WATER RESEARCH FOUNDATION℠

ADVANCING THE SCIENCE OF WATER®

Tailored Collaboration

Zero Liquid Discharge Desalination

Subject Area: Water Resources and Environmental Sustainability




Zero Liquid Discharge Desalination

About the Water Research Foundation

The Water Research Foundation (formerly Awwa Research Foundation or AwwaRF) is a member-supported, international, 501(c)3 nonprofit organization that sponsors research to enable water utilities, public health agencies, and other professionals to provide safe and affordable drinking water to consumers.

The Foundation's mission is to advance the science of water to improve the quality of life. To achieve this mission, the Foundation sponsors studies on all aspects of drinking water, including resources, treatment, distribution, and health effects. Funding for research is provided primarily by subscription payments from close to 1,000 water utilities, consulting firms, and manufacturers in North America and abroad. Additional funding comes from collaborative partnerships with other national and international organizations and the U.S. federal government, allowing for resources to be leveraged, expertise to be shared, and broad-based knowledge to be developed and disseminated.

From its headquarters in Denver, Colorado, the Foundation's staff directs and supports the efforts of more than 800 volunteers who serve on the board of trustees and various committees. These volunteers represent many facets of the water industry, and contribute their expertise to select and monitor research studies that benefit the entire drinking water community.

The results of research are disseminated through a number of channels, including reports, the Web site, Webcasts, conferences, and periodicals.

For its subscribers, the Foundation serves as a cooperative program in which water suppliers unite to pool their resources. By applying Foundation research findings, these water suppliers can save substantial costs and stay on the leading edge of drinking water science and technology. Since its inception, the Foundation has supplied the water community with more than $460 million in applied research value.

More information about the Foundation and how to become a subscriber is available on the Web at www.WaterResearchFoundation.org.

Zero Liquid Discharge Desalination

Prepared by:
Rick Bond, **Benjamin Klayman**, **Catherine Spencer**, and **Vasu Veerapaneni**
Black & Veatch, 8400 Ward Parkway, Kansas City, MO 64114

Tom Davis
University of Texas at El Paso, 500 West University Avenue, El Paso, TX 79968
and
Bill Batchelor
Texas A&M University, 3136 TAMU, College Station, TX 77843-3136

Jointly sponsored by:
Water Research Foundation
6666 West Quincy Avenue, Denver, CO 80235-3098

Orlando Utilities Commission
3800 Gardenia Avenue, Orlando FL 32802

Tampa Bay Water
2575 Enterprise Road, Clearwater, FL 33763

Saint Johns River Water Management District
Box 1429, Palatka, FL 32178-1429

South Florida Water Management District
P.O. Box 24680, West Palm Beach, FL 33416-4680
and
Southwest Florida Water Management District
2379 Broad Street, Brooksville, FL 34604-6899

Published by:

WATER RESEARCH FOUNDATION℠
ADVANCING THE SCIENCE OF WATER®

DISCLAIMER

This study was jointly funded by the Water Research Foundation (Foundation), Orlando Utilities Commission, Tampa Bay Water, Saint Johns River Water Management District, South Florida Water Management District, and Southwest Florida Water Management District (the co-funding utilities). The Foundation and the co-funding utilities assume no responsibility for the content of the research study reported in this publication or for the opinions or statements of fact expressed in the report. The mention of trade names for commercial products does not represent or imply the approval or endorsement of the Foundation or the co-funding utilities. This report is presented solely for informational purposes.

ISBN 978-1-60573-143-8

Printed in the U.S.A.

Printed on recycled paper

CONTENTS

TABLES

FIGURES

FOREWORD

The Water Research Foundation (Foundation) is a nonprofit corporation that is dedicated to the implementation of a research effort to help drinking water utilities respond to regulatory requirements and address high-priority concerns of the water sector. The research agenda is developed through a process of consultation with Foundation subscribers and other drinking water professionals. Under the umbrella of a Strategic Research Plan, the Board of Trustees and Board-appointed volunteer committees prioritize and select research projects for funding based upon current and future needs, applicability, and past work. The Foundation sponsors research projects through the Focus Area, Emerging Opportunities, and Tailored Collaboration programs, as well as various joint research efforts with organizations such as the U.S. Environmental Protection Agency and the U.S. Bureau of Reclamation.

This publication is a result of one of these sponsored studies, and it is hoped that its findings will be applied in communities throughout the world. The following report serves not only as a means of communicating the results of the water industry's centralized research program but also as a tool to enlist the further support of the nonmember utilities and individuals.

Projects are managed closely from their inception to the final report by the Foundation's staff and large cadre of volunteers who willingly contribute their time and expertise. The Foundation serves a planning and management function and awards contracts to other institutions such as water utilities, universities, and engineering firms. The funding for this research effort comes primarily from the Subscription Program, through which water utilities subscribe to the research program and make an annual payment proportionate to the volume of water they deliver and consultants and manufacturers subscribe based on their annual billings. The program offers a cost-effective and fair method for funding research in the public interest.

A broad spectrum of water supply issues is addressed by the Foundation's research agenda: resources, treatment and operations, distribution and storage, water quality and analysis, toxicology, economics, and management. The ultimate purpose of the coordinated effort is to assist water suppliers to provide the highest possible quality of water economically and reliably. The true benefits are realized when the results are implemented at the utility level. The Foundation's trustees are pleased to offer this publication as a contribution toward that end.

Roy L. Wolfe, Ph.D.
Chair, Board of Trustees
Water Research Foundation

Robert C. Renner, P.E.
Executive Director
Water Research Foundation

ACKNOWLEDGMENTS

This project was sponsored by the Water Research Foundation, Orlando Utilities Commission, Tampa Bay Water, St. Johns River Water Management District, South Florida Water Management District, and Southwest Florida Water Management District. The authors wish to express their thanks to Robert Teegarden and Keith Browning of OUC and Chris Owen of Tampa Bay Water for their support throughout the project.

Several agencies contributed time and materials to this research effort. Collier County, Sarasota County, and the City of Ormond Beach provided materials, water samples, and data. Special thanks are due Collier County for hosting the pilot study, and the authors wish to thank Paul Mattausch, Howard Brogdon, and Barry Erickson of Collier County for their support and assistance over several months of testing. Michael Bourke of Orica Watercare provided MIEX® resin for testing and consulted with the research team on use of ion exchange for TOC removal.

EXECUTIVE SUMMARY

Population growth, changing climate patterns, and pollution have combined to exert unprecedented stress on water supplies around the world. There is consensus in the water industry that increased use of desalination will be needed to meet future water demands and protect consumers and aquatic life from exposure to a growing list of emerging contaminants. Implementing desalination, however, can be constrained by the difficulty and expense of managing the concentrate byproduct generated by reverse osmosis (RO) and other membrane separation technologies. The options for managing concentrate are as follows:

- Direct discharge
- Deep well injection
- Discharge to a wastewater treatment facility
- Zero liquid discharge (ZLD) desalination

Discharge of concentrate by the first three methods can contaminate other water sources and diminish the value of reclaimed water for irrigation or industrial purposes. In ZLD desalination, concentrate is treated to produce product water and essentially dry salts. Consequently, there is no discharge of liquid waste from the site, and salts are removed from the water cycle.

Currently ZLD desalination is applied primarily to industrial waste streams or power plant cooling water, and the established technologies for ZLD are thermal desalination and evaporation ponds. Each has disadvantages that make it prohibitively expensive for drinking water applications. Consequently, there is a vital need by the drinking water industry for economical and environmentally sustainable methods for ZLD desalination.

OBJECTIVES

The overall goal of this research was to investigate methods that reduce the cost for ZLD desalination of brackish water. Specific project objectives were as follows:

- Evaluate and compare treatment technologies for ZLD desalination.
- Evaluate the effect of high concentrations of natural organic matter (NOM) on ZLD treatment requirements and costs.
- Evaluate the effect of total dissolved solids (TDS) concentration on ZLD costs.
- Evaluate the viability of ZLD desalination as a treatment approach for removal of a single contaminant.

BACKGROUND

Recovery in membrane separation processes, such as RO, electrodialysis (ED), and electrodialysis reversal (EDR) is limited by the membrane fouling potential of inorganic and organic precipitates. Inorganic fouling, also referred to as scaling, occurs when sparingly soluble salts precipitate and deposit on the membrane surface. Common salts of concern for brackish water desalination are calcium carbonate ($CaCO_3$), calcium sulfate ($CaSO_4$), and silica (SiO_2). Similarly,

organic fouling is caused by the precipitation of organic compounds onto the membrane, and the fouling potential of organic compounds is increased in the presence of calcium.

One approach to reducing the costs for ZLD is to treat RO concentrate to reduce its membrane fouling potential, and then desalinate the treated concentrate in a second membrane application. The hypothesis is treatment costs will be reduced by a concurrent increase in the percentage of water recovered with membrane processes and decrease in reliance on thermal technologies. Treatment processes that can be used to reduce the membrane fouling potential of concentrate include softening, fluidized bed crystallization, activated alumina, coagulation with metal salts, and ion exchange. The most highly developed options for the second membrane desalination step are RO and electrodialysis.

A new electrodialysis technology, referred to as electrodialysis metathesis (EDM), was integral to the ZLD approach investigated in this project. Electrodialysis has been used for decades in the drinking water industry to produce potable water and in the chemical and food industries to recover valuable salts or brine products.

In electrodialysis, water is desalinated by the transport of ions through ion exchange membranes under the driving force of an electric potential between a cathode and an anode. Cations are pulled from the feed water toward the cathode and anions are pulled toward the anode. Cations pass through cation selective membranes into the concentrate compartment and are held there by repulsion from the anion selective membrane. Anions similarly pass through anion exchange membranes and are held in the concentrate compartment by cation exchange membranes, The results is alternating compartments of desalinated product water and a byproduct concentrate containing all of the removed ions.

EDM differs from conventional electrodialysis by an innovative arrangement of ion exchange membranes and use of NaCl solution. These innovations cause EDM concentrate to be separated into two streams of highly soluble salts. One stream contains sodium and anions and the other chloride with cations. Separation of concentrate into two streams with highly soluble salts allows desalination at high rates of recovery that would lead to membrane fouling with RO or conventional electrodialysis. This characteristic makes EDM an attractive process for the second desalination step in ZLD.

APPROACH

The investigative approach comprised the following steps:

- Preliminary analyses to evaluate water quality and establish treatment goals.
- Preliminary testing to compare treatment options and select a ZLD approach for pilot-scale testing.
- Pilot-scale testing with the selected treatment approach.
- Evaluation of results to estimate full-scale treatment costs.

Five water sources were evaluated with bench- and pilot-scale testing. The test results were used to conduct desktop studies on two additional sources. Diverse water types were evaluated to maximize the applicability of this work. Raw water TDS concentrations in the sources ranged from 270 to 28,000 mg/L, and total organic carbon (TOC) concentrations ranged from 2 to 20 mg/L. The geographical focus of this study was Florida where natural organic matter (NOM) is found in many brackish water sources.

RESULTS/CONCLUSIONS

Three ZLD options were identified in the preliminary analyses and evaluated in preliminary testing. The first two options included combinations of ion exchange, softening, and coagulation processes for concentrate treatment followed by secondary desalination with RO. The third option comprised only EDM for secondary desalination, except for two sources for which ion exchange preceded EDM for TOC removal. Based on minimization of cost, waste byproducts, and energy consumption, the option with EDM was selected for further evaluation at pilot-scale.

EDM was pilot tested with concentrate samples from four of the water sources. The TDS range of the concentrate samples was 3000 to 16,000 mg/L, and the samples were supersaturated with salts that would foul RO or ED membrane systems if either were used for further treatment. Water quality and EDM performance parameters were monitored to evaluate: (1) the effectiveness of EDM in separating the concentrate into two streams of highly soluble salts, (2) the rate of product water recovery by EDM, and (3) energy requirements for desalination with EDM. Water quality analyses of the EDM concentrate streams showed the process was highly effective separating the concentrate into two highly soluble streams. Recovery of RO concentrate during EDM pilot tests ranged between 99.8 and 99.9 percent, and the EDM operated without any sign of membrane fouling.

Pilot test results were scaled up to calculate EDM recovery, water quality, and energy requirements for full-scale application. Full-scale ZLD treatment costs were calculated for each of the seven water sources. The treatment process comprised EDM followed by thermal desalination in a crystallizer. The ion exchange process, MIEX®, was included for TOC removal ahead of EDM for two of the sources.

Treatment costs were calculated per volume of RO concentrate recovered. (Cost on the basis of total plant production can be calculated by dividing these costs by 5 for an RO plant operating at 80 percent recovery or by 4 for a RO recovery of 75 percent.) Treatment costs included amortized equipment capital cost and O&M cost. Capital cost was amortized over 20 years at a 6 percent rate of return. O&M comprised energy, chemicals, and membrane replacement. Similar treatment costs were calculated for conventional ZLD with thermal desalination to assess the potential for cost reduction with the EDM method.

The treatment costs for ZLD with EDM were highly dependent on TDS. Five of the sources evaluated had raw water TDS concentrations of 1400 mg/L or less. The ZLD treatment costs for these sources ranged from $2.42 to $4.35 per kgal. The two other sources had TDS concentrations of 5300 and 28,000 mg/L. Treatment cost for the 5300 mg/L TDS source was $15.90 per kgal, and the cost for the 28,000 mg/L TDS source was $42.43 per kgal. Compared with conventional ZLD, treatment costs for the five lower TDS sources were 22 to 37 percent of the ZLD cost with thermal desalination. Treatment cost for the 5300 mg/L TDs source was comparable to that of conventional ZLD, and the EDM method was 60 percent more expensive than ZLD with thermal desalination for the 28,000 mg/L TDS source. Consequently, this approach appears to particularly advantageous for the higher quality brackish sources that utilities would first seek to use.

ZLD costs with the EDM method were reduced thirty percent for six of the sources by treating the EDM concentrate to develop beneficial products. This was not evaluated for the 28,000 mg/L TDS source because its treatment costs for the EDM option were prohibitive. The cost savings resulted primarily from recycle of the EDM concentrate to the process to replace NaCl consumed during electrodialysis. This reduced the flow treated by thermal desalination and reduced NaCl costs for EDM desalination. The salt products generated would be gypsum, calcium

carbonate, and dolomite. Although these salts have commercial value, in this analysis the final salt products were treated as cost neutral, having neither commercial value nor disposal cost. In the two options that included MIEX for TOC removal, treatment to remove TOC increased the ZLD treatment cost by 28 to 36 percent.

APPLICATIONS/RECOMMENDATIONS

As utilities face the challenges of increased use of alternative water sources and the need to remove emerging contaminants at very low concentrations, economical and sustainable management of RO concentrate will assume increasing importance. This research demonstrated a promising method of zero liquid discharge desalination using a new electrodialysis technology.

Although EDM is a new technology, it is nevertheless simply electrodialysis with an innovative arrangement of ion exchange membranes. Electrodialysis has been in use in large scale applications for more than 50 years, and its principles have been understood for more than 100 years. Consequently, there is little left to overcome in the learning curve for this technology, and it is likely that EDM will be available for full-scale implementation in the near future.

It is recommended that utilities faced with current or projected concentrate management challenges consider the ZLD approach evaluated in this research. The calculations in this report can be used as a model to evaluate ZLD with EDM and compare costs for this ZLD approach with other concentrate management options. If this preliminary evaluation looks promising, a utility is advised to conduct a pilot study with EDM to develop design and cost criteria specific to its water source.

RESEARCH PARTNERS

This research was supported by the following agencies:

- Orlando Utilities Commission
- Tampa Bay Water
- St. Johns Water Management District
- South Florida Water Management District
- Southwest Florida Water Management District

PARTICIPANTS

The following agencies provided data, water samples, facilities, and staff time to support this research:

- Orlando Utilities Commission
- Tampa Bay Water
- City of Ormond Beach
- Collier County Water Department
- Sarasota County Water Department

CHAPTER 1
INTRODUCTION

OVERVIEW

Population growth, changing weather patterns, and pollution have combined to exert unprecedented stress on water supplies around the world. In 2008, large areas of the United States were in a prolonged and severe drought. In the arid western states, the two largest manmade reservoirs in the U.S., Lakes Powell and Mead on the Colorado River, were at their lowest levels ever. In the Southeastern United States, the United States Department of Agriculture (USDA) reported that five states experienced Exceptional Drought Conditions, the department's most severe drought classification. In Florida, Lake Okeechobee reached its lowest recorded level, and significant portions of the state were classified as priority water resource caution areas, defined as areas where existing and reasonably expected sources of water and water conservation are not expected to be adequate to meet future needs.

In the U.S., water supply challenges have been exacerbated by high rates of population growth in regions with limited water resources. In 2005, the U.S. Census Bureau projected Nevada, Arizona, Florida, and Texas would experience the greatest population growth of any states from 2000 to 2030 (U.S. Census Bureau 2005). Utilities are increasingly exploring use of reclaimed water and brackish sources to mitigate existing and projected water shortages. Treatment of these sources generally involves desalination with reverse osmosis (RO) membranes or similar membrane separation technologies.

Water quality challenges grow with repeated use of limited water resources by an expanding population. RO is a best available technology (BAT) for many anthropological pollutants such as endocrine disrupting compounds, pharmaceuticals, and personal care products. Concerns about the adverse health and ecological effects of emerging contaminants and the ability to measure these contaminants at very low concentrations portends increased use of RO treatment, particularly for reclaimed water.

There is consensus in the water industry that increased use of desalination will be needed to meet water demand and protect public health and aquatic ecosystems. Implementation of desalination, however, is often constrained by the difficulty and expense of managing the concentrate byproduct generated by RO and other membrane separation technologies commonly used for desalination. The options for managing concentrate are as follows:

- Direct discharge.
- Deep well injection.
- Discharge to a wastewater treatment facility.
- Zero liquid discharge (ZLD) desalination

Discharge of concentrate by the first three methods risks contamination of other water resources. Furthermore, discharge to a wastewater treatment facility diminishes the value of reclaimed water for irrigation or industrial purposes. In ZLD desalination, concentrate is treated to produce product water and essentially dry salts. Consequently, there is no discharge of liquid waste from the site, and salts are removed from the water cycle.

Currently ZLD desalination is applied primarily to industrial waste streams or power plant cooling water. The established technologies for ZLD are thermal desalination and evaporation ponds. Each has disadvantages that make its use prohibitively expensive for drinking water applications.

Thermal desalination equipment is expensive because of the specialized materials required to withstand highly corrosive conditions. Furthermore, the process is energy intensive and therefore expensive to operate.

Evaporation ponds typically require leak-proof liners and leak monitoring systems, and large land areas are required, even in arid climates, to provide sufficient surface area for evaporation. Pond lining systems make ponds expensive to construct, and space requirements make them difficult to site. Furthermore, the water evaporated from ponds is lost as a resource to the community.

New ZLD approaches are being investigated that seek to reduce dependence on thermal desalination and evaporation ponds by increasing the percentage of water recovered by membrane separation processes, such as RO or electrodialysis. The ZLD approach investigated in this project involves treatment of concentrate to reduce its fouling potential, followed by desalination by electrodialysis to recover more water. This reduces the concentrate volume treated by evaporation ponds or thermal desalination and provides a significant reduction in ZLD treatment costs.

A similar approach was investigated in a recent Water Research Foundation research project to evaluate ZLD desalination of water sources for which removal of inorganic salts was the primary treatment goal (Bond and Veerapaneni 2007a). Reclaimed water and brackish water sources in humic rich environments, however, also contain high concentrations of natural organic matter (NOM). This is significant because:

1. NOM can adversely affect the processes used in ZLD to treat RO concentrate.
2. NOM can cause membrane fouling.
3. Reactions between NOM and divalent cations such as calcium increase the risk of membrane fouling beyond that posed by either acting alone.

Consequently, water sources with high organic concentrations must be treated for reduction of total organic carbon (TOC) as well as removal of salts. This adds a layer of complexity to concentrate treatment that must be understood in order to implement effective ZLD desalination of reclaimed waters and brackish waters with high TOC concentrations. In the current report, ZLD research was expanded to include waters with high organic concentrations.

Several factors made Florida an ideal location to investigate the challenges associated with ZLD desalination of water with high NOM. The state has an abundance of brackish sources with high NOM concentrations and is a leader in use of reclaimed water. Historically, Florida has relied on fresh groundwater for its water supply, but these sources alone will be inadequate to meet future needs. Consequently, significant portions of the state have been identified as priority water resource caution areas, defined as areas where existing and reasonably expected sources of water and water conservation are not expected to be adequate to meet future needs. Use of brackish and reclaimed sources can mitigate projected water shortages, but only if affordable and sustainable concentrate management solutions are available.

Understanding the need for concentrate management in Florida, the following Florida utilities and agencies came together to sponsor this research:

- Orlando Utilities Commission (OUC)
- Tampa Bay Water (TBW)
- Saint Johns River Water Management District (SJRWMD)
- South Florida Water Management District (SFWMD)
- Southwest Florida Water Management District (SWFWMD)

PROJECT OBJECTIVES

The overall goal of this research was to investigate methods that reduce the cost for ZLD desalination. Diverse water types and treatment approaches were evaluated to maximize the applicability of this work. Specific project objectives were as follows:

- *Evaluate and compare treatment technologies for ZLD desalination*. Several treatment technologies were evaluated to compare costs, energy requirements, and environmental sustainability. Of particular interest in this study was the evaluation of a new electrodialysis technology, electrodialysis metathesis (EDM), because it provides unique advantages for concentrate treatment.
- *Evaluate the effect of high concentrations of natural organic matter (NOM) on ZLD treatment requirements and costs*. To the best of our knowledge, ZLD desalination of waters with high organic content has never been investigated. Filling in this piece of the knowledge base will be critical to sustainable desalination of reclaimed water and brackish waters with high TOC concentrations.
- *Evaluate the effect of total dissolved solids (TDS) concentration on ZLD costs*. The five sources tested covered a broad range of TDS concentrations, from 270 mg/L to 5300 mg/L.
- *Evaluate the viability of ZLD desalination as a treatment approach for removal of a single contaminant*. The source with 270 mg/L TDS would not otherwise require desalination, but it is subject to fluoride concentrations as high as 10 mg/L. RO is a BAT for fluoride removal.

PROJECT APPROACH

Investigative Approach

The investigative approach comprised the following steps:

- Preliminary analyses to evaluate water quality and set treatment goals.
- Preliminary testing to compare treatment options and select one ZLD approach for pilot-scale testing.
- Pilot-scale testing with the selected treatment approach.
- Evaluation of results to estimate full-scale treatment costs.

Computer modeling programs were used throughout to project treatment goals, evaluate test results, and guide testing. Bench-scale testing was conducted with each of the five water sources to compare treatment options and select the best treatment approach for evaluation at pilot-scale. Pilot-scale testing was conducted with each of the water sources to evaluate the selected

treatment approach. Bench- and pilot-scale treatment results along with computer modeling were used to determine full-scale ZLD treatment costs and energy requirements for each water source. Desktop studies were conducted on two additional sources.

Treatment Approach

The treatment approach evaluated in this project comprised the following three steps:

1. Treatment of the concentrate to prepare it for secondary desalination.
2. Secondary desalination with one or more membrane separation processes.
3. Evaporation.

The percentage of product water recovered during desalination by membrane separation processes is limited by the membrane fouling potential of the water. The membranes can be fouled by inorganic salts, organic compounds, or both. The goal of concentrate treatment in the first step is to reduce the membrane fouling potential of concentrate so that it can be treated in a secondary desalination process with a high recovery of product water. The processes evaluated for concentrate treatment were coagulation, softening, fluidized bed crystallization (FBC), activated alumina (AA), magnetic ion exchange (MIEX®), and EDM.

The processes evaluated for secondary desalination were RO and EDM. In general, ZLD treatment costs are minimized by maximizing the percentage of concentrate recovered as product water in secondary desalination.

A final evaporative step is needed to completely separate salts from water. Available technologies for this step are thermal desalination, evaporation pond, and various enhanced evaporation technologies that use pumping energy to increase surface area and accelerate the rate of evaporation. Thermal desalination is the most practical of these options in Florida and similar climates where high rainfall rates make natural evaporation impractical.

BACKGROUND

Membrane Fouling

Recovery in membrane separation processes, such as RO, electrodialysis (ED), and electrodialysis reversal (EDR) is constrained by the membrane fouling potential of inorganic and organic precipitates.

Inorganic Fouling

Inorganic fouling, also referred to as scaling, occurs when sparingly soluble salts precipitate and deposit on the feed side of the membrane surface. The most common salts of concern for brackish water desalination are calcium carbonate ($CaCO_3$), calcium sulfate ($CaSO_4$), barium sulfate ($BaSO_4$), and silica (SiO_2).

Precipitation of these salts is driven by the concentration of their constituent ions. For example, the precipitation potential of $CaSO_4$ increases as concentrations of calcium (Ca) and sulfate (SO_4) in solution increase. The propensity of ions to react and form salts is also affected by the concentration of all other ions in the water. As solution ionic strength increases, electrostatic

interactions between ions reduce their reactivity with one another. An activity coefficient, γ, is used for each ion to reflect its attenuated reactivity, and the product of the activity coefficient and concentration is defined as activity. The activity of calcium, $\{Ca^{2+}\}$, for example, when reacting with sulfate to form $CaSO_4$ is its activity coefficient, $\gamma_{Ca,}$ times its molar concentration $[Ca^{2+}]$.

$$\{Ca^{2+}\} = \gamma_{Ca}[Ca^{2+}]$$

The ion activity product (IAP) for calcium sulfate is calculated as

$$IAP = \gamma_{Ca}[Ca^{2+}]\ \gamma_{SO4}[SO_4^{2-}] = \{Ca^{2+}\}\ \{SO_4^{2-}\}$$

The IAP at which dissolved ions of a salt and its solid phase are in equilibrium is referred to as the equilibrium solubility product, K_{s0}. The saturation state, S, of a solution is the ratio of IAP to K_{s0}.

$$S = \left(\frac{IAP}{Ksp}\right)$$

A solution is supersaturated with respect to a particular salt when $IAP > K_{s0}$ and undersaturated when $IAP < K_{s0}$.

$IAP < K_{s0}$ (solution is undersaturated)
$IAP = K_{s0}$ (solution is at equilibrium, saturated)
$IAP > K_{s0}$ (solution is supersaturated)

The potential for precipitation exists when $S > 1$, but precipitation is affected by many other factors including kinetics, hydrodynamics, and the presence of impurities. Consequently, there is often a discrepancy between the phase predicted by solubility equilibrium and that actually observed in a supersaturated solution. Even though solutions are supersaturated when $S > 1$, precipitation is virtually nonexistent until a sufficiently high state of supersaturation is reached. Until such a state is reached, ions can remain in solution indefinitely in supersaturated solutions.

In RO desalination, the supersaturation of sparingly soluble salts is highest near the surface of the membrane. This phenomenon is referred to as concentration polarization, and it occurs because the membrane surface is where water diffuses through the membrane and dissolved solids are rejected.

Chemicals that inhibit precipitation, commonly referred to as antiscalants, are used to pretreat RO feed water with the goal of increasing RO recovery. Antiscalants inhibit precipitation by adsorbing to the surface of precipitates to block integration of new ions or by sequestering ions to prevent formation of orderly crystals in precipitation reactions. Polyphosphates, organophosphonates, and polymers have been studied for their ability to inhibit precipitation, and many commercial antiscalants today are proprietary formulations of phosphonates, polymers, or phosphonate/polymer blends.

Organic Fouling

TOC in natural waters comprises a complex mix of thousands of organic compounds, many of which have yet to be identified. This heterogeneous group spans molecular weights ranging from several hundred to several hundred thousand and includes acids, bases, and neutral compounds.

Because characterization of TOC by identification of all of its individual compounds is not practical or even currently technically feasible, operational classes have evolved over several decades based on functional characteristics. The behavior of organic compounds in water treatment is related to certain functional characteristics, such as hydrophobicity.

Carboxylic acids are contained in 90 percent of natural organic matter in water and occur on humic substances at a frequency of 5 to 10 per molecule (Thurman 1985). The carboxylic acid group is an important functional group because it contributes to the solubility and metal binding capacity of TOC. In the pH range of natural waters, carboxylic acids are completely ionized giving TOC molecules a negative charge. Ionization increases the solubility of TOC and provides binding sites for major cations and trace metals. Disassociation of carboxylic acids causes hydrophobicity of TOC to decrease as pH increases. Egeberg and Alberts (2002), for example, found that hydrophobicity of NOM samples decreased by a factor of 3 when pH was increased from 4.7 to 7.

Fouling of membranes by organic matter is affected by the chemical characteristics of NOM, including size, charge, and functional groups of the molecules. The potential for organic fouling also depends upon membrane characteristics (particularly surface charge), chemical composition of the feed water, and hydrodynamic conditions in the membrane system (Hong and Elimelech 1997).

Jucker and Clark (1994) compared the adsorbability of fulvic and humic acids onto ultrafiltration membranes. The membranes tested had less adsorption capacity for fulvic than for humic acid. The influences of inorganic water chemistry and of membrane charge on NOM adsorption were also studied. Adsorption increased with high calcium concentrations, low pH, and high membrane pore zeta potential.

Nilson and DiGiano (1996) examined the influence of NOM composition on fouling of nanofiltration membranes. The hydrophobic NOM fraction, which was rejected to greater extent than the hydrophilic fraction, was responsible for membrane fouling. Schaefer, Fane, and Waite (1998) also found that the NOM fraction that absorbed UV the strongest and was the most hydrophobic deposited preferentially on the membrane surface.

Hong and Elimelech (1997) examined the chemical and physical interactions that affect NOM fouling of NF membranes with a focus on the combined effect of high concentrations of NOM and calcium. Using three humic acids, they found membrane fouling increased with increased solution ionic strength, decreased pH, and increased divalent cation concentration. Of these factors, the greatest fouling effect was caused by divalent cations.

Braghetta, DiGiano, and Ball (1998) evaluated the effects of NOM concentration, pH, solution ionic strength, and cross flow velocity on NF membrane fouling in bench-scale tests. The rate of membrane fouling was greater at pH 4 than at pH 7 or 10, and this was attributed to less electrostatic repulsion between the membrane and NOM at pH 4. A NaCl solution was used to increase ionic strength so the solution contained monovalent ions only. Membrane fouling and the amount of TOC adsorbed to the membrane surface increased as solution ionic strength increased. Two cross flow velocities were evaluated. Membrane flux decline was less for the higher cross flow velocity.

Li and Elimelech (2004) examined the mechanisms of organic fouling under different solution conditions of pH, total ionic strength, and divalent cation concentration by measuring the attraction and adhesion forces between an organic foulant and the membrane surface. Bench-scale fouling experiments were conducted to evaluate the effect of divalent cations on organic fouling. The test solution had a humic acid concentration of 20 mg/L and a total ionic strength of 10 mM.

Three samples were tested, one with Na^+ as the only cation, one with 1 mM of Ca^{2+}, and one with 1 mM of Mg^{2+}.

Over a period of 300 minutes, flux declined 11 percent for the solution without divalent cations, 16 percent for the solution with Mg^{2+}, and 49 percent in the solution with Ca^{2+}. Attraction forces between the clean membrane surface and humic acid were comparable for the three solutions, but there were significant differences in adhesion forces. There was no adhesion force for the monovalent solution, slight adhesion for the Mg^{2+} solution, and significantly greater adhesion force for the solution with Ca^{2+}. Hence, there was a much stronger interaction between humic acid and the clean membrane surface when calcium was present. The test was repeated using a fouled membrane with the same result. There was a much stronger interaction between humic acid and the fouled membrane surface in the presence of calcium.

It was concluded that organic fouling was not observed with the monovalent solution because electrostatic repulsion between the negatively charged membrane surface and the negatively charged humic acid prevented deposition of humic acid on the membrane. In contrast, divalent cations form complexes with humic acids, thereby reducing the charge of humic acid and reducing the electrostatic repulsion between it and the membrane surface. It was concluded that calcium caused more severe fouling than magnesium because the adhesion force between calcium and the membrane surface was significantly stronger.

Processes for Concentrate Treatment

Inorganic ions can be removed by precipitative processes, ion exchange, electrodialysis, or RO membranes. Organic compounds can be removed by precipitative processes, ion exchange, or adsorption to granular activated carbon (GAC).

Chemical Softening

Lime-soda ash softening has long been standard practice in drinking water treatment for removing calcium and magnesium hardness. Under appropriate conditions, it can also be effective for removal of TOC, trace metals, and silica. Consequently, softening has the potential to have an impact on all of the treatment goals for primary RO concentrate.

Calcium carbonate ($CaCO_{3(s)}$) precipitation depends on the ion activity product of the calcium (Ca^{2+}) and carbonate (CO_3^{2-}) ions. Because CO_3^{2-} concentration is pH dependent, the softening process is indirectly dependent on pH and is generally optimized around pH 10.3. Precipitation of magnesium hydroxide ($Mg(OH)_2$) is directly dependent on pH, and higher pH, typically 10.8 or greater, is required to achieve magnesium removal.

Trace elements are removed during softening by incorporation in the $CaCO_{3(s)}$ lattice structure. Bond and Veerapaneni (2007a) found that barium was removed in proportion to calcium in chemical softening jar tests with RO concentrate and that the percentage of barium removed increased with increasing barium-to-calcium ratio in the concentrate.

Although calcium carbonate is not an effective adsorbate (Powell 1954, Iler 1979), silica can be removed from water by adsorption to metal hydroxides such as $Mg(OH)_2$ (Betz, Noll, and Maguire 1940; Iler 1979). It has long been known that silica removal in chemical softening occurs by adsorption to freshly precipitated magnesium hydroxide (Straub 1936, Behrman and Gustafson 1940). Although dolomitic lime is 35 percent MgO, Behrman and Gustafson (1940) reported that it was not effective for silica removal because the magnesium was not freshly precipitated.

Correlation of silica removal to magnesium removal has been reported for chemical softening of RO concentrate. Bond and Veerapaneni (2007b) found that silica was removed in proportion to magnesium and that neither was removed effectively below pH 10.5.

TOC removal occurs during chemical softening, but there are inherent disadvantages compared with coagulation using iron or aluminum salts. Chemical softening is practiced at a much higher pH where TOC is more negatively charged and hydrophilic, making its removal more challenging. $CaCO_{3(s)}$ particles have a specific surface area about two orders of magnitude less than that of $Fe(OH)_{3(s)}$ or $Al(OH)_{3(s)}$, and in the pH range used for softening $CaCO_{3(s)}$ particles carry a net negative charge and therefore repulse negatively charged TOC molecules.

Nevertheless, TOC removal does occur during softening because of the affinity of certain TOC functional groups, notably carboxyl acids, for calcium. Furthermore, TOC removal during softening can be enhanced by addition of iron or aluminum coagulants during chemical softening and by precipitation of $Mg(OH)_2$. Water sources with the potential for substantial magnesium removal have an added advantage for TOC removal because $Mg(OH)_{2(s)}$ particles are amorphous, highly adsorbent, and remain positively charged at high pH.

Randtke (1988) concluded the following from several years of research regarding TOC removal by lime softening:

- Lime softening preferentially removes humic substances, and removal is increased by increasing pH and by precipitating $Mg(OH)_2$.
- TOC removal increases with addition of magnesium or phosphate.
- TOC removal increases with the amount of solids precipitated up to a point before ceasing to increase.
- The percent of TOC removed for a constant lime dose decreased as initial TOC concentration increased and the residual calcium concentration increased. It was concluded that TOC interfered with $CaCO_3$ precipitation.

Optimal conditions for hardness removal and TOC removal by softening do not coincide. $CaCO_3$ particles are positively charged in the presence of excess Ca^{2+} ions and negatively charged in the presence of excess CO_3^{2-} ions (Thompson and Pownall 1988; Cicerone, Regazzoni, and Blesa 1992; Nilsson and Sternbeck 1999; Lin and Singer 2005). TOC removal is enhanced by formation of amorphous $CaCO_3$ solids with poor crystallinity, excess Ca^{2+}, and low CO_3^{2-} concentration (Liao and Randtke 1985). Conversely, the rate of calcium carbonate precipitation increases as the molar ratio of CO_3^{2-}/Ca^{2+} increases (Zuddas and Mucci 1994, Lebron and Suarez 1998, Nilsson and Sternbeck 1999, Lin and Singer, and Aiken 2005). Liao and Randtke (1985) suggested that optimization of TOC and hardness removal might be achieved by using a two-stage process with one optimized for hardness removal and the other for TOC removal.

Furthermore, it is well known that the precipitation of $CaCO_3$ is inhibited by TOC, (Lebron and Suarez 1998, Lin, Singer, and Aiken 2005). The widely accepted method of inhibition is adsorption of TOC onto $CaCO_3$ and the blockage of $CaCO_3$ growth sites.

Batchelor and co-workers (Batchelor and McDevitt 1984; Batchelor, McDevitt, and Chan 1985; Abdel-Wahab and Batchelor 2002) proposed an interesting modification to lime softening, referred to as ultra high lime (UHL) softening, which has the potential to provide enhanced removals of silica, TOC, and sulfate compared with conventional softening.

UHL was conceptualized as a two-stage process in which ultra-high doses of lime are added to the first stage to raise pH to between 11 and 12. Calcium, silica, sulfate, magnesium,

and TOC are removed in the first stage, and excess calcium is carried over to the second stage. Carbonate (CO_2 or Na_2CO_3) is added in the second stage to precipitate mostly pure $CaCO_3$. It was suggested that a fluidized bed crystallizer might be appropriate for the second stage due to the purity of $CaCO_3$ solids expected.

Calcium is removed in the first stage by precipitation of $CaCO_3$. Some calcium and sulfate removal may occur with calcium sulfate precipitation. Increased sulfate removal can be achieved by the addition of aluminum to precipitate calcium sulfoaluminate ($Ca_6(SO_4)_2(Al)_2(OH)_{12}$) (Batchelor, McDevitt, and Chan 1985). In jar tests, sulfate removal increased with lime dose and with aluminum dose. At a lime dose of 18.5 mM and an aluminum dose of 8 mM, an initial sulfate concentration of 19 mM was reduced to 1 mM.

High calcium concentrations and high pH in the first stage result in removal of silica by adsorption to precipitated $Mg(OH)_2$, as in conventional softening, but also by precipitation of calcium silicate (CaH_2SiO_4). Reported values for the solubility product of calcium silicate range from $10^{-6.6}$ to $10^{-7.8}$ (Roller and Ervin 1940, Greenberg and Chang 1965, Mujeriego 1976, Batchelor and McDevitt 1984). Reduction in silica concentrations from 72 to 0.4 mg/L has been reported when sufficient lime was added to raise pH to 11.5 to 12 (Cleary and Grazdis 1982).

Although TOC removal was not studied in the work by Batchelor and co-workers, it is conceivable that the conditions associated with UHL would enhance TOC removal relative to conventional softening. The calcium-rich, carbonate-poor conditions in the first stage would favor TOC removal, and if aluminum is added for sulfate removal, it is possible that TOC would co-precipitate with calcium sulfoaluminate.

Coagulation With Metal Salts

Coagulation with metal salts has been a standard practice in the water treatment industry for decades to reduce turbidity and condition water for filtration. It has also been used for removal of silica and TOC.

Hydroxide precipitates of iron, aluminum, and magnesium are effective adsorbates for silica removal (Powell 1954, Iler 1979). Powell (1954) noted the following about silica removal with metal hydroxides:

- Removal occurs by adsorption and silica removal data typically conform to a Freundlich adsorption isotherm. As an adsorption process, the efficiency of the process falls off sharply as the silica concentration is reduced.
- There is an optimum pH for each process.
- Silica removal efficiency is dependent on the degree of hydration of the precipitate. Adsorption occurs on the hydrated form of the metal oxide.
- Metal oxides formed *in situ* are far more effective for silica removal than prepared oxides.
- The adsorption reactions are very rapid compared to typical hydraulic detention.
- Solids contact, as with return of magnesium hydroxide sludge in a clarifier, improves silica removal efficiency.

Early studies of silica removal focused on pretreatment of boiler feed water. Lindsay and Ryznar (1939) reported an optimal pH range of 8.3 to 8.7 for silica removal with sodium aluminate. Betz, Noll, and Maguire (1940) reported that silica removal by aluminum salts was most

effective in the pH range of 8.3 to 9.1, but lower pH, 7.6 to 8.0, was necessary to avoid residual dissolved aluminum concentrations. They evaluated silica removal with doses of freshly precipitated $Al(OH)_3$. An initial silica concentration was reduced from 23.9 mg/L to 9.5 mg/L at a dose of 200 mg/L. Removal efficiency decreased as the silica concentration decreased, and the data fit the Freundlich adsorption model. Schwartz (1938) reported that optimal silica removal with ferric hydroxide occurred at pH 9. Typical of an adsorption process, silica removal efficiency is higher for higher silica concentrations, but as silica concentrations decrease, increasingly large coagulant doses are required to increase removal.

Bond and Veerapaneni (2007a) evaluated silica removal from RO concentrate with alum and sodium aluminate. Silica was effectively removed at pH values between 8 and 9. The molar ratio of silica removed to aluminum added ranged from 0.4 to 1.0, and the ratio increased as pH increased between pH 8 and 9.

Aluminum and ferric salts are the most commonly used coagulants for dissolved organic carbon (DOC) removal. Randtke (1988) noted that studies to that point had not demonstrated superiority for either coagulant even though aluminum hydroxide is less soluble than ferric hydroxide in the pH range of 5 to 6 where DOC is less hydrophilic. The mechanisms for removal of DOC by coagulation are precipitation and adsorption to aluminum or ferric hydroxide (Dempsey, Ganho, and O'Melia 1984; Randtke 1988). Where precipitation is the dominant mechanism, there is a sharp increase in removal at the coagulant dose associated with minimum solubility of the DOC molecules. Where adsorption is predominant, DOC removal with increasing coagulant dose follows a more gradual slope.

Removal of DOC with coagulation is pH dependent (Dennett et al., 1996; Crozes, White, and Marshall 1995), and removal increases with coagulant dose up to a point where there is no further removal with increased dose (Weber and Jodellah 1985; Dempsey, Ganho, and O'Melia 1984; Semmens and Staples 1986). Hydrophobic, intermediate molecular weight (1K to 100K) substances are preferentially removed, and low molecular weight (< 1K) substances are poorly removed (Davis and Gloor 1981, Semmens and Ayers 1985, Semmens and Staples 1986).

Fluidized Bed Crystallizer

Fluidized bed crystallization achieves chemical softening within a fluidized bed. The treatment objectives are similar to those of conventional chemical softening, but the operating principles and the morphology of solids produced differ. Fluidized bed crystallization was first used for softening in 1938, and advancements to the technology and the extent of its use occurred in the 1980s when the process was selected to provide central water softening at main water treatment plants throughout the Netherlands (Graveland, de Moel, and Oomen 1983; Van der Veen and Graveland 1988).

Detailed descriptions of the fluidized bed crystallization process can be found elsewhere (Graveland, de Moel, and Oomen 1983; Van der Veen and Graveland 1988; Harms and Robinson 1990; van Dijk and Wilms 1991; Li, Jian, and Liao 2004; and Kim, Hirasawa, and Kim 2004). The following is a brief description of the process and the variables that govern its performance.

In fluidized bed crystallization, water and chemicals are fed at the bottom of a bed of $CaCO_3$ pellets to fluidize the bed and increase $CaCO_3$ supersaturation. Supersaturation induces calcium removal through crystal growth of pellets as calcium and carbonate ions diffuse from water to the surface of a $CaCO_3$ pellet and are incorporated in its crystal lattice structure. Sand is used as the starting seed material to develop new $CaCO_3$ pellets at startup of the unit, and new

sand is added periodically during operation to replace $CaCO_3$ pellets that are removed when they become too large. Clarification occurs in the column as treated water overflows the top of the reactor above the height of the fluidized bed.

The $CaCO_3$ pellets act as seed material to induce precipitation at lower supersaturation than required by chemical softening. In fact, supersaturation high enough to induce spontaneous nucleation of new $CaCO_3$ precipitates rather than crystal growth of existing pellets is undesirable because these smaller precipitates are more prone to carryover.

The bed is fluidized by the upflow velocity, and fluidization creates a vertical gradation of pellet size with the largest pellets at the bottom. The most important physical properties of the fluidized bed crystallizer are bed porosity, specific surface area of pellets in the bed, and pellet diameter, and these properties are interrelated. As pellet diameter increases, bed porosity increases, and specific surface area in the bed decreases. The rate of crystal growth decreases as pellet diameter increases because there is less specific surface area. The fluidized bed crystallization process is controlled by periodically removing the largest pellets from the bottom of the bed and adding sand to develop new $CaCO_3$ pellets.

The advantages of fluidized bed crystallization relative to conventional chemical softening are as follows:

- The solids generated by the process are near anhydrous pellets that are approximately 90 percent solid by weight. These pellets drain rapidly by gravity to a solids content of 99 percent.
- Precipitation occurs at lower supersaturation in the presence of $CaCO_3$ pellets, requiring lower pH and lower chemical doses to adjust pH before and after the process.
- The process has a high superficial velocity, up to 120 m/h (49 gpm/ft^2) and therefore requires less space.

Perhaps the most important of the above advantages is the formation of near dry solids. The solids volume from fluidized bed crystallization is approximately 10 percent of conventional softening sludge. Furthermore, there is potential beneficial use of the fluidized bed crystallization $CaCO_3$ pellets in agriculture and industry. In the Netherlands, all of the pellets are sold for beneficial use, including treatment of aggressive groundwater, neutralization of acidic wastewater, for road construction, cement manufacture, and in the metal industry (Graveland, de Moel, and Oomen 1983).

Bond and Veerapaneni (2007a) applied fluidized bed crystallization to treatment of concentrate for ZLD desalination. Calcium and barium were effectively removed at pH between 8 and 9. Silica, however, was not effectively removed at pH < 10. This deficiency was overcome by addition of aluminum salts to the fluidized bed crystallization process. With addition of alum or sodium aluminate, silica was effectively removed between pH 8 and 9.

Fluidized bed crystallization can be used to remove trace contaminants such as heavy metals (Zhou et al., 1999; Chen and Yu 2000; Guillard and Lewis 2001). An interesting application is the removal of fluoride (Aldaco, Garea, and Irabien 2006; Yang et al., 1999; Reardon and Wang 2000).

There are disadvantages, however, associated with treatment of concentrate with fluidized bed crystallization. Crystal morphology and purity can be affected by other inorganic ions such as magnesium and sulfate (Reddy and Wang 1980; Gratz and Hillner 1993; Astilleros et al., 2002; Tlili et al., 2003) and by organic compounds (Zhou et al., 1994; Hoch, Reddy, and Aiken 2000).

This may affect the beneficial use of pellets for some applications. Organic compounds can also reduce the rate of crystal growth (Lebron and Suarez 1998). Because of its supersaturation limits, fluidized bed crystallization is not an effective process for magnesium removal. Consequently, a metal salt coagulant must be added to the process to achieve silica removal.

Activated Alumina

Activated alumina is produced by dehydrating precipitated $Al(OH)_3$. The result is a highly porous (0.3 to 0.5 cm^3/g) mixture of amorphous and gamma aluminum oxide (γ-Al_2O_3) with a relatively high specific surface area (200 to 400 m^2/g). Removal of inorganic and organic contaminants by AA is sensitive to pH. Typical AA has a positive surface charge below pH 8.2 and a negative surface charge at higher pH values. AA has both anion and cation adsorption sites, but it has been used predominantly in drinking water treatment to remove anions. Anions are preferred by AA in the following order:

$$OH^- > H_2AsO_4^- > Si(OH)_3O^- > F^- > HSeO_3^- > SO_4^{2-} > CrO_4^{2-} >> HCO_3^- > Cl^- > NO_3^- > Br^- > I^-$$

AA was first investigated for silica removal from industrial waters. Behrman and Gustafson (1940) reported successful experiments removing silica with AA in investigating AA for treatment of boiler feed water. They noted that the AA could be regenerated by rinsing it successively with alkali and acid solutions.

Mouche and Matson (1980) proposed use of AA to remove silica from cooling tower water. The bulk of silica removal was reported to occur within the first 10 minutes of contact time. The suggested adsorption-regeneration cycle was as follows:

Step 1
Acidification
The AA is first treated with acid to form acidic AA.

$$Alumina \cdot HOH + HCl \rightarrow Alumina \cdot HCl + HOH$$

Step 2
Adsorption
Silica displaces chloride and adsorbs to the AA (provided pH is low enough to avoid competition from the more preferred hydroxide ions).

$$Alumina \cdot HCl + NaSi(OH)_3O \rightarrow Alumina \cdot H\,Si(OH)_3O + NaCl$$

Step 3
Regeneration
The AA is regenerated with caustic.

$$Alumina \cdot H\,Si(OH)_3O + 2NaOH \rightarrow Alumina \cdot NaOH + Na\,Si(OH)_3 + H_2O$$

Step 4
Acidification

Step 1 is repeated to restore fluoride removal capacity.

$$Alumina \cdot NaOH + 2HCl \rightarrow Alumina \cdot HCl + NaCl + HOH$$

Clifford, Matson, and Kennedy (1978) reported the optimum pH for silica removal with AA to be between 8 and 8.5. It was noted that this pH range was high enough for some of silicic acid to be in its anionic form ($Si(OH)_3O^-$) yet low enough to avoid competition from the preferred hydroxide (OH^-) ion. It was reported that sulfate had no impact on silica removal. Bouguerra et al., (2007) reported optimal silica removal between pH 8.0 and 8.5. Removal conformed to the Freundlich adsorption model.

AA can be used for TOC removal. Eberle, Stober, and Donnert (1976) reported stable 60 percent removal of TOC from river water with an initial TOC concentration of 7 mg/L after treatment of 1500 bed volumes. Because TOC removal was not increased by adding AA beds in series, it was concluded that 40 percent of the TOC was not adsorbable by the AA. Chen, Snoeyink, and Fiessinger (1987) evaluated AA for removal of TOC. AA was found to adsorb better as solution pH decreased, and this was attributed to increased negative charge on the TOC and increased positive charge on the AA. A percentage of the TOC was nonadsorbable.

AA has adsorption sites for cations and anions and, therefore, can achieve simultaneous removal of calcium, barium, silica, and TOC. Bond and Veerapaneni (2007a) evaluated removal of barium, calcium, and silica from brackish water with AA. The water quality characteristics of the brackish water were 4250 mg/L TDS, 420 mg/L Ca, 0.046 mg/L Ba, and 60 mg/L SiO_2. In isotherm experiments, with a contact time of 10 minutes and at pH 7.7, a 30 g/L AA dose reduced Ca by 30 percent, Ba by 83 percent, and SiO_2 by 76 percent. At a 50 g/L dose, calcium was reduced by 46 percent, barium by 90 percent, and silica by 89 percent.

MIEX®

MIEX® is a magnetic ion exchange resin developed for continuous use in a fixed or fluidized bed reactor. The MIEX® resin is a micro size, macroporous, strong base ion exchange resin with a built-in magnetic component. The MIEX® process comprises contact with the resin, resin separation and recycle, and regeneration. The magnetic component of the resin enhances its settling velocity. Most of the settled resin is collected and recycled to the process. A percentage of the recycled resin is continuously removed, regenerated, and returned to the contactor vessel.

The MIEX® resin was designed specifically for TOC removal, but other anions such as sulfate and silica can be removed by the process. The efficiency of removal of each depends on competition from other anions. Where MIEX® is used for treatment of RO concentrate, there is potential for sulfate concentrations to affect removal efficiencies for TOC.

The MIEX® resin is regenerated with a NaCl solution. The spent regenerant will be rich in sodium and chloride and the ions removed during treatment, and this stream must be managed along with RO concentrate to achieve ZLD desalination. The volume of spent regenerant that must be managed will depend on the regeneration frequency required to achieve treatment goals.

GAC

GAC is typically applied in fixed beds for removal of organic contaminants. As water is contacted with GAC, organic contaminants diffuse from solution and are adsorbed to the surface

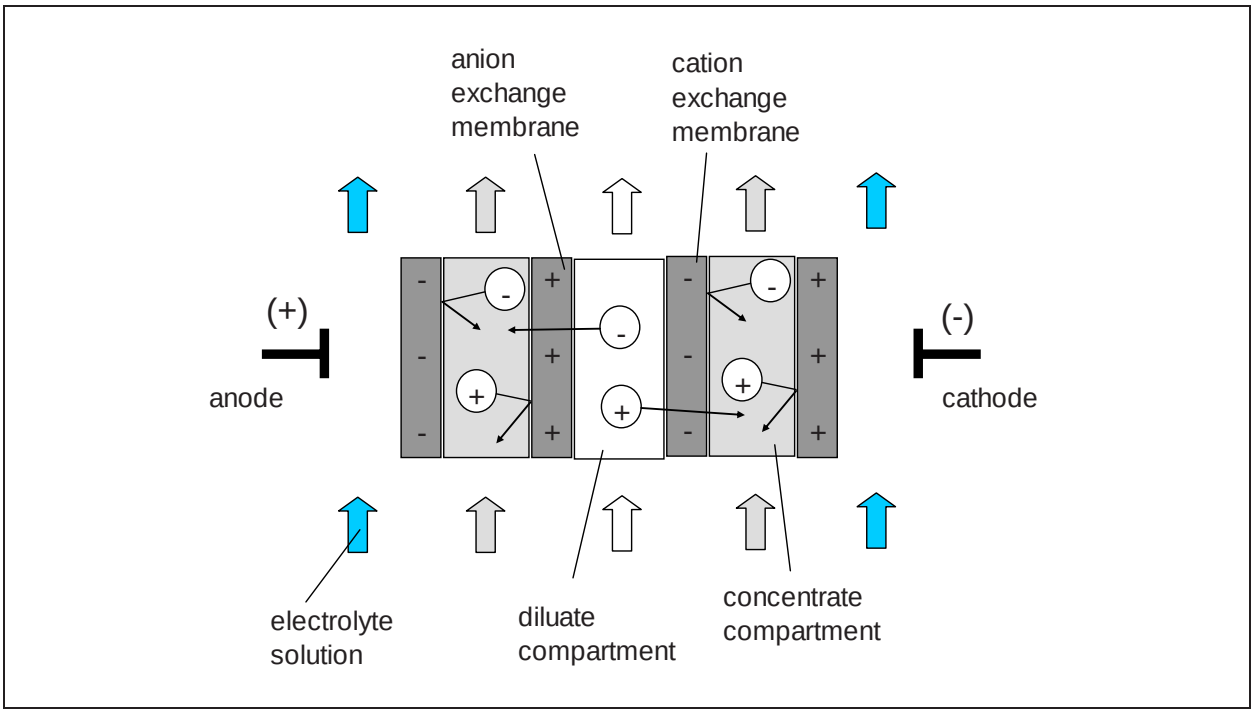

Figure 1.1 Electrodialysis cell schematic

of GAC particles. The adsorption capacity of GAC varies among organic contaminants. The adsorption front for a contaminant passes through the bed as the adsorption capacity of GAC is exhausted until the contaminant breaks through the bed. The media must be replaced before the level of contaminant breakthrough exceeds treatment goals. At typical water treatment TOC concentrations of 2 to 4 mg/L, media replacement frequency may be as often as 3 to 4 times per year. TOC concentrations in RO concentrate of high organic waters in this study exceeded 50 mg/L. Consequently, GAC treatment of concentrate would be economically infeasible and logistically impractical because of the need for frequent replacement of the GAC.

Electrodialysis

Electrodialysis (ED) is has been used for decades to remove ions from water. In drinking water applications, the objective has been to produce desalinated water for potable use. In the chemical and food industries, ED has been used to concentrate solutions for recovery of valuable salts or brine products. Chlorine gas and caustic, for example, are produced by electrodialysis of sodium chloride (NaCl) solutions in the chlor-alkali process.

The ED process is illustrated schematically in Figure 1.1. The ED stack comprises alternating cation and anion selective membranes between a cathode and an anode. The flat sheet membranes are separated by spacers that comprise a perimeter gasket and a plastic netting through which the solutions flow. The driving force for ED is the electric potential between the anode and cathode. Anions are drawn to the positively charged anode, and cations are drawn to the negatively charged cathode. Cations pass through the negatively charged cation exchange membrane and are rejected by the positively charged anion exchange membrane. Similarly, anions pass through the anion exchange membrane and are rejected by the cation exchange membrane. As a result,

solutions flowing through alternate compartments are depleted of ions and concentrated with ions. In terminology typically used in the ED industry, the solution being depleted of ions is referred to as diluate, and the solution receiving ions is referred to as concentrate.

Electrolyte solutions are fed in the compartments adjacent to the cathode and anode to carry current and maintain electric charge neutrality. Oxidation/reduction reactions occur at the electrodes, and the specific reactions depend on the type of electrolyte solutions used. When NaCl is the electrolyte solution, water can be reduced at the cathode to form hydrogen gas and hydroxide ions, and chloride and water can be oxidized at the anode to form chlorine gas, oxygen gas, and hydrogen ions.

$$\begin{aligned} &Cathode \quad 2H_2O + 2e^- \Rightarrow H_{2(g)} + 2OH^- \\ &Anode \quad 2Cl^- \Rightarrow Cl_{2(g)} + 2e^- \\ &\qquad H_2O \Rightarrow \frac{1}{2}O_{2(g)} + 2H^+ + 2e^- \end{aligned}$$

An ED cell pair comprises a cation exchange membrane, an anion exchange membrane, a diluate compartment, and a concentrate compartment. In typical full-scale applications, each ED stack contains several hundred cell pairs, and the plant might comprise several stages of ED stacks in series to achieve water quality goals and parallel series of these stacks to achieve production capacity.

An important distinction between ED and pressure driven membrane separation processes such as RO is that ions rather than water pass through the membranes. Consequently, only charged species are removed by ED, and uncharged species, such as silica at neutral pH, remain in the product water. This characteristic can be an advantage for ED in treating water sources with significant silica concentrations.

ED current is carried by the migration of ions. By Faraday's Law, the current required for the transfer of a given quantity of ions, I (A), is proportional to Faraday's constant, F (96,500 A·s eq^{-1}), diluate flow, q (L s^{-1}), the change in concentration between the influent and effluent of the diluate stream, ΔC (eq L^{-1}), and the inverse of the current efficiency factor, ζ.

$$I = \frac{Fq\Delta C}{\zeta}$$

The current efficiency factor is the electrical efficiency of the stack. It is the ratio of actual equivalents transferred to the theoretical number of equivalents transferred by Faraday's Law with ideal membranes and no electrical short-circuiting. Generally, industrial electrodialysis stacks have current utilization factors between 70 and 90 percent.

$$\zeta = \frac{\Delta C_{observed}}{\Delta C_{theoretical}}$$

Current density, i (A m^{-2}), is defined as the current divided by membrane area, A (m^2).

$$i = \frac{I}{A}$$

Current is related to applied voltage by Ohm's law, where V is the difference in electric potential in volts and R is resistance in ohms.

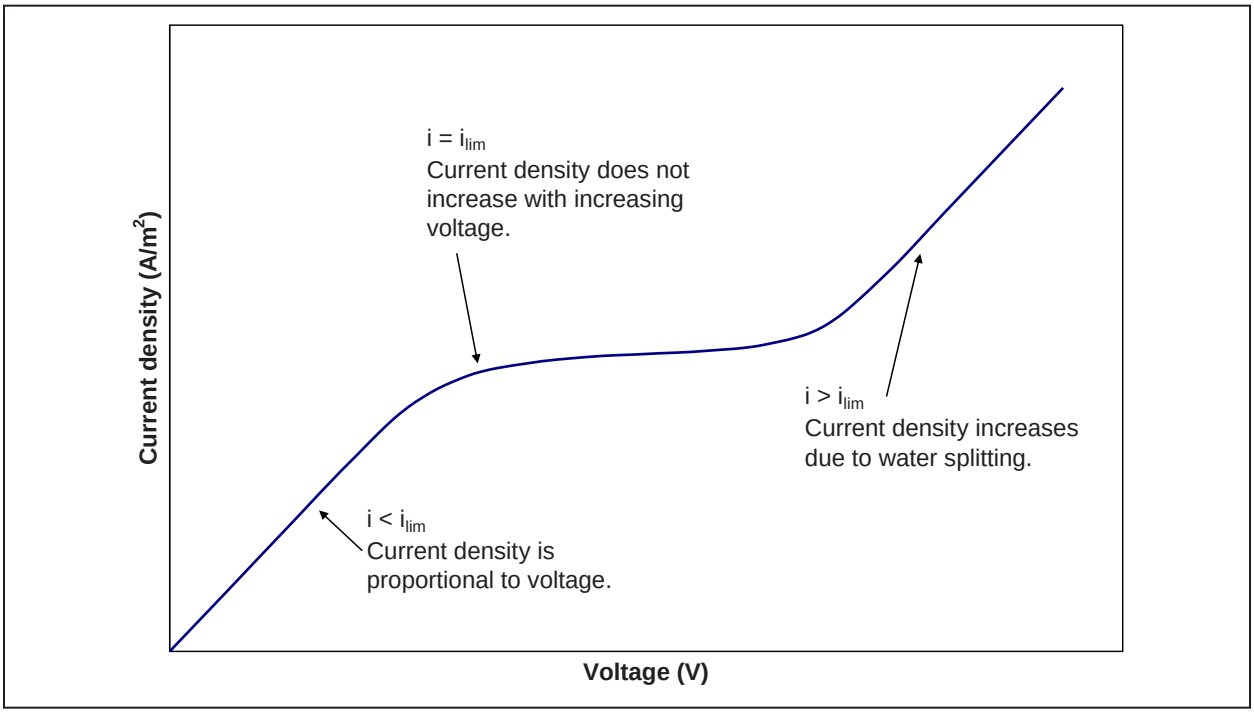

Figure 1.2 Electrodialysis limiting current density

$$I = \frac{V}{R}$$

The resistance of an ED cell pair is the sum of the resistances in the diluate channel, the concentrate channel, the anion exchange membrane, and the cation exchange membrane. Electrical resistance through an electrolyte solution increases as ionic strength of the solution decreases.

The transfer of ions through the membranes creates a concentration polarization effect, analogous to concentration polarization in RO desalination. In RO, ions are concentrated in the channel at the membrane surface because water diffuses through the membrane and ions are left behind. Concentration polarization in ED has an opposite effect.

In ED, ions rather than water are transported through the membrane. The concentration polarization effect occurs in ED because ions are transported through the membrane faster than they are transported through solution. Consequently, ion concentrations increase with distance from the membrane in the diluate solution compartment and decrease with distance from the membrane in concentrate solution compartment. A limiting current density is reached when the concentration of ions available to transfer current approaches zero at the membrane surface in the diluate compartment.

At the limiting current density, increases in voltage do not increase current density until voltage is high enough to split water molecules into H^+ and OH^-, at which point current is carried by H^+ and OH^- ions. Operation of ED near the limiting current density must be avoided because of energy inefficiency and the potential damage to membranes from pH extremes.

The concept of limiting current density (LCD) is illustrated in Figure 1.2. The graph depicts the response of current density as voltage is steadily increased. Initially, current density increases in proportion to voltage indicating current densities are less than the limiting value. The limiting

current density is reached where current density does not increase with increased voltage due to resistance across the ion-depleted diffusion boundary layer. As voltage is increased, current density remains flat until voltage is sufficient to cause water splitting and current is carried by H^+ and OH^- ions.

The LCD value depends on the concentration of ions in the water, cell geometry, and hydrodynamic conditions in the ED channels between membranes. LCD increases as the concentration of ions in the water increases and as the thickness of the membrane boundary layer decreases. The thickness of the boundary layer is affected by channel velocity and the geometry of the spacer. As velocity increases, flow becomes more turbulent, and the boundary layer thickness decreases. Increasing flow velocity, however, also reduces the residence time through the stack and the time available for ion transfer.

The energy consumed by electrodialysis comprises the energy required for ion transfer and the energy required for pumping. The energy required for ion transfer dominates because pumping pressures are minimal. The power required for ion transfer is by Ohm's Law:

$$P = VI$$

ED has been tailored for specific goals through the arrangement of membranes and the use of specialty membranes. ED has been used for decades to generate products from waste streams or saline solutions. Bipolar membranes have been used to produce hydrochloric acid (HCl) and sodium hydroxide (NaOH) from sodium chloride (NaCl) (Mazrou et al., 1998; Wilhelm et al., 2002).

Japan, Korea, and Taiwan use ED followed by evaporative crystallization to produce table salt from seawater (The Salt Industry Center of Japan 2009). In this application, monovalent selective membranes are used to separate divalent ions (Ca^{2+}, Mg^{2+}, SO_4^{2-}) from monovalent ions (Na^+, Cl^-). This serves two purposes. The content of divalent ions in the salt product is controlled and the membrane scaling potential by salts such as $CaSO_4$ is reduced. Alheritiere, Ernst, and Davis (1998) proposed the use of ED to produce magnesium sulfate and sodium chloride from magnesium chloride and sodium sulfate.

An innovation of ED, referred to as electrodialysis metathesis (EDM) was evaluated for concentrate treatment in this research. EDM is a recently patented process (U.S. Patents 7,083,730 and 7,459,088). The primary difference between EDM and ED or electrodialysis reversal (EDR) is an innovative arrangement of ion exchange membranes designed to separate concentrate into two streams of highly soluble salts.

A simplified schematic of the EDM process is shown in Figure 1.3. Compared with the ED repeating cell pair, EDM contains repeating cell sets comprising four membranes and four solution compartments. Each cell set has an anion exchange membrane (A), a cation exchange membrane (C), a monovalent selective anion exchange membrane (SA) and a monovalent selective cation exchange membrane (SC). Anions are pulled toward the anode and cations are pulled toward the cathode. Feed water is introduced to the diluate compartment between the anion (A) and cation (C) exchange membranes. Cations pass through the C membrane to concentrate 1 compartment, and anions pass through the A membrane to concentrate 2 compartment.

A sodium chloride solution is recirculated between membranes SC and SA. Chloride (Cl^-) passes through membrane SA to concentrate 2 and sodium (Na^+) passes through membrane SC to concentrate 1. Monovalent selective membranes (SA and SC) are used to prevent transfer of any divalent impurities the sodium chloride solution might contain.

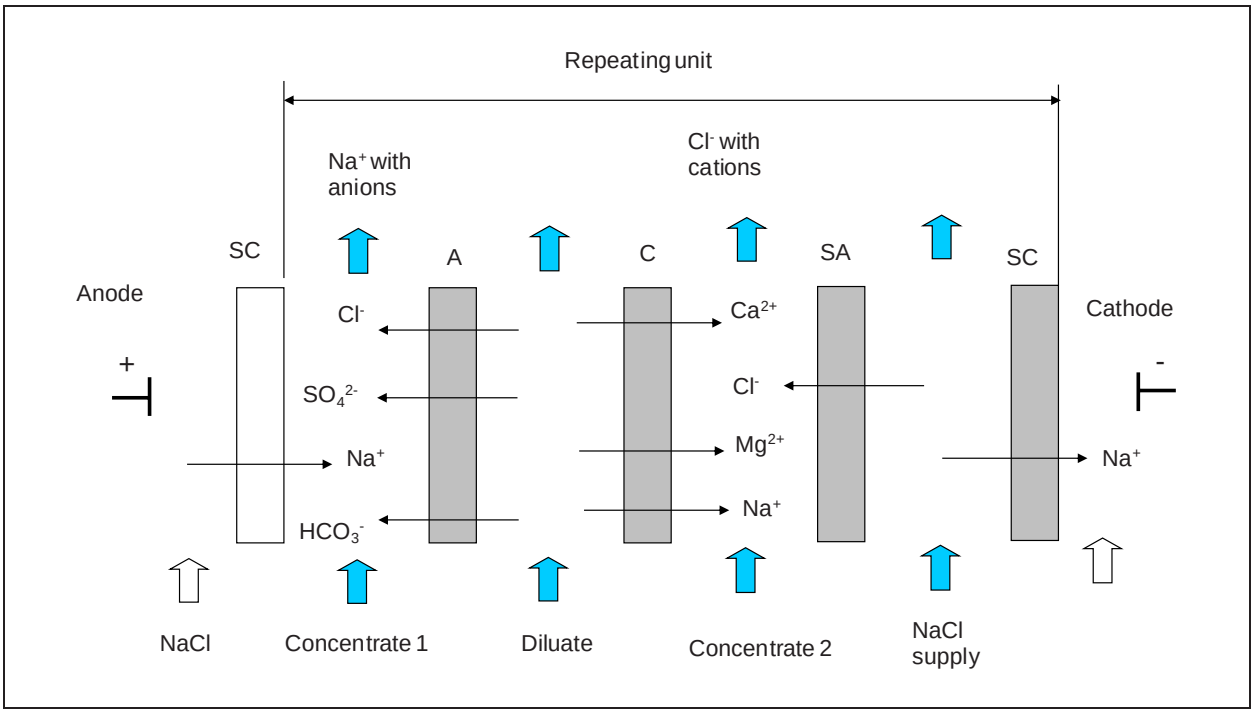

Figure 1.3 Electrodialysis metathesis cell schematic

This arrangement of cells causes the concentrate from the EDM process to be separated into two streams, one containing Na_2SO_4, HCO_3^-, and NaCl and the other containing $CaCl_2$, NaCl, and $MgCl_2$. The salts in these streams are significantly more soluble than the sulfate and carbonate salts that have the potential to precipitate in the single concentrate stream generated by ED or RO treating the same water. Consequently, recovery is not limited by the precipitation potential of sparingly soluble salts but rather by the transport of water from the diluate compartment to the concentrate compartments that occurs naturally.

Water transport from diluate to concentrate compartments occurs in electrodialysis by two mechanisms: (1) electroosmosis, the transport of water molecules associated with ions, and (2) osmosis driven by the concentration difference between the diluate concentrate streams. This loss of diluate determines recovery in EDM treatment. Water transport by electroosmosis is greater at lower diluate concentrations (Spiegler 1958). Transport by osmosis increases with osmotic pressure, i.e., as the concentration difference between the diluate and concentrate streams increases. Total water flux from osmosis and electroosmosis is relatively small, and, as discussed in Chapter 3, EDM recoveries in excess of 99 percent were observed in the pilot test.

Depending on water quality, there may be several options for managing concentrate from EDM. The two streams could be combined to precipitate product salts such as calcium carbonate and gypsum. The sodium chloride rich supernatant could be reused in the EDM process or used to regenerate MIEX.

Uncharged species such as silica are not significantly affected by electrodialysis and are therefore present in the product stream at the same concentration as in the feed stream. Consequently, an additional treatment process may be required for silica removal in some cases where EDM is used as pretreatment for secondary RO. Conversely, use of EDM as the sole secondary desalination process can obviate the need for silica removal.

Reverse Osmosis

Reverse osmosis (RO) is a pressure driven membrane separation process in which a semipermeable membrane allows the passage of water but rejects most dissolved salts. When two liquids of different salinity are separated by a semipermeable membrane there is a difference in chemical potential energy that causes water to diffuse from the fresh water side to the saline side. This diffusive transfer of water is called osmosis. The goal in RO desalination, however, is to force water to flow from the saline side to the fresh water side of the membrane to produce desalinated water. The system reaches osmotic equilibrium when the pressure differential between the two sides is equal to the difference in their chemical potentials. This pressure differential is referred to as the osmotic pressure of the system. The pressure that must be applied in RO desalination is the sum of the osmotic pressure and the losses resulting from flow through RO system.

The predominant type of RO membrane in use today is the spiral wound configuration. The spiral wound membrane is constructed of flat membrane sheets folded to form an envelope with a permeate channel between the membrane surfaces. Each envelope is connected to a central permeate tube and wound around it in a spiral. The membrane envelopes are separated by a thin (approximately 3 mm) mesh spacer called a feed spacer. Feed water is pumped through the feed spacer parallel to the membrane surface. A portion of the water diffuses through the membrane to become permeate and the remainder exits the membrane as a concentrate stream containing most of the dissolved solids originally present in the feed water. RO recovery is defined as the percentage of feed water recovered as permeate. As recovery increases, the volume of the concentrate stream decreases, and there is a proportional increase in rejected dissolved solids concentration. This increase in concentrations of inorganic and organic dissolved solids limits RO recovery of brackish water.

Thermal Desalination

Thermal processes have been used for decades to desalinate water, particularly in the Middle East where energy has been relatively inexpensive. Thermal desalination is accomplished by evaporating water, condensing the resulting steam, and recovering the condensate as high quality product water. Thermal desalination is a very energy intensive process due to the thermodynamic properties of water. Two types of mechanical vapor compression thermal desalination devices were used in the process evaluations for ZLD: brine concentrator and crystallizer.

The brine concentrator is a falling film evaporator with a sump at the bottom of its column and condensation tubes extending vertically above the sump. Feed water is heated and discharged to the sump. Vapor above the sump is drawn off and compressed in a vapor compressor. Heated water in the bottom of the sump is pumped to the top of the condensate tubes and allowed to fall down the inside of the tubes. Compressed vapor is discharged to the outside of the condensate tubes. The temperature of the compressed vapor is greater than that of the water inside the tubes, and heat exchange between the vapor and the water inside the tubes causes the vapor to condense on the outside of the tubes. This condensate is captured as product water.

Thermal desalination produces a high quality distillate, typically with TDS less than 10 mg/L. Recovery in the brine concentrator is limited by the scaling potential of the salts, and concentrations of TDS in the sump can reach 250,000 mg/L. Corrosion resistant and in some cases, highly specialized materials are required for construction of the brine concentrator to protect it against corrosion over its life span. Consequently, capital costs for brine concentrators are high.

Recovery in a brine concentrator treating brackish water RO concentrate is typically 95 to 98 percent. The remaining water is discharged from the sump as a highly saline concentrate.

The crystallizer is similar to the brine concentrator but is designed to treat higher TDS water. In a ZLD system with thermal desalination, concentrate from the brine concentrator would be treated in the crystallizer. Virtually all of the water would be recovered in the crystallizer, and the byproduct would be essentially dry salts.

Processes for Fluoride Treatment

Fluoride can be removed by adsorption, precipitation, membrane separation, and electrodialysis processes. The processes listed by USEPA as best technologies generally available (BTGA) are activated alumina (AA) and reverse osmosis (RO) (USEPA 2003).

AA for Fluoride Removal

The most commonly used adsorbent for fluoride removal is activated alumina. Adsorption of fluoride by AA is affected by pH, concentrations of competing anions such as hydroxide and sulfate, and initial fluoride concentrations. In contrast to ion exchange, AA has a high affinity for fluoride relative to other anions. Anions are preferred by AA in the following order:

$$OH^- > H_2AsO_4^- > Si(OH)_3O^- > F^- > HSeO_3^- > SO_4^{2-} > CrO_4^{2-} >> HCO_3^- > Cl^- > NO_3^- > Br^- > I^-$$

The optimal pH range for fluoride removal is between 5 and 6 (Choi and Chen 1979, Wu and Nitya 1979), but operation at pH > 6 may be desirable to prevent alumina from dissolving (Hao and Huang 1986). As pH or alkalinity increase, the capacity of AA to adsorb fluoride decreases due to increased competition from other anions (Bishop and Sansoucy 1978, Schoeman and McLeod 1987). The amount of fluoride adsorbed per unit of AA on a mass per mass basis increases with increasing initial fluoride concentration (Hao and Huang 1986, Bishop and Sansoucy 1978).

Bishop and Sansoucy (1978) evaluated fluoride removal with AA in a fluidized bed and noted two significant advantages relative to a downflow, gravity contactor. A higher adsorption capacity (mass per mass) was observed and attributed to more exposed AA surface area when the media was fluidized compared with packed in a bed. The second advantage was a higher loading rate in the fluidized bed because loading rate in the gravity bed was limited by headloss.

The adsorption-regeneration cycle for removal of fluoride with AA is as follows (Clifford, Matson, and Kennedy 1978):

Step 1
Acidification
The AA is first treated with acid to form acidic AA.

$$Alumina \cdot HOH + HCl \rightarrow Alumina \cdot HCl + HOH$$

Step 2
Adsorption
Fluoride ions displace the chloride ions and adsorb to the AA (provided pH is low enough to avoid competition from the more preferred hydroxide ions).

$$Alumina \cdot HCl + NaF \rightarrow Alumina \cdot HF + NaCl$$

Step 3
Regeneration
The AA is regenerated with caustic.

$$Alumina \cdot HF + 2NaOH \rightarrow Alumina \cdot NaOH + NaF$$

Step 4
Acidification
Step 1 is repeated to restore fluoride removal capacity.

$$Alumina \cdot NaOH + 2HCl \rightarrow Alumina \cdot HCl + NaCl + HOH$$

Alternatively, the feed water may be acidified to combine acidification and adsorption into one step.

$$Alumina \cdot NaOH + NaF + 2HCl \rightarrow Alumina \cdot HF + 2NaCl + HOH$$

Fluoride Removal by Precipitation With Calcium

Fluoride can be removed through precipitation of fluorite ($CaF_{2(s)}$) by introducing calcium to exceed the $CaF_{2(s)}$ solubility product ($K_{s0} = 10^{-10.3}$). In practice, however, the solubility product of fluorite often must be exceeded by several times before precipitation occurs, and it is difficult to reduce fluoride concentrations to levels that meet drinking water standards even with large doses of calcium.

$$CaF_{2(s)} \leftrightarrow Ca^{2+} + 2F^{-} \quad K_{s0} = 10^{-10.3}$$

A seeded precipitation approach, however, has been applied successfully to reduce fluoride concentrations to acceptable drinking water levels. A fixed bed of calcite has been used to achieve efficient fluoride removal without production of sludge (Yang et al., 1999; Reardon and Wang 2000). In this process, calcite is dissolved in the undersaturated feed water releasing calcium. The dissolved calcium creates supersaturation with respect to fluorite, and fluoride is removed by CaF_2 precipitation.

$$CaCO_{3(s)} \leftrightarrow Ca^{2+} + CO_3^{2-}$$
$$CaF_{2(s)} \leftrightarrow Ca^{2+} + 2F^{-}$$

Reardon and Wang (2000) suggested using two calcite beds in series. The objective was to remove fluoride in the first bed and to remove excess calcium in the second bed.

Turner, Binning, and Stipp (2005) demonstrated that fluoride removal in a calcite bed occurs not only by precipitation but also by adsorption of fluoride to the surface of the calcite particles. Fluoride removal was found to be dependent on pH and calcite surface area. Removal increased as pH decreased between pH 6 and 10, and removal increased as calcite surface area increased.

Fluidized bed crystallization employs calcite pellets in a fluidized bed to soften water. The process has been used for decades (Graveland, de Moel, and Oomen 1983) and is used for centralized softening throughout the Netherlands (Van der Veen and Graveland 1988). No studies of fluoride removal with fluidized bed crystallization were found in the literature, but it is logical that fluoride removal would occur by the same mechanisms as those responsible for fluoride removal in a fixed bed of calcite.

Zhang et al., (2005) evaluated coagulation with alum for fluoride removal. In this process, fluoride is removed by adsorption to precipitated $Al(OH)_{3(s)}$. Fluoride concentrations were reduced from 5 mg/L to less than 1 mg/L. The optimal pH for fluoride removal was found to be between 6 and 6.7, and an alum dose of approximately 50 mg/L was required for each 1 mg/L of fluoride removed.

Fluoride Removal by RO/NF Membranes

Fluoride is rejected by nanofiltration (NF) and RO membranes. An RO plant has been used for defluoridation in Finland for three years (Sehn 2008). Fluoride concentrations of 1.4 to 2.0 mg/L in the feed water are reduced to between 0.02 and 0.03 mg/L in the permeate. Tahaikt et al. (2007) evaluated two NF membranes for fluoride removal, one with a molecular weight cutoff (MWC) of 90 Da and the other with a MWC of 400 Da. Fluoride feed concentrations from 1.8 to 20 mg/L were tested. The 90 Da MWC membrane rejected virtually all of the fluoride at all feed concentrations. Permeate fluoride concentrations were less than 0.1 mg/L. Permeate fluoride concentrations for the 400 Da MWC membrane increased as the feed concentration increased. The permeate fluoride concentrations ranged from 0.9 mg/L at a feed concentration of 1.8 mg/L to 2.8 mg/L at a feed concentration of 20 mg/L.

RO or NF membranes are often determined to be the best solution for reducing salinity or for removing multiple contaminants with one process, but they generate a concentrate stream that must be managed. The cost for concentrate management can make other treatment options more economical than RO or NF when the treatment objective is removal of a single contaminant.

Fluoride Removal by Electrodialysis

Fluoride can be removed by electrodialysis (ED) and electrodialysis reversal (EDR). ED and EDR are membrane separation processes that use ion selective membranes. In contrast to RO and NF membranes, the driving force for ED/EDR is electric potential rather than pressure, and ions rather than water are transferred through the membranes.

Amor et al. (1998) evaluated fluoride removal in an ED system treating brackish groundwater with a TDS of 3000 mg/L. The fluoride concentration in the feed water was 3 mg/L. Product water fluoride concentrations were affected by the voltage applied to each ED cell. Product fluoride concentrations were 2.9 mg/L at 5 volts, 0.7 mg/L at 10 volts, and 0.21 mg/L at 15 volts.

WATER SOURCES EVALUATED

The water sources tested in this study were as follows:

Figure 1.4 Map of water sources tested

- Groundwater from the Tamiami aquifer treated at the Collier County North Regional Water Treatment Plant (CCNRWTP) with nanofiltration (NF) membranes, hereafter referred to as Tamiami groundwater (TGW).
- Lower Hawthorn aquifer groundwater treated at the CCNRWTP with RO membranes. This source is hereafter referred to as Lower Hawthorne groundwater (LHGW).
- Groundwater treated at the T. Mabry Carlton, Jr. Water Treatment Plant (TMCWTP) near Venice, Fl., with electrodialysis reversal (EDR), hereafter referred to as Carlton groundwater (CGW).
- Groundwater treated at the City of Ormond Beach Water Treatment Plant (OBWTP) with NF membranes, hereafter referred to as Ormond Beach groundwater (OBGW).
- Alafia River (AR) near Tampa treated at the Tampa Bay Regional Surface Water Treatment Plant (TBRSWTP).

The water sources evaluated in desktop studies were the following:

- St. Johns River (SJR) system water represented by water quality of Lake Monroe.
- Indian River Lagoon (IRL).

Locations of these sources are shown in Figure 1.4. Samples of each source used for testing were collected from the concentrate of the associated treatment plant except for the Alafia River. Finished water samples were collected at the TBRSWTP for evaluation of the Alafia River.

Table 1.1
Raw water data

Analyte	Units	TGW	LHGW	CGW	OBGW	AR	SJR	IR
Ca	mg/L	120	210	231	120	40	53	319
Mg	mg/L	21	200	114	15	12	22	1100
Na	mg/L	70	1400	54	65	30	158	8360
K	mg/L	6	67	4	3		7	324
Fe	mg/L	0.02	0.02	0	0.22		0.14	0.49
Mn	mg/L	0.003	0.003	0	0.01	0.01		0.01
Ba	mg/L	0.02	0.03	0.017	0.02	0.03	0.03	0.04
Sr	mg/L	0.68	16	13	0.5		1.5	7.6
Al	mg/L	0.05	0.05	0.17		0.28		0.54
Cl	mg/L	100	2800	97	130	27	285	13,600
SO_4	mg/L	50	730	722	250	80	90	2100
HCO_3	mg/L	378	207	166	329	109	55	148
NO_3	mg/L	>2.5	0.5	0	0.01	5		8.4
F	mg/L	0.4	2.2	1.4	0.19	10		0.15
SiO_2	mg/L	3.4	16	25	20	10	5	1.3
TDS	mg/L	560	5300	1412	630	270	750	28,700
TOC	mg/L	8.0	2.0	2.7	7.2	11	20	10.7
pH	SU	7.4	7.4	7.3	7.4	7.6	7.5	7.7

Average raw water data for each source tested are shown in Table 1.1. TOC concentrations ranged from 2.0 to 11.0 mg/L, and TDS ranged from 270 to 5300 mg/L. The treatment goal for the Alafia River was reduction of fluoride concentrations, which could exceed 10 mg/L. Although the TDS of the Alafia River was only 270 mg/L, RO is a best available technology (BAT) for removing fluoride. Unit conversion factors are given in Appendix A.

CHAPTER 2
METHODS AND MATERIALS

PRELIMINARY PROCESS ANALYSES

Preliminary process analyses were performed to provide a first estimate of concentrate treatment goals for each water source. Several antiscalant manufacturers have developed software programs specific to their products that can be used to project RO performance for a specific set of water quality data. One such program (Argo Analyzer by GE-Betz) was used to predict the effect of concentrate treatment on recovery in a secondary RO.

Scaling potential and recovery limits calculated with Argo Analyzer for each antiscalant product are based on thermodynamic relationships and empirical results from bench-, pilot-, and full-scale testing. To use this software, one enters RO feed water quality data and specifies pretreatment conditions including the type of antiscalant used and any pH adjustment. The output includes recommended maximum sustainable RO recovery, concentrate water quality values at the selected recovery, supersaturation of key salts such as $CaSO_4$, $BaSO_4$, SiO_2, CaF, and $SrSO_4$, recommended antiscalant dose, and identification of the recovery limiting salts.

The results of these analyses were used to estimate treatment goals for calcium, silica, and sulfate to avoid fouling secondary RO membranes with inorganic scalants. These results represented a starting point or a minimum level of treatment because organic fouling and interaction between organic compounds and cations were not included. Treatment goals identified in the preliminary analyses were used to guide the evaluation of concentrate treatment options.

TESTING

Bench- and pilot-scale tests were conducted with the TGW, LHGW, CGW, AR, and OBGW water sources.

Preliminary Testing

Bench-scale tests were conducted to evaluate and compare concentrate treatment options. The following processes were evaluated individually and in combination for treatment of primary concentrate:

- Chemical softening
- Fluidized bed crystallization
- MIEX
- Coagulation
- AA

Table 2.1
R1 milled limestone particle size distribution

Size	Percent passing
16 mesh (1190 µm)	100
20 mesh (840 µm)	92.6
30 mesh (590 µm)	70.3
100 mesh (150 µm)	7.3
120 mesh (125 µm)	6.5
140 mesh (105 µm)	5.8
200 mesh (75 µm)	5.1

Chemical Softening

Jar tests were conducted with concentrate samples to evaluate chemical softening for removal of calcium, sulfate, silica, and TOC. Softening was tested with caustic (NaOH) and soda ash (Na_2CO_3) or lime (CaO) and soda ash.

Concentrate samples were poured into 2-L jars and placed under a Phipps & Bird 6-paddle mixer. Chemicals were injected at the start of mixing, and the jars were mixed at 200 rpm for 30 seconds to simulate full-scale rapid mix. The jars were then mixed for 10 minutes each at 80, 60, and 50 rpm to simulate tapered flocculation. A 5-minute sedimentation period followed the last mixing period, after which samples were drawn from each jar and filtered through 1.0 µm pore glass fiber filters. Water quality analyses were conducted with the filtered samples.

Fluidized Bed Crystallization

Fluidized bed crystallization experiments were conducted with concentrate samples to evaluate removal of calcium, sulfate, silica, and TOC and with the AR sample to evaluate removal of fluoride. A 200 mL sample of concentrate was placed in a 500 mL beaker with 135 mL of R1 milled limestone (Mississippi Lime™). The material was 98.4 percent calcium carbonate by weight and had an apparent density of 56 lbs/ft^3. The size distribution is shown in Table 2.1.

Caustic was added to raise pH, and the beakers were mixed for 2 minutes at 200 rpm then allowed to settle for 5 minutes. The treated samples were filtered through 1.0 µm pore glass fiber filters, and water quality analyses were performed with the filtered samples.

Fluidized bed crystallization was evaluated for fluoride removal from AR samples. Alafia River raw water was spiked to a fluoride concentration of 24 mg/L. The test was conducted at two pH values, 6.2 and 8.2. A 200 mL volume of spiked sample was placed in a 500 mL beaker with 200 g of milled limestone. For the low pH test, no other chemicals were added. For the 8.2 pH test, NaOH was added to raise pH. The samples were mixed at 200 rpm with a contact time of 2 minutes. After settling for 5 minutes, the samples were filtered, and fluoride was field measured.

MIEX®

Two methods were used to test MIEX® for the TGW concentrate. In the first, bed volume treatment (BVT) rates were evaluated by contacting resin with a series of sample volumes,

compositing the treated samples, and measuring water quality in the composite sample. In the second method, the MIEX® resin was contacted with a single concentrate sample, and different doses of MIEX® were used to represent different BVTs. No difference was observed in results between the two methods, and the majority of MIEX® testing was conducted with the direct dose (second) method for simplicity.

For the composite method, a 2-L sample of concentrate was placed in beaker under the jar stirrer. In jars where pH adjustment was specified, NaOH was added to reach the desired pH. A 5 mL/L MIEX® resin dose was added to the jar, and the contents were mixed at 100 rpm for 15 minutes. After mixing, the sample was decanted to a 5-gallon bucket, and the MIEX® resin was retained in the beaker. The treated sample was analyzed for pH, UV254, and sulfate, and samples were collected for laboratory analyses of TOC and sulfate. This cycle represented 200-bed volume treatment with MIEX®.

A fresh 2-liter sample of concentrate was poured into the beaker containing the retained MIEX® resin, and the sample was mixed at 100 rpm for 15 minutes. At the end of mixing, the sample was decanted to the 5-gallon bucket, and the MIEX® resin again was retained in the beaker. The composite sample volume was stirred by hand, and samples were collected for water quality analyses from the composite sample volume. This represented 400 BVT.

This sequence of steps was repeated for 5 cycles. The composite samples thus analyzed represented 200, 400, 600, 800, and 1000 BVT.

In the direct dose method, a MIEX® dose was used in each jar that represented the prescribed BVT. For example, a 40 mL/L MIEX® dose was used to evaluate 25 BVT (1000mL/40mL = 25 bed volumes). As with the composite sample method, the samples were mixed at 100 rpm for 15 minutes. The samples were filtered, and UV254 was measured. Samples were collected for laboratory measurement of TOC and sulfate.

Coagulation With Ferric Chloride

Coagulation with ferric chloride was evaluated for removal of silica and TOC and for fluoride removal from the AR source. One-liter samples were mixed with ferric chloride for one minute at 200 rpm followed by three 10-minute mixing periods at 30, 20, and 12 rpm. The samples were allowed to settle for 5 minutes then filtered through 1.0 µm pore glass fiber filters. The filtered samples were field tested for UV absorbance, pH, and silica.

Activated Alumina

AA was tested for removal of silica, calcium, and fluoride. The AA material tested was DD-6, 28 × 30 mesh provided by GE. Isotherm tests were conducted to evaluate AA capacity. One-liter sample volumes were placed in jars with AA of different doses. The jars were mixed for 10 minutes then filtered through 1.0 µm pore glass fiber filters. The filtered samples were field tested for UV absorbance, pH, calcium, fluoride, and silica, and samples were collected for laboratory analysis of silica, calcium, fluoride, and TOC.

In the AA tests for fluoride removal, samples were spiked with sodium fluoride (ACS grade 99.9 percent purity) to evaluate treatment at different influent fluoride concentrations. Experiments were conducted to evaluate the effectiveness of regeneration of AA used to treat for fluoride. Virgin AA was tested as described above. The AA was retained and regenerated. The regeneration

protocol was 15 minutes of contact with a 0.1 N NaOH solution, rinse, 15 minutes of contact with a 0.1 N HCl solution, and rinse. Fluoride removal capacity of the AA media was evaluated through 4 regeneration cycles.

MIEX® Followed by Chemical Softening

MIEX® treatment followed by chemical softening was evaluated as a two-step process. In the first step, 2-L concentrate samples were placed in beakers. Three of the samples were dosed with 10 mL/L MIEX® (200 BVT), and three were dosed with 40 mL/L (50 BVT). The jars were mixed at 100 rpm for 15 minutes then allowed to settle. The three jars dosed with 10 mL/L MIEX® were decanted to create one composite 200 BVT sample, and the remaining three jars were combined to create one 50 BVT sample. Calcium, pH, and UV absorbance of each composite sample were measured.

For the softening step, three 1-L samples were poured into beakers from each MIEX®-treated composite sample. One jar from each set received the same doses of NaOH and Na_2CO_3 dose to evaluate the effect of TOC removal on softening. The jars were mixed, settled, and filtered as described previously in the chemical softening test method. The filtered samples were analyzed for calcium, silica, and UV absorbance.

Coagulation With Ferric Chloride Followed by Chemical Softening

Ferric coagulation followed by chemical softening was also evaluated as a two-step process. In the first step, 2-L concentrate samples were placed in beakers with ferric chloride ($FeCl_3$) doses ranging from 50 to 800 mg/L. Caustic (NaOH) was added to maintain pH in the optimum range for ferric hydroxide precipitation and TOC removal. The jars were mixed for 1 minute at 200 rpm, 10 minutes at 60 rpm, 10 minutes at 20 rpm, and 10 minutes at 12 rpm before being allowed to settle for 5 minutes. Approximately 100 mL of the settled sample was filtered through 1.0-µm-pore glass fiber filters and analyzed for silica and UV absorbance. The remaining sample was retained for the chemical softening test.

In the second step to evaluate chemical softening, one liter of settled sample was decanted from each jar to another beaker. The samples were dosed with NaOH and Na_2CO_3. The jars were mixed, settled, and filtered as described previously. The filtered samples were analyzed for calcium, silica, and UV absorbance.

Pilot-Scale Testing

The following processes were evaluated at pilot-scale:

- EDM
- MIEX® followed by EDM
- AA
- Calcite bed

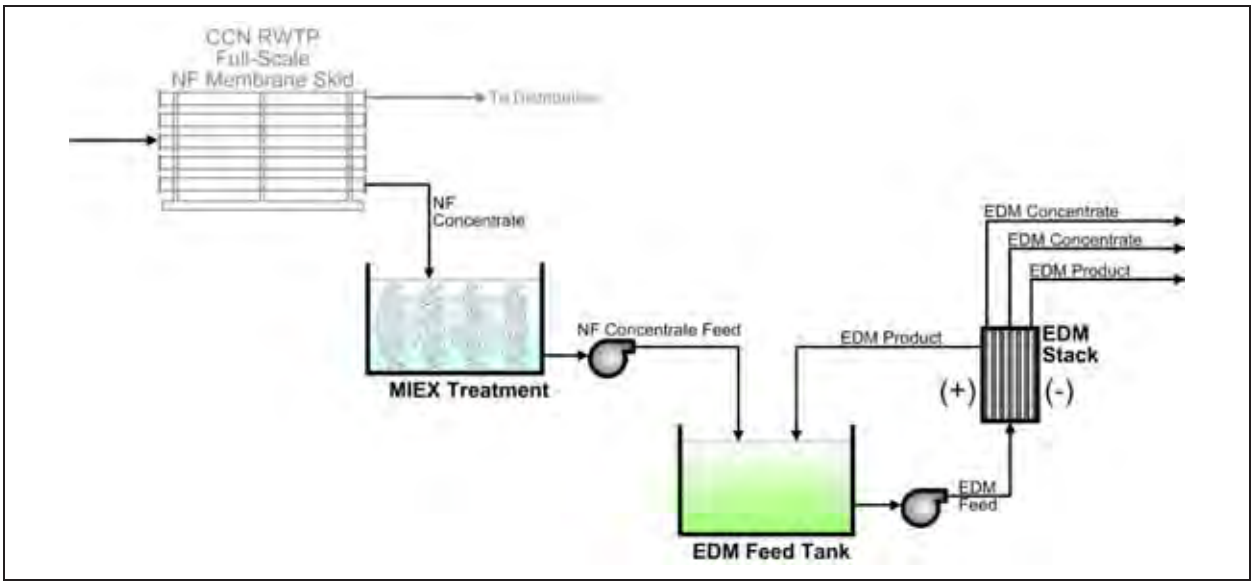

Figure 2.1 EDM pilot skid

EDM

Each of the concentrate samples was tested with EDM, and the typical arrangement for EDM pilot testing is shown in Figure 2.1. MIEX® treatment preceded EDM for the two sources with high TOC concentrations (TGW and OBGW).

The EDM pilot skid comprised an EDM stack containing five repeating cell sets (as shown previously in Figure 1.3) and feed tanks and pumps for the diluate, concentrate, NaCl, and Na_2SO_4 solutions. With the membrane arrangement shown in Figure 1.3, sodium ions and sulfate ions are removed from the electrode rinse solution through the cation-exchange membrane next to the anode and the anion-exchange membrane next to the cathode. Those ions are replaced by periodic addition of Na_2SO_4 crystals to the electrode rinse solution tank.

All solutions were recirculated through the stack. The two concentrate streams were bled periodically, and these volumes were measured to calculate stack recovery. Salt solutions were added to the NaCl and Na_2SO_4 feed tanks periodically to maintain concentrations in the NaCl supply and Na_2SO_4 electrode rinse. Concentrate was pumped from the holding tank to the EDM feed tank. The ratio of concentrate flow to EDM feed flow was controlled to simulate different stages of an EDM treatment train. Flow equal to the flow from the concentrate holding tank was bled continuously from the EDM feed tank.

The components of the EDM stack are described in Table 2.2. Each solution compartment was 10 cm wide by 20 cm long, so the active membrane area for each cell was 200 cm^2. The ion selective membranes were NEOSEPTA® by the Tokuyama Corporation. Each cell set contained a CMX (cation selective), CMS (monovalent cation selective), AMX (anion selective), and ACS (monovalent anion selective) membrane. Different membranes were selected for the end cell adjacent to each electrode for greater durability. The stack contained a CMB membrane at the anode and an AHA membrane at the cathode. The anode was a titanium plate coated with platinum, and the cathode was stainless steel.

Table 2.2
EDM stack description

Component	Description
Cationic membranes	5 CMX 5 CMS
Anionic membranes	5 AMX 5 ACS
End membranes	
• anode	CMB
• cathode	AHA
Active membrane area per cell	200 cm^2
Total active membrane area	0.1 m^2
Anode	Ti/Pt
Cathode	Stainless steel

The EDM unit contained rotameters and pressure sensors on the feed, concentrate, and electrolyte streams. All flows and pressures were recorded regularly. Concentrate flow from the holding tank to the EDM feed tank was measured volumetrically with a graduated cylinder and a stopwatch. Voltage and current were displayed continuously on the EDM control panel, and these measurements were recorded regularly.

Conductivity was measured regularly in the EDM feed, NaCl, Na_2SO_4, and concentrate tanks and in the concentrate holding tank typically at 30 minute intervals using a hand held conductivity meter. Samples were collected periodically from each stream for laboratory analyses.

MIEX® Followed by EDM

Two water sources (TGW and OBGW) were treated with MIEX® for TOC removal ahead of EDM. MIEX® treatment was conducted in batch mode. A 50-gallon volume of concentrate was mixed with a 25 BVT MIEX® dose for 15 minutes then allowed to settle. The settled water was pumped through a 1-µm cloth bag filter into the concentrate holding tank. The MIEX® treated concentrate was pumped with a diaphragm pump to the EDM diluate feed tank. Samples were collected of the concentrate before and after MIEX® treatment for analyses of TOC and ultraviolet absorption (UVA). The MIEX® treated concentrate was pumped from the concentrate holding tank to the EDM feed tank as previously described.

AA Column

AA was tested for removal of fluoride from the AR source in a 2.54 cm diameter pilot column. The column was loaded to a bed depth of 64 cm with DD-6, 28 × 30 mesh AA. The bed volume was 325 mL. AR water was spiked to a fluoride concentration of 6.2 mg/L, and pH in the sample was adjusted to 6.2. The spiked sample was pumped to the top of the AA bed at an average flow rate of 42 mL per minute. The average empty bed contact time (EBCT) was 7.8 minutes. Samples were collected at 30 minute intervals for fluoride measurement.

Calcite Column

Calcite was tested for removal of fluoride from the AR source in the same 2.54 cm diameter pilot column used in the AA test. Two sections of column were used in series to achieve a longer EBCT. Column A had a 66 cm bed depth and a 335 mL bed volume, and column B had a 64 cm bed depth and a 322 mL bed volume. Total bed volume of the columns was 656 mL. Each column was operated in downflow mode with an average flow of 41 mL per minute. The average EBCT was 7.8 minutes. Two experiments were conducted. In the first, fluoride was spiked to 3.9 mg/L, and pH was 6.97. In the second experiment, fluoride was 5.8 mg/L, and pH was 4.2. Samples were collected at 30 minute intervals for fluoride analysis.

WATER QUALITY ANALYSES

Several water characteristics were field measured during bench- and pilot-scale testing to obtain immediate results. Calcium was measured using the EDTA Titrimetric Method, Standard Method 3500-Ca B. Silica was measured with HACH method 8185, the silicomolybdate method. UV254 was measured with a Trojan P254C UV spectrometer. Sulfate was measured with HACH method 8051. Conductivity and pH were measured with probes. Fluoride was measured with a fluoride ion selective electrode.

Fluoride concentrations were field-measured with a fluoride ion selective electrode (Oakton model ISE fluoride electrode) and a mV meter (Oakton model Acorn pH 6) using the two-point calibration method. Two fluoride standards were prepared, 0.2 mg/L and 2 mg/L. The standard concentrations were selected to bracket the range of fluoride concentrations expected during testing. The potential of each standard was measured with the fluoride probe. A linear calibration slope was calculated as

$$s = \frac{E_1 - E_2}{C_1 - C_2}$$

where E_1 and E_2 are the potentials measured in standards 1 and 2, and C_1 and C_2 are the fluoride concentrations in standards 1 and 2. The potential of the sample was then measured, and the difference in potential between the sample and one of the standards was calculated as follows where E_X is the potential of the sample and E_1 is the potential of either of the standards:

$$\Delta E = E_X - E_1$$

The fluoride concentration in the sample, C_X, was calculated as

$$C_X = C_1 \times 10^{\frac{\Delta E}{s}}$$

CHAPTER 3
RESULTS AND DISCUSSION

PRELIMINARY ANALYSES

Preliminary analyses were conducted to evaluate treatment goals and select candidate treatment processes for each of the five water sources tested.

Water Quality Data

Typical water quality data for the five sources tested are shown in Table 3.1. The TGW, LHGW, CGW, and OBGW samples were collected from the existing RO, nanofiltration (NF), or EDR units at each plant. The AR water was a finished water sample from the TBWRSWTP. Desalination is not practiced at this plant, but RO is being considered for fluoride removal.

Evaluation of Treatment Goals

Treatment goals for each concentrate source depended on the type of secondary desalination process considered, RO or EDM. Treatment to reduce the membrane fouling potentials of TOC, calcium sulfate, and silica would be required ahead of secondary RO. Only TOC removal would be required for concentrate treatment ahead of secondary desalination with EDM because calcium and sulfate are separated into two concentrate streams within the EDM process and silica passes through the EDM stack unchanged.

The foulants that would limit recovery in secondary RO are shown for each water source in Table 3.2.

The primary treatment objective for the Alafia River water investigated in this project was fluoride removal. Fluoride concentrations as high as 10 mg/L have been observed, and the target for fluoride concentrations in the finished water is 1.5 mg/L. RO is a BAT for fluoride removal, but there are alternatives that do not involve desalination. The feasibility of RO for removal of a single contaminant with ZLD concentrate management was evaluated and compared with the following treatment alternatives: AA, fluidized bed crystallization, and calcite bed contactor.

Development of Treatment Options

Options for treating concentrate to reduce the membrane fouling potential of TOC, calcium sulfate, and silica are listed in Table 3.3. Calcium can be removed by softening, fluidized bed crystallization, or AA. EDM removes calcium and sulfate, and therefore has a dual effect on calcium sulfate precipitation potential. TOC can be removed by coagulation with alum or ferric salts, ion exchange (IX), or MIEX®. Silica can be removed by AA, coagulation, softening, or fluidized bed crystallization.

Three ZLD treatment system options (Table 3.4) were formulated from the treatment goals and list of viable treatment processes. Each ZLD option contained one or more process option for each of the three treatment steps (concentrate treatment, secondary desalination, and evaporation).

Table 3.1
Typical water quality data for sources tested (mg/L except pH (SU))

Analyte	TGW NF Concentrate	LHGW RO Concentrate	CGW EDR Concentrate	OBGW NF Concentrate	AR Finished Water
Ca	700	400	775	680	75
Mg	150	460	315	86	10
Na	250	4600	115	340	74
K	13	240	10	13	
Ba	0.14	0.07	0.5	0.09	0.008
Sr	4	18	0.06	3.1	
Cl	210	7300	575	750	100
SO_4	2300	3200	2300	1600	174
HCO_3	90	6	94	243	75
F	2	8	2	0.8	0.7
SiO_2	6	70	24	110	10
TDS	3800	16,000	4470	3900	388
TOC	50	9.6	4.7	46	2.3
pH	5.6	5.1	7.1	7.7	7.6

Table 3.2
Contaminants in the concentrate that would limit recovery by secondary RO

TGW NF Concentrate	LHGW RO Concentrate	CGW EDR Concentrate	OBGW NF Concentrate	AR Finished Water
$CaSO_4$ TOC	$CaSO_4$ SiO_2	$CaSO_4$ SiO_2	$CaSO_4$ TOC SiO_2	$CaSO_4$ SiO_2

Table 3.3
Treatment options to reduce the fouling potential of $CaSO_4$, TOC, and SiO_2

Foulant	Treatment options
$CaSO_4$	Softening Fluidized bed crystallization EDM Activated alumina (AA)
TOC	Coagulation Ion exchange (IX) Magnetic ion exchange (MIEX®)
SiO_2	AA Coagulation Softening Fluidized bed crystallization

Table 3.4
ZLD treatment systems evaluated

ZLD treatment system	Concentrate treatment	Secondary desalination	Evaporation
1	MIEX® or coagulation + Softening or FBC + Coagulation or AA	RO	Thermal
2	MIEX® + Coagulation or AA + EDM	RO	Thermal
3	MIEX®	EDM	Thermal

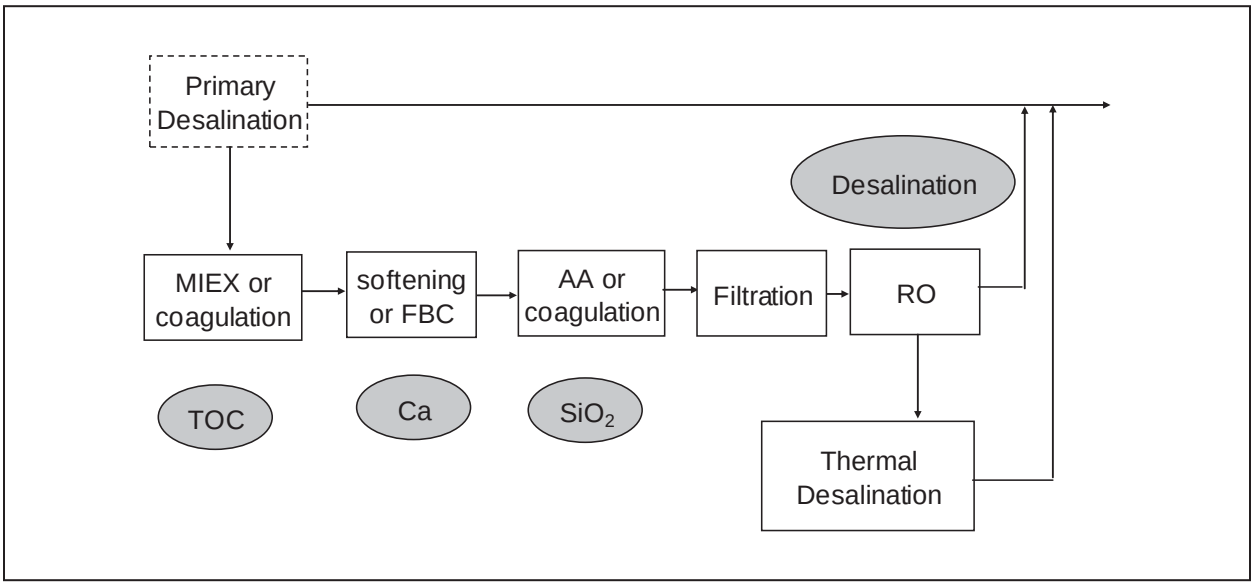

Figure 3.1 Option 1—coagulation/softening pretreatment with secondary RO

The first treatment option is illustrated in Figure 3.1. The concentrate treatment step comprises three processes: MIEX® or coagulation for TOC removal, softening or FBC for calcium removal, and coagulation or AA for silica removal. The treated concentrate is desalinated in the secondary RO, and concentrate from the secondary RO is treated with thermal desalination.

The second treatment option is shown in Figure 3.2. Concentrate is treated with MIEX® for TOC removal, EDM to remove calcium and sulfate, and coagulation or AA to remove silica. The treated concentrate is desalinated in the secondary RO, and concentrates from EDM and the secondary RO are treated with thermal desalination.

The third option is shown in Figure 3.3. EDM is used for secondary desalination, and the only concentrate treatment required ahead of EDM is MIEX® for TOC removal. Reduction of calcium sulfate fouling potential is not required, because EDM separates calcium and sulfate

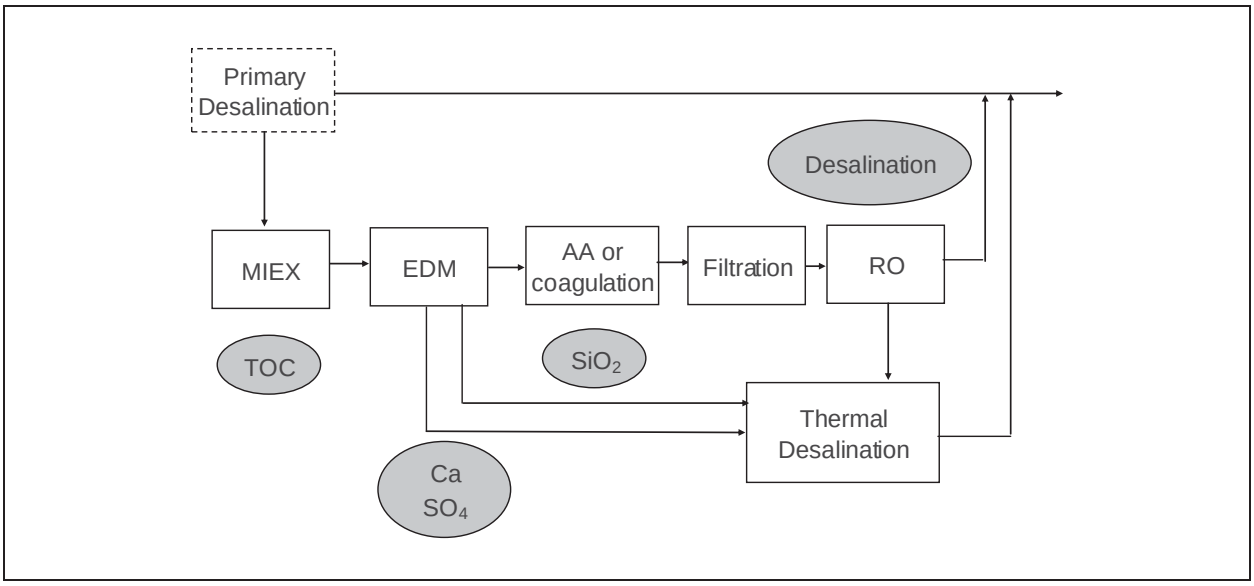

Figure 3.2 Option 2—EDM pretreatment with secondary RO

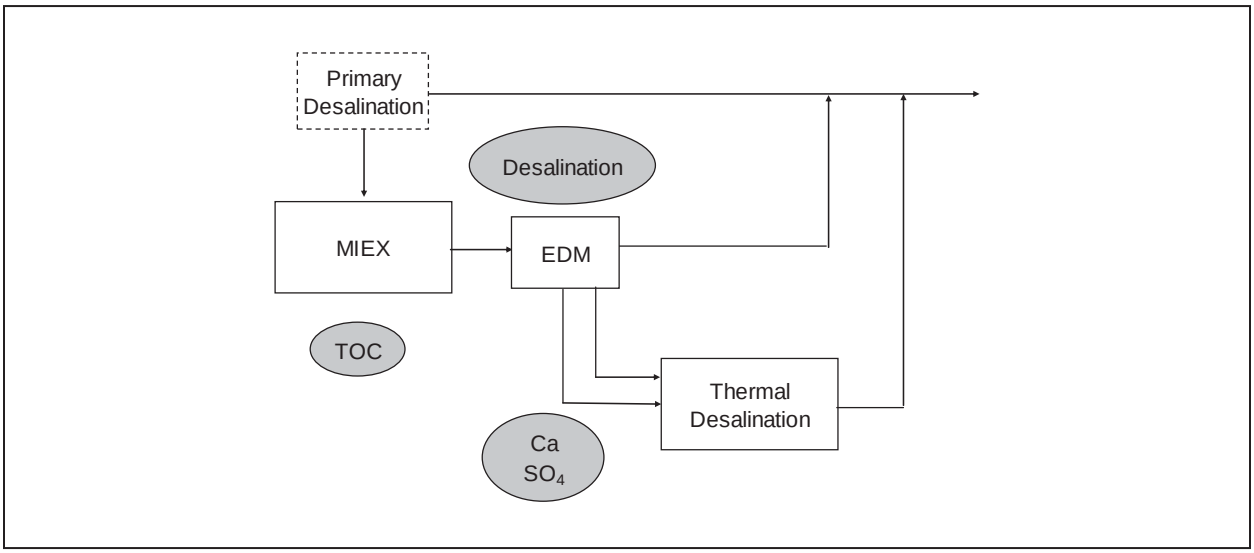

Figure 3.3 Option 3—EDM used for secondary desalination

into separate concentrate streams. Silica removal is not required, because silica molecules are uncharged and, therefore, exit EDM at the influent concentration. Concentrate from the EDM is treated with thermal desalination.

Alternatives to RO for fluoride removal from the Alafia River source were also investigated to provide a basis for comparison to desalination with ZLD. The treatment alternatives for fluoride removal tested at bench- or pilot-scale were fluidized bed crystallization, AA, and calcite bed contactor.

Table 3.5
Bench-scale testing matrix

	TGW NF concentrate	LHGW RO concentrate	CGW EDR concentrate	OBGW NF concentrate	AR finished water
Chemical softening (CS)	X	X	X	X	
FBC	X	X	X		X
MIEX	X			X	
MIEX + CS	X				
Coagulation	X	X		X	
Coagulation + CS	X				
AA		X	X	X	X
Calcite bed contactor					X
EDM	X				

PRELIMINARY TEST RESULTS

The following tests were conducted to evaluate the ZLD treatment options formulated in the preliminary analyses.

- Chemical softening
- Fluidized bed crystallization
- MIEX®
- MIEX® followed by chemical softening
- Coagulation with ferric chloride
- Coagulation with ferric chloride followed by chemical softening
- AA adsorption
- Calcite bed contactor

The matrix of treatment processes evaluated is shown in Table 3.5. All tests were conducted at bench-scale with the exception of EDM, which was conducted at pilot-scale.

Chemical Softening

Jar tests were conducted to evaluate chemical softening for removal of calcium, sulfate, and TOC on three of the water sources for the ZLD treatment option shown in Figure 3.1. In general, high chemical doses were required, and MIEX or coagulation still would be required for TOC removal for the high organic sources. Results of chemical softening jar tests for each water source are discussed below followed by a summary of all results.

TGW Chemical Softening Results

Results for caustic/soda ash softening of the TGW groundwater are shown in Figure 3.4. A titration experiment indicated a caustic (NaOH) dose of 400 mg/L was sufficient to raise the pH

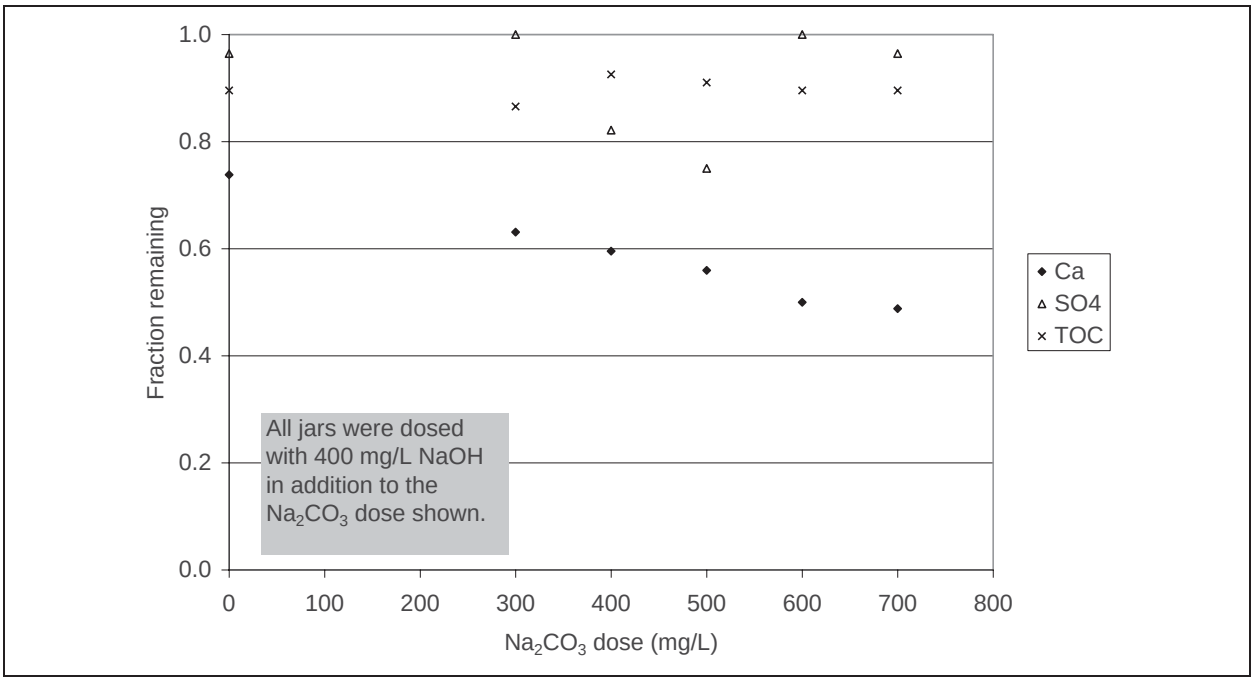

Figure 3.4 Jar test results for NaOH/soda ash softening of TGW concentrate

of the concentrate to 10. Soda ash was required because the concentrate contained a high percentage of noncarbonated hardness. A series of jars were tested each containing 400 mg/L NaOH and various doses of soda ash (Na_2CO_3). Calcium fraction remaining was about 0.7 without soda ash and decreased in proportion to soda ash dose to 0.5 fraction remaining in the jar with a 700 mg/L Na_2CO_3. Little to no sulfate removal was observed. TOC removal was consistently around 10 percent regardless of soda ash dose or calcium removal.

Jar tests results using lime and soda ash to soften TGW concentrate are shown in Figure 3.5. Calcium removal increased in proportion to soda ash dose. Calcium fraction remaining was 0.7 in the jar with 500 mg/L lime and 600 mg/L soda ash. TOC removal was around 15 percent, slightly greater than with NaOH. Sulfate removal was 7 percent for all soda ash doses.

Projected recoveries for secondary RO treatment of TGW concentrate are shown with soda ash doses in Figure 3.6. Recoveries projected for secondary RO were limited to less than 65 percent by calcium sulfate precipitation potential at the chemical doses evaluated.

CGW Chemical Softening Results

Jar test results for chemical softening with CGW concentrate are shown in Table 3.6 and Figures 3.7 and 3.8. Caustic and soda ash were used in the tests. The base dose shown for each jar is the sum of the NaOH and Na_2CO_3 doses. A soda ash dose of 1600 mg/L was required to reach a projected secondary RO recovery of 70 percent.

OBGW Chemical Softening Results

Jar test results for chemical softening with OBGW concentrate are shown in Figure 3.9. Base dose is the sum of NaOH and Na_2CO_3 doses. NaOH doses ranged from 640 to 800 mg/L, and

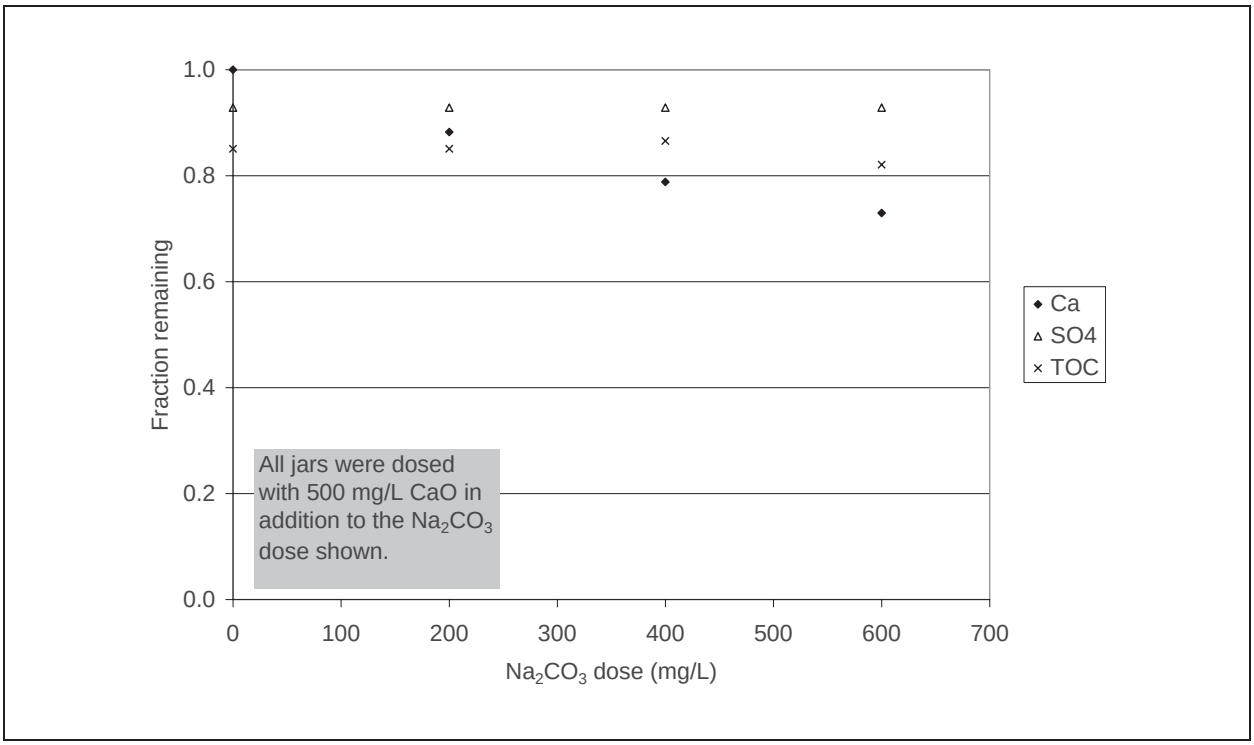

Figure 3.5 Jar test results for lime/soda ash softening of TGW concentrate

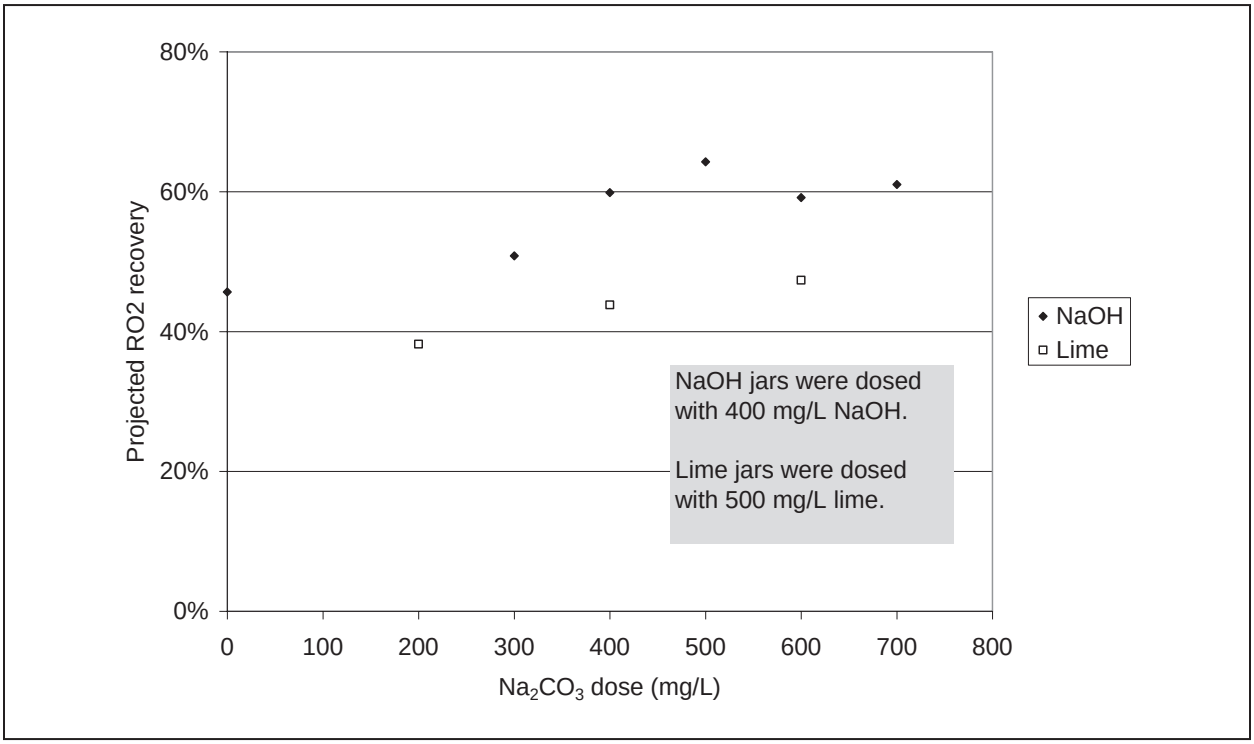

Figure 3.6 TGW projected secondary RO recovery after chemical softening

Table 3.6
CGW chemical softening jar test results

NaOH dose (mg/L)	Na_2CO_3 dose (mg/L)	Base dose (meq/L)	pH	Projected secondary RO recovery
40	200	4.7	9.6	41%
40	600	12.1	9.6	50%
40	1000	19.5	9.5	57%
80	200	5.7	9.9	45%
80	600	13.1	9.8	51%
80	1000	20.5	9.7	59%
100	200	6.2	9.8	45%
100	600	13.6	9.7	53%
100	1000	21.0	9.7	60%
120	200	6.7	9.9	45%
120	600	14.1	9.8	53%
120	1000	21.5	9.9	61%
40	1600	30.6	9.6	73%
80	1600	31.6	9.7	73%
120	1600	32.6	9.9	72%
200	600	16.1	10.2	55%
200	1000	23.5	10.1	60%
200	1600	34.6	10.2	72%

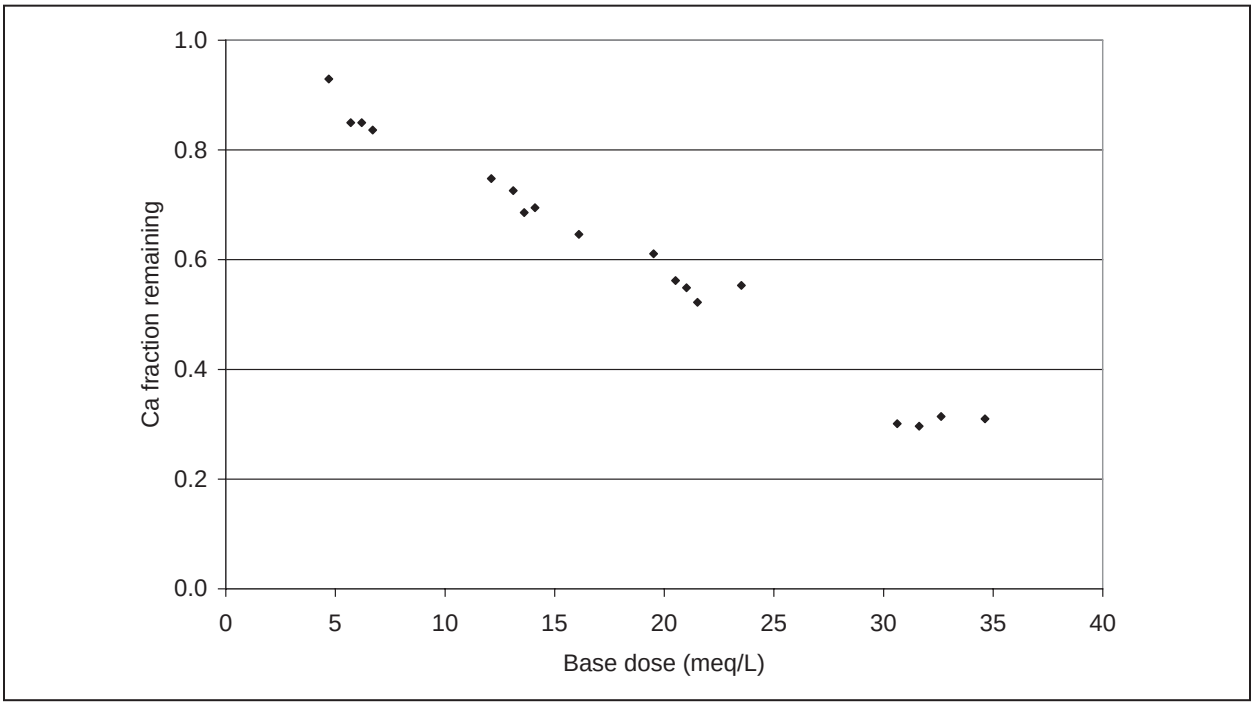

Figure 3.7 CGW—chemical softening jar test results

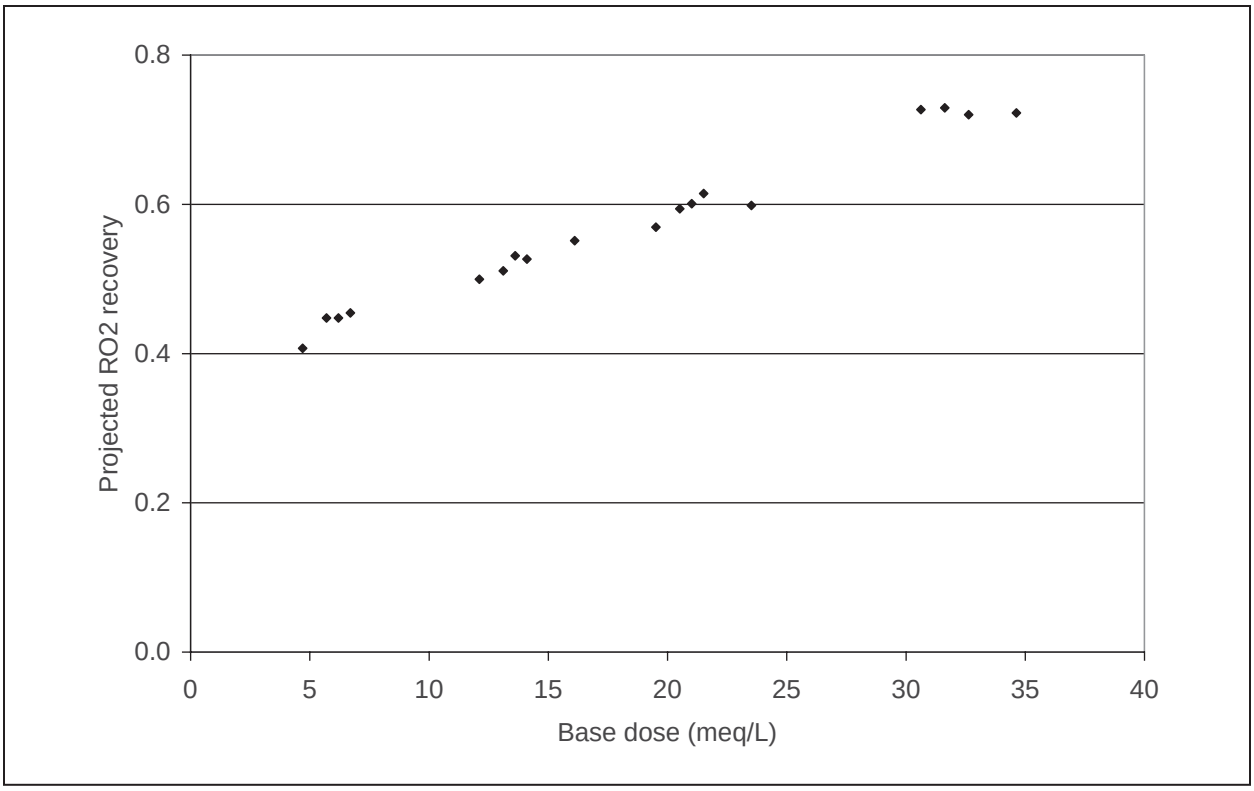

Figure 3.8 CGW—projected secondary RO recovery after chemical softening

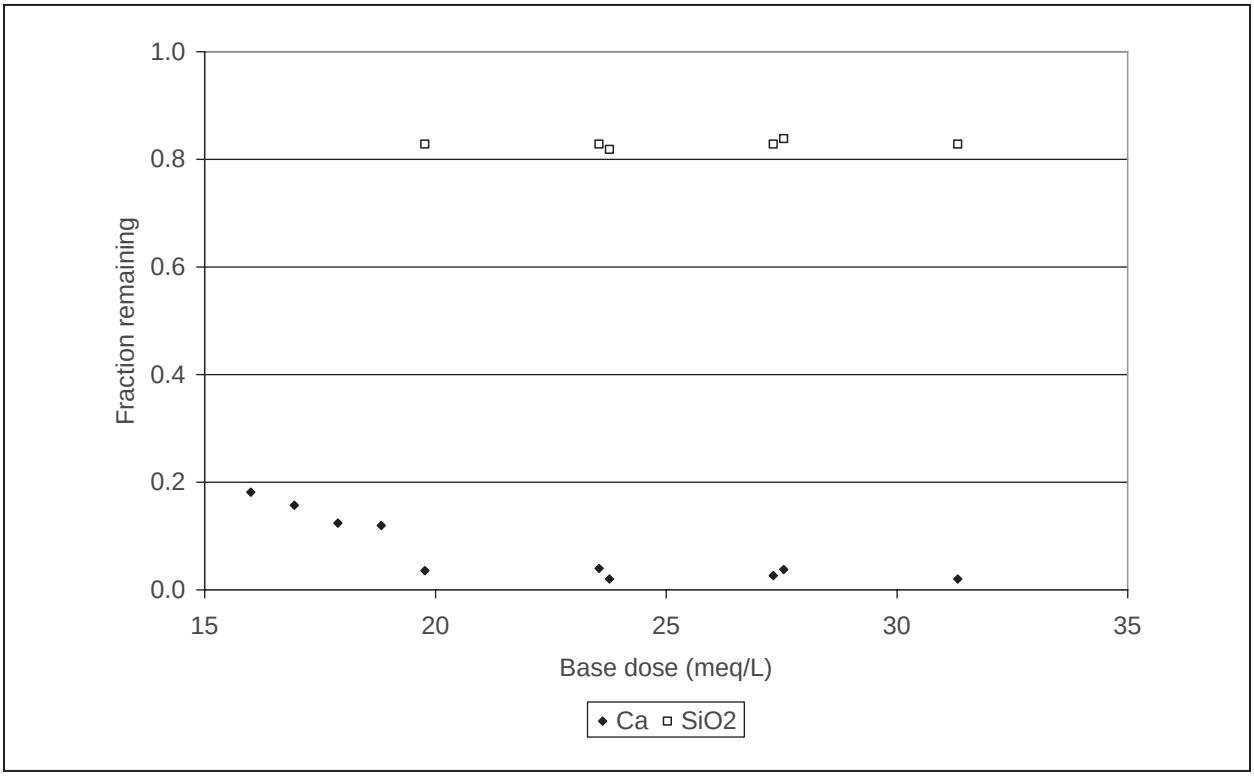

Figure 3.9 OBGW—chemical softening jar test results

Table 3.7
Summary of chemical softening jar test results

Sample	NaOH dose (mg/L)	Na_2CO_3 dose (mg/L)	Projected recovery secondary RO	Comments
TGW concentrate	400	500	62%	Additional process needed for TOC removal
CGW concentrate	80	1600	73%	
OBGW concentrate	640	100	90%	Additional processes needed for TOC and SiO_2 removal

Na_2CO_3 ranged from 100 to 1200 mg/L. Most of the calcium was removed, but only 20 percent of silica was removed because magnesium concentrations in this water were relatively low. Calcium sulfate precipitation potential was reduced sufficiently to achieve 90 percent recovery in secondary RO, but projected secondary RO recovery was limited to 50 percent by silica. Consequently, another process such as AA or coagulation with a metal salt would be required for silica removal.

Summary of Chemical Softening Results

Jar test results for chemical softening are summarized in Table 3.7. Modest secondary RO recoveries were projected for two of the sources, and chemical doses were high. Calcium removal was sufficient for 90 percent recovery in secondary RO for the OBGW concentrate, but two additional processes would be required, one for TOC and one for SiO_2, to achieve this recovery. A further disadvantage of chemical softening would be the need to manage large quantities of softening sludge.

Fluidized Bed Crystallization

Fluidized bed crystallization jar tests were conducted to evaluate FBC as an alternative to chemical softening in the ZLD Option 1. FBC was also evaluated for fluoride removal from the AR finished water.

TGW FBC Results

FBC jar test results for the TGW concentrate are shown in Figure 3.10. NaOH doses of 160 to 480 mg/L were tested without soda ash. Calcium removal ranged from 10 percent at 150 mg/L NaOH to 47 percent at a 480 mg/L NaOH. UVA reduction was about 20 percent at a NaOH dose of 150 mg/L, decreased to a minimum of 5 percent at 300 mg/L NaOH, and increased to 10 percent reduction at a NaOH dose of 500 mg/L. The parabolic shape of the dose response curve could be attributable to offsetting effects of pH and calcium removal on UVA. As pH increases, TOC becomes less hydrophobic and more difficult to remove, but calcium removal increases, favoring greater TOC removal.

Projected recovery for the secondary RO is plotted against caustic dose for the fluidized bed crystallization data in Figure 3.11. Projected recoveries for secondary RO were less than

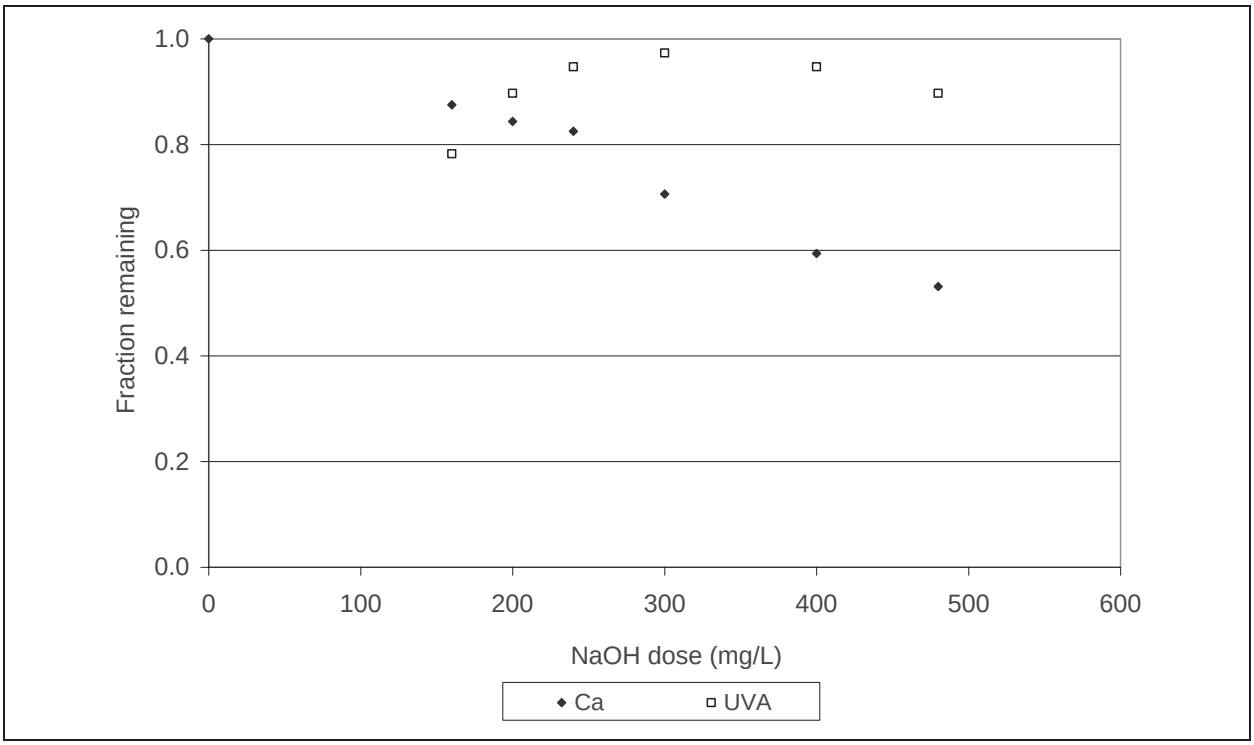

Figure 3.10 TGW fluidized bed crystallization jar test

70 percent. Comparing results for chemical softening with those for fluidized bed crystallization, greater chemical doses were required for calcium removal in the chemical softening test than in the fluidized bed crystallization test (Figure 3.12).

LHGW FBC Results

Jar tests were conducted to evaluate fluidized bed crystallization for removal of calcium and silica from LHGW concentrate (Figures 3.13 and 3.14). Calcium concentrations were reduced by approximately 50 percent with a NaOH dose of 140 mg/L, but calcium removal did not increase appreciably with increased NaOH doses because the concentrate contained insufficient carbonate for further precipitation of calcium carbonate. Silica removal, however, did increase as NaOH dose increased, particularly at pH greater than 9.5, due to magnesium hydroxide precipitation. Recovery projected for secondary RO was 70 percent at a NaOH dose of 260 mg/L.

A second set of jar tests was conducted in which Na_2CO_3 was added to provide additional carbonate. The NaOH dose was held at 140 mg/L and three Na_2CO_3 doses were evaluated, 250, 500, and 1000 mg/L. Calcium removal increased from 57 percent at 250 mg/L Na_2CO_3 to 78 percent at 1000 mg/L Na_2CO_3, and projected secondary RO recovery increased from 75 to 81 percent.

Although almost 90 percent silica removal was observed at the highest NaOH dose, operation of a fluidized bed crystallizer at high pH is not recommended because instantaneous nucleation of calcium carbonate precipitates would occur in lieu of crystal growth. This might be undesirable because these smaller precipitates have lower settling velocities and can be carried out of the fluidized bed crystallizer with the supernatant. Consequently, another process or addition of aluminum salt with the FBC likely would be required for silica removal.

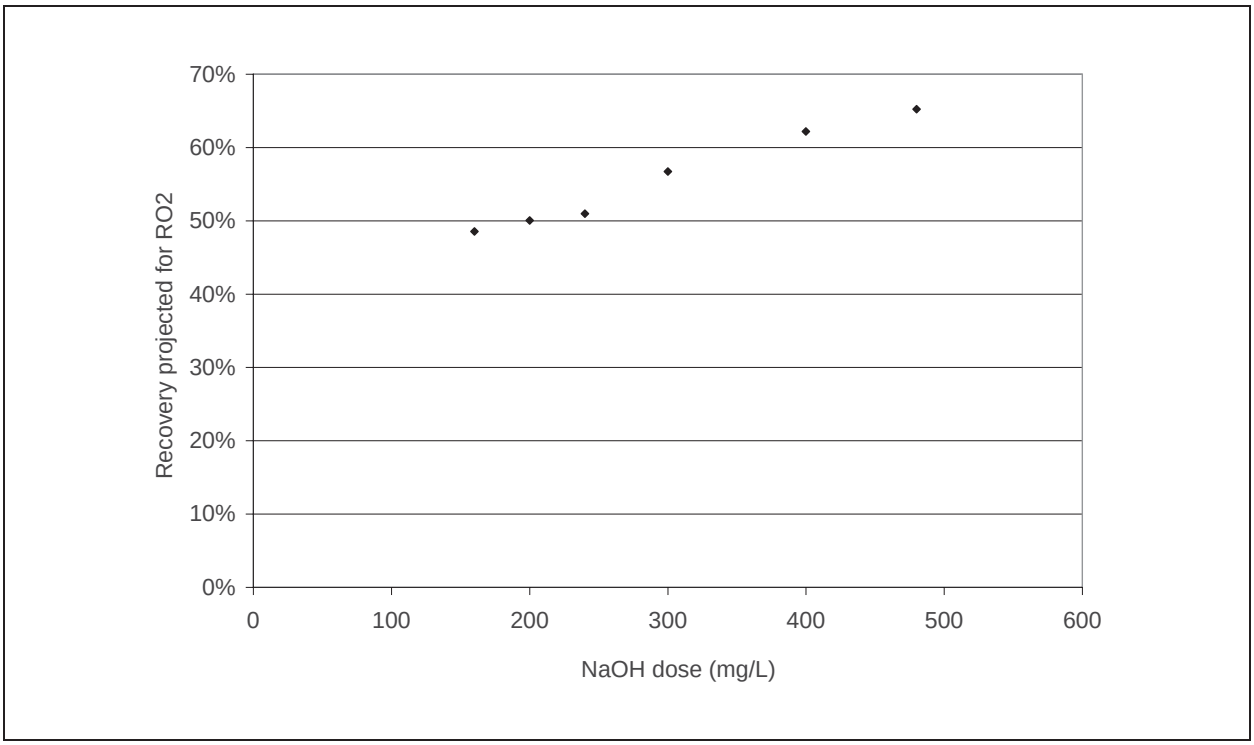

Figure 3.11 TGW projected secondary RO recovery after fluidized bed crystallization

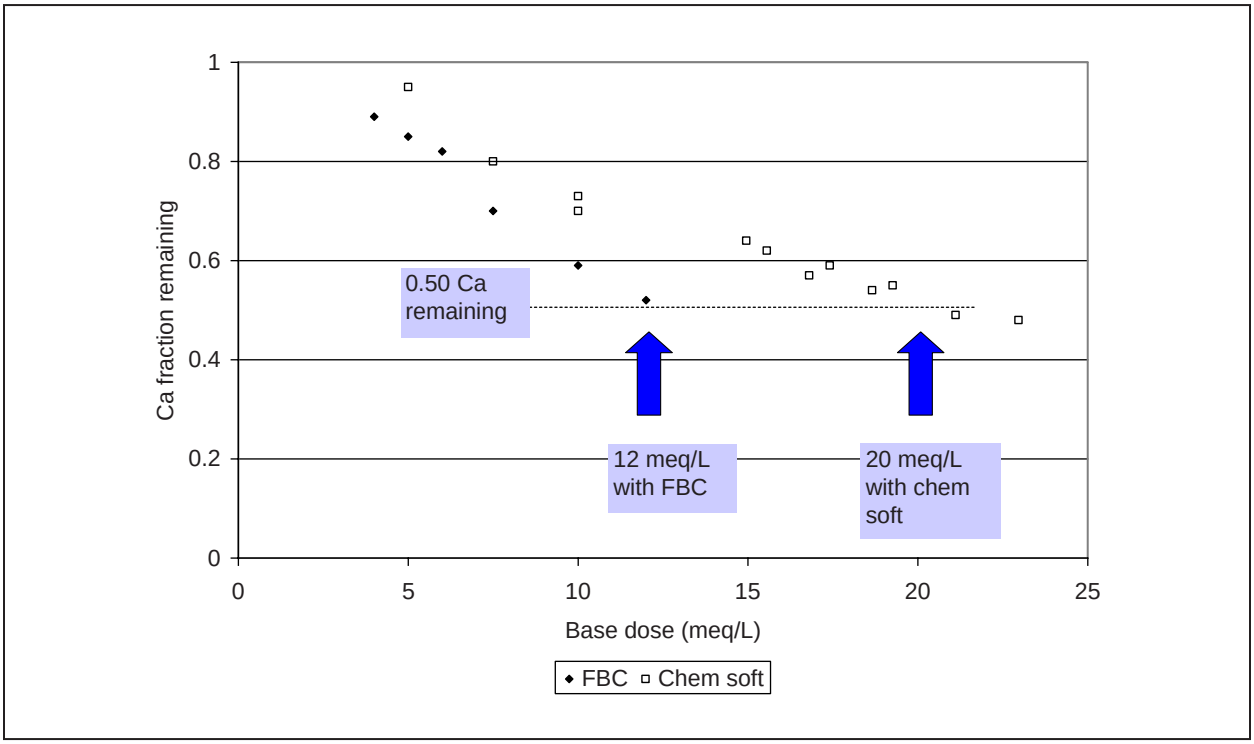

Figure 3.12 TGW comparison of chemical softening with fluidized bed crystallization

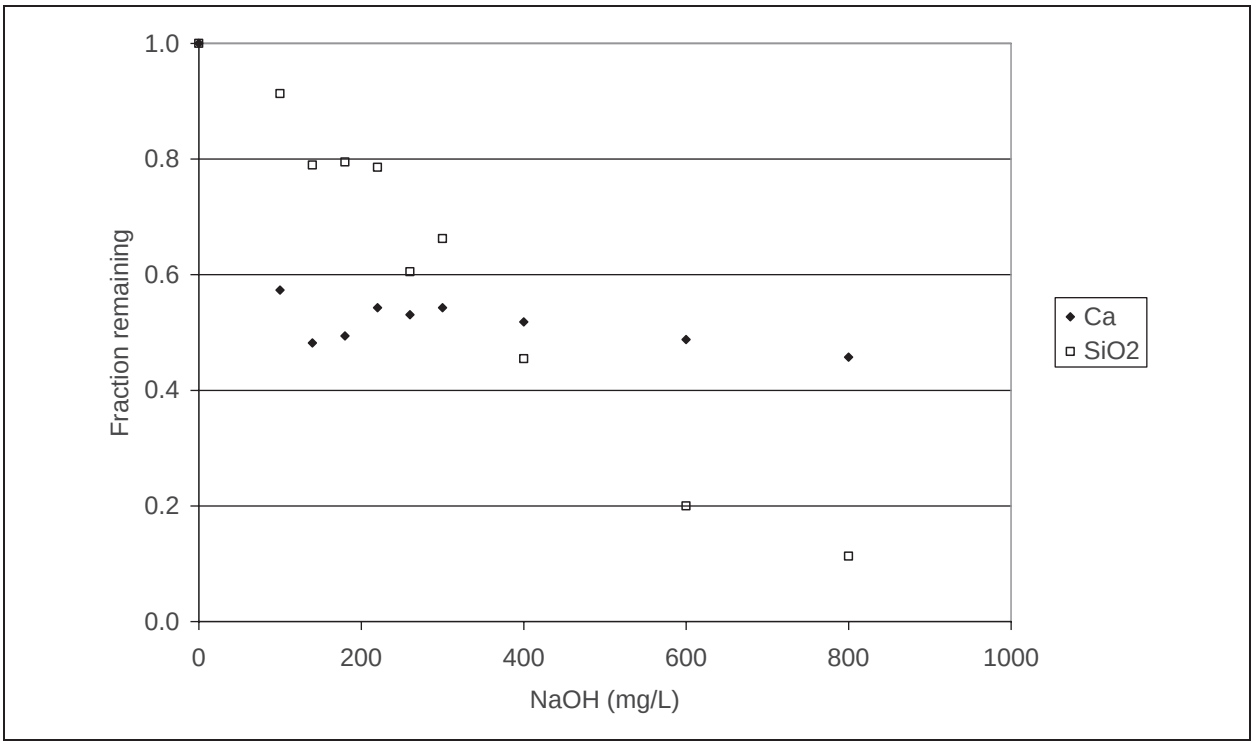

Figure 3.13 LHGW—FBC Ca and SiO_2 fractions remaining vs. NaOH dose

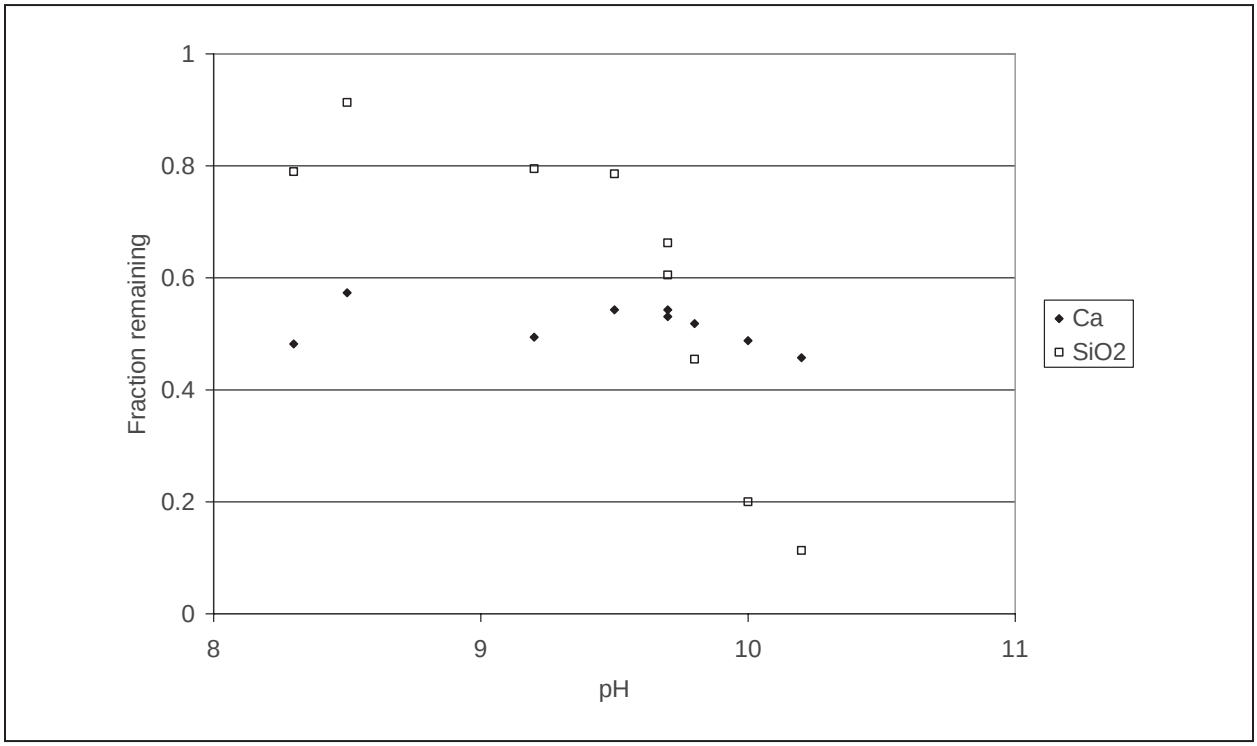

Figure 3.14 LHGW—FBC Ca and SiO_2 fractions remaining vs. pH

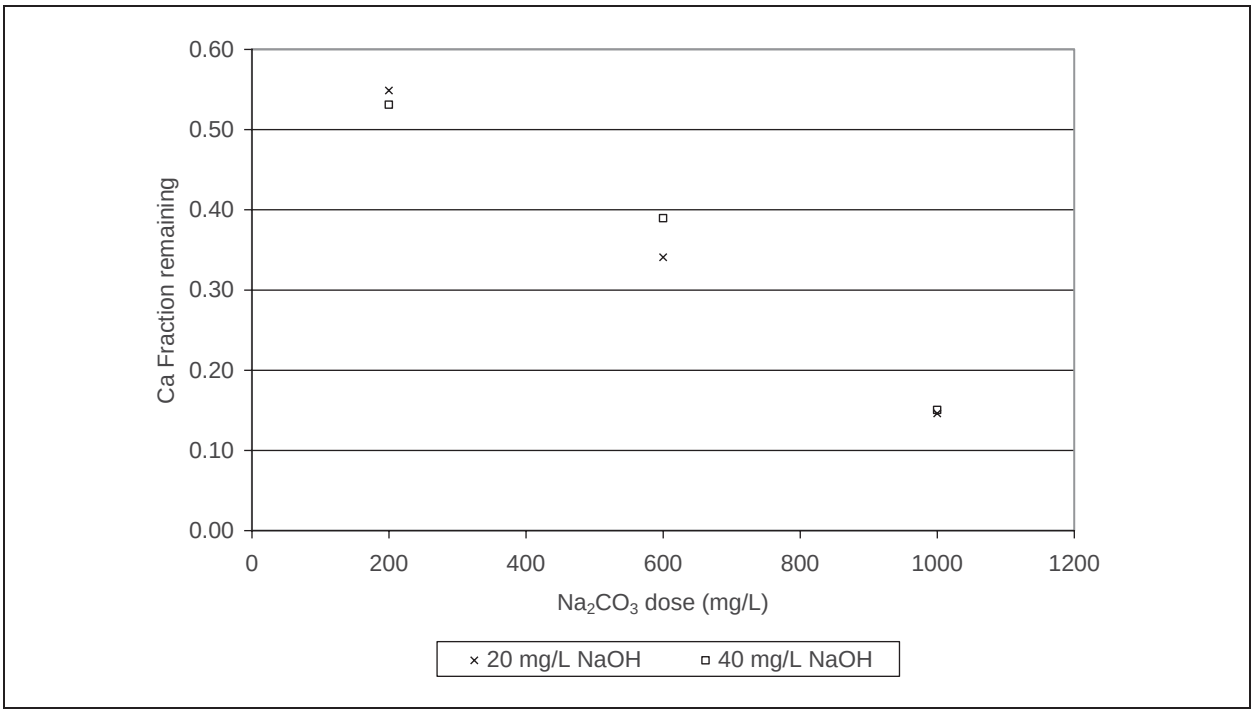

Figure 3.15 CGW—FBC jar test results

CGW FBC Results

Jar test results for fluidized bed crystallization with CGW concentrate are shown in Figures 3.15 and 3.16. Soda ash doses ranging from 200 to 1000 mg/L were added with either 20 or 40 mg/L NaOH doses. A secondary RO recovery of 70 percent was projected for a Na_2CO_3 dose of 600 mg/L, and 80 percent recovery was projected at 1000 mg/L Na_2CO_3 dose.

Summary of Fluidized Bed Crystallization Results

Jar test results for fluidized bed crystallization are summarized in Table 3.8. Chemical doses were lower than those for chemical softening to achieve similar secondary RO recovery, and the solids produced by fluidized bed crystallization are calcite crystals that are typically 10 percent of the volume of sludge produced by chemical softening. Projected secondary RO recoveries with fluidized bed crystallization were 65 to 80 percent.

MIEX®

MIEX® jar tests were conducted to evaluate removal of TOC from TGW and OBGW concentrate samples. MIEX® treatment is shown for TOC removal in all three of the ZLD options. UVA and TOC measurements were used to evaluate the effectiveness of MIEX® for removal of organic compounds. UVA measurement is particularly appropriate in this application because organic compounds with higher UVA generally pose the greatest membrane fouling potential. UVA was reduced by 70 to 80 percent at regeneration frequencies of 25 to 100 bed volumes treated.

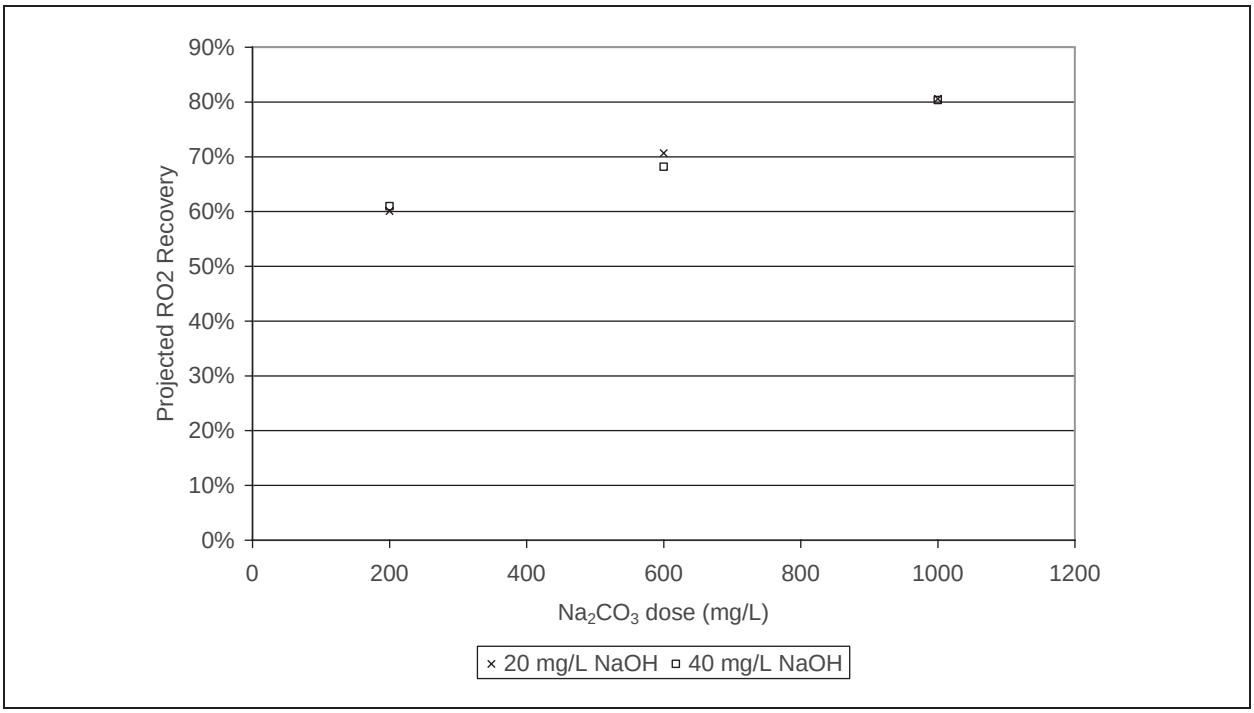

Figure 3.16 CGW—projected secondary RO recovery after FBC

Table 3.8
Summary of fluidized bed crystallization results for concentrate treatment

Sample	NaOH dose (mg/L)	Na_2CO_3 dose (mg/L)	Projected recovery secondary RO	Comments
TGW concentrate	480		65%	Additional process needed for TOC removal
LHGW concentrate	260		70%	
CGW concentrate	20	1000	80%	

TGW MIEX® Results

Results of jar tests conducted to evaluate the effect of pH on organics removal are shown in Figure 3.17. TOC has properties of a weak acid, becoming less protonated and more negatively charged as pH increases. Because MIEX® is an anion exchange resin, a change in pH that increases the negative charge density of TOC could improve its removal by MIEX®. UVA and TOC are plotted against bed volumes treated (BVT) for ambient pH 5.8 and for pH 7.0. Treatment appeared to be only slightly more effective at pH 7 than at pH 5.8.

The effect of BVT on organics removal at pH 5.8 (ambient condition) is shown in Figure 3.18. Regeneration frequency had little effect on treatment effectiveness between 200 and 1000 BVT. UVA fractions remaining were around 0.6 at 1000 BVT and 0.5 at 200 BVT. UVA reduction increased significantly, however, between 200 and 50 BVT. UVA fraction remaining was approximately 0.25 at 50 BVT.

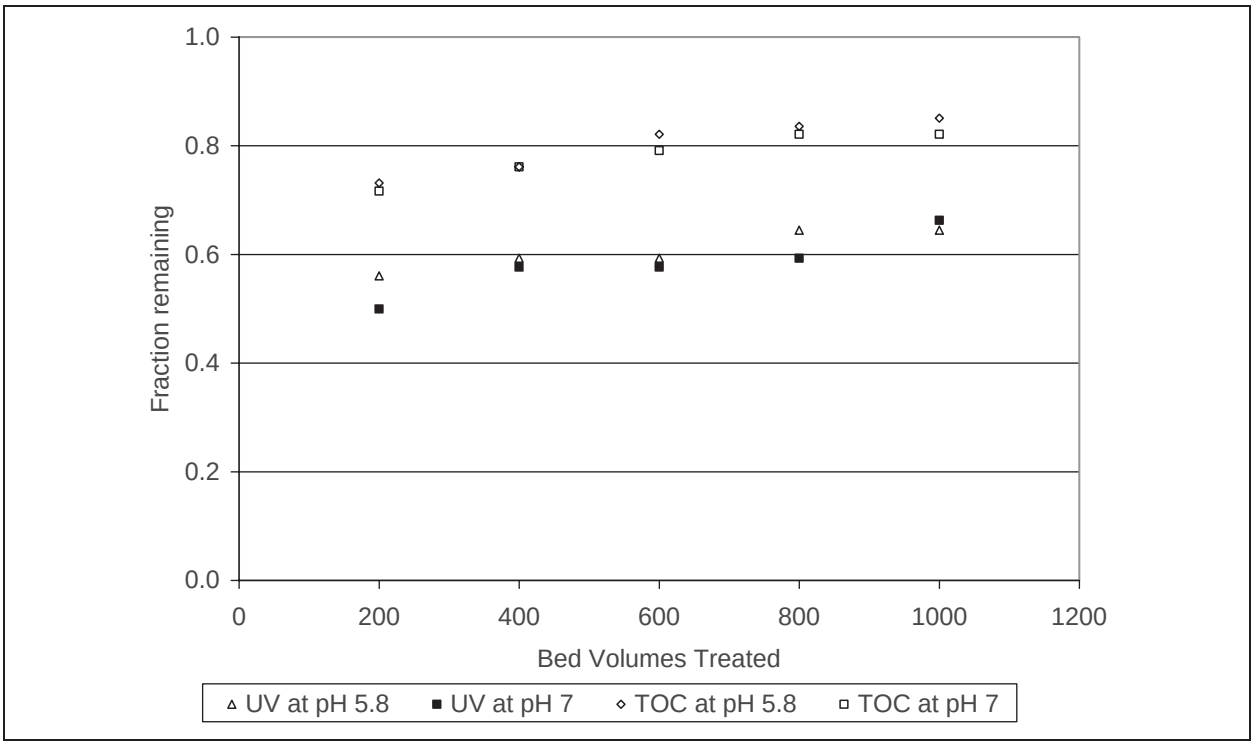

Figure 3.17 MIEX® treatment of TGW concentrate at pH 5.8 and 7.0

OBGW MIEX® Results

Jar test results for MIEX® are shown in Figure 3.19. UVA fraction remaining was reduced to less than 20 percent at 100 BVT and to about 10 percent remaining at 50 BVT.

Summary of MIEX® Results

Treatment with MIEX® was effective for reducing UVA in the concentrate samples even at the high TOC concentrations present in the TGW and OBGW concentrate samples tested. The results indicated that regeneration frequencies of 50 to 200 BVT would be expected to reduce UVA by 70 to 90 percent.

Activated Alumina

AA jar tests were conducted to evaluate removal of silica and calcium from the LHFW and CGW concentrates and for fluoride removal from the AR finished water.

LHGW AA Results

Jar test results for 10-minute contact time with AA are shown in Table 3.9 and Figure 3.20. The concentrate was tested without pH adjustment. A higher percentage of silica was removed than calcium or sulfate, but all were removed to some extent.

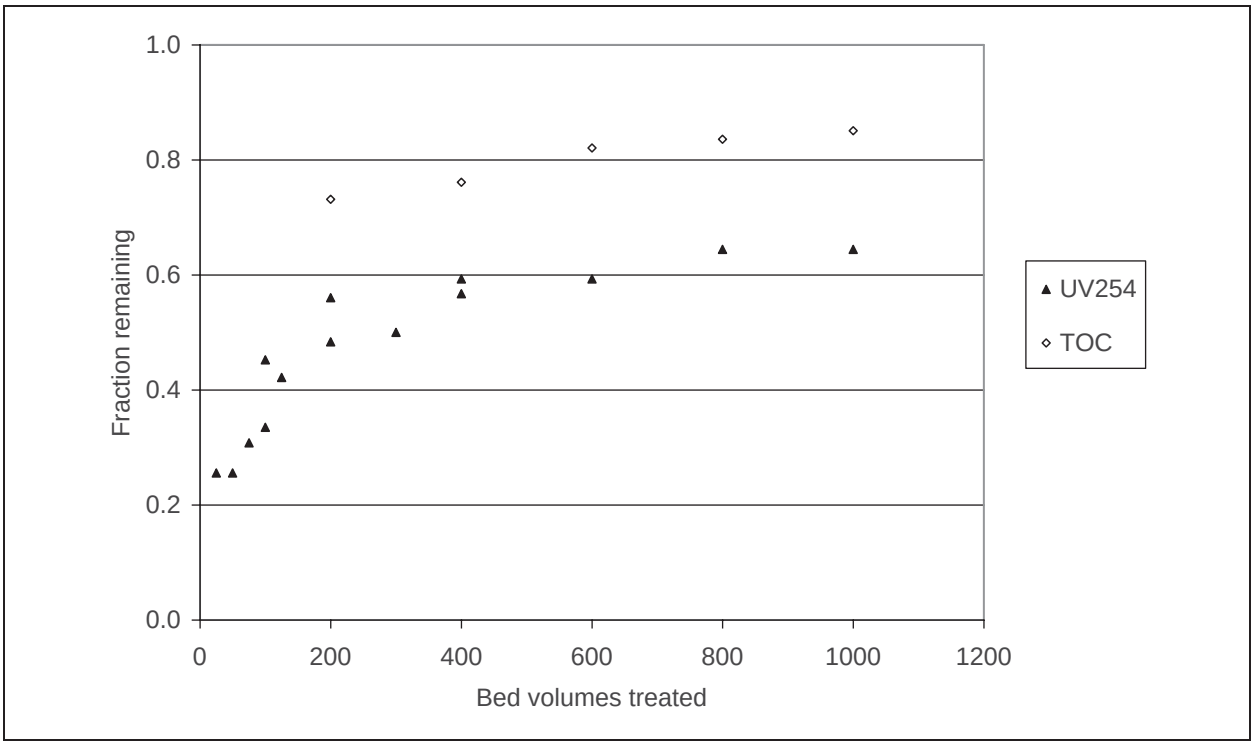

Figure 3.18 TGW—effect of MIEX® bed volumes treated at ambient pH 5.8

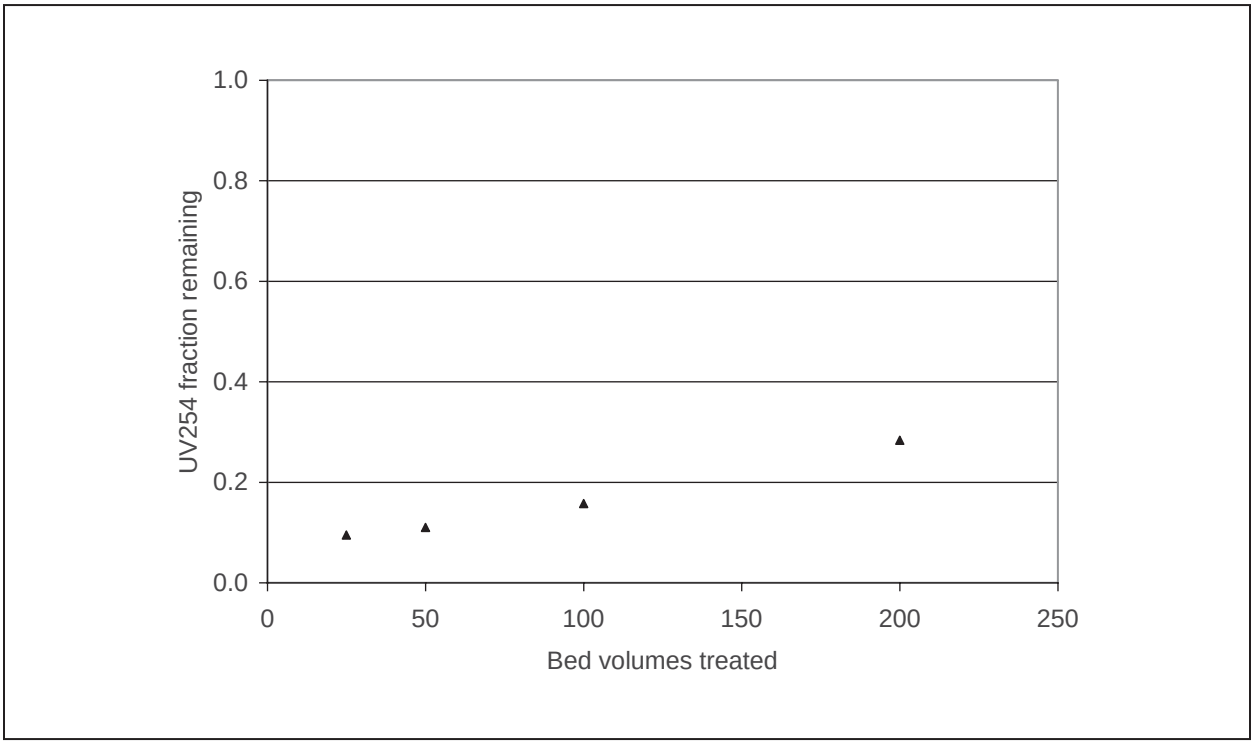

Figure 3.19 OBGW—MIEX® jar test results at ambient pH 7.8

Table 3.9
AA jar test results

BVT	SiO_2 (mg/L)	Ca (mg/L)	SO_4 (mg/L)	Al (mg/L)
	77	650	3800	0.05
200	49	450	3100	0.15
100	31	430	3000	0.20
50	16	390	2800	0.22
33	10	360	2600	0.12
20	4	310	2300	0.14

Secondary RO recovery projections are shown in Figure 3.21. There was a large disparity between the BVT required for calcium sulfate and the BVT for silica for the same recovery. To achieve 70 percent recovery, 15 BVT AA treatment would be required for calcium sulfate compared with 150 BVT for silica. Hence, AA treatment would be less economical for prevention of fouling of RO membranes with calcium sulfate than for fouling with silica, and if AA were the sole concentrate treatment process, AA media regeneration frequency would be governed by calcium sulfate treatment.

OBGW AA Results

Jar test results for AA treatment of the OBGW concentrate are shown in Figure 3.22. AA treatment effectively removed silica and calcium and reduced UVA. Maximum projected secondary RO recovery was limited to 76 percent by calcium sulfate and 89 percent by silica.

AR AA Results

Results for the AA jar test conducted to evaluate AA contact time are shown in Figure 3.23. Contact times from 2 to 15 minutes were evaluated. Typical of adsorption processes, the rate of removal tapered off with extended contact time. Based on the time experiment results, a contact time of 10 minutes was chosen for the isotherm test to evaluate AA capacity for fluoride removal.

Results of the isotherm test are shown in Table 3.10. Fluoride concentrations were reduced by 40 to 90 percent in the jars.

The isotherm data are plotted at log scale in Figure 3.24. Adsorption with AA is described by the Freundlich equilibrium adsorption model where C is the concentration of the fluoride in solution (mg/L), q is the concentration of fluoride on the AA media (mg F/ g AA), and K and n are model parameters fit to the data. The K and n parameters can be derived from the log plot of the data in the figure. For this experiment, K was 0.38 $(L/mg)^n$, and n was 0.33.

$$q = KC^n$$

$$\log q = n \log C + \log K$$

The Freundlich equation can be used to calculate AA usage rate (AAUR), the mass of AA required to treat a unit volume of water.

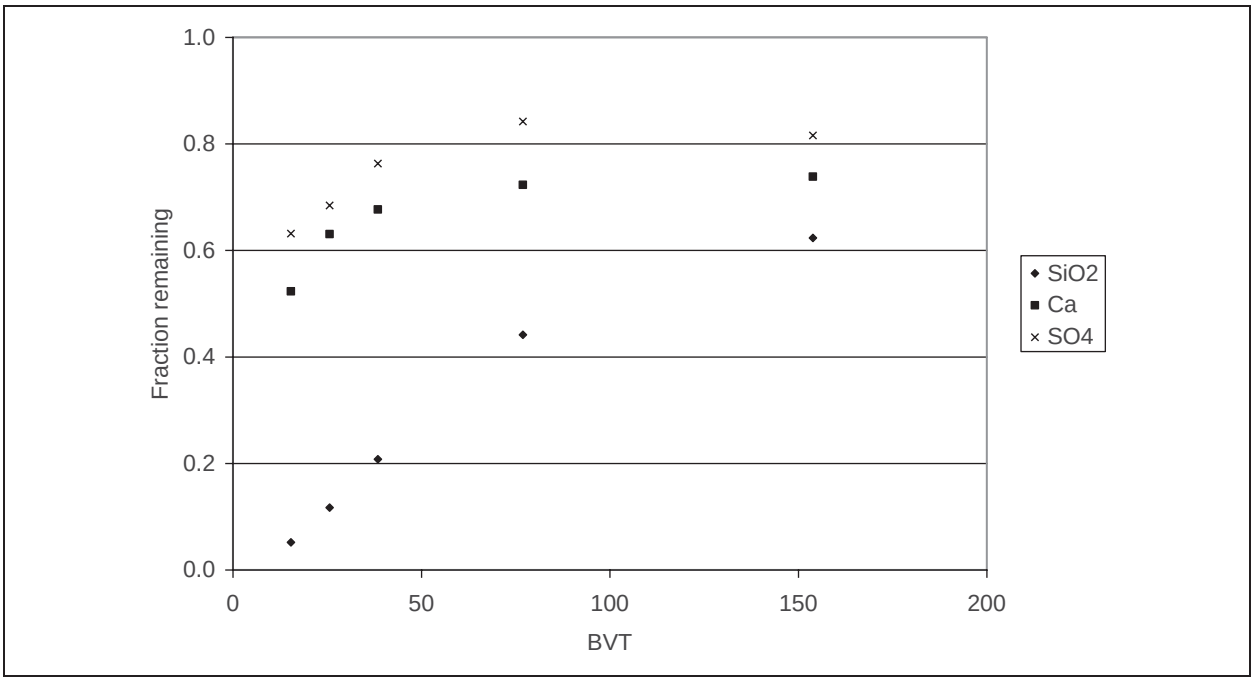

Figure 3.20 LHGW—AA jar test results

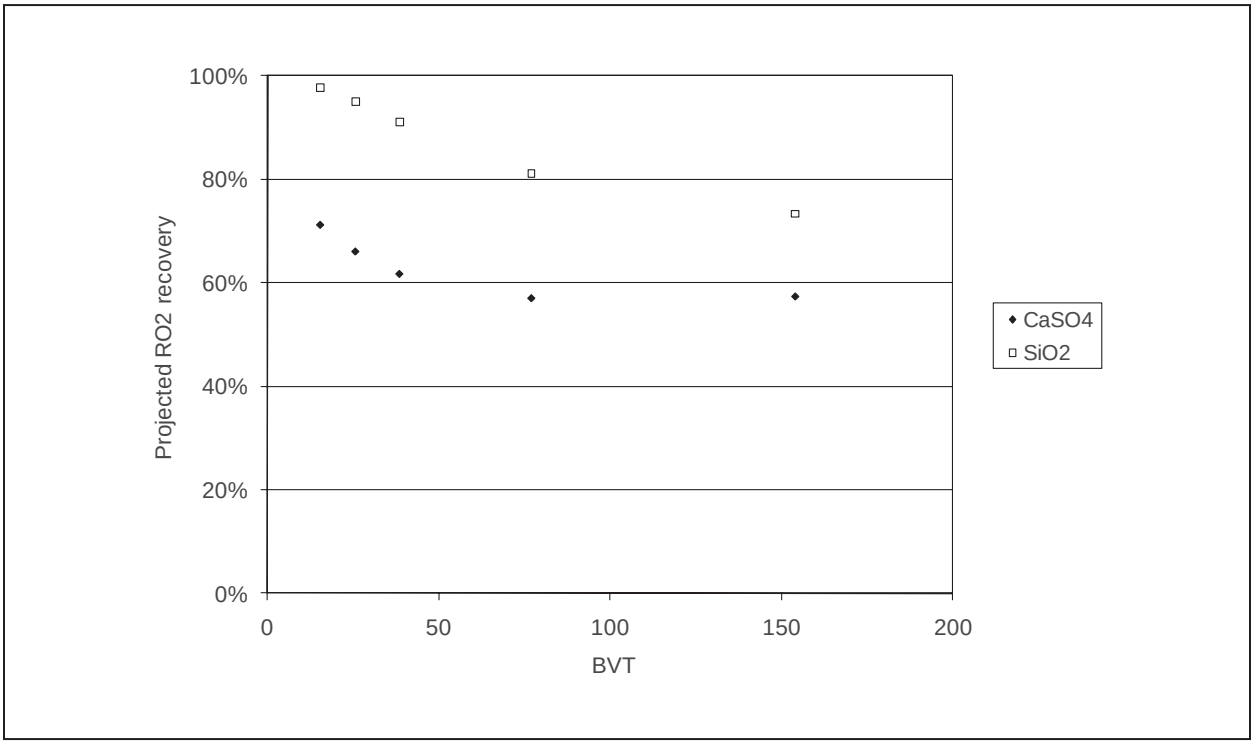

Figure 3.21 LHGW—projected secondary RO recovery after AA

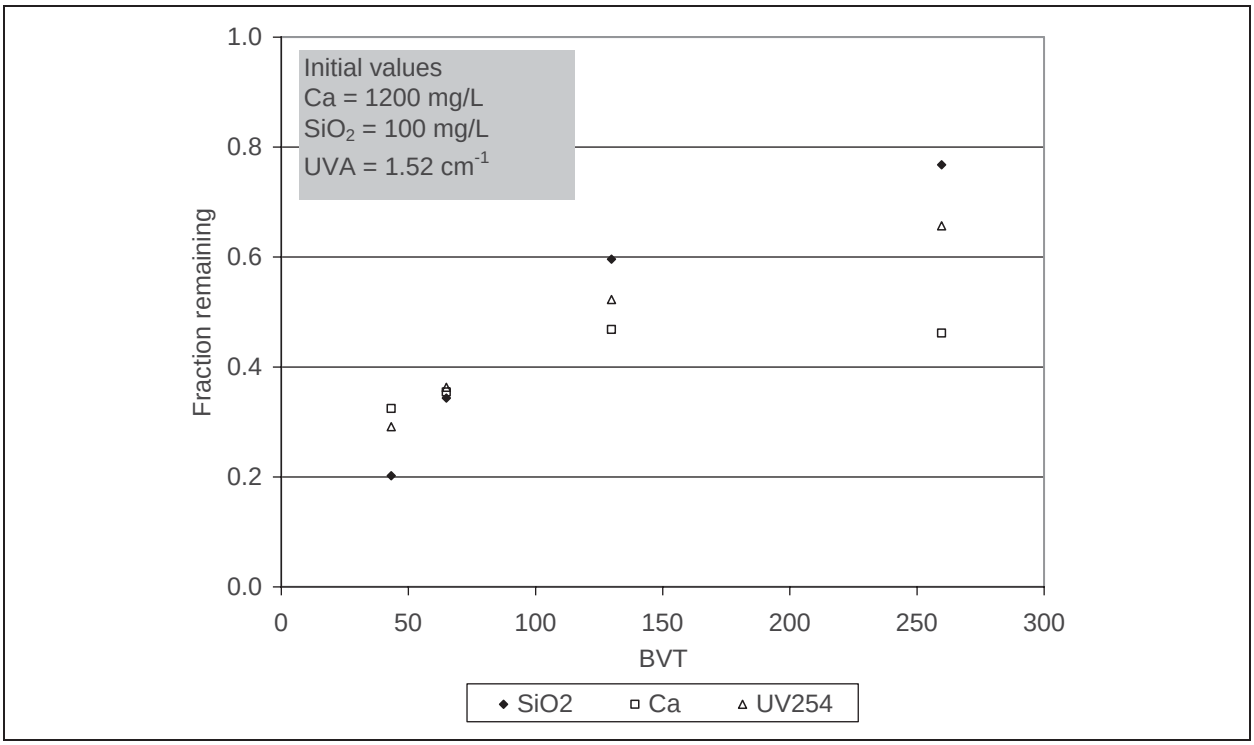

Figure 3.22 OBGW—AA jar test results

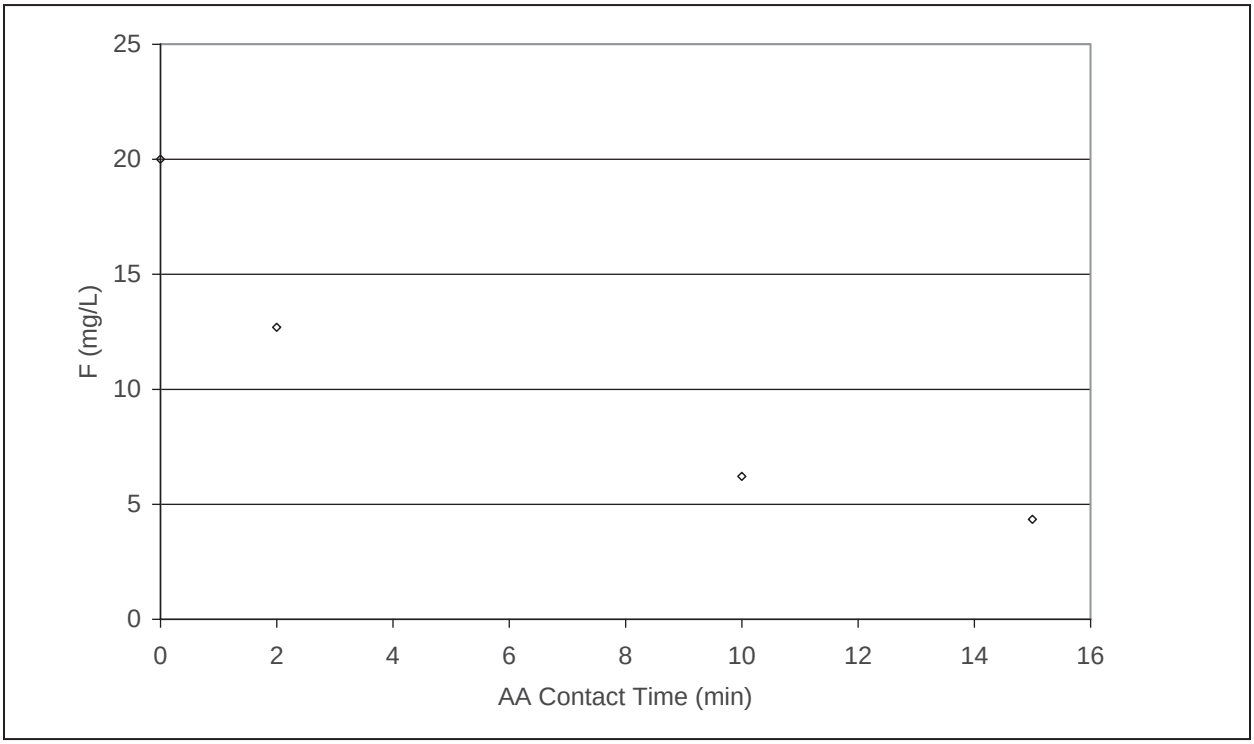

Figure 3.23 AR—jar test to evaluate AA contact time

Table 3.10
AA isotherm test results with AR finished water spiked to 20 mg/L fluoride

AA dose (g/L)	pH	F (mg/L)
10	8.4	12
20	8.2	6
30	8.3	3
40	8.5	2

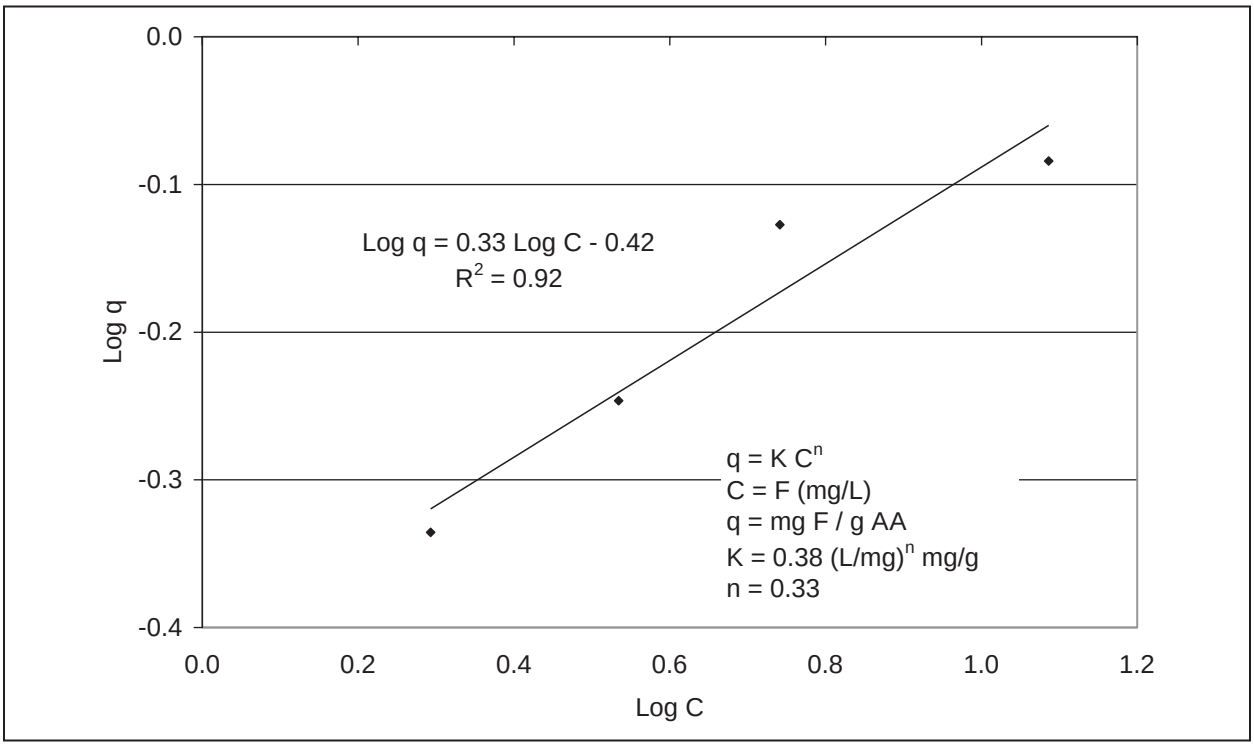

Figure 3.24 Log plot of AR isotherm data to derive Freundlich coefficients

$$q = KC^n$$
$$C_{in} = 5mg/L$$
$$C_{out} = 1mg/L$$
$$q = 0.38 \times 1^{0.33} = 0.38\frac{mg\,F}{g\,AA}$$
$$AAUR = \frac{(C_{in} - C_{out})}{q} = 4\frac{mg}{L} \times \frac{g\,AA}{0.38mg\,F} = 10.5\frac{g\,AA}{L} = 10.5\frac{kg\,AA}{m^3}$$

Figure 3.25 shows the AA usage rate required to achieve to a treated water goal of 1 mg/L fluoride for a range of influent fluoride concentrations. AAUR ranged from 3 kg/m^3 at an influent fluoride concentration of 2 mg/L to 24 kg/m^3 to treat 10 mg/L fluoride. The AAUR indicates AA regeneration frequency if the media is reused and replacement frequency if the media is used once then replaced. At the AAUR values observed, single use of the media would be prohibitively expensive.

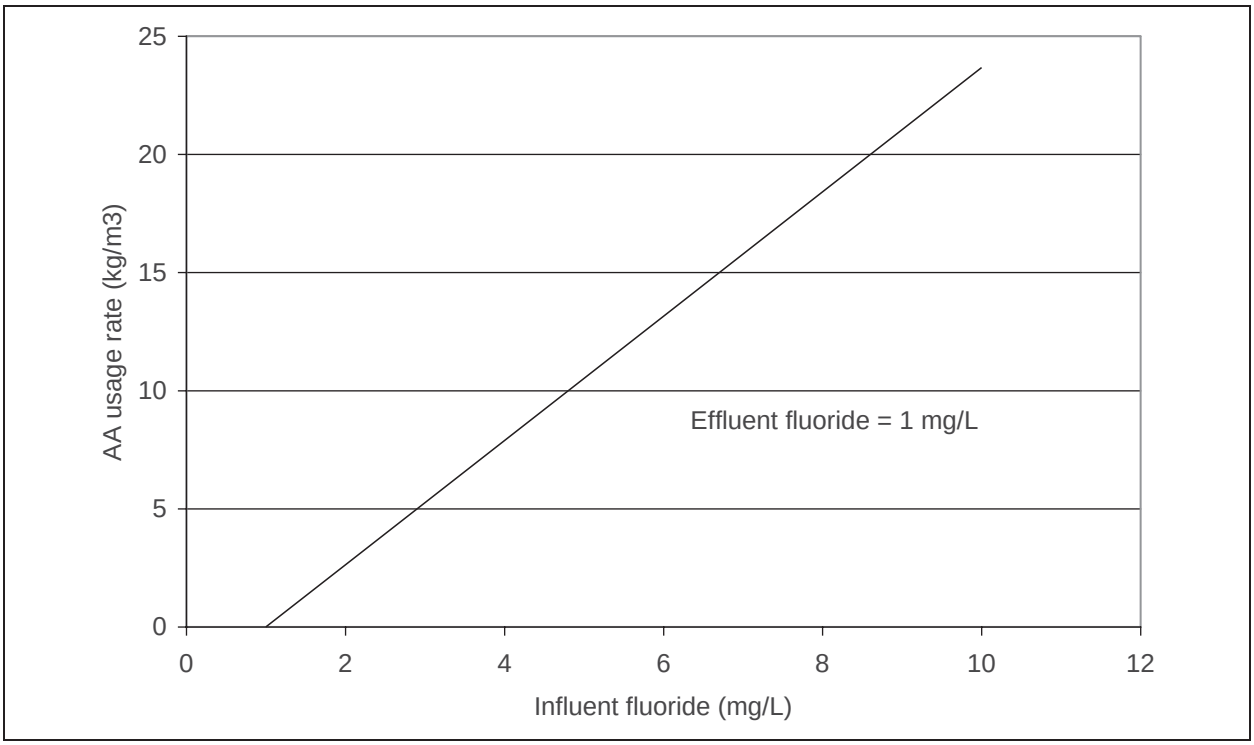

Figure 3.25 AA usage rate to produce AR finished water with 1 mg/L fluoride

The results of an experiment conducted to evaluate the effectiveness AA regeneration are shown in Figure 3.26. The AA dose was 25 g/L, and the sample fluoride concentration was spiked to 23 mg/L. The AA was used for 5 treatment cycles. Treatment after the first cycle with virgin media was compared to treatment after 4 cycles of regeneration. Ten percent virgin AA was added to the jar after each regeneration to replace media lost during the bench-scale regeneration process. Treatment with virgin media reduced fluoride from 23 mg/L to 4 mg/L. Some adsorption capacity was after the first regeneration, but adsorption capacity remaining after the first regeneration was maintained through the successive regeneration cycles.

AA Results Summary

AA was evaluated for silica removal in ZLD Options 1 and 2. AA treatment was effective for SiO_2 removal and also achieved reductions in calcium and UVA. AA was evaluated for fluoride removal from the AR source. Fluoride concentrations were effectively reduced by AA. Some AA adsorption capacity was lost after the first regeneration, but further reductions in capacity were not observed with successive regenerations.

Coagulation

Coagulation jar tests were conducted to evaluate removal of silica and TOC from the TGW, LHGW, and OBGW concentrates. Coagulation is an option for silica and TOC removal in ZLD Options 1 and 2.

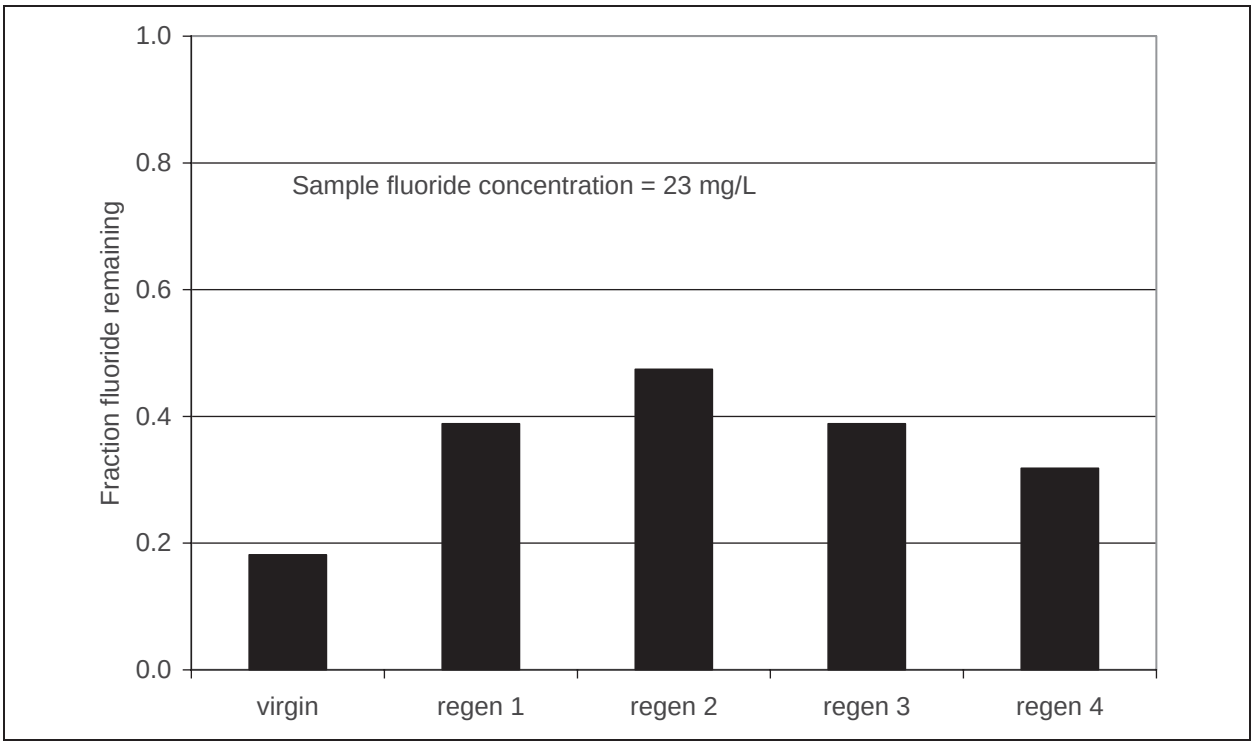

Figure 3.26 Effectiveness of AA regeneration treating AR spiked to 23 mg/L fluoride

Table 3.11
TGW ferric chloride coagulation jar test results

$FeCl_3$ (mg/L)	NaOH (mg/L)	pH	UVA (C/Co)	SiO_2 (C/Co)
50	120	6.7	0.95	0.74
200	200	6.9	0.82	0.61
400	280	6.9	0.78	0.52
550	280	6.5	0.54	0.48
700	320	6.4	0.54	0.39
800	320	6.0	0.36	0.35

TGW Coagulation Results

Coagulation jar tests were conducted with ferric chloride ($FeCl_3$) to evaluate its effect on UVA and SiO_2 (Table 3.11). Addition of $FeCl_3$ depresses pH, and consequently caustic was added to maintain pH in a range favorable for ferric hydroxide precipitation. At the maximum dose combination tested, 800 mg/L $FeCl_3$ and 320 mg/L NaOH, UVA and silica were reduced to about 35 percent of their original values. Silica removal was sufficient to achieve over 85 percent recovery in a secondary RO, but an additional treatment process would be required with coagulation for calcium removal to avoid membrane fouling by calcium sulfate.

Table 3.12
LHGW ferric chloride coagulation jar test results

$FeCl_3$ dose (mg/L)	NaOH dose (mg/L)	SiO_2 (mg/L)	pH	Projected RO2 recovery for SiO_2
50	120	60	6.3	67%
100	160	55	6.5	69%
200	280	45	6.6	75%
400	520	20	7.4	89%

LHGW Coagulation Results

The LHGW concentrate results to evaluate silica removal by ferric chloride coagulation are shown in Table 3.12. Caustic was added with ferric chloride to maintain pH in the optimal range. Projected RO2 recovery, based on SiO_2 scaling only, reached 89 percent at chemical doses of 400 mg/L $FeCl_3$ and 520 mg/L NaOH. As with the TGW concentrate, an additional process would be required for calcium removal.

OBGW Coagulation Results

Jar test results for coagulation with ferric chloride are shown in Figure 3.27. UVA was reduced to 30 percent remaining at a $FeCl_3$ dose of 600 mg/L. Silica was reduced to 75 percent remaining at a $FeCl_3$ dose of 400 mg/L. The maximum recovery projected for secondary RO based on silica removal was 59 percent. An additional process would be required for calcium removal.

Coagulation Followed by Softening

Jar tests were conducted with TGW concentrate to evaluate coagulation followed by chemical softening. The goal was to evaluate chemical doses required to achieve calcium and TOC treatment goals with coagulation followed by softening.

The coagulated samples from Table 3.8 were treated with the caustic and soda ash doses in Table 3.13 to evaluate coagulation followed by softening. The NaOH and total base doses in Table 3.13 include the NaOH dose added during coagulation from Table 3.8.

The results of this jar test are compared with softening without ferric coagulation pretreatment in Figure 3.28. More calcium was removed per meq/L of base added in the jars that were pretreated with ferric coagulation, but the benefit decreased as $FeCl_3$ and base doses increased because a portion of the base dose is consumed by the acidity added with ferric chloride. Recovery projected for secondary RO was less than 70 percent.

MIEX® Followed by Softening

Results for MIEX® treatment followed by chemical softening are shown in Figure 3.29. Softening doses in each jar were 600 mg/L NaOH plus a Na_2CO_3 dose that ranged from 200 to 600 mg/L. The base dose shown is the sum of the NaOH and Na_2CO_3 doses. Two MIEX® conditions were evaluated, 200 and 50 BVT. MIEX® treatment at 200 BVT increased calcium removal

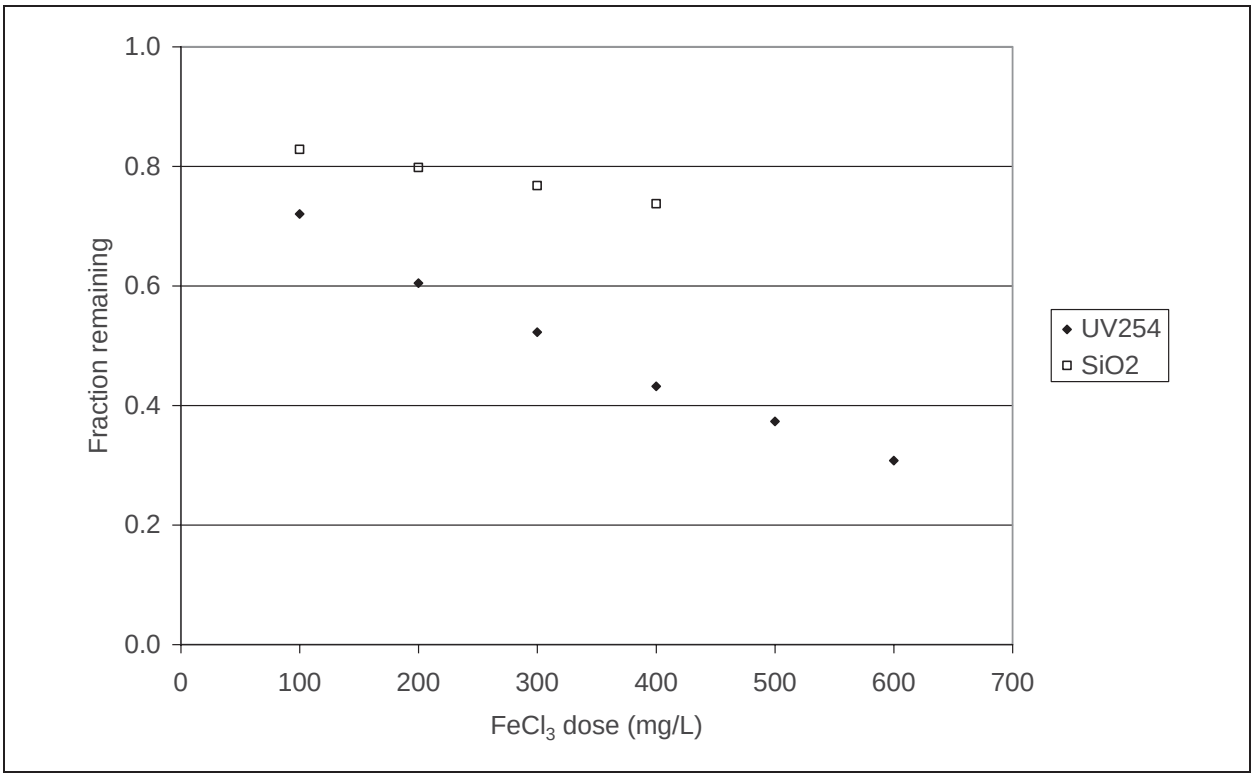

Figure 3.27 OBGW—coagulation with ferric chloride jar test results

Table 3.13
Jar test chemical doses for ferric chloride coagulation followed by softening

$FeCl_3$ (mg/L)	NaOH (mg/L)	Na_2CO_3 (mg/L)	Total base (meq/L)
50	220	100	7.4
200	400	200	13.7
400	680	400	24.4
550	880	600	33.1
700	1120	800	42.8
800	1420	1000	54.0

by 2 to 16 percent compared with softening alone. MIEX® treatment at 50 BVT resulted in 5 to 24 percent greater calcium removal.

Projected secondary RO recoveries projected are shown in Figure 3.30. A secondary RO recovery of 80 percent was projected for a base dose of 34 meq/L.

EDM

The results of pilot-scale tests to evaluate EDM treatment of TGW concentrate are shown in Figure 3.31. The figure shows conductivities of the feed, effluent, and concentrate streams over

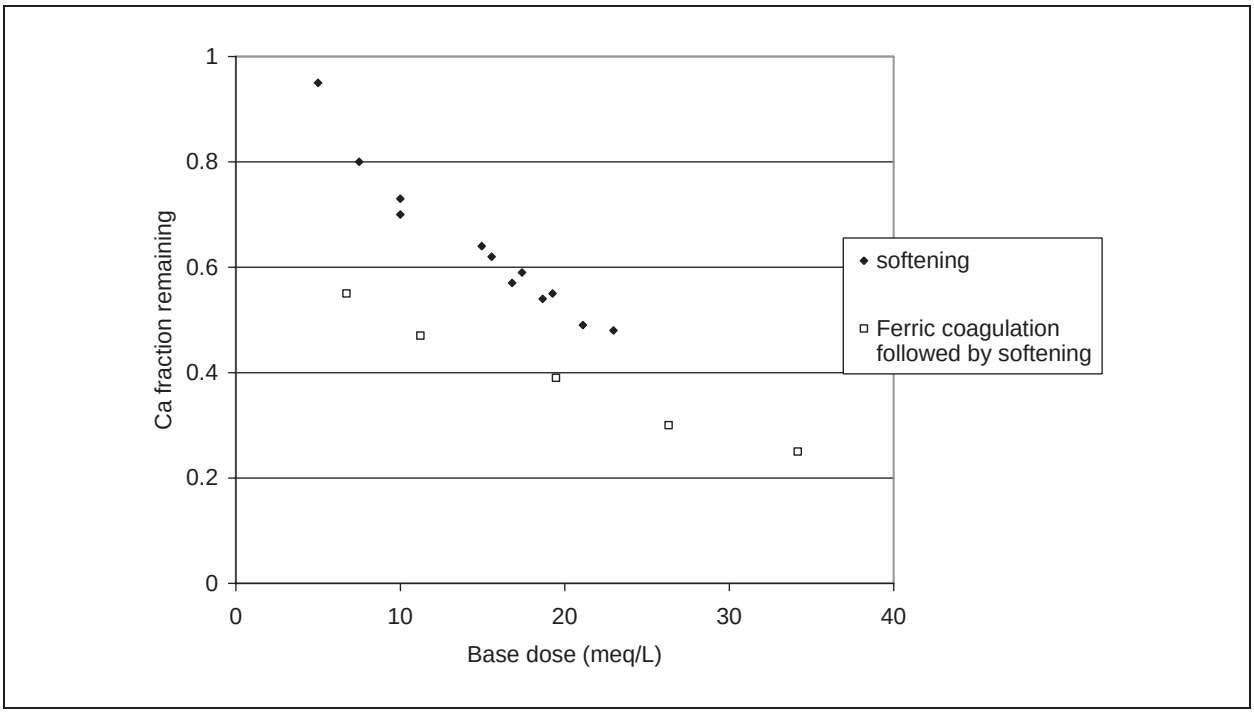

Figure 3.28 TGW effect of ferric coagulation on softening

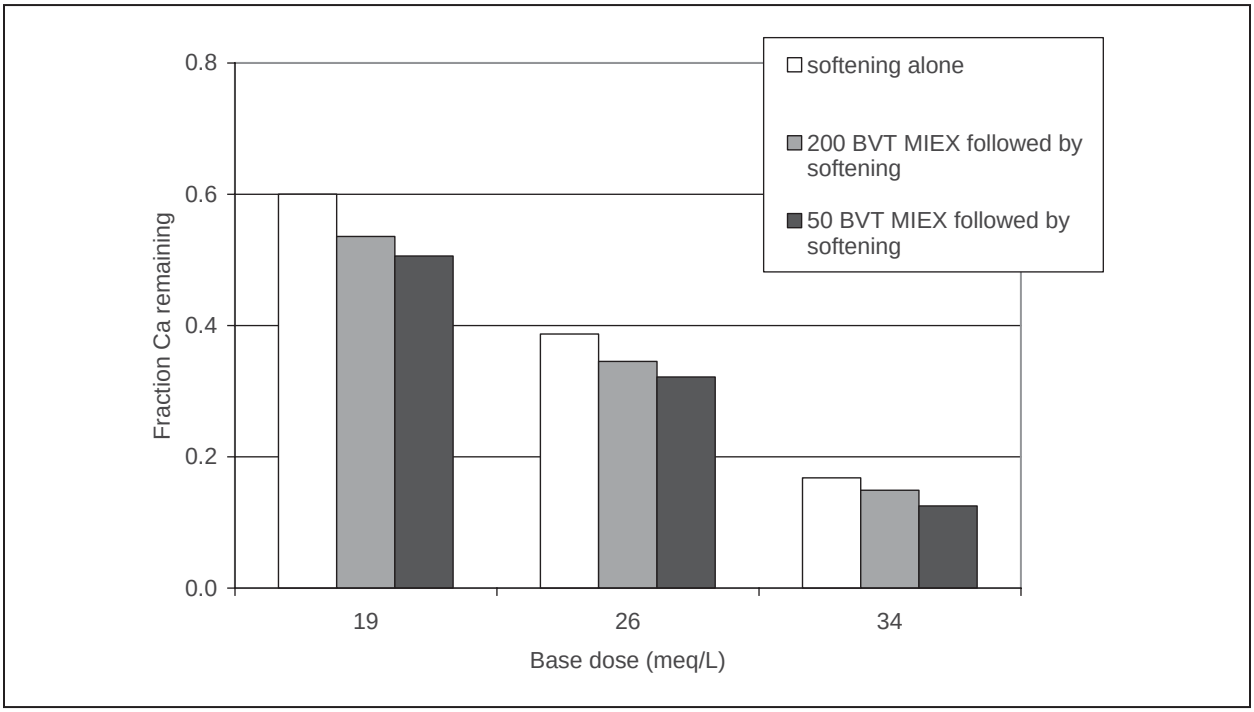

Figure 3.29 TGW effect of MIEX® pretreatment on calcium removal

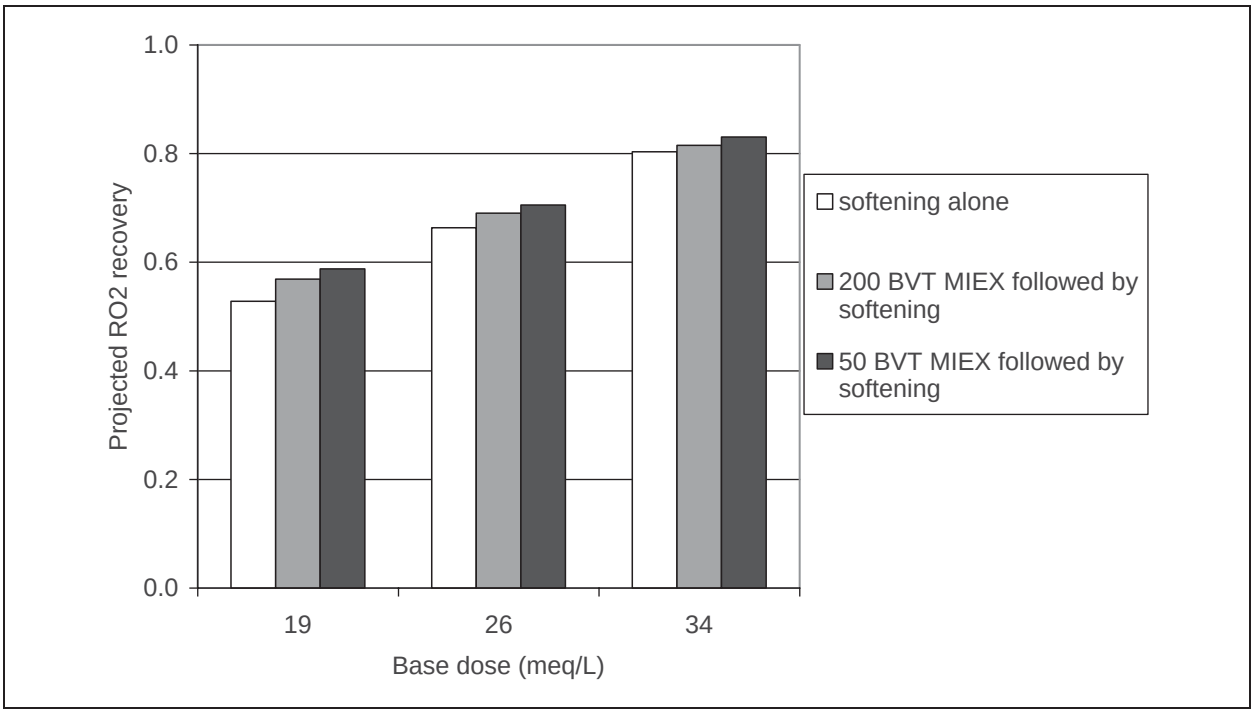

Figure 3.30 TGW projected secondary RO recovery for softening with and without MIEX® pretreatment

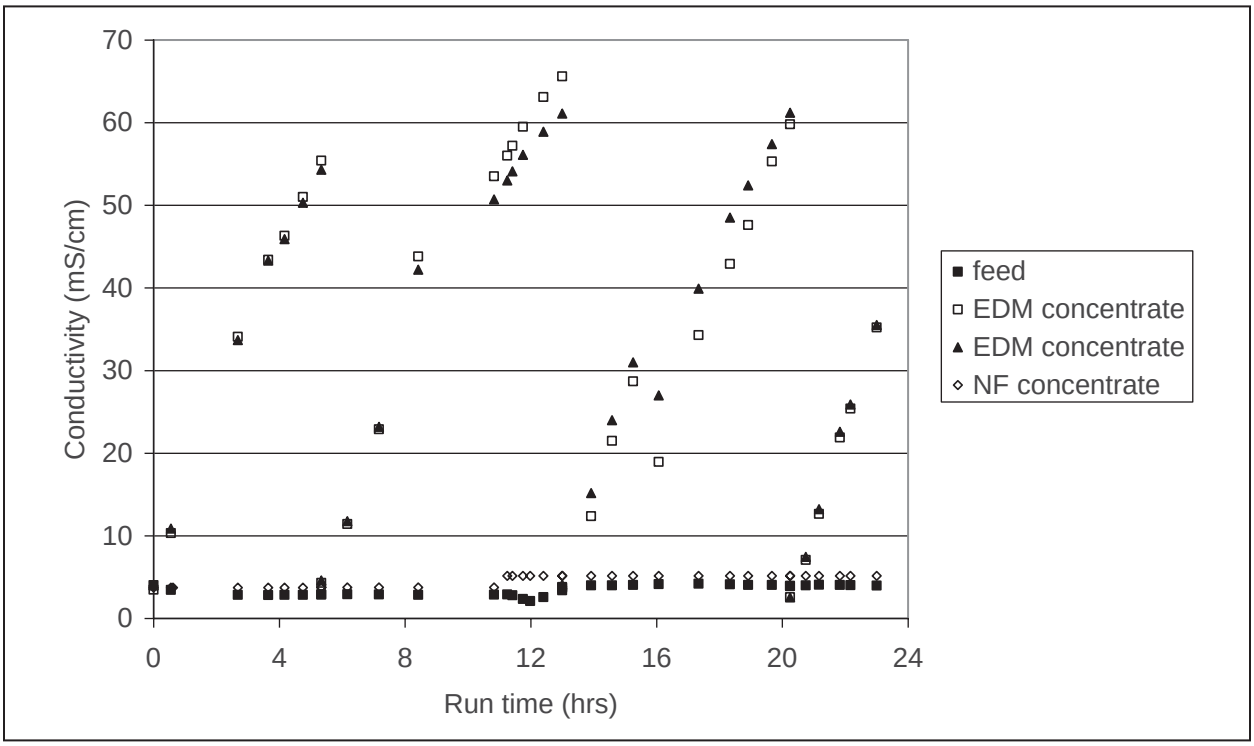

Figure 3.31 EDM pilot results with TGW concentrate

Table 3.14
Typical costs and energy requirements for ZLD treatment steps

		Capital cost ($/kgal)	Energy (kWh/kgal)
Secondary desalination	RO	$1.50	4
Final evaporation	Brine concentrator	$15	80
	Crystallizer	$100	350

a total 23 hours of operation. The experiments were feed-and-bleed operations that were restarted each morning and did not reach steady state. In the second experiment, which lasted 8 hours, the conductivity of the sodium salt concentrate reached 66 mS/cm and conductivity of the chloride salt concentrate reached 61 mS/cm. The NF concentrate entered the feed tank at 6.5 mS/cm and overflowed at 3.7 mS/cm. Calcium and sulfate concentrations in the effluent stream were measured to evaluate the effect EDM pretreatment would have on recovery in secondary RO. Calcium was reduced from 700 mg/L to 390 mg/L, and sulfate was reduced from 2300 mg/L to 980 mg/L. For EDM pretreatment followed by secondary RO (Option 2), the recovery projected for secondary RO at this level of EDM treatment was 81 percent. For EDM as the secondary desalination device (Option 3), the EDM pilot achieved 99.4 percent recovery of product water. The test was conducted at one set of operating conditions, but the extent of calcium and sulfate removal and overall ion removals (desalination) with EDM is adjustable by increasing the duration of flow through the stack or by increasing stack voltage.

ZLD Process Selection

Results from preliminary tests were used to compare ZLD treatment Options 1, 2, and 3 and select one for extensive pilot-scale testing. Treatment cost and energy requirements are key considerations in ZLD process selection. To achieve ZLD, water not recovered in secondary desalination must be removed in the final evaporation step. Depending on flow rate, the final evaporation step for each option would comprise a crystallizer or a brine concentrator followed by a crystallizer. There is a sharp demarcation in costs and energy between the secondary desalination and final evaporation steps.

Table 3.14 shows typical capital costs and energy requirements for secondary desalination and for the final evaporation step processes: brine concentrator and crystallizer. Costs and energy requirements for the evaporative processes are between one and two orders of magnitude greater than those for secondary desalination. It is evident that ZLD costs and energy requirements are minimized by maximizing the percentage of water recovered through secondary desalination and thereby minimizing the percentage of water that must be recovered in the final evaporation step.

Key characteristics of the three ZLD options are compared in Table 3.15. Option 3, use of EDM for secondary desalination, has the following advantages relative to Options 1 and 2:

- Option 3 provides higher recovery through secondary desalination and lower capacity required for final evaporation. For example, if recovery in the primary desalination device is 80 percent, recovery after secondary desalination would be 93 percent for

Table 3.15
Comparison of ZLD treatment options

	Option 1 coagulation softening secondary RO	Option 2 EDM secondary RO	Option 3 EDM
Recovery in secondary device	60–70 %	80%	98%
Number of treatment processes	7	7	4
Chemical usage	High	Low	Low
Byproducts	Sludge RO concentrate	RO concentrate EDM concentrate	EDM concentrate
Potential for beneficial use of byproducts	Low	Low	High

Option 1, 96 percent for Option 2, and 99.6 percent for Option 3. Consequently, the thermal desalination capacities required for Options 1 and 2 would be 17.5 and 10 times that required in Option 3, respectively.

- Option 3 requires fewer treatment processes than Options 1 and 2 because pretreatment to remove calcium and silica is not required for desalination with EDM.
- Option 3 has the lowest production of waste byproducts and lowest chemical consumption. Option 1 has high chemical usage relative to Options 2 and 3 and generates the greatest volume of waste byproducts. Byproducts in Option 2 are RO and EDM concentrate streams. The only byproduct in Option 3 is EDM concentrate.
- Option 3 offers the greatest potential for beneficial use of byproducts. The highly concentrated byproduct flow from EDM is amenable to development of beneficial salts such as $CaSO_4$ and $CaCO_3$ or for reuse in the EDM and MIEX processes.

EDM was selected for pilot testing based on the following considerations:

- Option 3 was judged to be the option with the greatest potential for affordable and sustainable ZLD desalination. Option 2 was second.
- EDM is a new technology and demonstrating the viability of this technology through pilot tests with several water sources was perceived to offer the greatest potential for the advancement of ZLD desalination.
- Preliminary calculations indicated that Option 3 would be less expensive and require less energy than Option 2 for the TGW, CGW, and OBGW concentrates. The LHGW concentrate, however, had a much higher TDS concentration (16,000 mg/L compared with about 4000 mg/L for the other concentrates), and costs for Options 2 and 3 for LHGW appeared to be comparable. EDM was selected for pilot testing because (1) use of brackish sources with lower TDS such as the TGW, CGW, and OBGW are preferred and will be used more frequently than with high TDS brackish sources, and (2) pilot test results for EDM could also be used to evaluate Option 2.

PILOT TEST RESULTS

The following pilot-scale tests were conducted on the five water sources:

- TGW—MIEX followed by EDM
- LHGW—EDM
- CGW—EDM
- OBGW—MIEX followed by EDM
- AR—AA bed and calcite contactor

EDM Pilot Results

Pilot tests were conducted to evaluate EDM performance regarding the following:

- Water quality in the product and concentrate streams.
- Recovery of product water without membrane fouling.
- Energy requirements.

The EDM pilot was operated with the same superficial velocity for each of the water sources, 5 cm/s, which is a typical design velocity for full-scale electrodialysis stacks. Consequently, flow per width of cell was the same at pilot-scale as it would be at full-scale. The length of the pilot cell (20 cm), however, was shorter than full-scale cell length (160 cm), and therefore the hydraulic residence time was shorter. To simulate full-scale hydraulic residence time, the EDM feed stream was recirculated, and a steady-state EDM feed conductivity was maintained by blending the concentrate source water with the recirculated EDM diluate in a constant ratio.

Water Quality

The EDM process was designed to separate concentrate into two highly soluble streams: one containing sodium and anions and the other containing chloride and cations. Silica was expected to pass through EDM unchanged because it is an uncharged molecule at neutral pH. Many compounds that comprise TOC have a negative charge at neutral pH, and therefore some passage of TOC through the anion selective membranes was expected.

Theoretically, higher recoveries are possible in EDM than in RO because calcium and sulfate are separated into different concentrate streams and because TOC and silica are not concentrated in EDM as they are in RO. Water quality in the pilot feed and concentrate streams were monitored to evaluate the effectiveness of the EDM process to separate calcium and sulfate in the concentrate streams and to avoid concentration of silica or TOC.

Water quality data for the EDM test with TGW NF concentrate are shown in Table 3.16. The following were key conclusions regarding this pilot test:

- MIEX® treatment step.
  - MIEX® treatment reduced TOC from 58.5 to 20.4 mg/L.
  - Other anions were also removed by MIEX® treatment. Sulfate concentrations were reduced from 1940 mg/L in the NF concentrate to 1010 mg/L after MIEX® treatment, and there was a slight reduction in silica concentration.

Table 3.16
EDM water quality results treating TGW NF concentrate

Analyte	NF concentrate (mg/L)	MIEX treated NF concentrate (mg/L)	EDM feed (mg/L)	EDM Concentrate 1 (mg/L)	EDM Concentrate 2 (mg/L)
Calcium	660	566	284	51	14,900
Magnesium	132	116	69	5	2220
Sodium	202	698	376	38,600	14,000
Chloride	144	1590	853	30,800	53,700
Sulfate	1940	1010	421	42,400	nondetect
HCO_3	41	38	29	352	nondetect
Silica	29.4	24.6	25.0	12.2	17.6
TOC	58.5	20.4	18.5	36.5	2.4

  - Sodium and chloride concentrations increased after MIEX® treatment. Chloride was exchanged for sulfate and TOC in MIEX® treatment, and chloride concentration increased from 144 mg/L in the untreated NF concentrate to 1590 mg/L after MIEX® treatment. There was also an increase in sodium concentration.
  - Ions with membrane fouling potential (TOC and sulfate) were replaced by ions with little to no membrane fouling potential (chloride and sodium) during MIEX® treatment.
- EDM treatment step.
  - The EDM pilot separated the concentrate into two streams: one containing sodium and anions and the other containing chloride and cations. Concentrate stream 1 contained high concentrations of sodium, chloride, and sulfate with low concentrations of calcium and magnesium. Concentrate stream 2 contained high concentrations of chloride, calcium, magnesium, and sodium, and sulfate was below the laboratory detection limit.
  - Silica and TOC went through EDM treatment largely unaffected. EDM feed concentrations approximate EDM diluate concentrations because the EDM diluate was recycled to the EDM feed tank with NF concentrate in a 10:1 ratio. Silica in the EDM feed was 25.0 mg/L compared with 24.6 mg/L in the MIEX treated concentrate. TOC in the EDM feed was 18.5 mg/L compared with 20.4 mg/L in the MIEX treated concentrate.
  - Modest levels of TOC and silica were found in the concentrate streams, but these concentrations were less than those in the NF concentrate and not great enough to pose membrane fouling risks. TOC generally carries a negative charge, and Concentrate stream 1 where anions were collected contained 36.5 mg/L of TOC. The membrane fouling potential of TOC increases in the presence of calcium, but calcium and TOC were separated by EDM into different concentrate streams.
  - No inorganic or organic compound concentrations were found in any of the EDM streams that would be considered potential membrane fouling threats. There was no variation in the EDM pilot pressures or flows throughout testing. It was

Table 3.17
EDM water quality results treating LHGW RO concentrate

Analyte	RO concentrate (mg/L)	EDM feed (mg/L)	EDM Concentrate 1 (mg/L)	EDM Concentrate 2 (mg/L)
Calcium	450	322	34	10,200
Magnesium	500	417	9	6500
Sodium	4700	4200	60,800	37,900
Chloride	7800	6280	65,800	102,000
Sulfate	2580	2220	34,200	nondetect
Silica	43.5	49.0	16	11

Table 3.18
EDM water quality results treating CGW EDR concentrate

Analyte	EDR concentrate (mg/L)	EDM feed (mg/L)	EDM Concentrate 1 (mg/L)	EDM Concentrate 2 (mg/L)
Calcium	520	226	43	14,400
Magnesium	236	43	7	5450
Sodium	163	114	31,800	3920
Chloride	400	222	11,400	45,900
Sulfate	1440	635	48,400	nondetect
Silica	22.8	25.2	15	13

concluded that the EDM pilot treated the TGW NF concentrate without fouling of the EDM membranes.

Water quality data for the EDM tests with LHGW, CGW, and OBGW concentrates are shown in Tables 3.17, 3.18, and 3.19. The results in these tests were as described for the TGW concentrate. The EDM concentrate was separated into two highly soluble streams, and silica was unaffected by EDM treatment. Pressures and flows did not vary in any of the tests. The water quality data and the operating pressures and flows indicated no membrane fouling occurred.

EDM Recovery

Recovery for EDM has the same definition as it does for RO: the ratio of product water flow to feed flow. The difference between feed and product flows is the flow that leaves the EDM stack as concentrate.

In EDM, concentrate flow comes from water transported from the diluate and NaCl cells to concentrate cells. This transport occurs by two mechanisms: (1) electroosmosis, the transport of water molecules associated with ions, and (2) osmosis driven by the concentration difference between the diluate and concentrate streams. This loss of product water determines recovery for

Table 3.19
EDM water quality results treating OBGW NF concentrate

Analyte	NF concentrate (mg/L)	EDM Concentrate 1 (mg/L)	EDM Concentrate 2 (mg/L)
Calcium	770	47	19,200
Magnesium	86	4	2600
Sodium	339	41,500	15,800
Chloride	683	37,800	64,300
Sulfate	135	40,900	147
Silica	65	12	13

Table 3.20
EDM recovery and water transfer rate in the pilot tests

Water	Total concentrate flow (L/h)	Total product flow (L/h)	Recovery	Rate of water transfer, λ (moles H_2O/eq)
TGW	0.16	125	99.9%	7.7
LHGW	0.28	125	99.8%	7.4
CGW	0.13	125	99.9%	8.2
OBGW	0.13	125	99.9%	7.6

an EDM stack, and the amount of water transferred to the concentrate cells by osmosis and electroosmosis is typically proportional to equivalents of ions transferred.

Recovery data from EDM pilot tests with the water sources are shown in Table 3.20. Recovery ranged between 99.8 and 99.9 percent for the water sources. The rate of water transfer by osmosis and electroosmosis, λ, ranged between 7.4 and 8.2 moles of water per equivalent of ions transferred.

EDM Energy

In electrolytic solutions under an applied electrical potential, current is carried by the movement of ions, and the current measured in an electrodialysis stack is proportional to the equivalents of ions removed. This relationship is expressed in Faraday's law, where F is Faraday's constant (96,500 A·s eq^{-1}), q is diluate flow (L s^{-1}), ΔC is the change in concentration between the influent and effluent of the diluate stream (eq L^{-1}), and ζ is the current efficiency factor.

$$I = \frac{Fq\Delta C}{\zeta}$$

Current is related to applied voltage and resistance by Ohm's law, and power is the product of current and voltage. Resistance across an electrodialysis stack depends on membrane characteristics and conductivities of solutions in the cells. The pilot-scale data required to determine energy requirements for full-scale EDM are voltage, current, and solution conductivities.

Table 3.21
EDM pilot results with TGW concentrate

Run time (hrs)	Current (A)	EDM feed conductivity (mS/cm)	Concentrate 1 conductivity (mS/cm)	Concentrate 2 conductivity (mS/cm)	NaCl conductivity (mS/cm)
0	1.9	4.94	43.2	52.9	50.8
0.7	2.0	4.98	49.5	57.6	49.6
1.17	2.0	4.55	56.1	64.3	48.2
1.67	1.9	4.21	62.0	69.5	46.9
2.17	1.9	3.99	66.2	73.2	45.2
2.67	1.9	3.87	70.7	75.2	44.1
3.17	1.9	3.83	80.4	80.4	42.8
5.17	1.9	3.72	92.9	92.5	62.1
5.67	1.9	3.73	97.2	96.1	60.9
6.17	1.9	3.74	98.8	96.8	59.9
6.67	1.9	3.74	102.7	102.5	58.9
7.17	1.9	3.73	105.8	105.6	57.6

$$I = \frac{V}{R}$$
$$P = IV$$

During electrodialysis with EDM, ions are drawn from the diluate and NaCl cells into the concentrate cells. Concentrate cell conductivities increase while those in the diluate and NaCl cells decrease until equilibrium is reached between the forces promoting and resisting ion transfer.

Table 3.21 shows data from the EDM pilot as it progressed from startup to a steady rate of ion transfer. These data are from tests with the TGW concentrate, but they are representative of the pattern observed in tests with each water source. Stack voltage was held at 8 V. EDM diluate was blended with TGW NF concentrate in a 10:1 ratio in the EDM feed tank. The NF concentrate conductivity was 6.5 mS/cm. The conductivity of the Na_2SO_4 electrode rinse ranged between 31 and 33 mS/cm during the test. EDM feed and NaCl conductivities decreased with time and concentrate conductivities increased with time. NaCl conductivities spiked at 5.2 hours because more salt was added to the NaCl feed tank. EDM performance reached steady-state over the last two hours of the test with EDM feed conductivity at 3.7 mS/cm. This represented a 47 percent reduction of the NF concentrate conductivity.

Results from a similar EDM experiment with LHGW RO concentrate are shown graphically in Figure 3.32. Conductivities in the two concentrate streams increased from the start of the test and approached a steady-state plateau at hour 9. It took longer to approach steady-state with the LHGW concentrate because it the highest TDS of the sources test, but the parabolic shape of the concentrate conductivity profiles was observed with each water source. The pump feeding RO concentrate was turned off at hour 12 to evaluate EDM performance with a longer hydraulic residence time. After 150 minutes, EDM feed conductivity was reduced from 25.8 mS/cm to 10.6 mS/cm, calcium from 450 mg/L to 30 mg/L, and sulfate from 2600 mg/L to 900 mg/L.

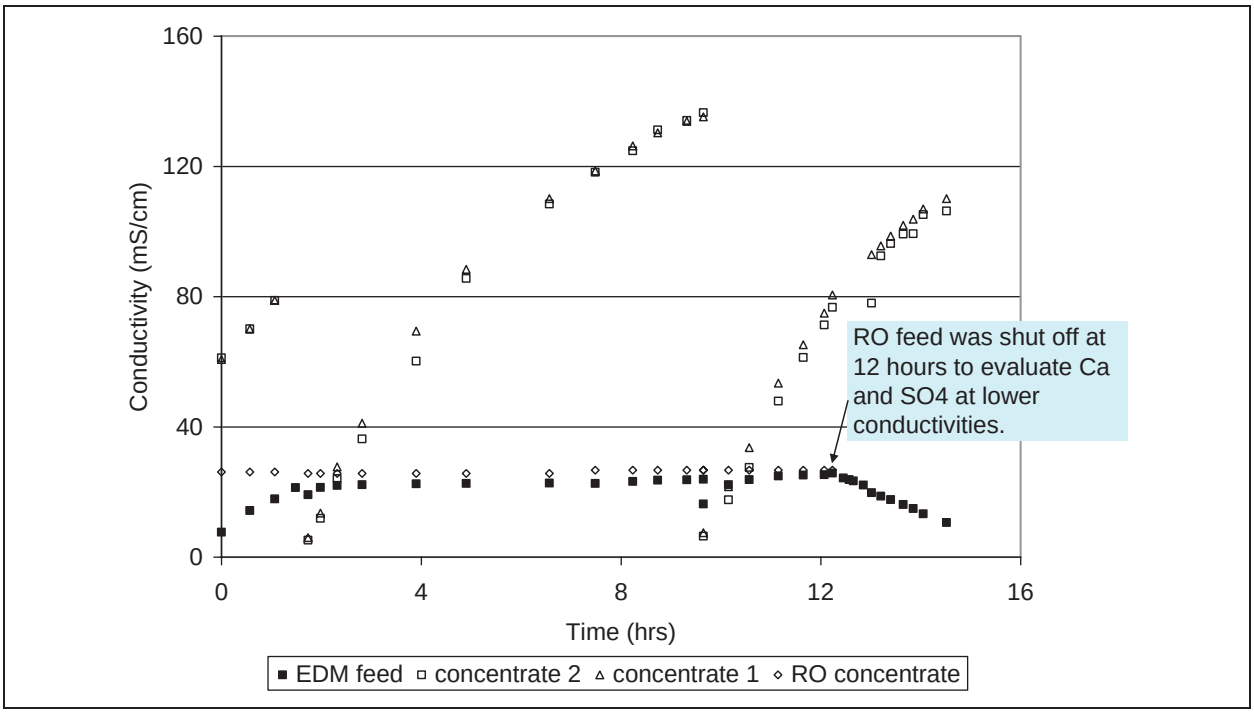

Figure 3.32 EDM test results with LHGW RO concentrate

Table 3.22
EDM pilot results for all sources

Source	Current (A)	EDM feed conductivity (mS/cm)	Concentrate 1 conductivity (mS/cm)	Concentrate 2 conductivity (mS/cm)	Current efficiency ζ
TGW	1.9	3.7	106	106	0.84
LHGW	3.0	22.4	170	160	0.87
CGW	1.4	2.4	80	76	0.77
OBGW	1.7	3.0	105	102	0.82

Results for each of the water sources at steady-state operation of the EDM pilot are shown in Table 3.22. The stack voltage was 8 V in each test. Current during the EDM tests ranged from 1.4 to 3.0 A. Current efficiency factors were between 0.77 and 0.87.

Each water source was tested with EDM voltage held constant at 8 volts to provide a consistent set of operating conditions for evaluation of EDM across a range of TDS concentrations. Experiments, however, were also conducted to evaluate the effect of voltage on ion transfer in the EDM pilot.

Figure 3.33 shows the relationship between voltage and current during one such experiment with the LHGW RO concentrate. EDM stack voltage was increased incrementally while recording current. Current and therefore the rate of ion extraction increased in proportion to an increase in voltage in the 3 to 12 volt range tested.

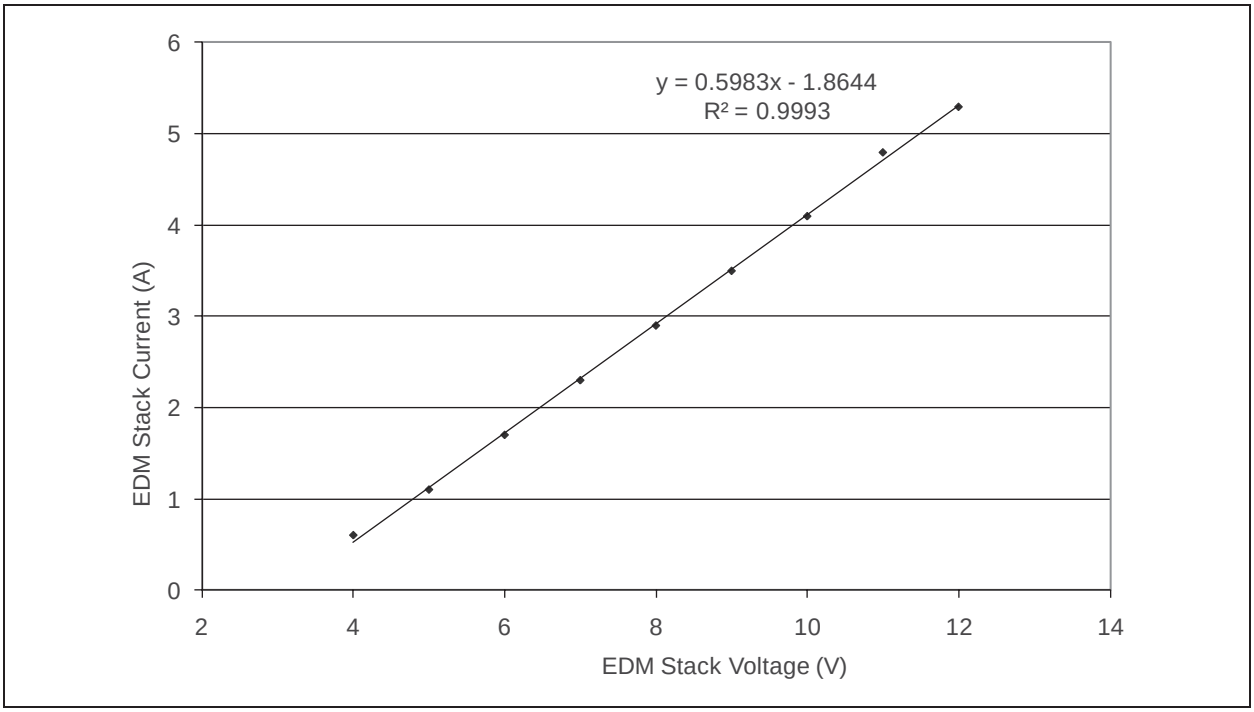

Figure 3.33 EDM experiment with LHGW RO concentrate illustrating the relationship between voltage and current

In addition to voltage drops across cells, there is also a voltage drop due to reactions at the electrodes. A typical full-scale EDM stack contains at least 100 cell sets between a pair of electrodes, and voltage drop at electrodes is negligible relative to voltage across all of the cell sets.

The EDM pilot stack, however, contained five cell sets between a pair of electrodes, and consequently voltage drop at the electrodes comprised a significant fraction of the stack voltage. In order to use pilot data to predict full-scale performance, voltage drop attributable to the pilot electrodes and electrode rinse solutions had to be quantified.

An experiment was conducted to determine voltage drop at the pilot stack electrodes. The pilot stack was disassembled and emptied of all membranes except a single cation exchange membrane (CMS). The modified EDM stack was operated with four different strength Na_2SO_4 solutions while varying voltage and measuring current to evaluate electrode voltage drop as a function of solution conductivity.

The results of this experiment are shown in Figure 3.34. A linear equation fit the data for each Na_2SO_4 solution with an intercept of 3 volts. Potential drop at electrodes is the sum of a fixed component due to resistance through stack materials and voltage drop due to solution and membrane resistances. Consequently, the intercept represents the fixed voltage drop at the electrodes (U_0), and the slope of each graph represents the sum of membrane resistance, R_m, and solution resistance, R_{sol}, at the solution conductivity tested. The resistance of the membrane is the area resistance, ρ (ohm·cm^2), divided by the membrane area A (cm^2). The voltage drop at the electrodes (U_e) is

$$U_e = U_0 + I(R_{sol} + R_m) = U_0 + I\left(R_{sol} + \frac{\rho}{A}\right)$$

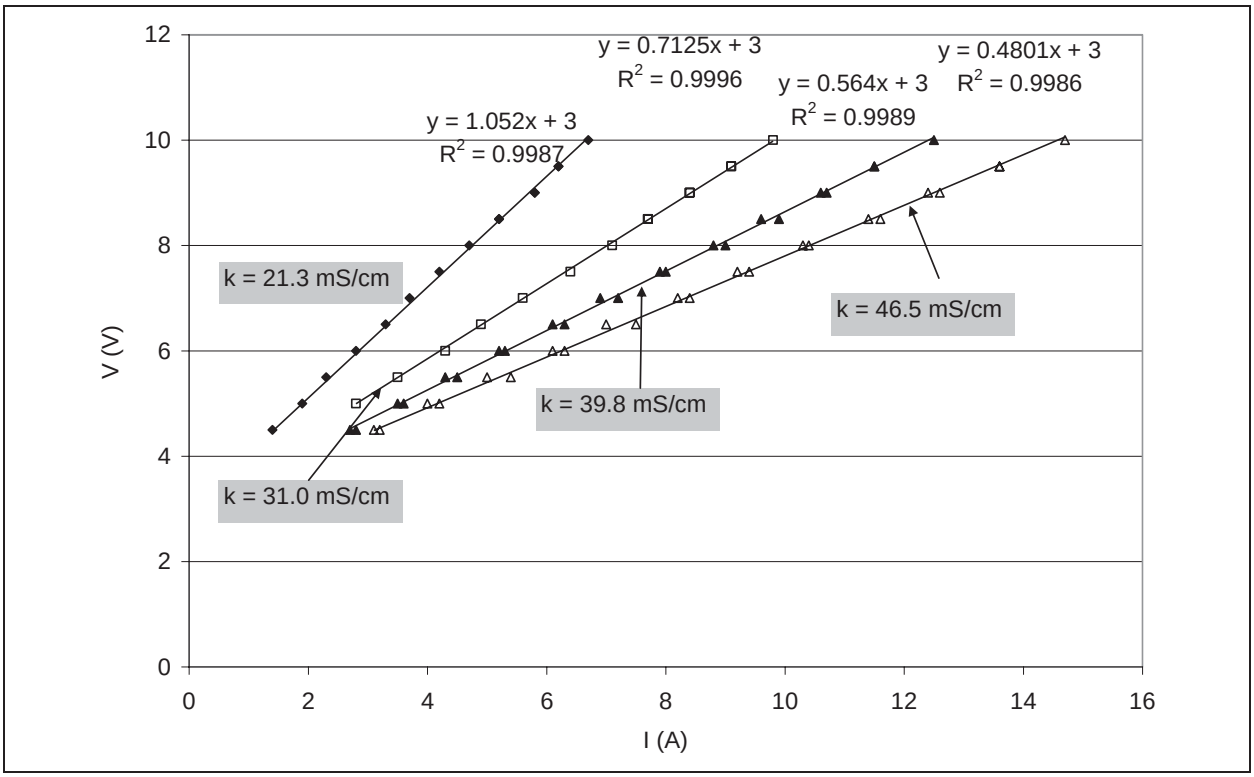

Figure 3.34 Results of pilot experiment to isolate voltage drop at the electrodes

The slope of the graph is $R_m + R_{sol}$. Therefore, R_{sol} can be calculated from the slope of the linear regression for each data set and the known area resistance of the membrane. The CMS membrane used in the experiment had an area resistance of 3 ohm·cm^2 and a membrane area of 200 cm^2. Therefore, the membrane resistance was 0.015 ohm. Because solution resistance varies linearly with conductivity, the product of R_{sol} and k was a constant.

Calculated values of R_{sol} and $R_{sol} \times k$ are shown in Table 3.23. Solution resistance was the difference between the graph slope and the membrane resistance. The calculated values of $R_{sol} \times k$ were within 2 percent of one another, and the average value was 21.8 ohms mS cm^{-1}. Therefore, the relationship $R_{sol} = 21.8\ k^{-1}$ was used in the model to calculate solution resistance in the electrode compartments as a function of solution conductivity.

During normal operation with all membranes in place, the pilot stack contained two electrode membranes, a CMB membrane at the anode and an AHA membrane at the cathode. The area resistances were 4.5 Ω cm^2 for the CMB membrane and 4.1 Ω cm^2 for the AHA membrane. The total membrane resistance was 0.043 Ω. Therefore, the electrode voltage drop in the pilot unit at any conductivity k was calculated as follows:

$$U_e = 3 + I\left(\frac{21.8}{k} + 0.043\right)$$

Voltage drop at the electrodes was subtracted from stack voltage to calculate the power used in each pilot test (Table 3.24). Power requirements for the pilot tests ranged from 1.1 to 1.8 W per cell.

Table 3.23
Calculated values of the product of solution resistance and conductivity (R_{sol} × k)

k (mS cm^{-1})	21.3	31.0	39.8	48.7
Slope (Ω)	1.052	0.713	0.713	0.480
R_{cm} (Ω)	0.015	0.015	0.015	0.015
R_{sol} (Ω)	1.037	0.698	0.549	0.465
R_{sol} × k (Ω mS cm^{-1})	22.0	21.6	21.9	21.7

Table 3.24
Power required per EDM cell in the pilot tests

Source	Current (A)	Voltage applied to stack (V)	Voltage drop at electrodes (V)	Voltage per cell (V)	Power (w/cell)
TGW	1.9	8	4.22	0.76	1.4
LHGW	3.0	8	4.80	0.60	1.8
CGW	1.4	8	3.96	0.81	1.1
OBGW	1.7	8	4.01	0.80	1.4

Fluoride Removal Pilot Results

Pilot tests were conducted to evaluate fluoride removal from the AR source with AA and with a calcite contactor. The objective was to compare each process with RO for fluoride removal followed by ZLD concentrate treatment using EDM, and a crystallizer.

AA Column Pilot Test

The pilot column was operated with an average EBCT of 7.8 minutes, and 36 bed volumes of AR sample spiked with fluoride were treated. The fluoride concentration in the feed was 6.2 mg/L, and the pH was 6.2. Effluent fluoride concentrations were below the detection limit of 0.1 mg/L for the duration of the test.

Calcite Column Pilot Test

The results of the calcite column test are shown in Table 3.25. The pilot column was operated with an average EBCT of 16 minutes. Two batches of AR sample were tested. In the first batch, fluoride was spiked to 3.8 mg/L and pH was 7.0. In the second batch, fluoride was spiked to 5.8 mg/L and pH was adjusted to 4.2. Fluoride removal in the calcite column was not effective at either pH.

FULL-SCALE EVALUATIONS

The results of the preliminary analyses, bench-scale tests, and pilot-scale tests were used to evaluate full-scale zero liquid discharge desalination for seven brackish water sources. The sources comprised the five water sources tested plus two additional sources evaluated in desktop studies.

Table 3.25
Calcite column test results

Run time (hrs)	Influent F (mg/L)	Effluent F (mg/L)	Influent pH	Effluent pH	Effluent Ca (mg/L)
3.5	3.8	3.2	7.0	7.5	130
5.5	5.8	5.6	4.2	7.6	120
8.0	5.8	5.6	4.2	7.6	150
9.5	5.8	5.6	4.2	7.6	145

Pilot tests were conducted to develop data for evaluation of full-scale performance of EDM, MIEX, AA, and calcite contactor. Full-scale evaluations were performed with pilot data by scaling pilot results up to full-scale. For MIEX, AA, and calcite, treatment criteria per unit of water treated developed at pilot-scale were appropriate for full-scale application. More detailed evaluation, however, was required to translate EDM pilot results to full-scale because of the number of variables that govern EDM performance and because of the disproportionate effect of resistances at the electrodes and across the stack manifold at pilot-scale.

Equations describing voltage drop and resistance in electrodialysis stacks are well known and have been used for decades in design and optimization of the electrodialysis process for a variety of applications (Strathmann 2004). These equations were used to develop a model for EDM (Appendix B). Input data for the model are influent water quality, EDM design and operating parameters, and desalination treatment goals. The input data are used to calculate voltage drop, concentrate flows, and concentrate water quality for EDM. The EDM model was calibrated with data from the EDM pilot test of each water source and used to calculate full-scale EDM power requirements.

Full-scale design parameters and treatment costs were developed for each water source. Treatment costs are summarized in the text and detailed cost calculations are presented in Appendix C.

The seven water sources and level of evaluation were as follows:

- TGW—bench- and pilot-scale testing.
- LHGW—bench- and pilot-scale testing.
- CGW—bench- and pilot-scale testing.
- OBGW—bench- and pilot-scale testing.
- AR—bench- and pilot-scale testing.
- St. Johns River (SJR)—desktop study
- Indian River Lagoon (IRL)—desktop study.

Variants of Option 3 (MIEX, EDM, and crystallizer) were evaluated for each water source. MIEX was omitted for the sources that did not have high NOM concentrations. Option 3 was evaluated with and without further treatment of EDM concentrate to develop beneficial products to assess potential economic and environmental advantages of this enhancement. An electricity cost of $0.12 per kWh was used for all cost calculations.

Option 3 costs for each source were compared to the cost for ZLD with the established method shown in Figure 3.35. The established ZLD method was labeled Option 4. In Option 4, all

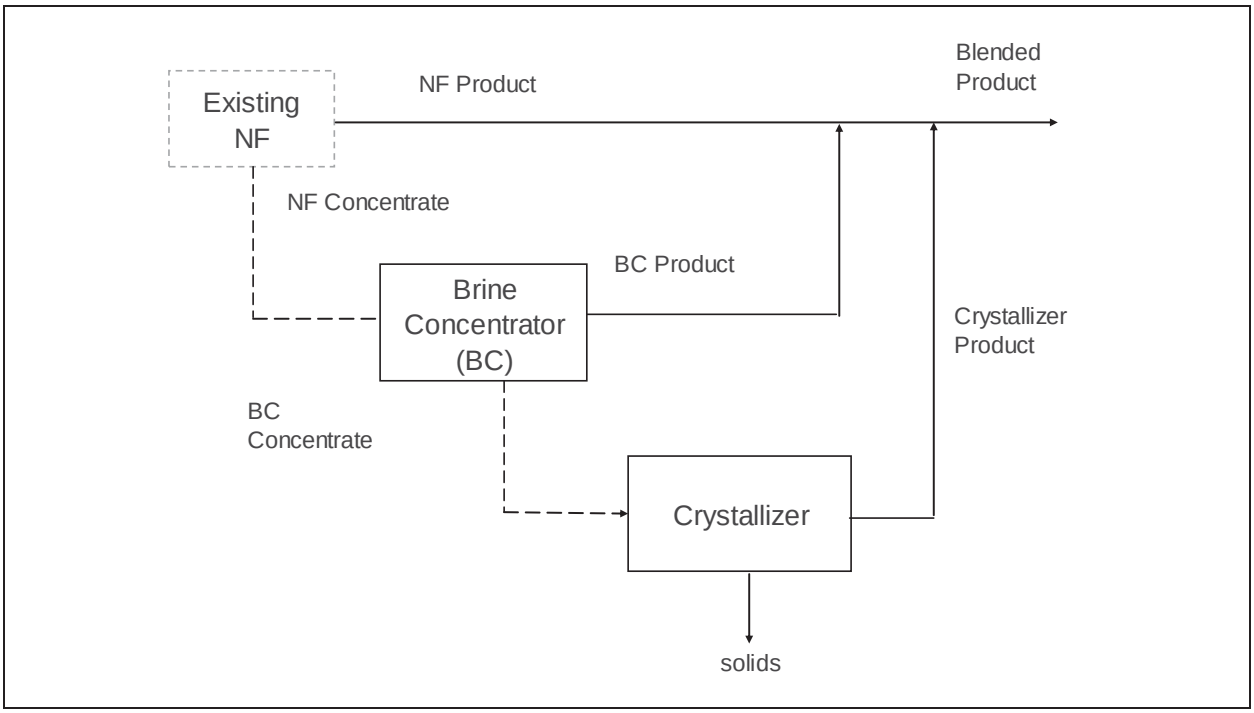

Figure 3.35 Option 3: Conventional ZLD approach with brine concentrator and crystallizer

of the concentrate from the primary desalination device is treated by thermal desalination: a brine concentrator followed by a crystallizer. This is a mature and proven method for achieving ZLD, but it is expensive and energy intensive. Option 4 costs provided a bench-mark for measuring the potential for reducing ZLD costs with Option 3.

TGW

The following three variations of the Option 3 ZLD process were evaluated for TGW and compared to the established ZLD method of Option 4:

- Option 3A—Option 3 without treatment of EDM concentrate to derive beneficial products.
- Option 3B—Option 3 with treatment of EDM concentrate to derive beneficial products.
- Option 3C—Option 3 without MIEX treatment and without treatment of EDM concentrate to derive beneficial products.
- Option 4 – thermal treatment of primary RO concentrate with a brine concentrator and crystallizer

The variants of Option 3 were identified to explore a range of potential costs for ZLD desalination of TGW. In Option 3A, no attempt is made to derive beneficial use of EDM concentrate, rather the EDM concentrate is discharged directly to the crystallizer. In Option 3B, EDM concentrate is treated further to derive beneficial products. Advantages of beneficial use of EDM concentrate include reduction in NaCl costs for EDM and reduction in required crystallizer capacity. These savings are counteracted to some extent by costs for the additional treatment processes

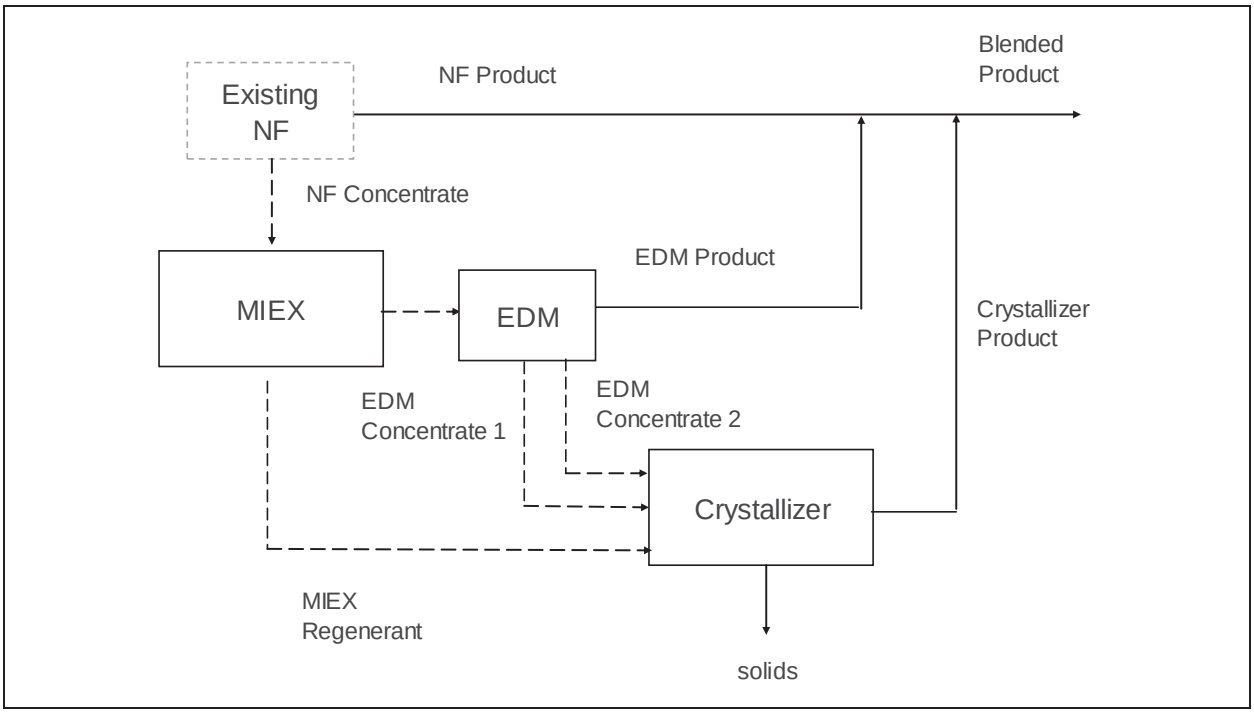

Figure 3.36 TGW Option 3A (Option 3 without treatment of EDM concentrate)

for EDM concentrate. Testing to demonstrate development of beneficial products from EDM concentrate was beyond the scope of this project, but the processes that would be used for this purpose are well understood with a long history of use in water treatment and industrial applications. Options 3A and 3B can be compared to assess the potential cost benefits effects of treating EDM concentrate to develop usable products. Options 3A and 3C can be compared to evaluate the effect of high organic concentrations on ZLD costs.

TGW Option 3A (Option 3 Without Treatment to Develop Beneficial Use of EDM Concentrate)

The basic ZLD process (Option 3A) for the TGW source is shown in Figure 3.36. Concentrate from the existing NF membranes is treated with MIEX for TOC removal. MIEX treated concentrate is desalinated with EDM. EDM generates two concentrate streams. The EDM concentrate streams and MIEX regenerant are treated in a crystallizer. The final product water is a blend of the NF, EDM, and crystallizer product waters.

MIEX criteria are shown in Table 3.26. MIEX was included in the process train for TOC removal. Average TOC concentrations for the TGW source were 8 mg/L in the NF feed, 0.4 mg/L in the NF permeate, and 50 mg/L in the NF concentrate. In the pilot test, the MIEX treatment reduced TOC to 20 mg/L in the EDM feed at 50 BVT. Jar tests with MIEX with TGW NF concentrate produced similar results. A 50 BV MIEX regeneration frequency was used for full-scale evaluation.

The treatment goal for EDM was calculated based on 80 percent recovery with the existing NF membranes, 200 mg/L TDS NF permeate, 2900 mg/L TDS NF concentrate, and a blended product goal of 400 mg/L TDS or less. The target TDS concentration for the EDM product, C_{EDM}, was 1200 mg/L.

Table 3.26
MIEX criteria and calculations for TGW

Parameter	Value
Regeneration frequency	50 BV
NaCl regenerant concentration	100 g/L
Regeneration loading	360 g NaCl/ L resin
Regeneration volume	0.072 m^3 /m^3 product water
Resin regeneration rate	0.02 m^3 resin/m^3 product water
Initial TOC	50 mg/L
Treated TOC	20 mg/L
TOC accumulated in regenerant	30 g/ m^3 product water
TOC limit in regenerant	10 g/L
Maximum reuse of regenerant	24 times
NaCl consumed per mass TOC removed	1.7 g/g TOC removed
NaCl consumption	50 g/ m^3 product water
Regenerant byproduct	0.003 m^3 /m^3 product water
MIEX attrition rate	0.002 L resin / m^3 product water
MIEX unit cost	$14 per L resin
NaCl unit cost	$0.11 per kg

$$0.2 \times C_{EDM} + 0.8 \times 200 = 400$$

$$C_{EDM} = 1200 \frac{mg}{L}$$

Input data used in the EDM power calculations for TGW are shown in Table 3.27. A design cell velocity of 6 cm/s was used, and therefore the flow per cell was 0.017 L/s. The EDM stack was evaluated with the membranes used in the EDM pilot. These membranes had area resistances ranged from 2.5 to 6.5 Ω cm^2. Current utilization factor and water transfer coefficient values were as determined during pilot testing. An average NaCl conductivity of 200 mS cm^{-1} was used. The solubility limit of NaCl is around 425 mS cm^{-1}, and therefore a higher NaCl concentration could have been selected.

The effect of NaCl conductivity on EDM energy required to meet the specified treatment goal for TGW is shown in Figure 3.37. Energy consumption decreases as NaCl conductivity increases because resistance in the NaCl solution decreases as its conductivity increases.

Results of the EDM energy calculations are shown in Table 3.28. A cell voltage of 0.58 V was required to generate the 56 A current needed to reduce TDS from 3000 mg/L in the EDM feed to 1200 mg/L in the EDM diluate. The current density was 0.0086 A/cm^2, and the polarization parameter (current density divided by normality of the diluate solution) was 62 A cm/eq. As a rule of thumb, power polarization in electrodialysis should be maintained below 200 A cm eq^{-1} to avoid operation near the limiting current density. Model current density for TGW was safely within good design practice. Cell flow rates were 0.0168 L/s in the feed, 0.0165 L/s in the diluate, and a total of 0.0003 L/s in the two concentrate cells. Recovery of the EDM stack was 98.4 percent. The stack

Table 3.27
EDM model input for TGW NF concentrate

Parameter	Value
Flow per cell set	0.0168 L/s
Cell sets per stack	100
Membrane width	40 cm
Membrane length	160 cm
Membrane area	6400 cm^2
Cell width	0.07 cm
Cell velocity	6 cm/s
Shadow factor	1.2
CMX membrane area resistance	3 Ω cm^2
AMX membrane area resistance	2.5 Ω cm^2
CMS membrane area resistance	6.5 Ω cm^2
AMS membrane area resistance	6.5 Ω cm^2
Water transfer coefficient	7.6 mol/eq
Current utilization factor	0.84
Average NaCl cell conductivity	200 mS cm^{-1}
Feed water TDS	3000 mg/L
Feed water temperature	298 K

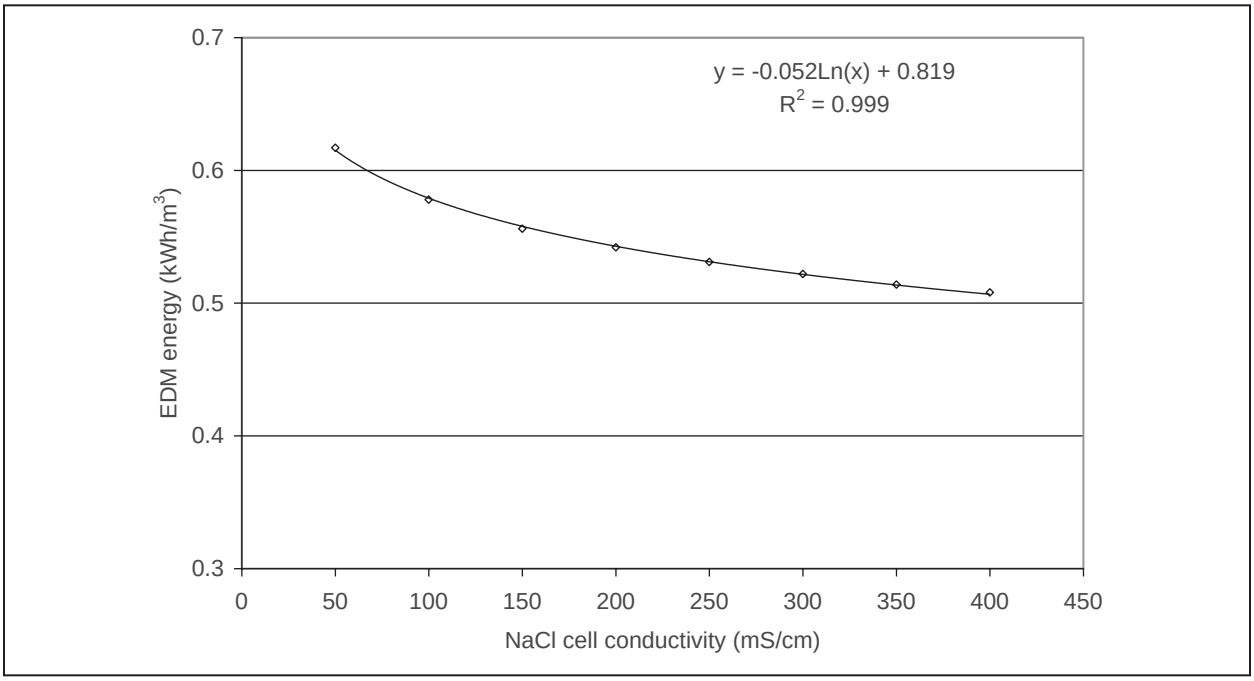

Figure 3.37 Effect of NaCl cell conductivity on EDM energy

Table 3.28
EDM model results for TGW NF concentrate

Parameter	Value
Diluate TDS	1200 mg/L
Current	56 A
Current density	0.0088 A/ cm^2
Power polarization	63 A cm/eq
Concentrate 1 conductivity	373 mS/cm
Concentrate 2 conductivity	373 mS/cm
Diluate flow per cell	0.0165 L/s
Total concentrate flow per cell	0.0003 L/s
EDM recovery	98.4 %
Voltage per cell	0.60 V
Electrode voltage	5 V
Stack voltage	65 V
Stack power	3.4 kW
EDM energy requirement	0.60 kWh/m^3

Table 3.29
Fraction of TGW NF concentrate treated by each process if EDM concentrate is not treated to produce beneficial products

Process	Fraction of NF concentrate treated
MIEX®	1.0
EDM	1.0
Crystallizer	0.019

power was 3.2 kW. The EDM energy required to meet the diluate treatment goal was 2.12 kWh/kgal of concentrate treated.

The fraction of TGW NF concentrate treated by each successive process if EDM concentrate is not treated to develop beneficial products is shown in Table 3.29. All of the NF concentrate would be treated with MIEX®, and the MIEX® product water would be treated in EDM. Approximately 0.003 m^3 of MIEX regenerant would be sent to the crystallizer for each m^3 product water. The EDM would achieve 98.4 percent recovery, and its concentrate would be treated in the crystallizer.

Treatment costs for TGW with Option 3A are summarized in Table 3.30. All costs are per m^3 of total concentrate recovered. Energy requirements for MIEX were considered negligible relative to those of the EDM and crystallizer. Sodium chloride is consumed by MIEX for regeneration of the resin and by EDM to balance ion transfer from the diluate to the concentrate cells. Materials costs comprise replacement of MIEX resin and replacement of EDM membranes. An attrition rate of 2 L MIEX resin per 1000 m^3 water treated was used for MIEX replacement cost. A replacement frequency of 7 years was used for EDM membrane replacement cost. Capital costs

Table 3.30
TGW Option 3A treatment costs

Process	Energy cost ($/m^3)	NaCl cost ($/m^3)	Materials ($/m^3)	O&M cost ($/m^3)	Capital cost ($/m^3)	Total cost ($/m^3)
MIEX®		$0.01	$0.03	$0.03	$0.22	$0.25
EDM	$0.06	$0.19	$0.01	$0.31	$0.11	$0.42
Crystallizer	$0.17			$0.17	$0.15	$0.32
Total	$0.23	$0.20	$0.04	$0.51	$0.48	$0.99

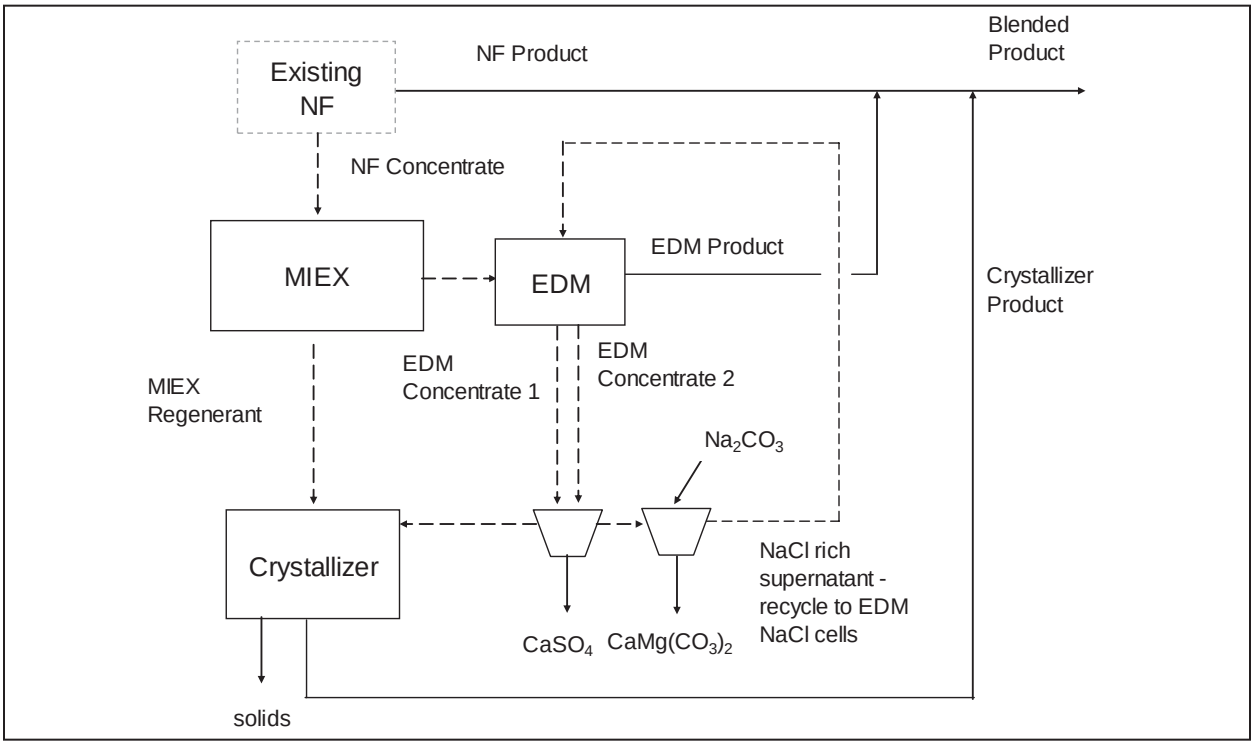

Figure 3.38 TGW Option 3B (Option 3 with treatment of EDM concentrate)

were amortized over 20 years at a 6 percent rate of return. For this version of Option 3, the total treatment cost was $0.99 per m^3 of concentrate treated, of which approximately half was capital cost and half O&M cost. The crystallizer accounted for one-third the total treatment cost even though it treated less than 2 percent of the flow.

TGW Option 3B (Option 3 With Treatment to Develop Beneficial Use of EDM Concentrate)

Option 3B is illustrated in Figure 3.38. In this option, EDM concentrate is treated to develop calcium sulfate, dolomite ($CaMg(CO_3)_2$), and a NaCl solution that is recycled to the EDM process. In the first step, the two concentrate streams, one rich in calcium and the other rich in sulfate, are combined to precipitate calcium sulfate. Calcium sulfate has many uses including: as a building product, as a coating agent in paper production, as a soil conditioner, as a paint conditioner, and in manufacture of sulfuric acid. Dolomite can be used as a material in concrete, in steel manufacture,

Table 3.31
TGW water quality through the EDM concentrate treatment steps

Ion	EDM Concentrate 1 (mg/L)	EDM Concentrate 2 (mg/L)	Step 1 feed (mg/L)	Step 1 supernatant (mg/L)	Step 2 supernatant (mg/L)
Ca	111	35,176	17,643	1645	136
Mg	11	5241	2626	2626	1735
Na	83,848	33,051	58,450	58,450	61,900
K	115	874	500	500	500
Cl	63,993	129,386	96,689	96,689	96,689
SO_4	88,094	0	44,047	5675	5675
HCO_3	719	0	360	360	349

and as a soil amendment in agriculture. Part of the supernatant is sent to the crystallizer, and the remainder is treated in a second precipitation step. The ratio of these flows depends on the amount of NaCl that can be reused in the EDM process. In the second step, Na_2CO_3 is added to precipitate dolomite. The supernatant from the second precipitation step is rich in sodium chloride and is recycled to the NaCl cells of the EDM to replace NaCl transferred during electrodialysis.

Results of calculations to project water quality through the EDM treatment steps are shown in Table 3.31. The feed to the Step 1 process is the blend of the two EDM concentrate streams. Calcium sulfate is precipitated in Step 1, and the supernatant from Step 1 is rich in magnesium, sodium, and chloride. Half the supernatant is discharged to the crystallizer to be evaporated and recovered as product water, and the remainder is treated in a second precipitation. A soda ash dose of 8,000 mg/L is added in Step 2 to precipitate dolomite. The sodium chloride rich supernatant from Step 2 is recycled to the EDM process to replace NaCl transferred to concentrate cells during electrodialysis. The solids produced are 69 kg $CaSO_4$ and 7.6 kg dolomite per m^3 EDM concentrate treated. The EDM concentrate flow is 1.6 percent of the total NF concentrate recovered in ZLD treatment. On the basis of total concentrate recovered, solids produced are 1.1 kg $CaSO_4$ and 0.1 kg dolomite per m^3 EDM concentrate treated product recovered from NF concentrate.

The advantages of treating the EDM concentrate for beneficial use would be as follows:

- The capacity required for the crystallizer would be reduced by 50 percent.
- The recycled EDM concentrate would provide the NaCl required by EDM and MIEX virtually eliminating the cost for new NaCl.
- The solids produced would be used beneficially rather than being transported to a landfill.

Treatment costs for TGW with Option 3B are summarized in Table 3.32. All costs are per m^3 of total concentrate volume recovered. Energy requirements for MIEX® and the precipitative processes used to treat EDM concentrate were considered negligible relative to those of EDM and the crystallizer. Materials costs for MIEX® and EDM were estimated on the same bases as for

Table 3.32
ZLD treatment costs for TGW with Option 3B

Process	Energy cost ($/m^3)	NaCl cost ($/m^3)	Materials ($/m^3)	O&M cost ($/m^3)	Capital cost ($/m^3)	Total cost ($/m^3)
MIEX®			$0.02	$0.02	$0.22	$0.25
EDM	$0.07		$0.06	$0.13	$0.11	$0.24
EDM concentrate treatment				$0.03	$0.01	$0.04
Crystallizer	$0.08			$0.08	$0.11	$0.19
Total	$0.15		$0.08	$0.27	$0.45	$0.71

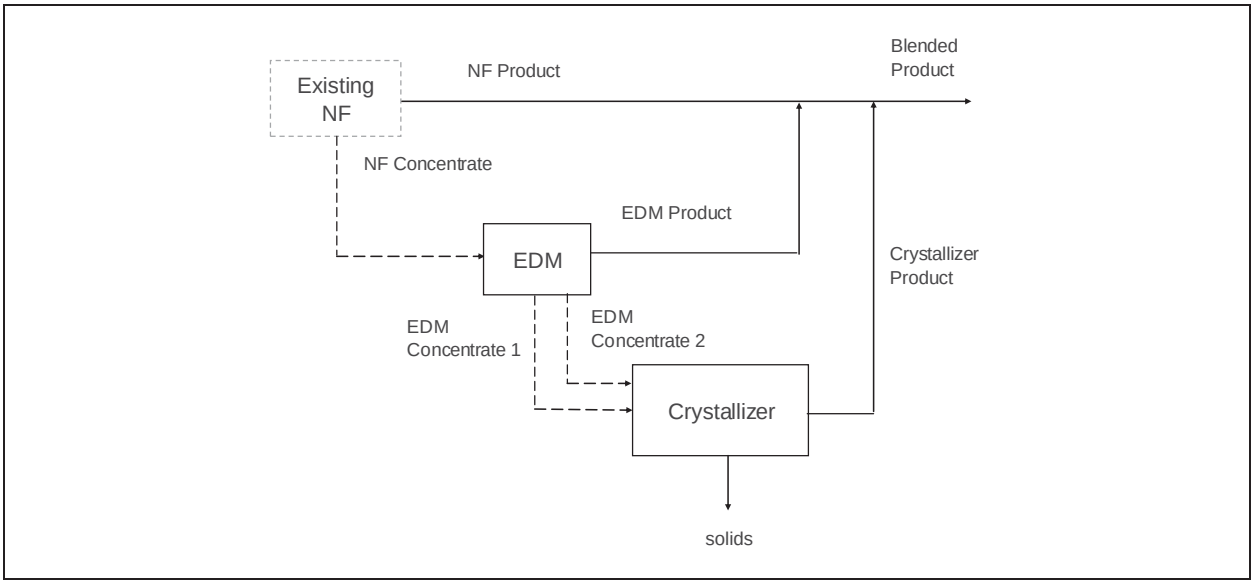

Figure 3.39 TGW Option 3C (Option 3 without MIEX® or treatment of EDM concentrate)

Option 3A. The material cost for the EDM concentrate treatment steps was the cost for soda ash. The capital cost for EDM concentrate treatment included both process steps.

TGW Option 3C: Option 3 Without MIEX® or Treatment to Develop Beneficial Use of EDM Concentrate

Option 3C is illustrated in Figure 3.39. This option is identical to Option 3A except MIEX is omitted. Options 3A and 3C can be compared to assess the effect of high NOM concentrations on ZLD treatment for the TGW source.

Treatment costs for TGW with Option 3C are summarized in Table 3.33. All costs are per m^3 of total concentrate recovered.

Table 3.33
ZLD treatment costs for TGW with Option 3C

Process	Energy cost ($/m^3)	NaCl cost ($/m^3)	Materials ($/m^3)	O&M cost ($/m^3)	Capital cost ($/m^3)	Total cost ($/m^3)
EDM	$0.07	$0.19	$0.06	$0.31	$0.11	$0.42
Crystallizer	$0.17			$0.17	$0.15	$0.32
Total	$0.24	$0.19	$0.01	$0.48	$0.26	$0.74

Table 3.34
ZLD treatment costs for TGW with Option 4

Process	Energy cost ($/m^3)	Capital cost ($/m^3)	Total cost ($/m^3)
Brine Concentrator	$2.28	$0.43	$2.71
Crystallizer	$0.21	$0.17	$0.38
Total	$2.49	$0.60	$3.09

TGW Option 4: Concentrate Treatment With a Brine Concentrator and Crystallizer

In Option 4, all of the NF concentrate is treated with thermal desalination using a brine concentrator and crystallizer. This option was included to compare the cost for ZLD desalination with Option 3 to the cost using the established ZLD approach of Option 4.

Treatment costs for TGW with Option 4 are summarized in Table 3.34. All costs are per m^3 of total concentrate recovered.

Comparison of TGW Treatment Options

The effect of treatment of EDM concentrate to develop beneficial byproducts and the effect of high organics concentrations on ZLD costs are illustrated in Figure 3.40. Comparing Option 3B with Option 3A, treating the EDM concentrate to develop products could reduce costs by almost 30 percent. Comparing Option 3C with Option 3A, treatment to remove organics appears to increase cost by about 25 percent. The ZLD approach for TGW of treating the NF concentrate with MIEX and EDM ahead of thermal desalination (Option 3) was estimated to be 3 to 5 times less expensive than treating all of the concentrate by thermal desalination (Option 4).

LHGW

The LHGW source did not contain high concentrations of organic compounds. Its unusual characteristic is a concentration of magnesium that is higher than the calcium concentration. Option 3 was evaluated without treatment of EDM concentrate for beneficial use (Option 3A) and with treatment of EDM concentrate to develop beneficial products (Option 3B). These variants of Option 3 were compared with the established ZLD method of concentrate treatment with a brine concentrator and crystallizer (Option 4).

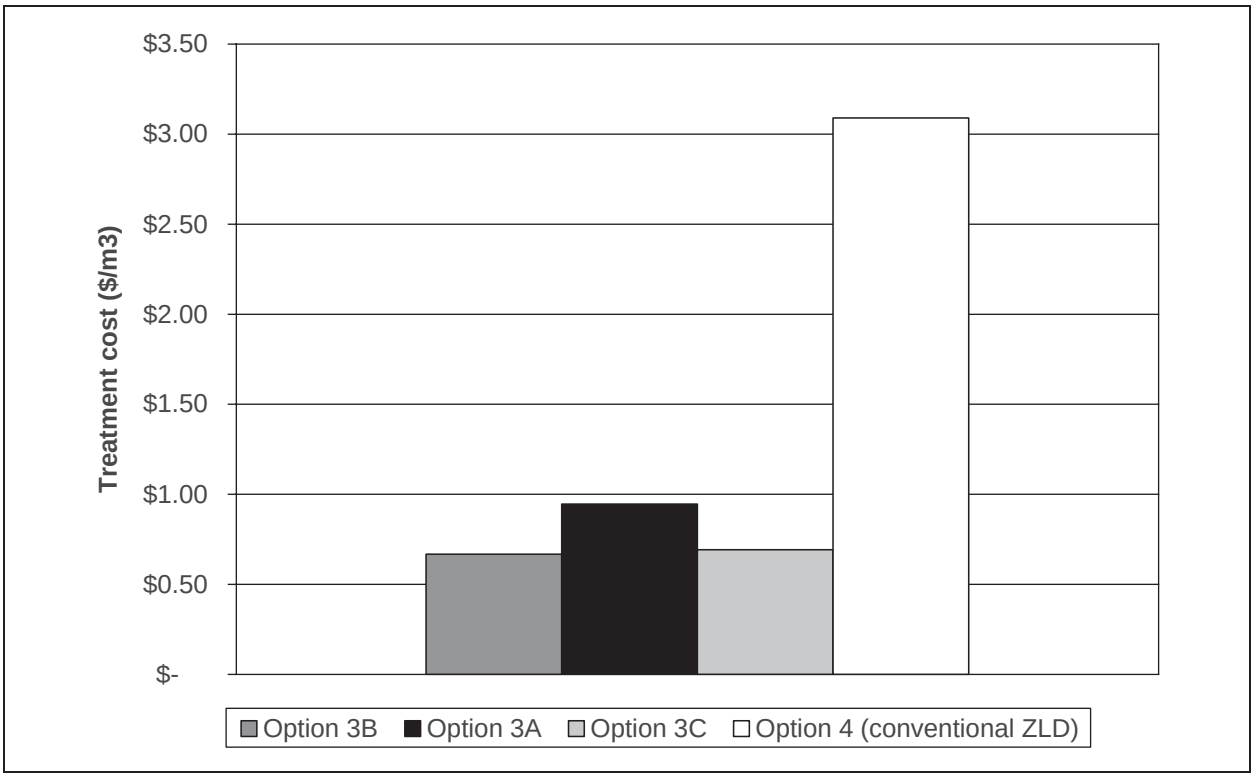

Figure 3.40 TGW comparison of ZLD treatment costs ($ per m^3 RO concentrate recovered)

LHGW Option 3A (Option 3 Without Treatment to Develop Beneficial Use of EDM Concentrate)

The basic ZLD process (Option 3A) for LHGW is shown in Figure 3.41. Concentrate from the existing RO membranes is treated with EDM. The concentrate from EDM is treated in a brine concentrator followed by a crystallizer. The final product water is a blend of the existing RO permeate, the EDM diluate, and distillate from the brine concentrator and crystallizer.

The treatment goal for EDM was calculated based on 80 percent recovery in the existing RO membranes, 100 mg/L TDS RO permeate, 16,000 mg/L TDS RO concentrate, and a blended product goal of 400 mg/L TDS or less. The target TDS concentration for the EDM product, C_{EDM}, was 1600 mg/L.

$$0.2 \times C_{EDM} + 0.8 \times 100 = 400$$

$$C_{EDM} = 1600 \frac{mg}{L}$$

Input data used in the EDM power calculations for LHGW are shown in Table 3.35. The cell velocity was 6 cm/s, and the flow per cell was 0.017 L/s. The EDM stack was evaluated with the membranes used in the EDM pilot. Current utilization factor and water transfer coefficient values were as determined during pilot testing. An average NaCl conductivity of 300 mS cm^{-1} was used. The demineralization requirement, reducing TDS from 16,000 to 1600 mg/L, was much greater than for the TGW source, and consequently two EDM stacks in series were used.

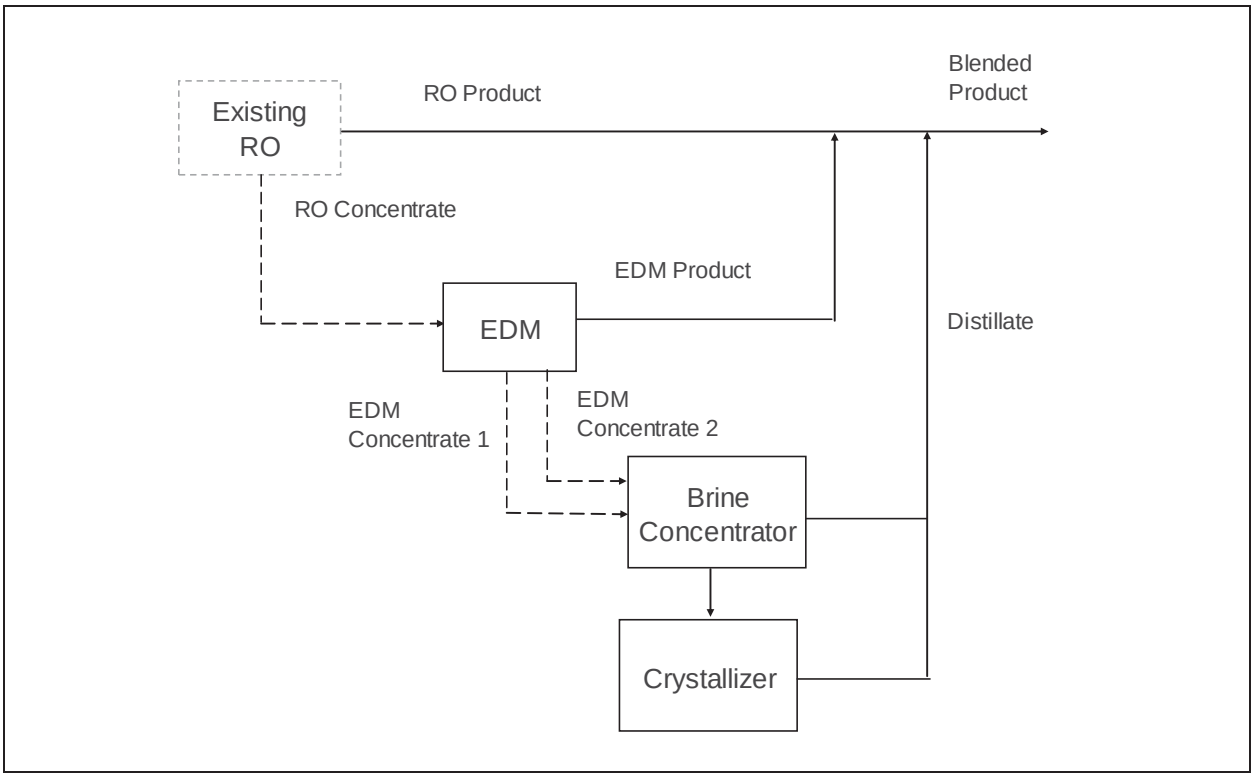

Figure 3.41 LHGW Option 3A (Option 3 without treatment of EDM concentrate)

Table 3.35
EDM model input for LHGW RO concentrate

Parameter	Value
Flow per cell set	0.0168 L/s
Cell sets per stack	100
Number of stacks in series	2
Membrane width	40 cm
Membrane length	160 cm
Membrane area	6400 cm^2
Cell width	0.07 cm
Cell velocity	6 cm/s
Shadow factor	1.2
CMX membrane area resistance	3 Ω cm^2
AMX membrane area resistance	2.5 Ω cm^2
CMS membrane area resistance	6.5 Ω cm^2
AMS membrane area resistance	6.5 Ω cm^2
Water transfer coefficient	7.6 mol/eq
Current utilization factor	0.90
Average NaCl cell conductivity	300 mS cm^{-1}
Feed water TDS	16,000 mg/L
Feed water temperature	298 K

Table 3.36
EDM model results for LHGW RO concentrate

Parameter	Value
Diluate TDS	1600 mg/L
Stack 1 current	300 A
Stack 1 current density	0.047 A/ cm^2
Stack 1 power polarization	63 A cm/eq
Stack 1 Concentrate 1 conductivity	272 mS/cm
Stack 1 Concentrate 2 conductivity	272 mS/cm
Stack 1 diluate flow per cell	0.0152 L/s
Stack 1 Total concentrate flow per cell	0.0016 L/s
Stack 1 EDM recovery	90.4 %
Stack 1 voltage per cell	1.41 V
Electrode voltage	5 V
Stack 1 voltage	146 V
Stack 1 power	44 kW
Stack 2 current	121 A
Stack 2 current density	0.019 A/ cm^2
Stack 2 power polarization	73 A cm/eq
Stack 2 Concentrate 1 conductivity	272 mS/cm
Stack 2 Concentrate 2 conductivity	272 mS/cm
Stack 2 diluate flow per cell	0.0147 L/s
Stack 2 Total concentrate flow per cell	0.0006 L/s
Stack 2 voltage per cell	1.45 V
Electrode voltage	5 V
Stack 2 voltage	150 V
Stack 2 power	18 kW
Total EDM recovery	87.2%
Total EDM energy	11.3 kWh/m^3

Results of the EDM energy calculations for LHGW are shown in Table 3.36. Cell voltages of 1.40 V in the first stack and 1.44 V in the second stack were required. The currents were 300 A in Stack 1 and 120 A in Stack 2. Power polarization factors were 63 A cm/eq in Stack 1 and 73 A cm/eq in Stack 2. Stack 1 cell flow rates were 0.0168 L/s in the feed, 0.0152 L/s in the diluate, and a total of 0.0016 L/s in the two concentrate cells. Stack 2 cell flow rates were 0.0152 L/s in the feed, 0.0145 L/s in the diluate, and a total of 0.0006 L/s in the two concentrate cells. Recovery of the two EDM stacks was 87.2 percent. The total power of the two stacks was 60 kW, and the total EDM energy required to meet the diluate treatment goal was 10.8 kWh/m^3.

Treatment costs for LHGW with Option 3A are summarized in Table 3.37. All costs are per m^3 of total concentrate recovered. The total treatment cost was $4.33 per m^3 of RO concentrate recovered.

Table 3.37
ZLD treatment costs for LHGW with Option 3A

Process	Energy cost ($/m^3)	NaCl cost ($/m^3)	Materials ($/m^3)	O&M cost ($/m^3)	Capital cost ($/m^3)	Total cost ($/m^3)
EDM	$1.35	$1.50	$0.11	$2.96	$0.22	$3.18
Brine concentrator	$0.29			$0.29	$0.14	$0.43
Crystallizer	$0.54			$0.54	$0.18	$0.72
Total	$2.14	$1.50	$0.03	$3.79	$0.54	$4.33

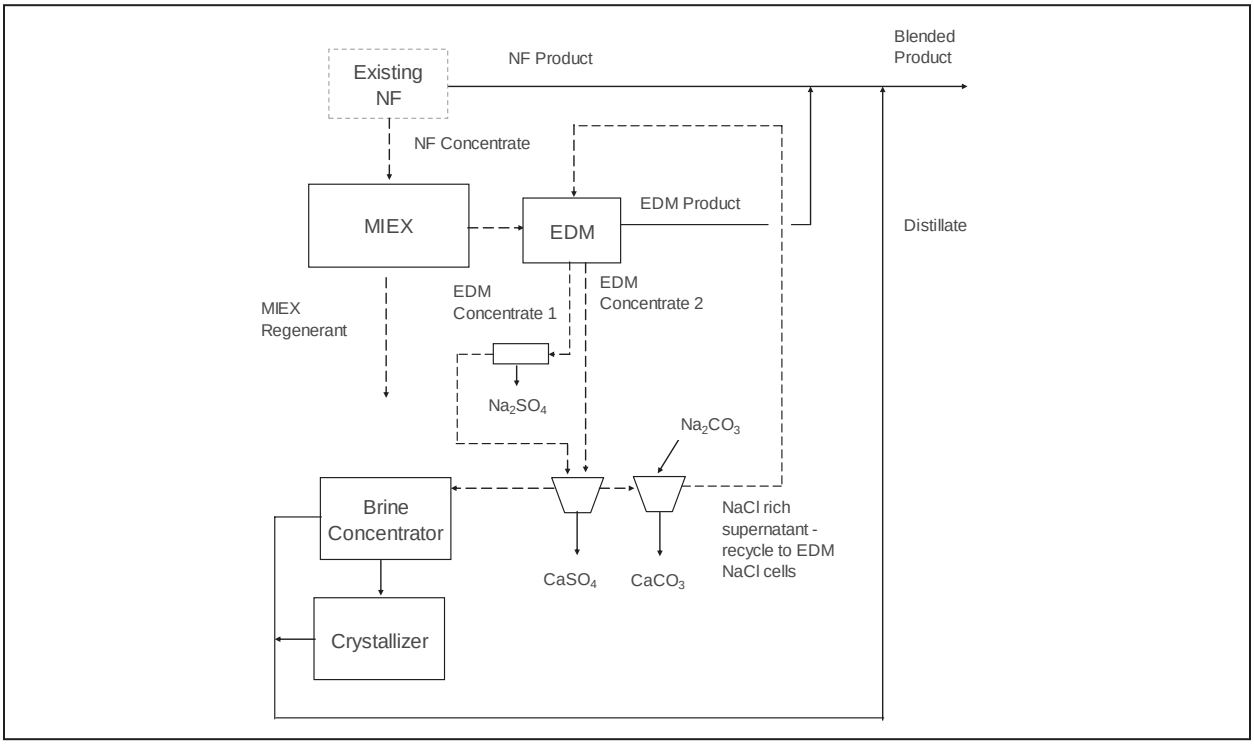

Figure 3.42 LHGW Option 3B (Option 3 with treatment of EDM concentrate)

LHGW Option 3B (Option 3 With Treatment to Develop Beneficial Use of EDM Concentrate)

Option 3B for LHGW is shown in Figure 3.42. The concentrate from EDM is treated in three steps. In the first, the concentrate stream 1 is cooled to crystallize $Na_2SO_4 \cdot 10\ H_2O$. This step is included because EDM concentrate contains a surplus of sulfate relative to calcium. In the second step, the concentrate streams are mixed to precipitate calcium sulfate. In the third step, soda ash is added to precipitate dolomite. Half of the EDM concentrate flow is used to replenish NaCl in the EDM and the remainder is treated in the crystallizer.

Projected water quality through the EDM treatment steps is shown in Table 3.38. A lime dose of 3600 mg/L as CaO is added to react with excess sulfate. A caustic dose of 9850 mg/L

Table 3.38
LHGW water quality through the EDM concentrate treatment steps

Ion	EDM Concentrate 1 (mg/L)	EDM Concentrate 2 (mg/L)	Step 2 feed (mg/L)	Step 2 supernatant (mg/L)	Step 3 supernatant (mg/L)
Ca	62	18,510	6791	2041	45
Mg	16	11,800	4319	4319	3162
Na	110,330	68,780	63,109	63,109	67,712
Cl	119,400	185,100	111,624	111,624	111,624
SO_4	62,100	0	16,474	5091	5091
HCO_3	0	0	0	0	0

Table 3.39
ZLD treatment costs for LHGW with Option 3B

Process	Energy cost ($/m^3)	Materials ($/m^3)	O&M cost ($/m^3)	Capital cost ($/m^3)	Total cost ($/m^3)
EDM	$1.35	$0.11	$1.46	$0.22	$1.68
EDM concentrate treatment		$0.60	$0.60	$0.02	$0.62
Brine concentrator	$0.14		$0.14	$0.12	$0.26
Crystallizer	$0.27		$0.27	$0.18	$0.45
Total	$1.76	$0.71	$2.47	$0.54	$3.01

is added in Step 2 to precipitate $Mg(OH)_2$. The sodium chloride rich supernatant from Step 2 is recycled to the EDM process to replace NaCl transferred to concentrate cells during electrodialysis. The solids produced are 222 kg $Mg(OH)_2$ and 358 kg $CaCO_3$ per 1000 m^3 product recovered from RO concentrate.

Treatment costs for LHGW with Option 3B are summarized in Table 3.39. All costs are per m^3 of total concentrate recovered. The EDM cost is significantly less than in Option 3A because EDM NaCl costs are eliminated and the crystallizer capacity is reduced by half.

LHGW Option 4

Treatment costs for LHGW using Option 4 are summarized in Table 3.40. All costs are per m^3 of total concentrate recovered. The total treatment cost for LHGW with conventional ZLD treatment was $4.02 per m^3 of RO concentrate recovered.

Comparison of LHGW Treatment Options

Treatment costs per m^3 of RO concentrate recovered for LHGW are shown in Figure 3.43. Option 3 without beneficial use of byproducts was about 5 percent more expensive than Option 4, and Option 3 with beneficial use of byproducts was 40 percent less than Option 4.

Table 3.40
ZLD treatment costs for LHGW with Option 4

Process	O&M cost ($/m^3)	Capital cost ($/m^3)	Total cost ($/m^3)
Brine concentrator	$2.28	$0.43	$2.71
Crystallizer	$0.84	$0.46	$1.30
Total	$3.12	$0.89	$4.02

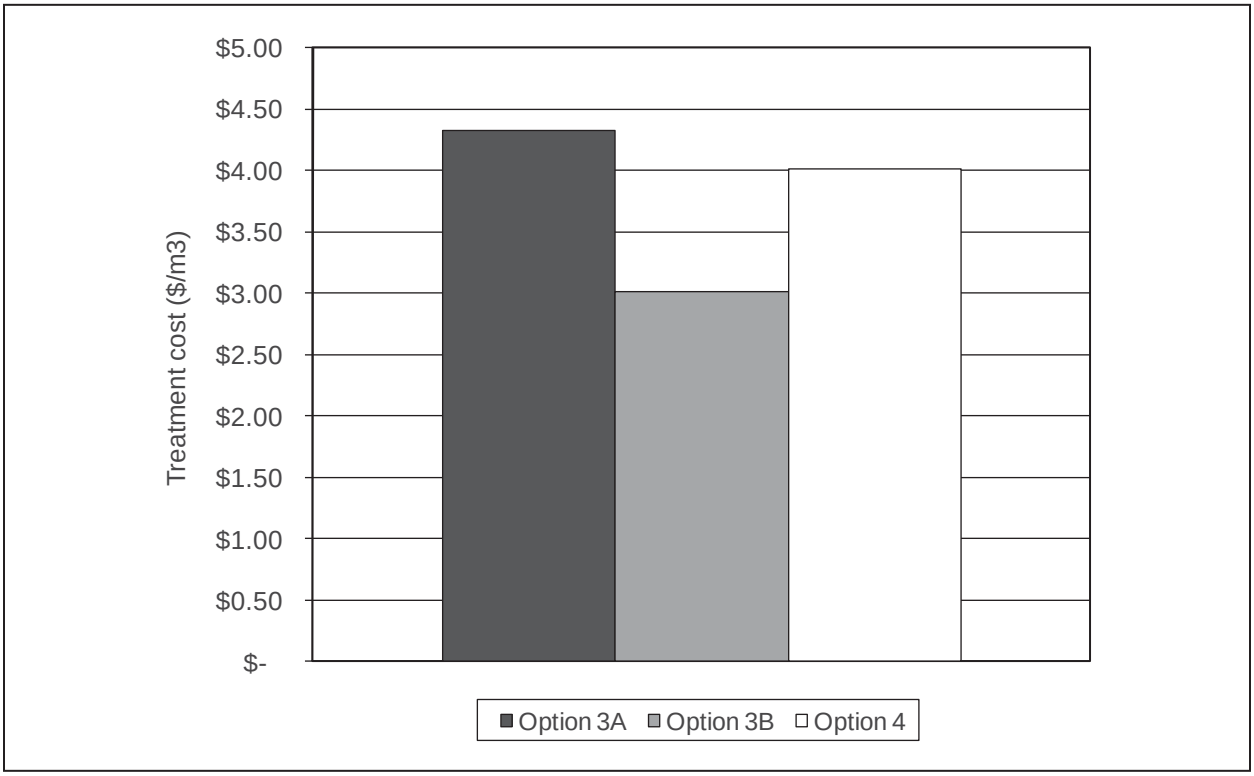

Figure 3.43 Comparison of treatment costs for LHGW ($ per m^3 RO concentrate recovered)

CGW

The options evaluated for CGW were as follows:

- Option 3A—EDM concentrate is discharged to the crystallizer.
- Option 3B—EDM concentrate is treated to derive beneficial products.
- Option 4—Treatment of concentrate with a brine concentrator and crystallizer.

CGW Option 3A (Option 3 Without Treatment to Develop Beneficial Use of EDM Concentrate)

The treatment train for CGW Option 3A is shown in Figure 3.44. In Option 3A, concentrate from the existing EDR is treated with EDM, and the concentrate from EDM is treated in the crystallizer. The final product water is a blend of the existing EDR product, the EDM diluate, and the crystallizer distillate.

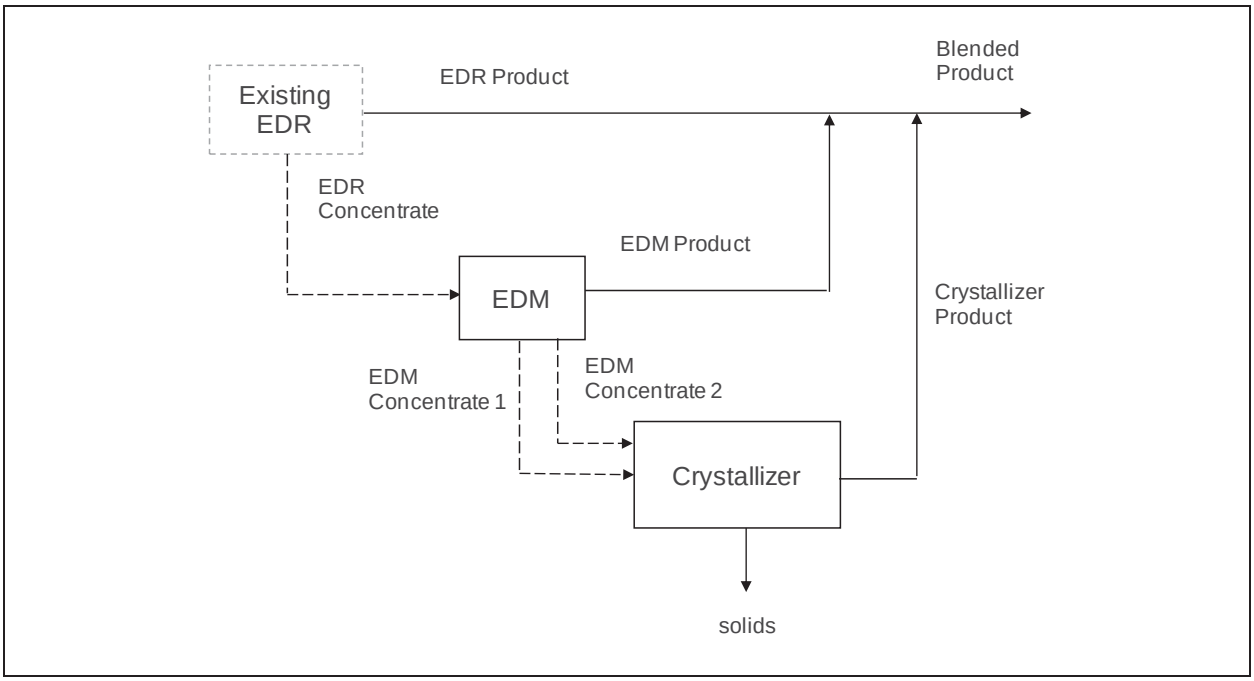

Figure 3.44 CGW Option 3A (Option 3 without treatment of EDM concentrate)

The treatment goal for EDM was calculated based on 80 percent recovery by the existing EDR membranes, 200 mg/L TDS EDR product water, 4175 mg/L TDS EDR concentrate, and a blended product goal of 400 mg/L TDS or less. The target TDS concentration for the EDM product, C_{EDM}, was 1200 mg/L.

Input data used in the EDM power calculations for CGW are shown in Table 3.41. A design cell velocity of 6 cm/s was used, and therefore the flow per cell was 0.017 L/s. The EDM stack was evaluated with the membranes used in the EDM pilot. Membrane area resistances ranged from 2.5 to 6.5 Ω cm^2. Current utilization factor and water transfer coefficient values were as determined during pilot testing. An average NaCl conductivity of 200 mS cm^{-1} was used.

Results of the EDM energy calculations are shown in Table 3.42. A cell voltage of 0.80 V and a current of 93 A were required to reduce TDS from 4175 mg/L in the EDM feed to 1200 mg/L in the EDM diluate. The current density was 0.0145 A/cm, and the polarization parameter was 82 A cm/eq. Cell flow rates were 0.0168 L/s in the feed, 0.0163 L/s in the diluate, and a total of 0.0005 L/s in the two concentrate cells. Recovery of the EDM stack was 97.3 percent. The stack power was 7.9 kW, and the EDM energy required to meet the diluate treatment goal was 1.31 kWh/m^3.

Treatment costs for CGW with Option 3A are summarized in Table 3.43. All costs are per m^3 of total concentrate recovered. The total treatment cost was $1.29 per m^3, of which 50 percent was capital and 50 percent O&M. The crystallizer accounted for half the total treatment cost even though it treated less than 3 percent of the flow.

CGW Option 3B (Option 3 With Treatment to Develop Beneficial Use of EDM Concentrate)

Option 3B for CGW is shown in Figure 3.45. In the first step, flow from concentrate stream 1 is cooled to crystallize $Na_2SO_4 \cdot 10H_2O$. In the second step, the two concentrate streams are mixed

Table 3.41
EDM model input for CGW EDR concentrate

Parameter	Value
Flow per cell set	0.0168 L/s
Cell sets per stack	100
Membrane width	40 cm
Membrane length	160 cm
Membrane area	6400 cm^2
Cell width	0.07 cm
Cell velocity	6 cm/s
Shadow factor	1.2
CMX membrane area resistance	3 Ω cm^2
AMX membrane area resistance	2.5 Ω cm^2
CMS membrane area resistance	6.5 Ω cm^2
AMS membrane area resistance	6.5 Ω cm^2
Water transfer coefficient	7.6 mol/eq
Current utilization factor	0.84
Average NaCl cell conductivity	200 mS cm^{-1}
Feed water TDS	4175 mg/L
Feed water temperature	298 K

Table 3.42
EDM model results for CGW EDR concentrate

Parameter	Value
Diluate TDS	1200 mg/L
Current	93 A
Current density	0.0145 A/ cm^2
Power polarization	82 A cm/eq
Concentrate 1 conductivity	267 mS/cm
Concentrate 2 conductivity	267 mS/cm
Diluate flow per cell	0.0163 L/s
Total concentrate flow per cell	0.00046 L/s
EDM recovery	97.3 %
Voltage per cell	0.80 V
Electrode voltage	5 V
Stack voltage	85 V
Stack power	7.9 kW
EDM energy requirement	1.31 kWh/m^3

Table 3.43
CGW Option 3A treatment costs

Process	Energy cost ($/m^3)	NaCl cost ($/m^3)	Materials ($/m^3)	O&M cost ($/m^3)	Capital cost ($/m^3)	Total cost ($/m^3)
EDM	$0.16	$0.31	$0.06	$0.53	$0.11	$0.63
Crystallizer	$0.28			$0.28	$0.18	$0.47
Total	$0.44	$0.31	$0.06	$0.81	$0.29	$1.10

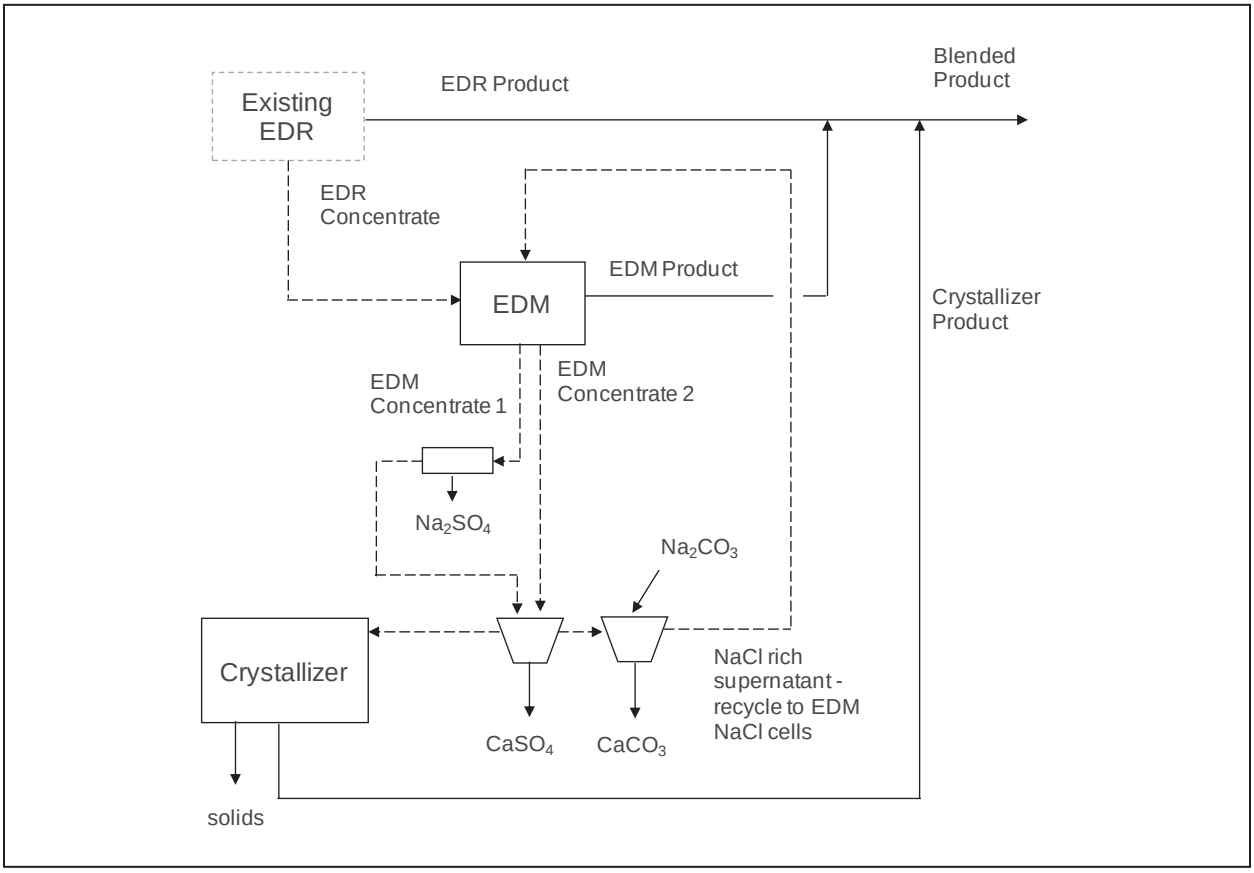

Figure 3.45 CGW Option 3B (Option 3 with treatment of EDM concentrate)

to precipitate $CaSO_4$. Half of the supernatant is discharged to the crystallizer and the remainder is mixed with soda ash in the third step to precipitate dolomite.

Water quality results through the EDM concentrate treatment steps are shown in Table 3.44. Concentrate stream 1 is treated to remove Na_2SO_4 so that when the two concentrate streams are blended in Step 2 calcium and sulfate concentrations are stoichiometrically proportionate. In Step 2, the two concentrate steams are mixed without chemical addition to precipitate calcium sulfate. Calcium and sulfate molar concentrations are reduced by more than 80 percent in this step. The supernatant from Step 2 contains mostly sodium and chloride. Half of the supernatant flow from Step 2 evaporated in the crystallizer and recovered as distillate, and the remainder is treated in Step 3. In step 3, the concentrate is mixed with a soda ash dose of 14,840 mg/L to precipitate dolomite. The supernatant from this step contains mostly sodium and chloride. The supernatant is

Table 3.44
CGW water quality through the EDM concentrate treatment steps

Ion	EDM Concentrate 1 (mg/L)	EDM Concentrate 2 (mg/L)	Step 2 feed (mg/L)	Step 2 supernatant (mg/L)	Step 3 supernatant (mg/L)
Ca	113	38,925	19,876	3010	200
Mg	18	14,731	7510	7510	5905
Na	83,900	10,595	37,478	37,478	43,907
K	0	805	410	410	410
Cl	31,175	129,386	81,186	81,186	81,186
SO_4	132,348	0	45,978	5503	5503
HCO_3	1027	0	504	500	10

Table 3.45
ZLD treatment costs for CGW with Option 3B

Process	Energy cost ($/m^3)	NaCl cost ($/m^3)	Materials ($/m^3)	O&M cost ($/m^3)	Capital cost ($/m^3)	Total cost ($/m^3)
EDM	$0.16		$0.06	$0.21	$0.11	$0.32
EDM concentrate treatment			$0.18	$0.18	$0.01	$0.19
Crystallizer	$0.14			$0.14	$0.14	$0.28
Total	$0.30		$0.24	$0.53	$0.26	$0.79

Table 3.46
ZLD treatment costs for CGW with Option 4

Process	O&M cost ($/m^3)	Capital cost ($/m^3)	Total cost ($/m^3)
Brine concentrator	$2.28	$0.43	$2.71
Crystallizer	$0.24	$0.18	$0.42
Total	$2.52	$0.62	$3.13

recycled to the EDM to replenish NaCl used during electrodialysis. Solids generated are 65 kg/m^3 Na_2SO_4 in Step 1, 73 kg/m^3 $CaSO_4$ in Step 2, and 13 kg/m^3 dolomite in Step 3.

Treatment costs for CGW with Option 3B are summarized in Table 3.45. All costs are per m^3 of total concentrate recovered. The total treatment cost was $0.79 per m^3.

CGW Option 4

Treatment costs for CGW using Option 4 are summarized in Table 3.46. All costs are per m^3 of total concentrate recovered. The total treatment cost for CGW with conventional ZLD treatment was $3.13 per m^3 of EDR concentrate recovered.

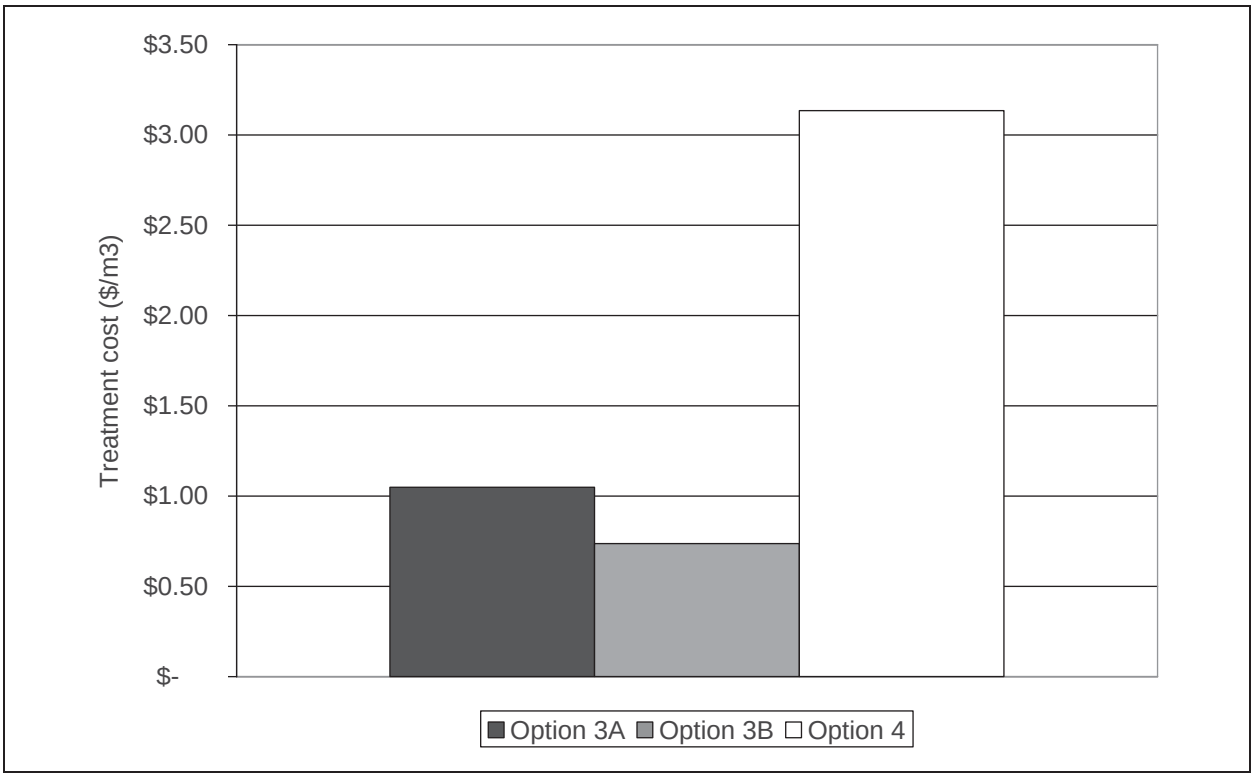

Figure 3.46 Comparison of treatment costs for CGW ($ per m^3 EDR concentrate recovered)

Comparison of CGW Treatment Options

Treatment costs per m^3 of EDR concentrate recovered for CGW are shown in Figure 3.46. Option 3 without beneficial use of byproducts was 33 percent of Option 4, and Option 3 with beneficial use of byproducts was 23 percent of Option 4.

OBGW

The following ZLD Options were evaluated for OBGW:

- Option 3A—EDM concentrator is discharged to the crystallizer.
- Option 3B—EDM concentrate is treated to derive beneficial products.
- Option 4—Treatment of concentrate with a brine concentrator and crystallizer.

OBGW Option 3A (Option 3 Without Treatment to Develop Beneficial Use of EDM Concentrate)

The process diagram for OBGW Option 3A is as shown for TGW Option 3A. Concentrate from the existing NF membranes is treated with MIEX for TOC removal. MIEX treated concentrate is desalinated with EDM. The EDM concentrate streams and MIEX regenerant are treated in a crystallizer. The final product water is a blend of the NF, EDM, and crystallizer product waters.

Table 3.47
MIEX criteria and calculations

Parameter	Value
Regeneration frequency	100 BV
NaCl regenerant concentration	100 g/L
Regeneration loading	360 g NaCl/ L resin
Regeneration volume	0.036 m^3 /m^3 product water
Resin regeneration rate	0.01 m^3 resin/m^3 product water
Initial TOC	48 mg/L
Treated TOC	14 mg/L
TOC accumulated in regenerant	34 g/ m^3 product water
TOC limit in regenerant	10 g/L
Maximum reuse of regenerant	11 times
NaCl consumed per mass TOC removed	1.7 g/g TOC removed
NaCl consumption	56 g/ m^3 product water
Regenerant byproduct	0.003 m^3 /m^3 product water
MIEX attrition rate	0.002 L resin / m^3 product water
MIEX unit cost	$14 per L resin
NaCl unit cost	$0.11 per kg

MIEX criteria are shown in Table 3.47. Average TOC concentrations for the OBGW source were 7.5 mg/L in the NF feed, 0.4 mg/L in the NF permeate, and 48 mg/L in the NF concentrate. In the bench-scale test, MIEX treatment reduced UVA by 80 percent at 100 BVT. A MIEX regeneration frequency of 100 BV was used for full-scale evaluation.

The treatment goal for EDM was calculated based on 80 percent recovery in the existing NF membranes, 200 mg/L TDS NF permeate, 2900 mg/L TDS NF concentrate, and a blended product goal of 400 mg/L TDS or less. The target TDS concentration for the EDM product, C_{EDM}, was 1200 mg/L.

$$0.2 \times C_{EDM} + 0.8 \times 200 = 400$$

$$C_{EDM} = 1200 \frac{mg}{L}$$

Input data used in the EDM power calculations for OBGW are shown in Table 3.48. A design cell velocity of 6 cm/s was used, and therefore the flow per cell was 0.017 L/s. The EDM stack was evaluated with the membranes used in the EDM pilot. Current utilization factor and water transfer coefficient values were as determined during pilot testing. An average NaCl conductivity of 200 mS cm^{-1} was used.

Results of the EDM energy calculations are shown in Table 3.49. A cell voltage of 0.71 V was required to generate the 77 A current needed to reduce TDS from 3700 mg/L in the EDM feed to 1200 mg/L in the EDM diluate. The current density was 0.0120 A/cm, and the polarization parameter was 77 A cm/eq. Cell flow rates were 0.0168 L/s in the feed, 0.0164 L/s in the diluate, and a total of 0.00038 L/s in the two concentrate cells. Therefore, recovery of the EDM stack was

Table 3.48
EDM model input for OBGW NF concentrate

Parameter	Value
Flow per cell set	0.0168 L/s
Cell sets per stack	100
Membrane width	40 cm
Membrane length	160 cm
Membrane area	6400 cm^2
Cell width	0.07 cm
Cell velocity	6 cm/s
Shadow factor	1.2
CMX membrane area resistance	3 Ω cm^2
AMX membrane area resistance	2.5 Ω cm^2
CMS membrane area resistance	6.5 Ω cm^2
AMS membrane area resistance	6.5 Ω cm^2
Water transfer coefficient	7.6 mol/eq
Current utilization factor	0.84
Average NaCl cell conductivity	200 mS cm^{-1}
Feed water TDS	3000 mg/L
Feed water temperature	298 K

Table 3.49
EDM model results for OBGW NF concentrate

Parameter	Value
Diluate TDS	1200 mg/L
Current	77 A
Current density	0.012 A/ cm^2
Power polarization	77 A cm/eq
Concentrate 1 conductivity	308 mS/cm
Concentrate 2 conductivity	308 mS/cm
Diluate flow per cell	0.0165 L/s
Total concentrate flow per cell	0.00038 L/s
EDM recovery	97.8 %
Voltage per cell	0.71 V
Electrode voltage	5 V
Stack voltage	76 V
Stack power	5.9 kW
EDM energy requirement	0.97 kWh/m^3

Table 3.50
Fraction of OBGW NF concentrate treated by each process if EDM concentrate is not treated to produce beneficial products

Process	Fraction of NF concentrate treated
MIEX®	1.0
EDM	1.0
Crystallizer	0.022

Table 3.51
OBGW Option 3A treatment costs

Process	Energy cost ($/m^3)	NaCl cost ($/m^3)	Materials ($/m^3)	O&M cost ($/m^3)	Capital cost ($/m^3)	Total cost ($/m^3)
MIEX®		$0.01	$0.03	$0.04	$0.22	$0.26
EDM	$0.12	$0.26	$0.06	$0.43	$0.11	$0.54
Crystallizer	$0.23			$0.23	$0.17	$0.41
Total	$0.35	$0.27	$0.08	$0.70	$0.50	$1.20

97.8 percent. The stack power was 5.9 kW. The EDM energy required to meet the diluate treatment goal was 0.97 kWh/m^3.

The fraction of OBGW NF concentrate treated by each successive process if EDM concentrate is not treated to develop beneficial products is shown in Table 3.50. All of the NF concentrate would be treated with MIEX®, and the MIEX® product water would be treated in EDM. The EDM would achieve 97.8 percent recovery, and its concentrate would be treated in the crystallizer.

Treatment costs for OBGW with Option 3A are summarized in Table 3.51. All costs are per m^3 of total concentrate recovered. The total treatment cost for Option 3A was $1.20 per m^3.

OBGW Option 3B: EDM Concentrate Is Treated to Develop Beneficial Products

Option 3B is illustrated in Figure 3.47. In this option, EDM concentrate is treated in two precipitation steps. In the first, the two concentrate streams are mixed without chemical addition to precipitate $CaSO_4$ and $CaCO_3$. Half the supernatant is discharged to the crystallizer and the other half is treated in the second step. In Step 2, soda ash is added to precipitate dolomite. Supernatant from Step 2 is recycled to the EDM to provide NaCl.

Water quality results for the EDM concentrate through each treatment step are shown in Table 3.52. The feed to the first precipitation step is the blend of the two concentrate streams. Calcium carbonate and calcium sulfate precipitate in this step because the blended concentrate contains high concentrations of calcium, sulfate, and carbonate. Step 2 supernatant contains mostly sodium and chloride. The solids generated are 14 kg/m^3 calcium carbonate and 26 kg/m^3 calcium sulfate in Step 1, and 8 kg/m^3 dolomite in Step 2.

Treatment costs for OBGW with Option 3B are summarized in Table 3.53. All costs are per m^3 of total concentrate recovered. The total treatment cost was $0.77 per m^3.

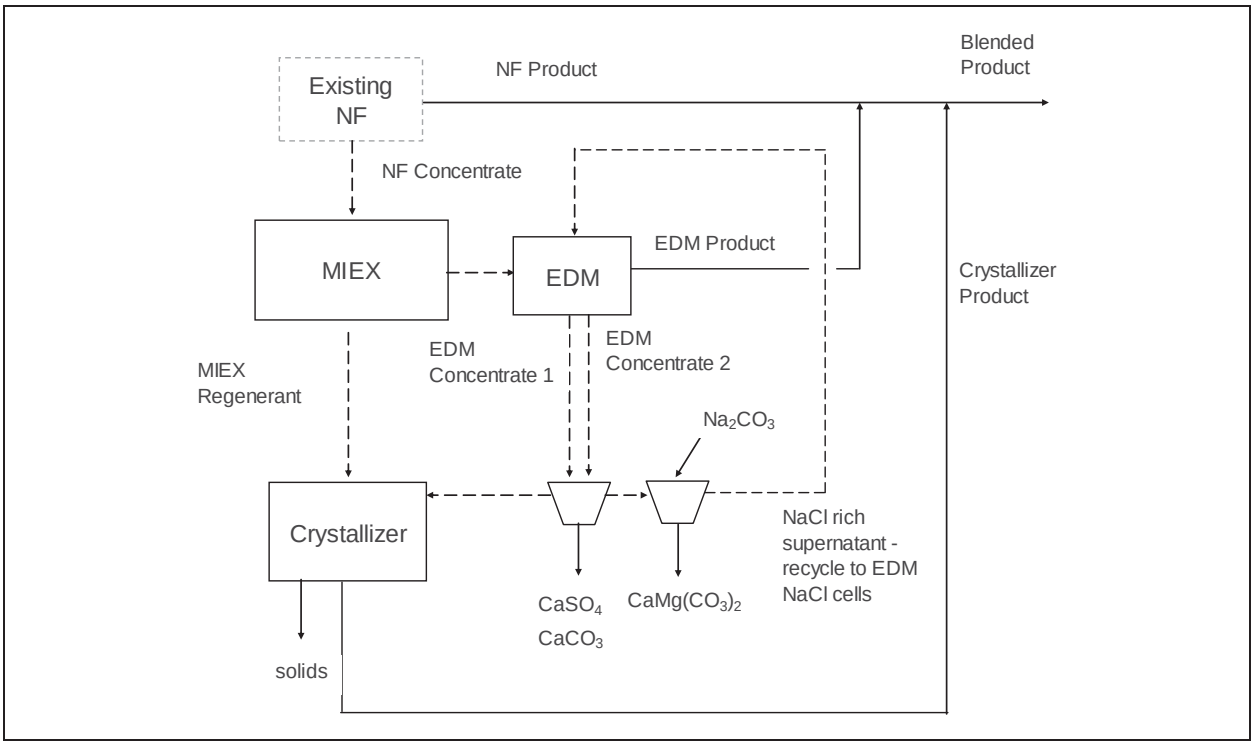

Figure 3.47 OBGW Option 3B (Option 3 with treatment of EDM concentrate)

Table 3.52
OBGW water quality through the EDM concentrate treatment steps

Ion	EDM Concentrate 1 (mg/L)	EDM Concentrate 2 (mg/L)	Step 1 feed (mg/L)	Step 1 supernatant (mg/L)	Step 2 supernatant (mg/L)
Ca	48	27,280	13,664	1825	53
Mg	4	3694	1849	1849	786
Na	83,940	44,898	64,419	64,419	69,023
K	105	1211	658	658	658
Cl	74,727	129,277	102,000	102,000	102,000
SO_4	40,428	148	20,288	5599	5599
HCO_3	42,108	0	21,054	12,438	7060

Table 3.53
OBGW Option 3B treatment costs

Process	Energy cost ($/m^3)	Materials ($/m^3)	O&M cost ($/m^3)	Capital cost ($/m^3)	Total cost ($/m^3)
MIEX		$0.03	$0.03	$0.22	$0.25
EDM	$0.12	$0.06	$0.17	$0.11	$0.28
EDM concentrate treatment		$0.08	$0.08	$0.02	$0.10
Crystallizer	$0.08		$0.08	$0.11	$0.19
Total	$0.20	$0.17	$0.37	$0.45	$0.82

Table 3.54
ZLD treatment costs for OBGW with Option 4

Process	O&M cost ($/m^3)	Capital cost ($/m^3)	Total cost ($/m^3)
Brine concentrator	$2.28	$0.43	$2.71
Crystallizer	$0.21	$0.17	$0.38
Total	$2.49	$0.60	$3.09

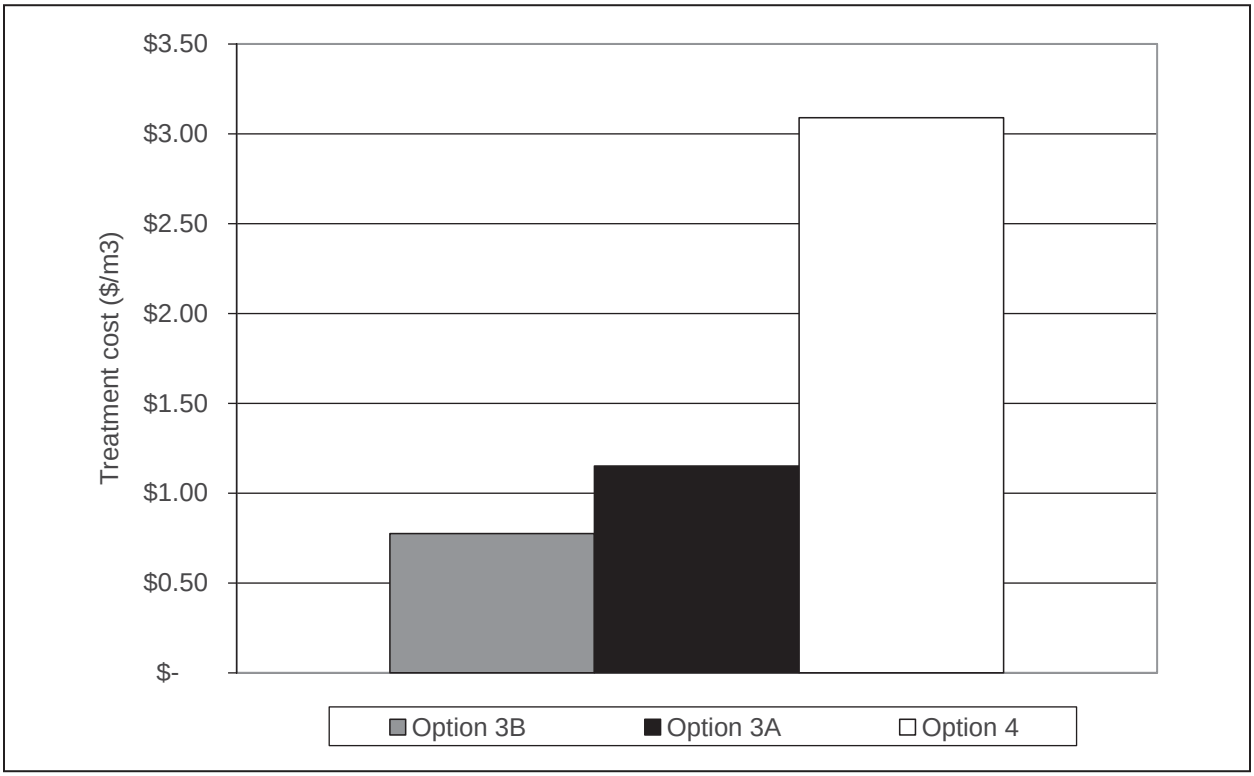

Figure 3.48 Comparison of treatment costs for OBGW ($ per m^3 NF concentrate recovered)

OBGW Option 4

Treatment costs for OBGW using Option 4 are summarized in Table 3.54. All costs are per m^3 of total concentrate recovered. The total treatment cost for OBGW with conventional ZLD treatment was $3.09 per m^3 of NF concentrate recovered.

Comparison of OBGW Treatment Options

Treatment costs per m^3 of RO concentrate recovered for CGW are shown in Figure 3.48. Option 3 without beneficial use of byproducts was 37 percent of Option 4, and Option 3 with beneficial use of byproducts was 25 percent of Option 4.

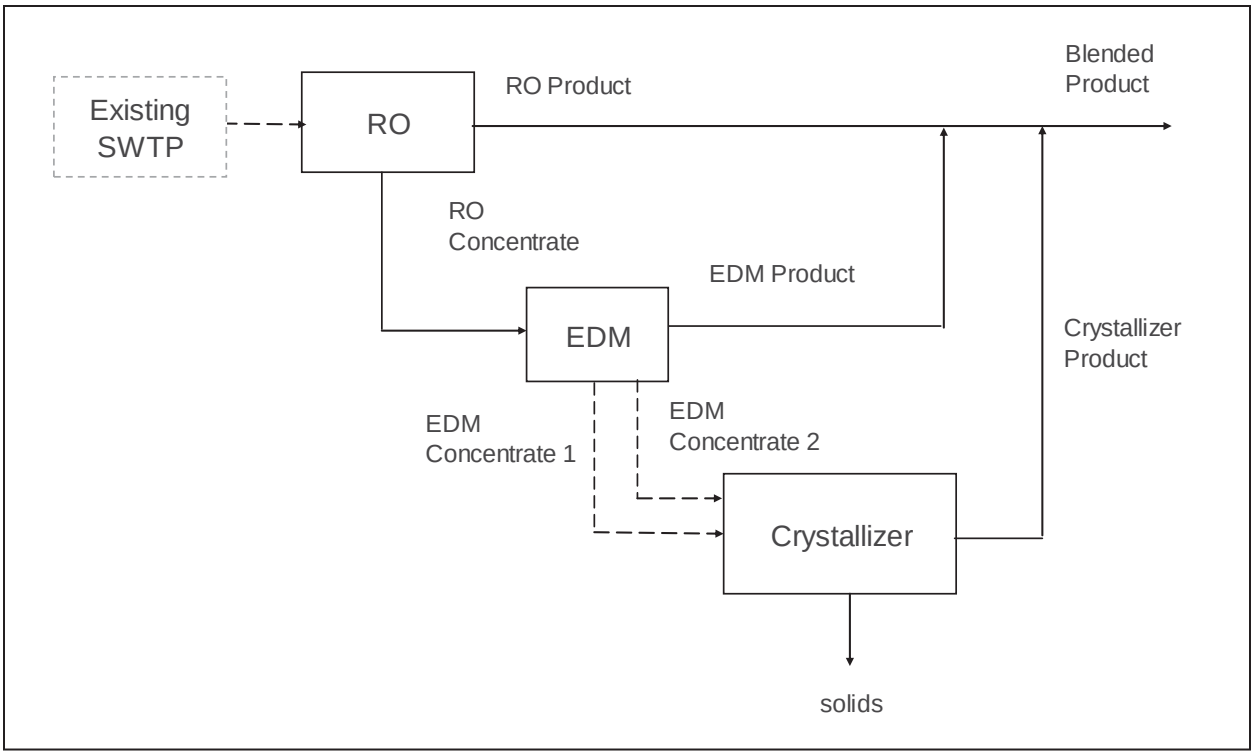

Figure 3.49 AR Option 3A (Option 3 without treatment of EDM concentrate)

AR

The objective for this source was to assess the feasibility of RO treatment with zero liquid discharge for removal treatment of a single contaminant, fluoride. RO with ZLD was compared to the most effective non-RO option tested, activated alumina. The options evaluated for AR were as follows:

- Option 3A—Option 3 without treatment of EDM concentrate to develop products.
- Option 3B—Option 3 with treatment of EDM concentrate to develop products.
- Option 4—Treatment of primary RO concentrate with a brine concentrator and crystallizer.
- Option 5—Activated alumina for fluoride removal.

AR Option 3A (Option 3 Without Treatment to Develop Beneficial Use of EDM Concentrate)

Option 3A for AR is shown in Figure 3.49. Finished water from the existing surface water treatment plant (SWTP) is treated with RO for fluoride removal. RO concentrate is treated with EDM, and EDM concentrate is recovered in the crystallizer. The blended product comprises the RO permeate, EDM diluate, and crystallizer distillate.

The treatment goal for EDM was calculated based on the fluoride treatment goal. A recovery of 85 percent was used for the primary RO. The fluoride concentrations were 10 mg/L in the RO feed, 67 mg/L in the RO concentrate, and 0.5 mg/L in the RO permeate (95 percent rejection).

Table 3.55
EDM model input for AR RO concentrate

Parameter	Value
Flow per cell set	0.0168 L/s
Cell sets per stack	100
Membrane width	40 cm
Membrane length	160 cm
Membrane area	6400 cm^2
Cell width	0.07 cm
Cell velocity	6 cm/s
Shadow factor	1.2
CMX membrane area resistance	3 Ω cm^2
AMX membrane area resistance	2.5 Ω cm^2
CMS membrane area resistance	6.5 Ω cm^2
AMS membrane area resistance	6.5 Ω cm^2
Water transfer coefficient	7.6 mol/eq
Current utilization factor	0.84
Average NaCl cell conductivity	200 mS cm^{-1}
Feed water TDS	3000 mg/L
Feed water temperature	298 K

The EDM was required to reduce fluoride in the RO concentrate from 67 mg/L to 7 mg/L to meet the fluoride treatment goal of 1.5 mg/L in the blended product water.

$$0.15 \times C_{EDM} + 0.85 \times 0.5 = 1.5$$

$$C_{EDM} = 7 \frac{mg}{L} F$$

Input data used in the EDM power calculations for AR are shown in Table 3.55. A design cell velocity of 6 cm/s was used, and therefore the flow per cell was 0.017 L/s. The EDM stack was evaluated with the membranes used in the EDM pilot. Current utilization factor and water transfer coefficient values were as determined during pilot testing. An average NaCl conductivity of 200 mS cm^{-1} was used.

Results of the EDM energy calculations are shown in Table 3.56. A cell voltage of 0.65 V was required to generate the 49 A current needed to reduce fluoride from 67 mg/L in the EDM feed to 7 mg/L in the EDM diluate. The current density was 0.0077 A/cm, and the polarization parameter was 123 A cm/eq. Cell flow rates were 0.0168 L/s in the feed, 0.0166 L/s in the diluate, and a total of 0.00024 L/s in the two concentrate cells. Therefore, recovery of the EDM stack was 98.6 percent. The stack power was 3.4 kW. The EDM energy required to meet the diluate treatment goal was 0.57 kWh/m^3.

Treatment costs for AR with Option 3A are summarized in Table 3.57. All costs are per m^3 of total concentrate recovered. The total treatment cost for concentrate treatment with Option 3A was $0.69 per m^3 of RO concentrate recovered.

Table 3.56
EDM model results for AR RO concentrate

Parameter	Value
Diluate fluoride	7 mg/L
Current	49 A
Current density	0.008 A/ cm^2
Power polarization	123 A cm/eq
Concentrate 1 conductivity	454 mS/cm
Concentrate 2 conductivity	454 mS/cm
Diluate flow per cell	0.0166 L/s
Total concentrate flow per cell	0.00024 L/s
EDM recovery	98.6 %
Voltage per cell	0.65 V
Electrode voltage	5 V
Stack voltage	70 V
Stack power	3.4 kW
EDM energy requirement	0.57 kWh/m^3

Table 3.57
AR Option 3A treatment costs

Process	Energy cost ($/$m^3$)	NaCl cost ($/$m^3$)	Materials ($/$m^3$)	O&M cost ($/$m^3$)	Capital cost ($/$m^3$)	Total cost ($/$m^3$)
EDM	$0.07	$0.16	$0.06	$0.29	$0.11	$0.40
Crystallizer	$0.15			$0.15	$0.14	$0.29
Total	$0.22	$0.16	$0.06	$0.44	$0.25	$0.69

With the cost for the primary RO included, the cost to treat the SWTP finished water with RO and Option 3A treatment of the RO concentrate was $0.30 per m^3 of SWTP finished water. Thus this option for fluoride removal would add about $0.30 to the existing plant treatment cost.

AR Option 3B: EDM Concentrate Is Treated to Develop Beneficial Products

Option 3B for AR is illustrated in Figure 3.50. In this option, EDM concentrate is treated in two precipitation steps. In the first, the two concentrate streams are mixed without chemical addition to precipitate $CaSO_4$ and dolomite. Half the supernatant is discharged to the crystallizer and the other half is treated in the second step. In Step 2, caustic is added to precipitate dolomite. Supernatant from Step 2 is recycled to the EDM to provide NaCl.

Water quality results through the EDM concentrate treatment steps are shown in Table 3.58. The solids precipitated were 0.19 kg dolomite and 0.27 kg gypsum per m^3 primary RO concentrate treated in the first precipitation step, and 0.06 kg dolomite per m^3 primary RO concentrate treated in the second precipitation step. The supernatant from the second step is predominantly sodium chloride.

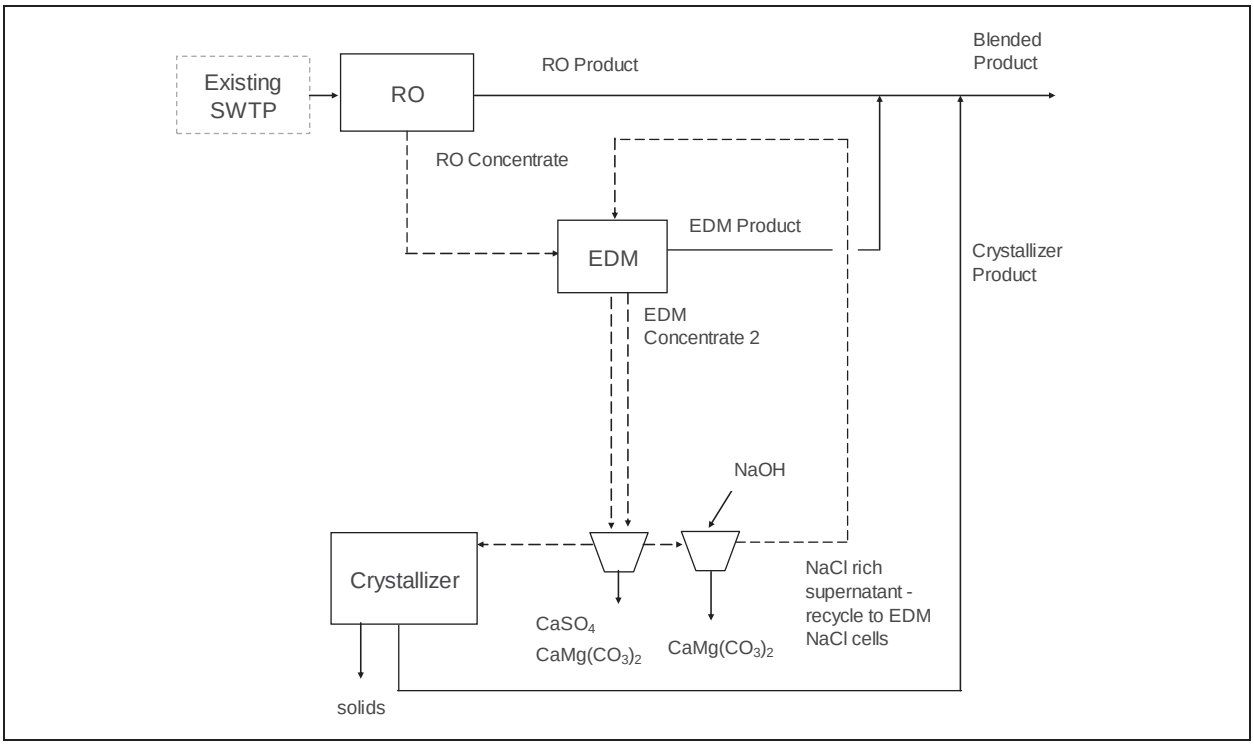

Figure 3.50 AR Option 3B (Option 3 with treatment of EDM concentrate)

Table 3.58
AR water quality through the EDM concentrate treatment steps

Ion	EDM Concentrate 1 (mg/L)	EDM Concentrate 2 (mg/L)	Step 1 feed (mg/L)	Step 1 supernatant (mg/L)	Step 2 supernatant (mg/L)
Ca	0	16,930	8465	957	32
Mg	0	5079	2539	884	311
Na	41,860	12,697	27,279	27,279	30,820
K	0	0	0	0	0
Cl	11,428	65,490	38,459	38,459	38,586
SO_4	33,860	0	16,930	6693	6720
HCO_3	46,134	0	23,067	13,834	11,000

Treatment costs for AR with Option 3B are summarized in Table 3.59. All costs are per m^3 of total concentrate recovered. The total treatment cost was \$0.48 per m^3.

With the cost for the primary RO included, the cost to treat the SWTP finished water with RO and Option 3B treatment of the RO concentrate was \$0.27 per m^3 of SWTP finished water. Thus this option for fluoride removal would add about \$0.27 to the existing plant treatment cost.

Table 3.59
AR Option 3B treatment costs

Process	Energy cost ($/m^3)	Materials ($/m^3)	O&M cost ($/m^3)	Capital cost ($/m^3)	Total cost ($/m^3)
EDM	$0.07	$0.06	$0.12	$0.11	$0.23
EDM concentrate treatment		$0.06	$0.06	$0.01	$0.07
Crystallizer	$0.07		$0.07	$0.10	$0.18
Total	$0.14	$0.12	$0.25	$0.22	$0.48

Table 3.60
ZLD treatment costs for AR with Option 4

Process	O&M cost ($/m^3)	Capital cost ($/m^3)	Total cost ($/m^3)
Brine concentrator	$2.28	$0.43	$2.71
Crystallizer	$0.11	$0.12	$0.23
Total	$2.39	$0.55	$2.94

AR Option 4

Treatment costs for AR using Option 4 are summarized in Table 3.60. All costs are per m^3 of total concentrate recovered. The total treatment cost for AR with conventional ZLD treatment was $2.94 per m^3 of RO concentrate recovered. With the cost for the primary RO included, the cost to treat the SWTP finished water with RO and Option 4 treatment of the RO concentrate was $0.64 per m^3 of SWTP finished water.

AR Option 5

Treatment costs for AR using Option 5, fluoride removal with AA, were evaluated with an influent fluoride concentration of 10 mg/L and a treatment goal of 1.5 mg/L. The AA usage rate based on isotherm test results was 20 kg AA per m^3 water treated. For a 10 minute empty bed contact time (EBCT) and an AA usage rate of 20 kg AA per m^3, the bed would be regenerated every 39 bed volumes (BV).

A typical regeneration protocol would be as shown in Table 3.61. In the first step with NaOH, fluoride adsorbed to the AA is displaced by hydroxide (OH^-). The AA is rinsed to expel excess NaOH. To restore AA adsorption capacity the media is acidified with H_2SO_4 or HCl. A 2 BV rinse follows to remove acid. A fast rinse of 20 to 30 BV is used to remove any fluoride that may have leaked from the bed.

The costs for Option 5 are shown in Table 3.62. The treatment cost is dominated by the chemical cost included in the O&M total. At a regeneration frequency of 39 BV, chemical usage would be 4.1 kg 0.5 NaOH and 1.9 kg 0.93 H_2SO_4 per m^3 water treated. At unit costs of $0.66 per kg for NaOH and $0.11 per kg for H_2SO_4, the chemical costs would be $2.89 per m^3 water treated.

Table 3.61
Typical AA regeneration protocol

Step	BV
Regenerate with 1% NaOH	5
Rinse	2
Acidify with 2% H_2SO_4	2
Rinse	2
Fast rinse	20 to 30

Table 3.62
ZLD treatment costs for AR with Option 5 at ambient pH

Process	O&M cost ($/m^3)	Capital cost ($/m^3)	Total cost ($/m^3)
AA contactors	$2.91	$0.06	$2.97

Table 3.63
ZLD treatment costs for AR with Option 5 at pH 5.5 to 6.0

Process	O&M cost ($/m^3)	Capital cost ($/m^3)	Total cost ($/m^3)
AA contactors	$0.30	$0.06	$0.36

It should be noted that the jar test was conducted at ambient pH (7.6), and that higher AA adsorption capacities for fluoride have been reported at pH 6 and lower. Clifford (1999) states that a 1000 BV regeneration rate can be expected for a water source containing 3 to 6 mg/L fluoride if pH is lowered to 5.5 to 6.0.

Treated costs for treatment at reduced pH assuming a regeneration frequency of 500 BV for 10 mg/L source water are shown in Table 3.63. An acid dose of 70 mg/L H_2SO_4 must be added to the feed water to lower pH to 6.0, and a post treatment NaOH dose of 50 mg/L must be added to bring pH back to 7.8. The chemical cost for AA regeneration, however, is decreased significantly. The total treatment cost was $0.36 per m^3 of water treated.

Comparison of AR Treatment Options

Treatment costs per m^3 of RO concentrate recovered for AR are shown in Figure 3.51 for Option 3 and Option 4. Option 3 without beneficial use of byproducts (Option 3B) was 22 percent of Option 4, and Option 3 with beneficial use of byproducts (Option 3A) was 15 percent of Option 4.

Treatment costs per m^3 of total product for AR are shown in Figure 3.52. Options 3 and 4 are compared with Option 5 on the basis of total production to assess the feasibility of RO with ZLD for fluoride treatment. AA treatment at ambient pH is not economically viable because of the high chemical cost for frequent regeneration. The treatment cost for AA at pH 6 is comparable to that of Option 3, but there are other factors to consider with this AA option. Approximately 8 percent of product water would be used for regeneration and rinses. The NaOH regenerant stream in

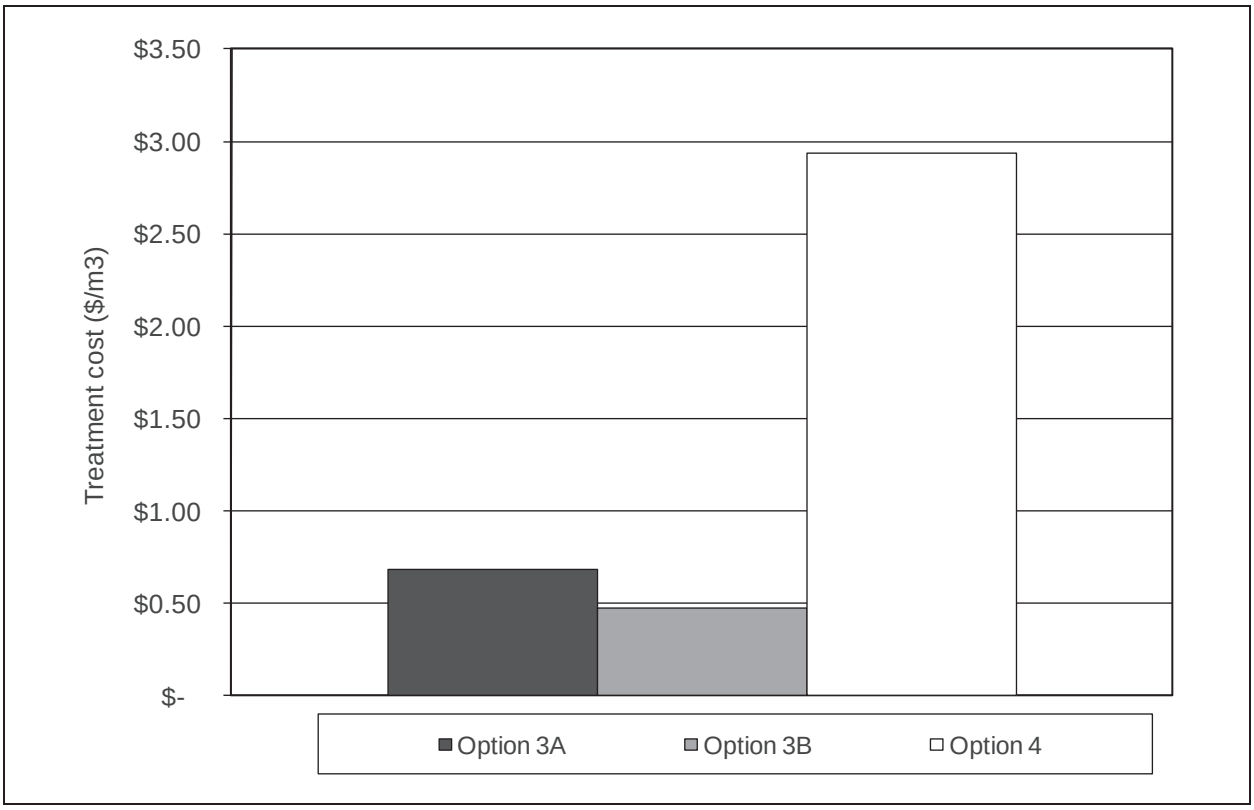

Figure 3.51 Comparison of concentrate treatment costs for AR ($ per m^3 NF concentrate recovered)

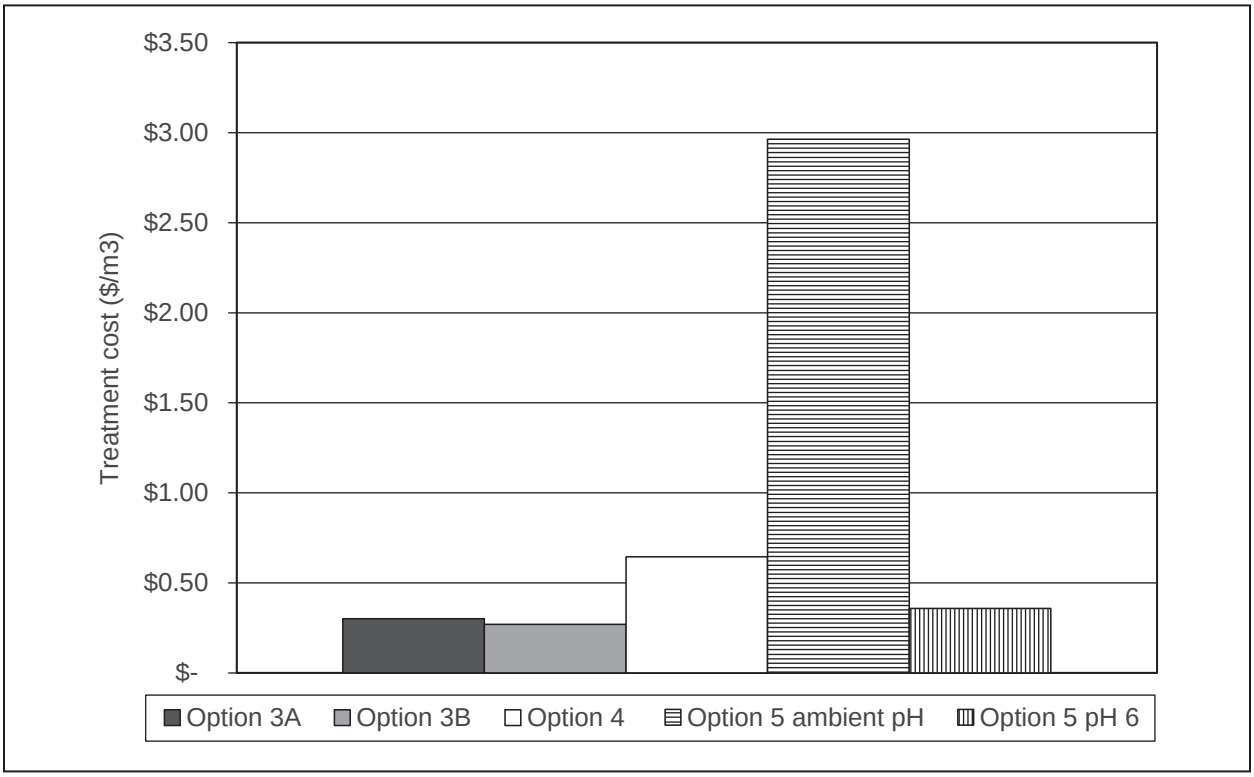

Figure 3.52 Comparison of finished water treatment costs for AR ($ per m^3 total production)

Table 3.64
SJR RO concentrate average water quality data

Analyte	Concentration (mg/L)
Ca	267
Mg	80
Na	200
Cl	180
SO_4	533
HCO_3	727
TDS	2942

particular would contain high concentrations of fluoride. This waste stream must be managed, and discharge to a sewer may be difficult because of the fluoride concentration.

The cost for AA treatment, however, would be more sensitive to the initial fluoride concentration than Option 3 because AA treatment more directly targets fluoride than do RO or electrodialysis. At an influent fluoride concentration of 5 mg/L, for example, the cost for AA treatment would be approximately halved while the cost for Option 3 would decrease by about 5 percent.

SJR

A desktop study was conducted for SJR to develop costs for ZLD concentrate management of this surface water source. The options evaluated for SJR were as follows:

- Option 3A—Option 3 without treatment of EDM concentrate to develop products.
- Option 3B—Option 3 with treatment of EDM concentrate to develop products.
- Option 4—Treatment of primary RO concentrate with a brine concentrator and crystallizer.

Water quality data for RO concentrate for SJR are shown in Table 3.64. The data were taken from a St. Johns River Water Management District report, Special Publication SJ2004-SP20, Surface Water Treatability and Demineralization Study (2004).

SJR Option 3A (Option 3 Without Treatment to Develop Beneficial Use of EDM Concentrate)

Option 3A for SJR is shown in Figure 3.53. Finished water from the surface water treatment plant (SWTP) is treated with RO to reduce TDS. RO concentrate is treated with EDM, and EDM concentrate is recovered in the crystallizer. The blended product comprises the RO permeate, EDM diluate, and crystallizer distillate.

The treatment goal for EDM was calculated based on a TDS treatment goal of 400 mg/L, RO recovery of 80 percent, and RO permeate TDS of 200 mg/L.

$$0.20 \times C_{EDM} + 0.80 \times 200 = 400$$

$$C_{EDM} = 1200 \frac{mg}{L}$$

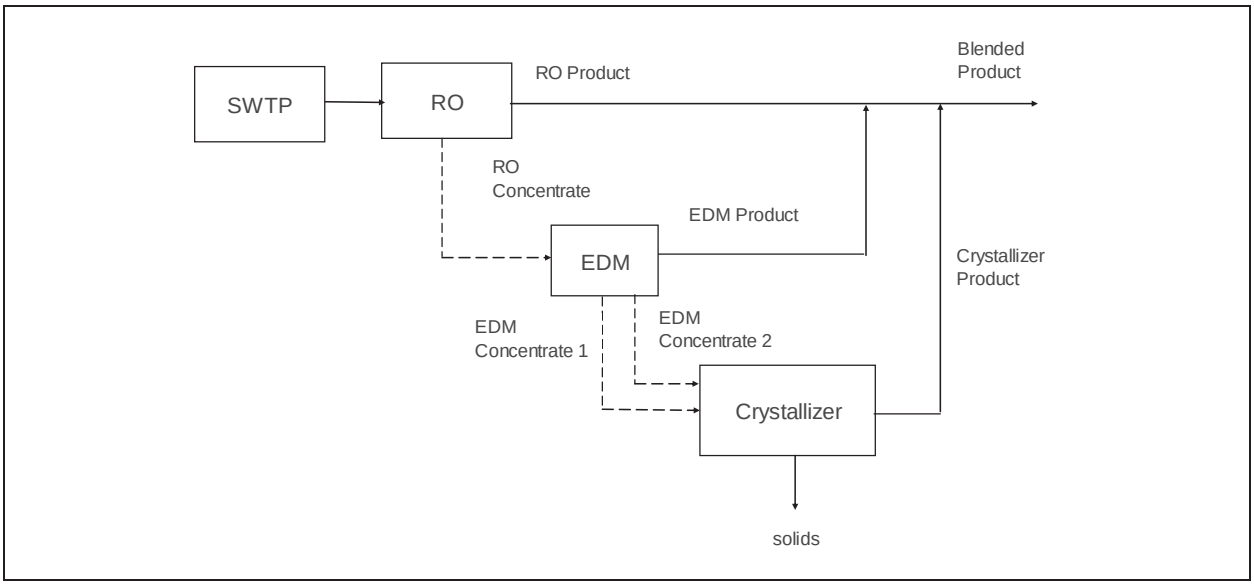

Figure 3.53 SJR Option 3A (Option 3 without treatment of EDM concentrate)

Table 3.65
EDM model input for SJR RO concentrate

Parameter	Value
Flow per cell set	0.0168 L/s
Cell sets per stack	100
Membrane width	40 cm
Membrane length	160 cm
Membrane area	6400 cm^2
Cell width	0.07 cm
Cell velocity	6 cm/s
Shadow factor	1.2
CMX membrane area resistance	3 Ω cm^2
AMX membrane area resistance	2.5 Ω cm^2
CMS membrane area resistance	6.5 Ω cm^2
AMS membrane area resistance	6.5 Ω cm^2
Water transfer coefficient	7.6 mol/eq
Current utilization factor	0.84
Average NaCl cell conductivity	200 mS cm^{-1}
Feed water TDS	2942 mg/L
Feed water temperature	298 K

Table 3.66
EDM model results for SJR RO concentrate

Parameter	Value
Diluate TDS	1200 mg/L
Current	54 A
Current density	0.0084 A/ cm^2
Power polarization	62 A cm/eq
Concentrate 1 conductivity	380 mS/cm
Concentrate 2 conductivity	380 mS/cm
Diluate flow per cell	0.0165 L/s
Total concentrate flow per cell	0.00026 L/s
EDM recovery	98.5 %
Voltage per cell	0.59 V
Electrode voltage	5 V
Stack voltage	59 V
Stack power	3.5 kW
EDM energy requirement	0.57 kWh/m^3

Table 3.67
SJR Option 3A treatment costs

Process	Energy cost ($/$m^3$)	NaCl cost ($/$m^3$)	Materials ($/$m^3$)	O&M cost ($/$m^3$)	Capital cost ($/$m^3$)	Total cost ($/$m^3$)
EDM	$0.07	$0.18	$0.06	$0.31	$0.13	$0.44
Crystallizer	$0.16			$0.16	$0.15	$0.31
Total	$0.23	$0.18	$0.06	$0.47	$0.28	$0.75

Input data used in the EDM power calculations for AR are shown in Table 3.65. A design cell velocity of 6 cm/s was used, and therefore the flow per cell was 0.017 L/s. The EDM stack was evaluated with the membranes used in the EDM pilot. An average NaCl conductivity of 200 mS cm^{-1} was used.

Results of the EDM energy calculations are shown in Table 3.66. The cell voltage was 0.59 V, and the current was 54 A. The current density was 0.0084 A/cm, and the polarization parameter was 62 A cm/eq. Cell flow rates were 0.0168 L/s in the feed, 0.0165 L/s in the diluate, and a total of 0.00026 L/s in the two concentrate cells. Therefore, recovery of the EDM stack was 98.5 percent. The stack power was 3.2 kW. The EDM energy required to meet the diluate treatment goal was 0.53 kWh/m^3.

Treatment costs for SJR with Option 3A are summarized in Table 3.67. All costs are per m^3 of total concentrate recovered. The total treatment cost for concentrate treatment with Option 3A was $0.75 per m^3 of RO concentrate recovered.

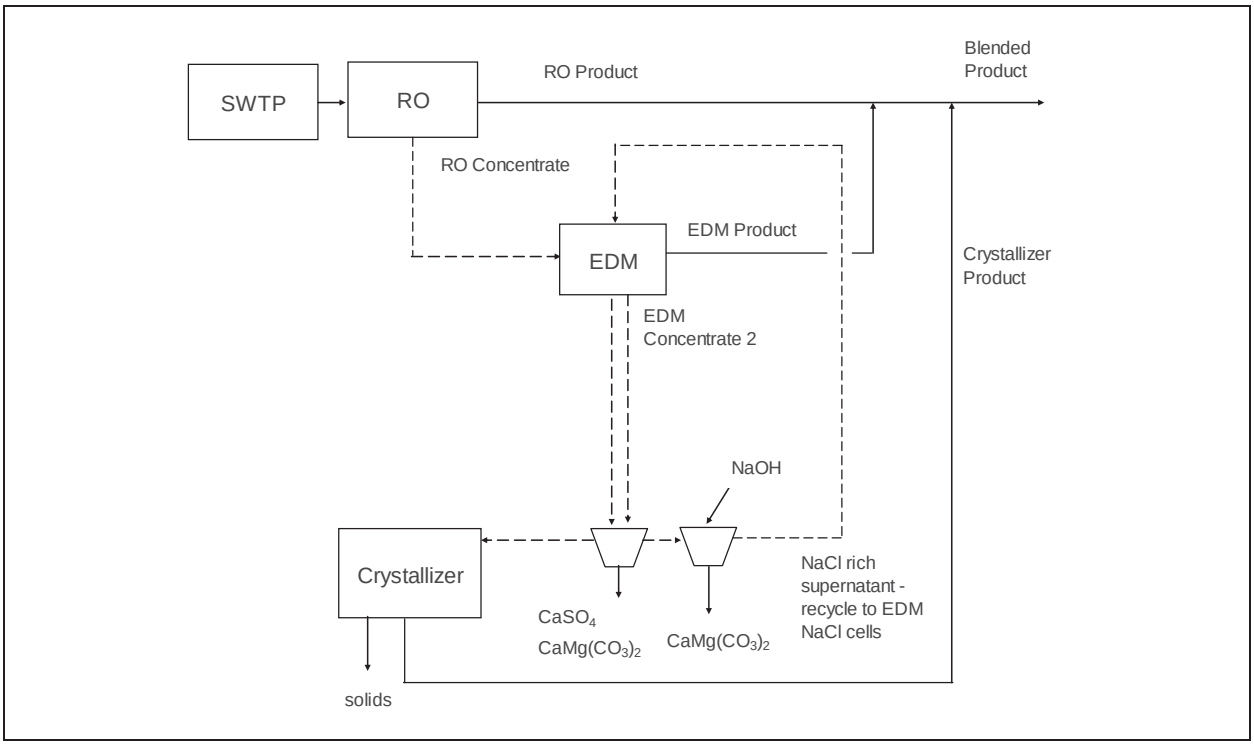

Figure 3.54 SJR Option 3B (Option 3 with treatment of EDM concentrate)

Table 3.68
SJR water quality through the EDM concentrate treatment steps

Ion	EDM Concentrate 1 (mg/L)	EDM Concentrate 2 (mg/L)	Step 1 feed (mg/L)	Step 1 supernatant (mg/L)	Step 2 supernatant (mg/L)
Ca	0	10,192	5096	931	48
Mg	0	3058	1529	813	272
Na	24,883	7644	16,263	16,261	18,791
K	0	0	0	0	0
Cl	6879	38,824	22,852	22,868	22,868
SO_4	20,384	0	10,192	5567	5568
HCO_3	27,773	0	23,067	8684	6083

SJR Option 3B: EDM Concentrate Is Treated to Develop Beneficial Products

Option 3B for SJR is illustrated in Figure 3.54. In this option, EDM concentrate is treated in two precipitation steps. In the first, the two concentrate streams are mixed without chemical addition to precipitate calcium carbonate, $CaSO_4$, and dolomite. Half the supernatant is discharged to the crystallizer and the other half is treated in the second step where caustic is added to precipitate dolomite. Supernatant from Step 2 is recycled to the EDM to provide NaCl.

Water quality results through the EDM concentrate treatment steps are shown in Table 3.68. The solids precipitated were 3 kg calcium carbonate, 6 kg dolomite, and 8 kg gypsum per m^3

Table 3.69
SJR Option 3B treatment costs

Process	Energy cost ($/m^3)	Materials ($/m^3)	O&M cost ($/m^3)	Capital cost ($/m^3)	Total cost ($/m^3)
EDM	$0.06	$0.06	$0.12	$0.13	$0.25
EDM concentrate treatment		$0.05	$0.05	$0.01	$0.06
Crystallizer	$0.08		$0.08	$0.11	$0.19
Total	$0.15	$0.11	$0.25	$0.25	$0.50

Table 3.70
ZLD treatment costs for SJR with Option 4

Process	O&M cost ($/m^3)	Capital cost ($/m^3)	Total cost ($/m^3)
Brine concentrator	$2.28	$0.43	$2.71
Crystallizer	$0.16	$0.17	$0.32
Total	$2.44	$0.60	$3.04

primary RO concentrate treated in the first precipitation step, and 4 kg dolomite per m^3 primary RO concentrate treated in the second precipitation step. The supernatant from the second step is predominantly sodium chloride.

Treatment costs for SJR with Option 3B are summarized in Table 3.69. All costs are per m^3 of total concentrate recovered. The total treatment cost was $0.50 per m^3.

SJR Option 4

Treatment costs for SJR using Option 4 are summarized in Table 3.70. All costs are per m^3 of total concentrate recovered. The total treatment cost for SJR with conventional ZLD treatment was $2.94 per m^3 of RO concentrate recovered.

Comparison of SJR Treatment Options

Treatment costs per m^3 of RO concentrate recovered for SJR are shown in Figure 3.55 for Option 3 and Option 4. Option 3 without beneficial use of byproducts (Option 3B) was 25 percent of Option 4, and Option 3 with beneficial use of byproducts (Option 3A) was 16 percent of Option 4.

IR

A desktop study was conducted for IR to develop costs for ZLD desalination of the IR source. Average water quality data for IR are shown in Table 3.71. The IR source differs significantly from the other sources evaluated. TDS is approximately 28,000 mg/L and is predominantly sodium and chloride. Calcium concentration is relatively low.

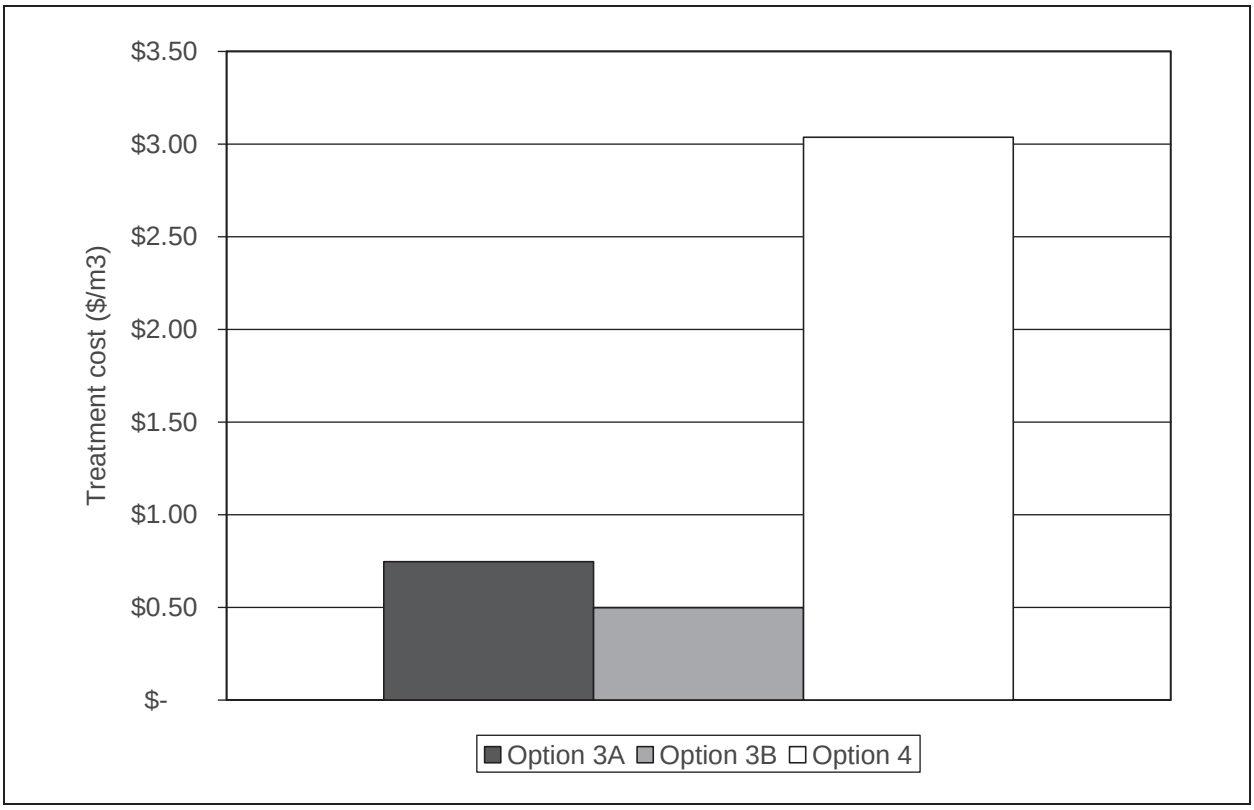

Figure 3.55 Comparison of concentrate treatment costs for SJR ($ per m^3 RO concentrate recovered)

Table 3.71
IR RO concentrate average water quality data

Analyte	Concentration (mg/L)
Ca	319
Mg	1100
Na	8360
Cl	15,336
SO_4	2100
HCO_3	148
TDS	27,687

The treatment options evaluated for this source differed slightly from the other sources because of the unique water quality characteristics of IR. The options evaluated for IR were as follows:

- Option 3A—Option 3 without treatment of EDM concentrate to develop products.
- Option 4—Treatment of primary RO concentrate with a brine concentrator and crystallizer.
- Option 6—RO followed by EDM and a crystallizer.

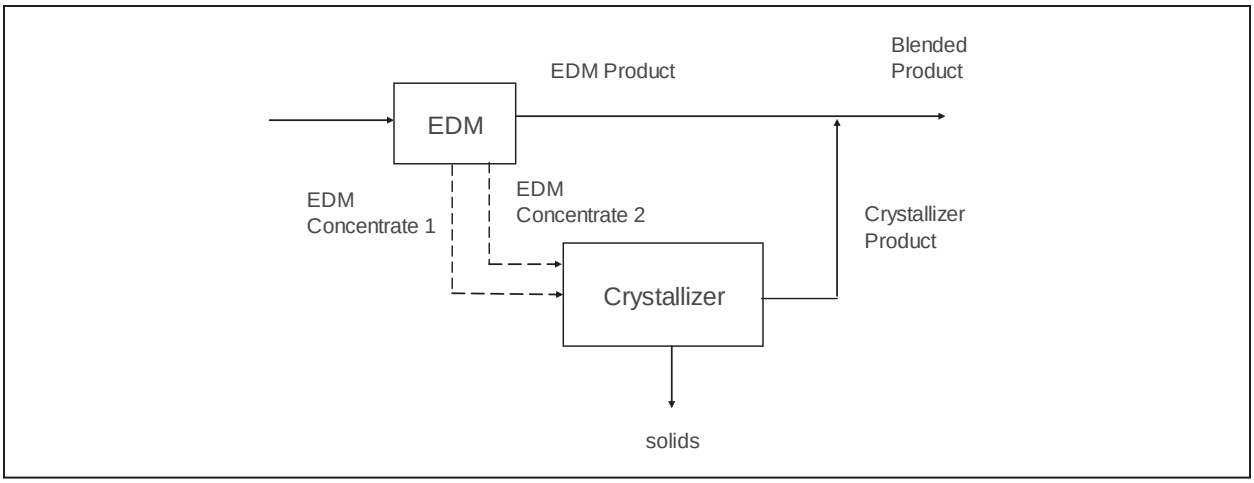

Figure 3.56 IR Option 3A (Option 3 without treatment of EDM concentrate)

Table 3.72
EDM model input for IR

Parameter	Value
Flow per cell set	0.0168 L/s
Cell sets per stack	100
Number of stacks in series	2
Membrane width	40 cm
Membrane length	160 cm
Membrane area	6400 cm^2
Cell width	0.07 cm
Cell velocity	6 cm/s
Shadow factor	1.2
CMX membrane area resistance	3 Ω cm^2
AMX membrane area resistance	2.5 Ω cm^2
CMS membrane area resistance	6.5 Ω cm^2
AMS membrane area resistance	6.5 Ω cm^2
Water transfer coefficient	7.6 mol/eq
Current utilization factor	0.90
Average NaCl cell conductivity	300 mS cm^{-1}
Feed water TDS	27,690 mg/L
Feed water temperature	298 K

IR Option 3A (Option 3 Without Treatment to Develop Beneficial Use of EDM Concentrate)

Option 3A for IR is shown in Figure 3.56. The blended product comprises the EDM diluate and crystallizer distillate. This option differs from Option 3A of the other sources because there is no existing RO. Rather the water was concentrated through several cycles through a power plant cooling tower, and the TDS of this water is higher than the RO concentrate from any of the sources.

Table 3.73
EDM model results for IR

Parameter	Value
Diluate TDS	500 mg/L
Stack 1 current	500 A
Stack 1 current density	0.0781 A/ cm^2
Stack 1 power polarization	57 A cm/eq
Stack 1 Concentrate 1 conductivity	269 mS/cm
Stack 1 Concentrate 2 conductivity	269 mS/cm
Stack 1 diluate flow per cell	0.0142 L/s
Stack 1 Total concentrate flow per cell	0.0025 L/s
Stack 1 EDM recovery	84.8 %
Stack 1 voltage per cell	2.09 V
Electrode voltage	5 V
Stack 1 voltage	214 V
Stack 1 power	107 kW
Stack 2 current	295 A
Stack 2 current density	0.0461 A/ cm^2
Stack 2 power polarization	109 A cm/eq
Stack 2 Concentrate 1 conductivity	269 mS/cm
Stack 2 Concentrate 2 conductivity	269 mS/cm
Stack 2 diluate flow per cell	0.0127 L/s
Stack 2 Total concentrate flow per cell	0.0015 L/s
Stack 2 voltage per cell	2.18 V
Electrode voltage	5 V
Stack 2 voltage	223 V
Stack 2 power	66 kW
Total EDM recovery	75.8%
Total EDM energy	33.7 kWh/m^3

Input data used in the EDM power calculations for IR are shown in Table 3.72. The treatment goal for EDM was a diluate TDS of 500 mg/L. As with the LHGW source, two EDM stacks in series were required to achieve the treatment goal because of the high initial TDS. An average NaCl conductivity of 300 mS cm^{-1} was used.

Results of the EDM energy calculations for IR are shown in Table 3.73. Without a RO permeate source to blend with, the EDM energy requirements for this source were much greater than the other sources because 98 percent removal of TDS by electrolysis was required. Cell voltages of 1.40 V in the first stack and 1.44 V in the second stack were required. The currents were 300 A in Stack 1 and 120 A in Stack 2. Power polarization factors were 63 A cm/eq in Stack 1 and 73 A cm/eq in Stack 2. Stack 1 cell flow rates were 0.0168 L/s in the feed, 0.0152 L/s in the diluate, and a total of 0.0016 L/s in the two concentrate cells. Stack 2 cell flow rates were 0.0152 L/s in the feed, 0.0145 L/s in the diluate, and a total of 0.0006 L/s in the two concentrate cells. Recovery of

Table 3.74
IR Option 3A treatment costs

Process	Energy cost ($/m^3)	NaCl cost ($/m^3)	Materials ($/m^3)	O&M cost ($/m^3)	Capital cost ($/m^3)	Total cost ($/m^3)
EDM	$4.04	$4.05	$0.11	$8.20	$0.24	$8.44
Crystallizer	$2.55			$2.55	$0.31	$2.86
Total	$6.59	$4.05	$0.11	$10.75	$0.55	$11.30

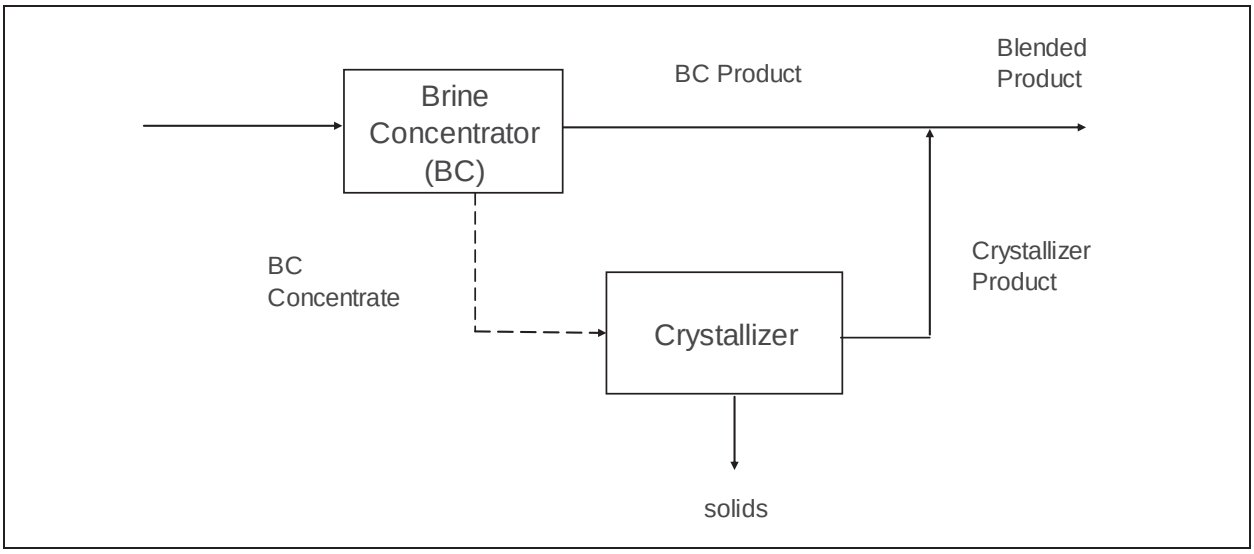

Figure 3.57 IR Option 4, treatment of primary RO concentrate with a brine concentrator and crystallizer

the two EDM stacks was 87.2 percent. The total power of the two stacks was 60 kW, and the total EDM energy required to meet the diluate treatment goal was 10.8 kWh/m^3.

Treatment costs for IR with Option 3A are summarized in Table 3.74. All costs are per m^3 of total concentrate recovered. The total treatment cost for concentrate treatment with Option 3A was $11.21 per m^3 of RO concentrate recovered.

IR Option 4

Option 4 for IR is shown in Figure 3.57. The blended product comprises the brine concentrator and crystallizer distillates.

Treatment costs for IR with Option 4 are summarized in Table 3.75. All costs are per m^3 of total concentrate recovered. The total treatment cost for IR with conventional ZLD treatment was $6.91 per m^3 of RO concentrate recovered.

IR Option 6

Option 6 for IR is shown in Figure 3.58. In this option, IR water is desalinated with RO with a recovery of around 50 percent. RO concentrate is treated with EDM. EDM recovery would

Table 3.75
ZLD treatment costs for IR with Option 4

Process	O&M cost ($/m^3)	Capital cost ($/m^3)	Total cost ($/m^3)
Brine concentrator	$2.28	$0.39	$2.67
Crystallizer	$1.46	$2.78	$4.24
Total	$3.74	$3.17	$6.91

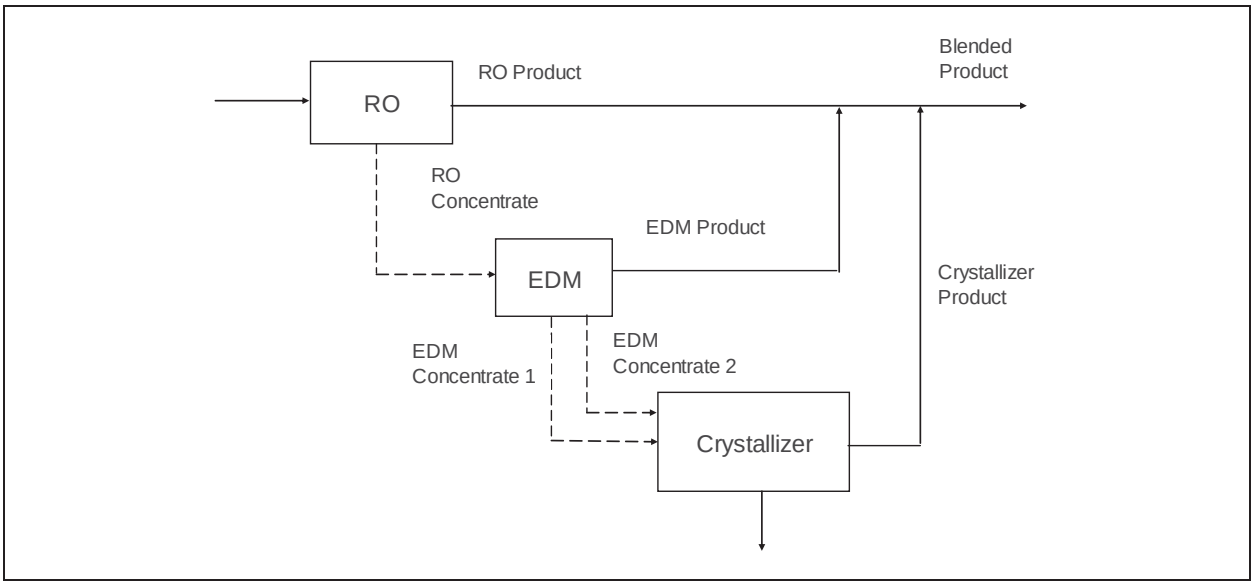

Figure 3.58 IR Option 6—RO followed by EDM and crystallizer

be 55 percent, and the EDM concentrate is treated in the crystallizer. The blended product comprises RO permeate, EDM diluate, and crystallizer distillate.

Input data used in the EDM power calculations for Option 6 are shown in Table 3.76. The feed to the EDM, the RO concentrate, had 55,374 mg/L TDS. The treatment goal for EDM was a diluate TDS of 800 mg/L. Blended with the RO permeate, this would produce a TDS of 500 mg/L. Two EDM stacks in series were required. An average NaCl conductivity of 300 mS cm^{-1} was used.

Results of the EDM energy calculations for Option 6 are shown in Table 3.77. Cell voltages of 1.40 V in the first stack and 1.44 V in the second stack were required. The currents were 300 A in Stack 1 and 120 A in Stack 2. Power polarization factors were 63 A cm/eq in Stack 1 and 73 A cm/eq in Stack 2. Stack 1 cell flow rates were 0.0168 L/s in the feed, 0.0152 L/s in the diluate, and a total of 0.0016 L/s in the two concentrate cells. Stack 2 cell flow rates were 0.0152 L/s in the feed, 0.0145 L/s in the diluate, and a total of 0.0006 L/s in the two concentrate cells. Recovery of the two EDM stacks was 87.2 percent. The total power of the two stacks was 60 kW, and the total EDM energy required to meet the diluate treatment goal was 10.8 kWh/m^3.

Treatment costs for IR with Option 6 are summarized in Table 3.78. All costs are per m^3 of total product water. The total treatment cost for Option 6 was $17.01 per m^3 of product water. The costs were dominated by the energy and NaCl costs for EDM.

Table 3.76
EDM model input for IR

Parameter	Value
Flow per cell set	0.0168 L/s
Cell sets per stack	100
Number of stacks in series	2
Membrane width	40 cm
Membrane length	160 cm
Membrane area	6400 cm^2
Cell width	0.07 cm
Cell velocity	6 cm/s
Shadow factor	1.2
CMX membrane area resistance	3 Ω cm^2
AMX membrane area resistance	2.5 Ω cm^2
CMS membrane area resistance	6.5 Ω cm^2
AMS membrane area resistance	6.5 Ω cm^2
Water transfer coefficient	7.6 mol/eq
Current utilization factor	0.90
Average NaCl cell conductivity	300 mS cm^{-1}
Feed water TDS	55,374 mg/L
Feed water temperature	298 K

IR Option 7

Option 7 for IR is shown in Figure 3.59. In this option, IR water is desalinated with RO with a recovery of around 50 percent. RO concentrate is treated with brine concentrator followed by a crystallizer. The blended product comprises RO permeate and brine concentrator and crystallizer distillate.

Treatment costs for IR with Option 7 are summarized in Table 3.79. All costs are per m^3 of total product water. The total treatment cost was $4.06 per m^3 of product water.

Comparison of IR Treatment Options

Treatment costs per m^3 of RO concentrate recovered for IR are shown in Figure 3.60. Option 7, treating the water with RO followed by thermal desalination was the least expensive option. Option 4, treatment of all of the water with thermal desalination, was 70 percent more expensive than Option 7. EDM was not cost effective for this water source. Option 3A was almost three times as expensive as Option 7, and Option 6 was four times as expensive.

Table 3.77
EDM model results for IR

Parameter	Value
Diluate TDS	800 mg/L
Stack 1 current	950 A
Stack 1 current density	0.148 A/ cm^2
Stack 1 power polarization	53 A cm/eq
Stack 1 Concentrate 1 conductivity	134 mS/cm
Stack 1 Concentrate 2 conductivity	134 mS/cm
Stack 1 diluate flow per cell	0.0120 L/s
Stack 1 Total concentrate flow per cell	0.0049 L/s
Stack 1 EDM recovery	71.1 %
Stack 1 voltage per cell	3.90 V
Stack 1 voltage	390 V
Stack 1 power	371 kW
Stack 2 current	540 A
Stack 2 current density	0.084 A/ cm^2
Stack 2 power polarization	95 A cm/eq
Stack 2 Concentrate 1 conductivity	134 mS/cm
Stack 2 Concentrate 2 conductivity	134 mS/cm
Stack 2 diluate flow per cell	0.0092 L/s
Stack 2 Total concentrate flow per cell	0.0028 L/s
Stack 2 voltage per cell	3.94 V
Stack 2 voltage	394 V
Stack 2 power	213 kW
Total EDM recovery	54.7%
Total EDM energy	135.6 kWh/m^3

Table 3.78
ZLD treatment costs for IR with Option 6

Process	O&M cost ($/$m^3$)	Capital cost ($/$m^3$)	Total cost ($/$m^3$)
RO	$0.29	$0.05	$0.35
EDM	$13.47	$0.12	$13.60
Crystallizer	$2.16	$1.25	$3.42
Total	$15.64	$1.38	$17.01

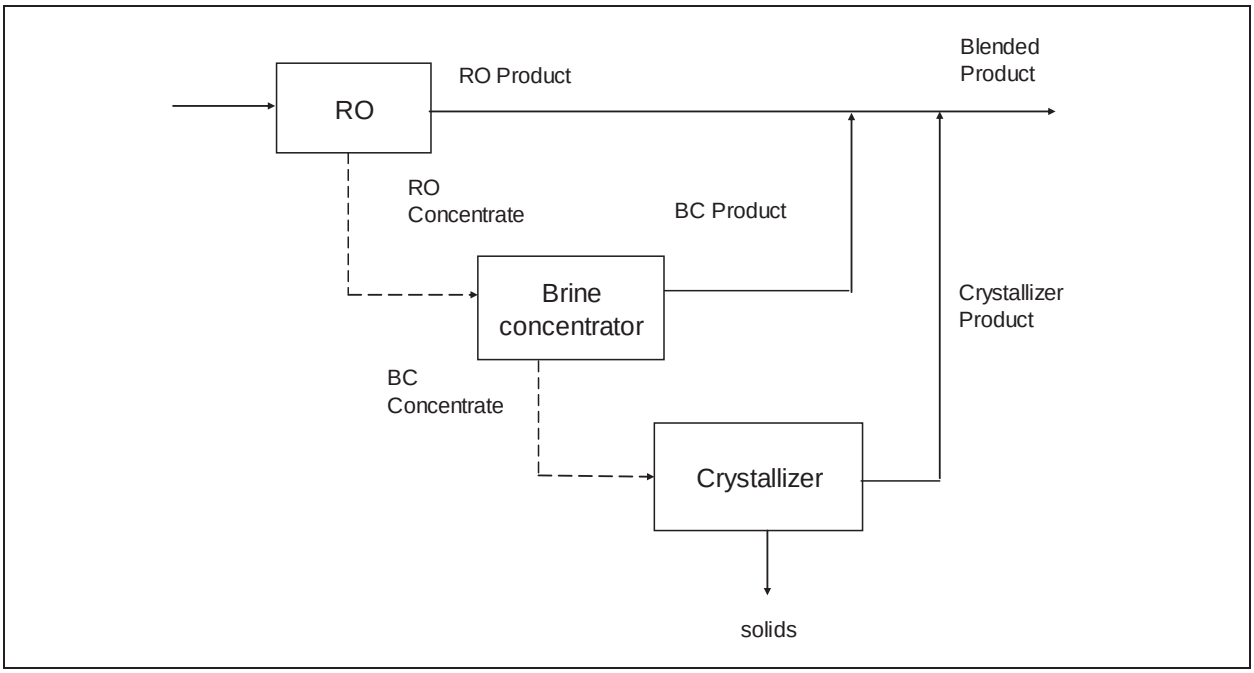

Figure 3.59 IR Option 7—RO followed by brine concentrator and crystallizer

Table 3.79
ZLD treatment costs for IR with Option 7

Process	O&M cost ($/m^3)	Capital cost ($/m^3)	Total cost ($/m^3)
RO	$0.30	$0.10	$0.40
Brine concentrator	$1.14	$0.22	$1.36
Crystallizer	$1.46	$0.84	$2.30
Total	$2.90	$1.16	$4.06

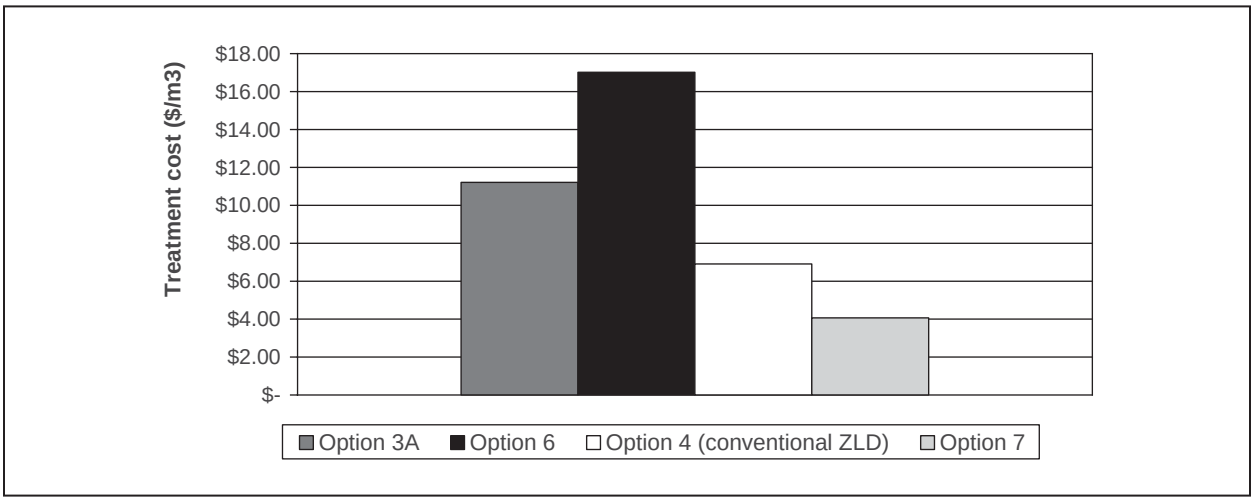

Figure 3.60 Comparison of concentrate treatment costs for IR ($ per m^3 RO concentrate recovered)

CHAPTER 4
SUMMARY AND CONCLUSIONS

SUMMARY

The objective of this research was to investigate methods for reducing the costs of desalination with zero liquid discharge management of concentrate. Seven water sources were evaluated, and these sources comprised a diverse set of water quality characteristics and water types. TDS in the sources ranged from 270 to 28,000 mg/L. Five of the sources had high concentrations of natural organic matter (NOM) with TOC concentrations ranging from 7 to 20 mg/L. Four of the sources were groundwater, and three were surface water. Four of the sources were treated at existing desalination facilities, two were potential water supply sources, and one was blowdown water from a power plant cooling tower. Bench- and pilot-scale tests were conducted with five of the sources. These test results were used to conduct desktop studies with two additional sources. Results from testing, modeling efforts, and desktop studies were used to develop full-scale ZLD treatment costs for each water.

The research approach comprised the following steps:

- Preliminary analyses to evaluate water quality and set treatment goals.
- Bench-scale testing to compare treatment options and select one ZLD approach for pilot-scale testing.
- Pilot-scale testing with the selected treatment approach.
- Evaluation of results to estimate full-scale treatment costs.

Preliminary analyses were conducted with each water source to select treatment options and set treatment goals. Treatment technologies evaluated included combinations of chemical softening, ion exchange, fluidized bed crystallization, activated alumina, coagulation with ferric chloride, electrodialysis, RO, calcite bed contactor, brine concentrator, and crystallizer.

Three ZLD approaches were formulated from the preliminary analyses of treatment goals and treatment options. Each approach comprised three steps: (1) concentrate treatment, (2) secondary desalination, and (3) evaporation. In the first step, concentrate is treated to reduce its membrane fouling potential. Treatment goals for this step included removal of calcium, sulfate, TOC, and silica. The treated concentrate is desalinated in the second step to generate product water and reduce the volume of concentrate. A final evaporation step is needed to treat concentrate from the secondary desalination device.

The ZLD approaches compared for further evaluation are shown in Table 4.1. MIEX or coagulation was included for TOC removal, softening or FBC for calcium removal, coagulation or AA for silica removal, and RO for secondary desalination in Options 1 and 2. EDM provided secondary desalination in Option 3, and MIEX® for TOC removal was the only concentrate treatment step. Thermal processes were used for the final evaporation step for each option.

Option 3, with EDM secondary desalination, was selected for further evaluation. EDM is a new electrodialysis technology that has advantages for concentrate treatment. Unlike RO and conventional electrodialysis technologies, the EDM concentrate is separated into two streams of highly soluble salts. This feature allows much higher recoveries to be achieved with EDM than

Table 4.1
ZLD treatment systems evaluated

ZLD treatment system	Concentrate treatment	Secondary desalination	Evaporation
1	MIEX® or coagulation + Softening or FBC + Coagulation or AA	RO	Thermal
2	MIEX® + Coagulation or AA + EDM	RO	Thermal
3	MIEX®	EDM	Thermal

with RO or other forms of electrodialysis. The concentrate streams from EDM are amenable to further treatment to develop solid and liquid products for beneficial use, which reduces the amount of solid waste byproducts from the ZLD process.

Option 3 was judged to be the option with the greatest potential for affordable and sustainable ZLD desalination for the following reasons:

- Higher recovery in the secondary desalination step.
- Fewest treatment processes required.
- Lowest production of solid byproducts.
- Lowest chemical usage.
- Greatest potential for beneficial use of byproducts.
- EDM is a new technology, and demonstrating the viability of this technology through pilot tests with several water sources was perceived to offer the greatest potential for the advancement of ZLD desalination.
- Preliminary calculations indicated Option 3 would be the least expensive and require the least energy.

Pilot tests were conducted with MIEX® followed by EDM. MIEX® was included only for the water sources with high TOC concentrations. MIEX® treatment was effective for reducing TOC concentrations ahead of EDM, and there was no sign of organic fouling of the EDM membranes during testing. MIEX® treatment also reduced sulfate concentrations.

Electrodialysis with EDM separated concentrate into two highly soluble streams, one containing sodium and anions and the other containing chloride and cations. Concentrate stream 1 contained high concentrations of sodium, chloride, and sulfate with low concentrations of calcium and magnesium. Concentrate stream 2 contained high concentrations of chloride, calcium, magnesium, and sodium.

Recovery of product water during EDM pilot tests ranged between 99.8 and 99.9 percent. The rate of water transfer by osmosis and electroosmosis, λ, ranged between 7.4 and 8.2 moles of water per equivalent of ions transferred.

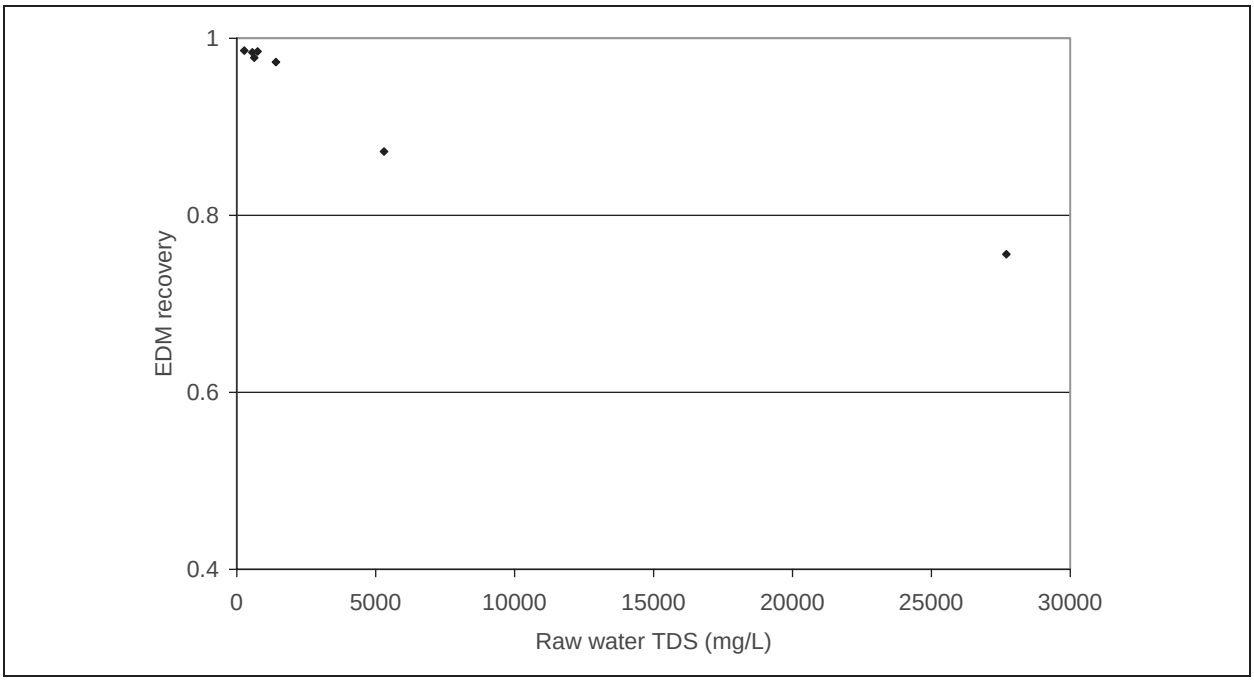

Figure 4.1 Effect of raw water TDS on EDM recovery in Option 3

Pilot test results were scaled up to calculate EDM recovery, water quality, and energy requirements for full-scale applications. Current in electrodialysis is proportional to the number and charge of ions removed from the diluate. Current is related to voltage and resistance by Ohm's law, and power is the product of current and voltage.

Figure 4.1 shows calculated full-scale EDM recovery for Option 3. The water lost as concentrate during desalination with EDM is proportional to the quantity of ions removed. Consequently, EDM recovery decreased as feed water TDS and the EDM desalination requirement increased.

Figure 4.2 shows the effect of raw water TDS on the EDM energy required in Option 3. The energy required for desalination with electrodialysis is proportional to the quantity of ions removed. Consequently, EDM energy increased in proportion to TDS. The alternative to EDM for treating RO concentrate is a thermal brine concentrator. Typical energy required for a brine concentrator is 20 kWh/m^3.

Figure 4.3 shows treatment costs for Option 3 compared with treatment costs for the currently established ZLD method using thermal desalination, Option 4. The energy requirement for electrodialysis depends on ionic concentration while the energy required for thermal desalination depends more strongly on the volume of water to be evaporated. Consequently, the rate of cost increase with TDS in the figure is steeper for Option 3 than for Option 4. At a raw water TDS of 3000 mg/L or less, Option 3 was significantly less expensive than Option 4. The costs appear to be comparable in the 5000 to 10,000 mg/L TDS range and to favor thermal desalination above 10,000 mg/L TDS.

TDS of the IR source was 28,000 mg/L. The estimated treatment cost for Option 3 was \$11.21 per m^3, and the estimated cost for Option 4 was \$6.91 per m^3. Option 7, treating this water with RO followed by thermal desalination, however, was less expensive than thermal treatment alone. The treatment cost for Option 7 was \$4.06 per m^3. This result, however, is qualified by the caveat that the membrane fouling potential of the IR water was very low relative to the other

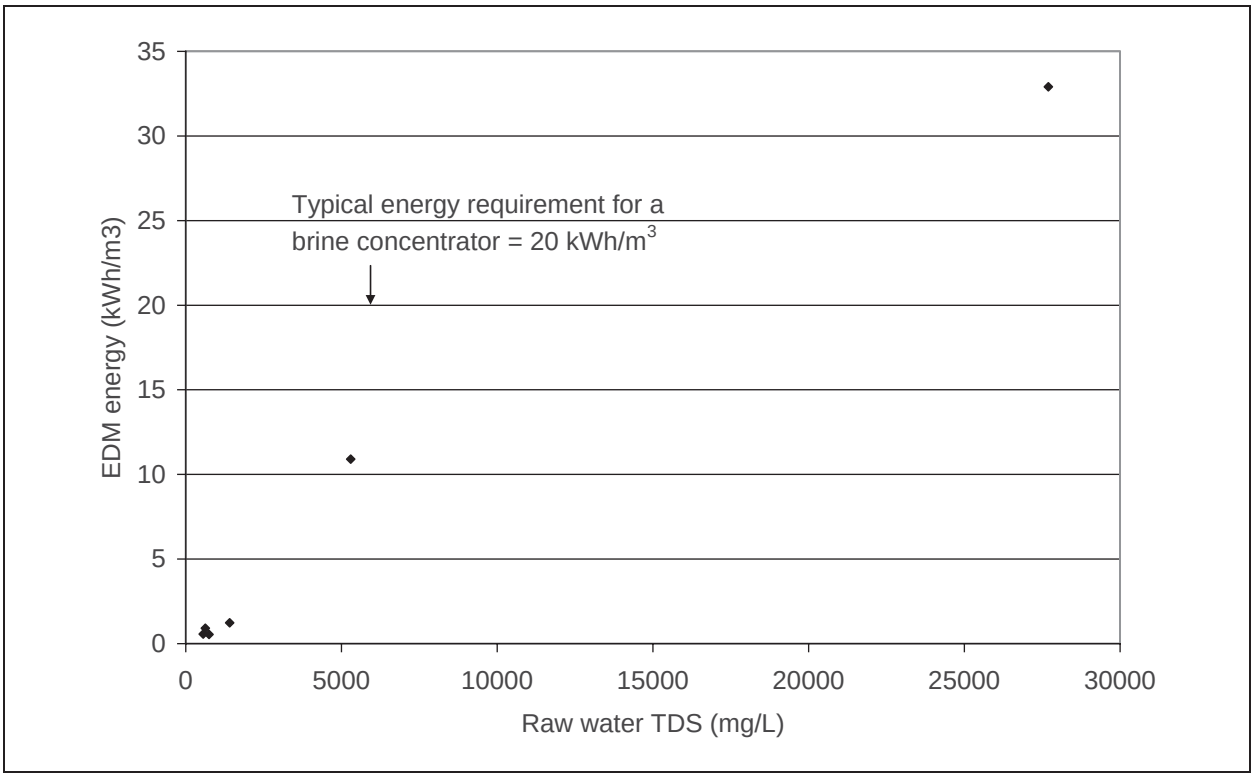

Figure 4.2 Effect of raw water TDS on energy required for EDM in Option 3

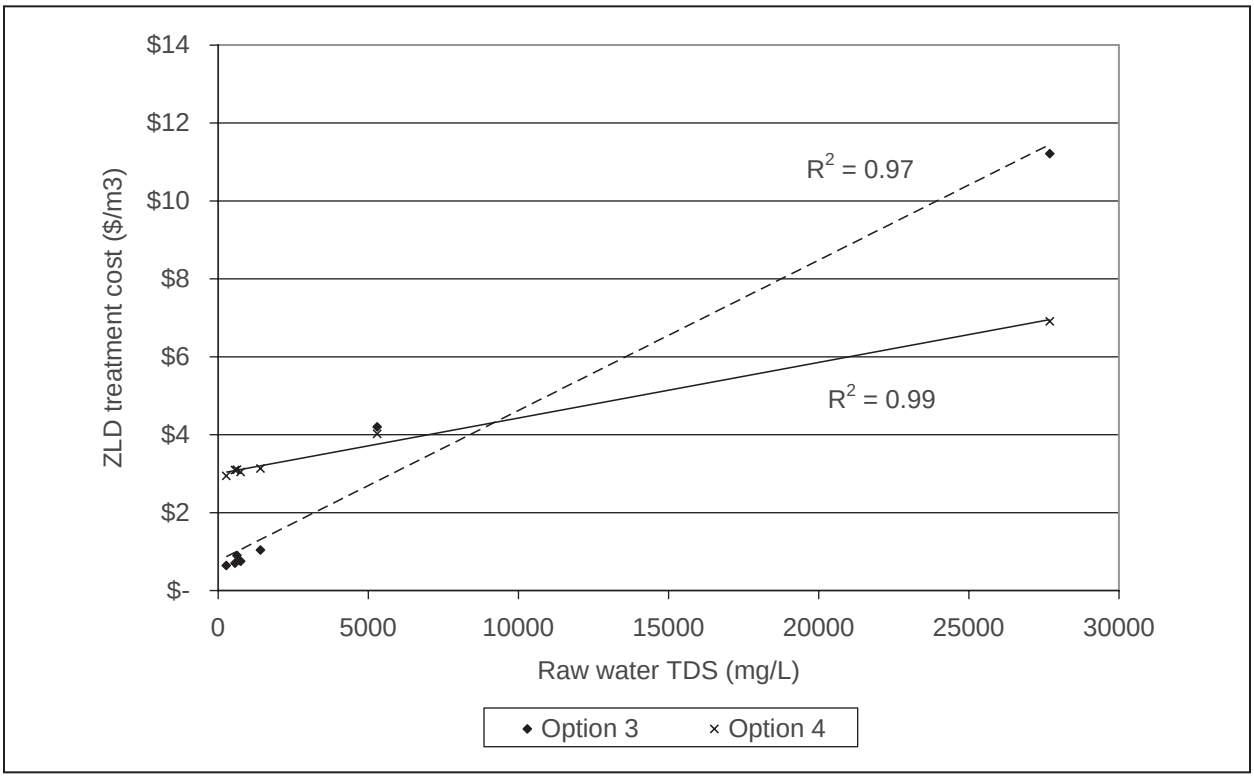

Figure 4.3 Effect of raw water TDS on relative costs for Options 3 and 4

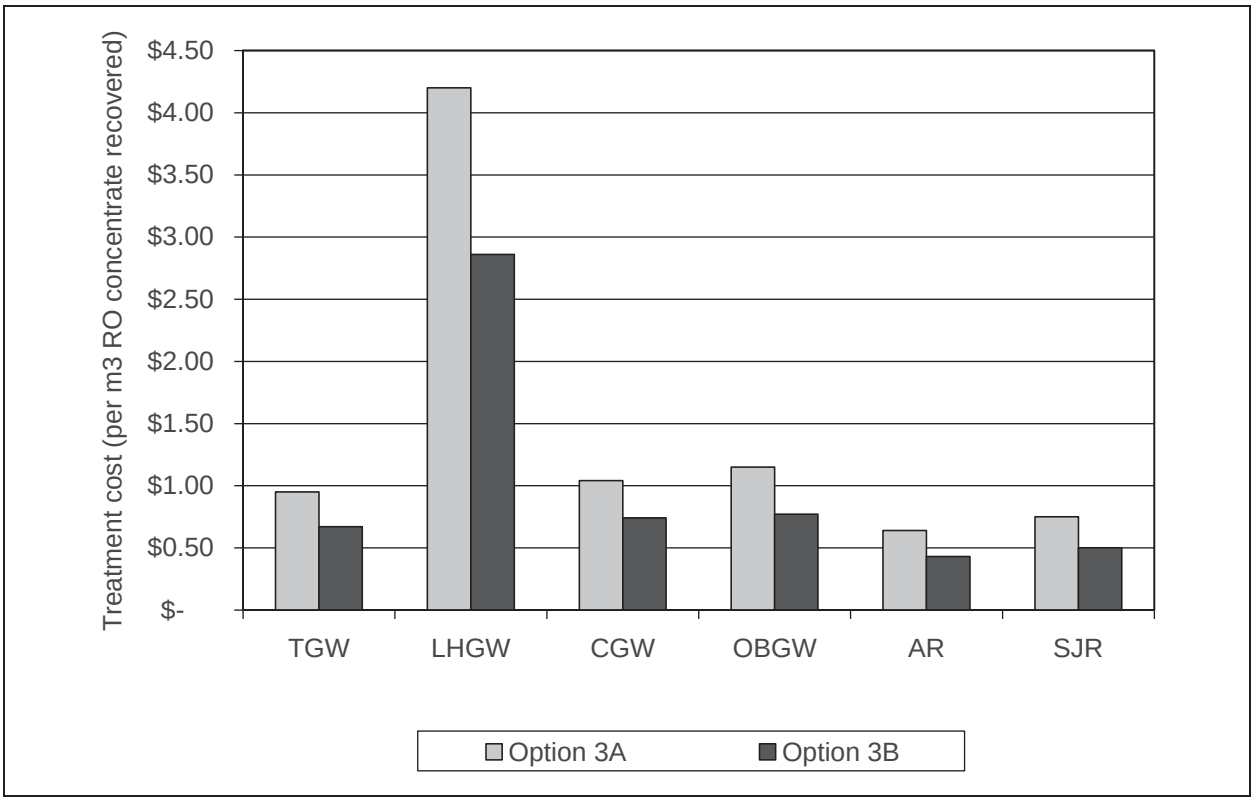

Figure 4.4 Improvements in ZLD treatment cost when beneficial chemicals are recovered from EDM concentrate

waters evaluated, because calcium comprised only 1 percent of the total TDS. At calcium to TDS ratios found in the other water sources, RO desalination of 28,000 mg/L TDS water would not be possible.

The separation of concentrate into two streams with high concentrations of calcium in one stream and high concentrations of sulfate in the other provides unique opportunities to develop beneficial salts from the concentrate generated by EDM. Treatment of EDM concentrate to develop products was evaluated in Option 3B to assess the economic benefit of this additional treatment step. The salts generated were gypsum, calcium carbonate, and dolomite. Each of these salts has commercial uses, but the analysis was treated as if the salt products were cost neutral having neither economic value nor disposal cost.

The potential savings from treating the EDM concentrate is illustrated in Figure 4.4 comparing the costs of Options 3A and 3B. Treatment of the EDM concentrate (Option 3B) reduced the costs of Option 3 by one third for each of the water sources. The reason for the cost reduction is that part of the NaCl-rich water is recycled to the EDM as a supply of NaCl rather than treated by thermal evaporation.

CONCLUSIONS

This research indicated the use of electrodialysis with EDM is very promising for zero liquid discharge desalination of brackish water sources containing 5000 mg/L TDS or less. Above

10,000 mg/L TDS concentrations, energy requirements begin to shift the economics in favor of thermal desalination.

Compared with concentrate treatment approaches in which chemicals are added to precipitate targeted salts (e.g., Options 1 and 2), EDM requires only NaCl addition, and there is potential to recycle NaCl from concentrate back to the process. Consequently, the generation of solid byproducts is reduced substantially. This characteristic is an important advantage because chemical, treatment, and disposal costs for managing solid byproducts can be significant in ZLD desalination.

An advantage of using EDM rather than a second RO to desalinate RO concentrate is that less pretreatment is required. EDM separates ions of sparingly soluble salts into separate concentrate streams thereby eliminating the membrane scaling potential of calcium sulfate and calcium carbonate. Consequently calcium removal was not necessary in order to desalinate the sources tested with EDM, but softening would have been required for secondary desalination with RO. Silica passed through EDM unchanged because it is an uncharged molecule. Conversely silica is concentrated in RO, so silica removal ahead of RO would have been required for several of the water sources tested. Similarly TOC was not concentrated in EDM, but it is concentrated in desalination with RO. Therefore, TOC removal ahead of EDM was not as critical as it would have been for secondary desalination with RO.

Specific conclusions from test results were as follows:

- MIEX® treatment of RO concentrate with TOC concentrations of 50 mg/L reduced UVA by 70 to 90 percent at regeneration rates of 50 to 200 BV. There was no indication of organic fouling of the EDM membranes during the pilot tests.
- Prior to testing, the effectiveness of EDM in separating concentrate into two streams of highly soluble salts was recognized as a key to its success treating RO concentrate. The pilot tests reported herein demonstrated that EDM was highly effective in separating concentrate into two streams: one containing sodium and anions and the other containing chloride and cations.
- Silica and TOC went through EDM treatment largely unaffected. Silica in the EDM diluate was 25.0 mg/L compared with 24.6 mg/L in the feed. TOC in the EDM diluate was 18.5 mg/L compared with 20.4 mg/L in the feed.
- Modest levels of TOC and silica were found in the concentrate streams, but the concentrations were less than those in the primary RO concentrate and not great enough to pose membrane fouling risks. TOC generally carries a negative charge, and Concentrate Stream 1 where anions were collected contained 36.5 mg/L of TOC. The membrane fouling potential of TOC increases in the presence of calcium, but calcium and TOC were separated by EDM into different concentrate streams.
- Recovery of 99.8 to 99.9 percent of product water was achieved by the EDM pilot treating primary RO concentrate .
- Power consumption by the EDM pilot ranged from 1.1 to 1.8 watts per EDM cell.
- No inorganic or organic compound concentrations were found in any of the EDM streams that would be considered potential membrane fouling threats. There was no variation in the EDM pilot pressures or flows throughout testing. It was concluded that the EDM pilot treated primary RO concentrate from the sources without fouling the EDM membranes.

- Treatment costs for Option 3, EDM followed by a crystallizer, ranged from $0.64 to $11.21 per m^3 and were dependent on TDS concentration of the water. Treatment costs ranged from $0.64 to $0.90 per m^3 treated for the water sources with TDS less than 1500 mg/L TDS. The cost for the 5300 mg/L TDS source was $4.20 per m^3 treated, and the cost for the 28,000 mg/L TDS source was $11.21 per m^3 treated.
- Extending treatment in Option 3 to develop beneficial products from EDM concentrate reduced treatment costs by about one-third for each of the sources evaluated. (This enhancement was not evaluated for the IR source with 28,000 mg/L TDS because the cost for Option 3 was prohibitive). The salt products were gypsum, calcium carbonate, and dolomite. The salt products were assumed to be cost neutral in the analysis having neither commercial value nor disposal cost. Because of the high concentration of calcium in one EDM concentrate stream and sulfate in the other stream, gypsum was precipitated in the first EMD concentrate treatment step without chemical addition.
- Treatment to remove TOC ahead of EDM was evaluated for two of the sources. TOC treatment increased the cost for Option 3 by 28 and 36 percent.

RECOMMENDATIONS FOR FURTHER RESEARCH

This research demonstrated the viability of treating RO concentrate with EDM and the potential for ZLD cost savings using this approach. Suggestions for further research on this topic are as follows:

- The ZLD approach with EDM was very cost-effective for brackish waters with low TDS but prohibitively expensive for the water evaluated with 28,000 mg/L TDS. Conceivably there is a TDS transition range where thermal desalination becomes less expensive than EDM. From the sources tested, it appeared that this range might be between 5000 and 15,000 mg/L raw water TDS. Although utilities will preferentially use lower TDS brackish water rather than higher TDS water because it is less expensive, more study of water sources in the 5000 to 15,000 mg/L TDS range would help define the cost breakpoint between EDM and thermal processes.
- The treatment of EDM concentrate to develop salts with commercial value was treated as a desktop study using the EDM concentrate water chemistry data from the pilot study. This treatment enhancement helps reduce ZLD costs and provides better environmental management of solid byproducts generated in desalination. Further study to optimize treatment methods and evaluate marketability of potential products would be beneficial.
- Thermal desalination with a crystallizer was used for the final evaporation step. Crystallization is an expensive process because of the corrosion resistant materials required for the equipment and because of the energy required. Although a small percentage of the flow was treated with crystallization, the cost for crystallization comprised a significant fraction of the total treatment cost. With treatment of EDM concentrate to develop other beneficial products, this small residual of concentrate would contain mostly sodium and chloride. A significant cost reduction could be realized by finding beneficial uses for this sodium chloride solution that would otherwise be evaporated in a crystallizer in wet climates or discharged to an evaporation pond in arid climates.

CHAPTER 5
RECOMMENDATIONS TO UTILITIES

As utilities face the challenges of increased use of alternative water sources to meet water demands and treatment to remove emerging contaminants at very low concentrations, economic and environmentally sustainable management of RO concentrate will become increasingly important. This research demonstrated a promising method of zero liquid discharge desalination using a new electrodialysis technology, EDM, and thermal desalination to treat and recover RO concentrate. This approach appears to offer significant cost savings for ZLD treatment of brackish waters with TDS less than 5000 mg/L.

Thermal desalination with a crystallizer was used in this project for the final evaporation step because the climate in Florida is too wet for effective use of evaporation ponds. Utilities in more arid climates, however, would have the option of using an evaporation pond in lieu of a crystallizer. At a loading rate of 2 gpm per acre and a construction cost of $200,000 per acre, an evaporation pond in lieu of a crystallizer would reduce treatment costs for Option 3 by 12 to 36 percent for the water sources evaluated.

Although EDM is a new technology, it is nevertheless simply electrodialysis with an innovative arrangement of ion exchange membranes. Electrodialysis has been used for water desalination for more than three decades and in fact has a longer history of practice than RO. Electrodialysis theory and application are well understood, and the membranes used in the EDM pilot are widely available commercial membranes. For these reasons, it is conceivable that the EDM technology will be available for full-scale implementation within a short time frame.

It is recommended that utilities faced with current or projected concentrate management challenges consider the ZLD approach evaluated in this research using the EDM technology. The model developed in this research can be used to evaluate this ZLD approach and compare its costs with costs for other ZLD options. If this preliminary evaluation looks promising, a utility might choose to conduct a pilot study with EDM to develop design and cost criteria specific to its water source.

APPENDIX A
UNIT CONVERSION FACTORS

1 L = 0.264 U.S. gal
1 m^3 = 264 U.S. gal
1 kg = 2.204 lb
1 m = 3.281 ft
1m^3/d = 264gal/d

APPENDIX B
EDM MODEL

PREDICTIVE MODEL FOR ELECTRODIALYSIS METATHESIS ENERGY REQUIREMENTS

A mathematical model was developed to calculate energy requirements for desalination with electrodialysis metathesis (EDM). The input data are influent water quality, EDM design and operating parameters, and desalination treatment goals. The input data are used to calculate voltage drop, concentrate flows, and concentrate water quality for an EDM cell set. The model can be used to perform the following:

- Calculation of energy requirements for desalination of any water quality set.
- EDM process optimization.
- Evaluation and comparison of different treatment options, e.g., EDM followed by RO versus EDM alone.

Model equations are discussed first for basic electrodialysis then expanded for EDM. The primary difference between the two is the number of cells and membranes in the repeating unit. Electrodialysis stacks are comprised of cell pairs formed by a pair of membranes while the repeating unit in EDM stacks comprises four cells and four membranes.

BASIC ELECTRODIALYSIS CELL PAIR

A basic electrodialysis cell pair is illustrated in Figure B.1. In calculating the theoretical voltage for desalinating water in an electrodialysis stack, it is convenient to calculate the voltage drop across a single cell pair then multiply the result by the number of cell pairs in the stack. The cell pair comprises from left to right: a diluate compartment, an anion selective membrane (A), a concentrate compartment, and a cation selective membrane (C). A full-scale stack contains hundreds of such cell pairs between a cathode and anode.

Concentrate and diluate flows are co-current in the Y direction, and the figure shows a cross-section of the cell pair through the X-Z plane. The electrodes generate an electric potential difference in the X direction, perpendicular to the membranes.

Ion transport in the X direction occurs by two mechanisms: (1) as migration driven by the electrical potential gradient, and (2) as diffusion driven by chemical potential gradients due to concentration differences. Ion flux by diffusion is negligible relative to migration and can be accounted for within the current utilization factor. Nevertheless, the electromotive force exerted by the diffusion potential must be counteracted by electrical potential and therefore contributes to the voltage drop across the cell pair.

Ion transport in the Y direction occurs by convection. Ion concentrations in the diluate stream decrease in the Y direction from the inlet to the outlet of the cell pair, and those in the concentrate stream increase.

Figure B.1a shows salt concentrations across the cell pair in a plane perpendicular to the Y-axis. The points 1 through 9 in the figure mark concentration transition points that occur at

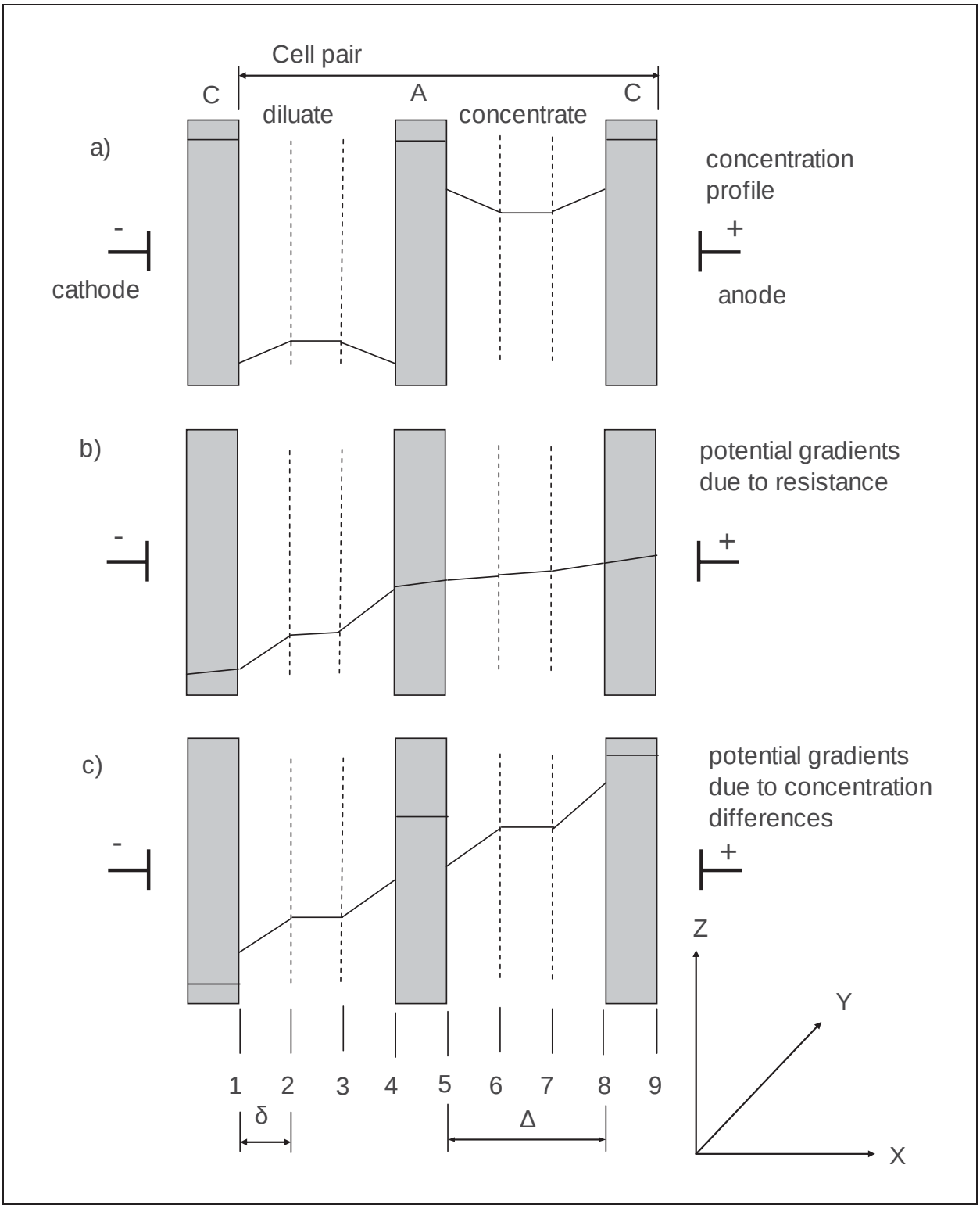

Figure B.1 Electrodialysis pair schematic illustrating (a) the electrolyte concentration profile, (b) the potential gradient profile due to resistances, and (c) the potential gradient profile due to concentration differences

membrane surfaces and boundary layers. Ions are transported much faster through the membranes, than they are through solution which causes depletion of ions at the membrane surface in the diluate and accumulation of ions at the membrane surface in the concentrate. Hence, boundary layer concentrations increase in the diluate and decrease in the concentrate with distance from the membrane surface. Ion concentrations are considerably higher in membranes than in solution to balance membrane fixed charges, and these ions are almost exclusively counterions, i.e., ions of opposite charge.

Voltage drop across a cell pair is the sum of the following components:

1. Voltage to overcome solution resistances.
2. Voltage to overcome membrane resistances.
3. Voltage to counteract the electromotive force from chemical potential differences.

Figure B.1b shows voltage drop across the cell pair due to resistance. Because resistance is inversely proportional to conductivity, voltage drops in solution are greatest in the diluate. Voltage drops across membranes are proportional to area resistances of the membranes. Energy requirements are minimized by maintaining narrow spacing between membranes, selecting low resistance membranes, and maintaining sufficient cross-flow velocity to minimize boundary layer thickness. The voltage drop across the cell pair is the sum of diffusion potentials and voltage drops due to resistances of the two solution compartments and the membranes.

Potential gradients due to concentration differences are shown in Figure B.1c. Differences in chemical potential exert an electromotive force that must be counteracted by the applied voltage difference. The voltage drop due to a difference in chemical potentials between two solutions is expressed as

$$\Delta U_{1-2dp} = \frac{\Re T}{F}\int_{1}^{2}(t_{-}^{\,d} - t_{+}^{\,d})\,d(\ln \gamma C)$$

Therefore, the voltage drop across the cell pair due to chemical potential differences is

$$\Delta U_{dp} = \frac{\Re T}{F}\left[\begin{array}{l}(t_{-}^{\,d} - t_{+}^{\,d})\displaystyle\int_{1}^{2} d(\ln \gamma C) + (t_{-}^{\,d} - t_{+}^{\,d})\int_{3}^{4} d(\ln \gamma C) + (t_{-}^{\,am} - t_{+}^{\,am})\int_{4}^{5} d(\ln \gamma C) + \\ (t_{-}^{\,c} - t_{+}^{\,c})\displaystyle\int_{5}^{6} d(\ln \gamma C) + (t_{-}^{\,c} - t_{+}^{\,c})\int_{7}^{8} d(\ln \gamma C) + (t_{-}^{\,cm} - t_{+}^{\,cm})\int_{8}^{9} d(\ln \gamma C)\end{array}\right]$$

The above expression can be simplified by recognizing the following characteristics of ion transport in solution and through the membranes:

- Transport numbers of cations and anions in a solution are similar. Assume $t_{-}^{\,d} = t_{+}^{\,d}$ and $t_{-}^{\,c} = t_{+}^{\,c}$.
- Current through the membranes is carried almost exclusively by counterions. Assume $t_{-}^{\,am} = 1$, $t_{+}^{\,am} = 0$, $t_{-}^{\,cm} = 0$, and $t_{+}^{\,cm} = 1$.

Therefore,

$$\Delta U_{dp} = \frac{\Re T}{F}\left[\int_4^5 d(\ln \gamma C) - \int_8^9 d(\ln \gamma C)\right]$$

$$\Delta U_{dp} = \frac{\Re T}{F}\left[\ln\left(\frac{\gamma_5 C_5}{\gamma_4 C_4}\right) - \ln\left(\frac{\gamma_9 C_9}{\gamma_8 C_8}\right)\right]$$

The potential drop in solution from point 1 to point 2 due to resistance is as follows:

$$\Delta U_{1-2IR} = i\int_1^2 \frac{dx}{\kappa}$$

Here κ is the conductivity of the solution with the units S/cm that can be measured with a conductivity meter and a conductivity cell with a known cell constant.

Potential drops through the anion and cation membranes are

$$\Delta U_{amIR} = i\rho_{am}$$

$$\Delta U_{cmIR} = i\rho_{cm}$$

Summing terms across the cell pair, the potential drop due to resistance is

$$\Delta U_{IR} = i\left[\int_1^2 \frac{dx}{\kappa} + \int_2^3 \frac{dx}{\kappa} + \int_3^4 \frac{dx}{\kappa} + \rho_{am} + \int_5^6 \frac{dx}{\kappa} + \int_6^7 \frac{dx}{\kappa} + \int_7^8 \frac{dx}{\kappa} + \rho_{cm}\right]$$

If it is assumed that concentration variations across each diluate and concentrate cell are kept a minimum to avoid concentration polarization and recognizing that Δ>>δ, the potential drop due to resistance can be simplified to

$$\Delta U_{IR} = +i\left[\frac{\Delta}{k_d} + \rho_{am} + \frac{\Delta}{k_c} + \rho_{cm}\right]$$

Combining diffusion potential and resistance terms, the total potential drop across the cell pair is

$$\Delta U = \frac{\Re T}{F}\left[\ln\left(\frac{\gamma_c C_c}{\gamma_d C_d}\right) - \ln\left(\frac{\gamma_d C_d}{\gamma_c C_c}\right)\right] + i\left[\frac{\Delta}{k_d} + \rho_{am} + \frac{\Delta}{k_c} + \rho_{cm}\right]$$

If ratios of diluate and concentrate activities are replaced with the ratios of their conductivities, the equation simplifies to

$$\Delta U = \frac{\Re T}{F}\left[\ln\left(\frac{k_c}{k_d}\right) - \ln\left(\frac{k_d}{k_c}\right)\right] + i\left[\frac{\Delta}{k_d} + \rho_{am} + \frac{\Delta}{k_c} + \rho_{cm}\right] \quad \text{(B.1)}$$

There are factors that reduce the efficiency of the applied voltage in real world applications and cause the actual voltage drop to be greater than the value calculated in Equation B.1. Membranes in a stack are separated by a mesh spacer. The spacer reduces the area available for current flux through solution and through the membranes, and reducing the area available for current increases resistance. This is referred to as shadow effect, and Equation B.1 is corrected by application of shadow effect factor, β, to the resistance terms.

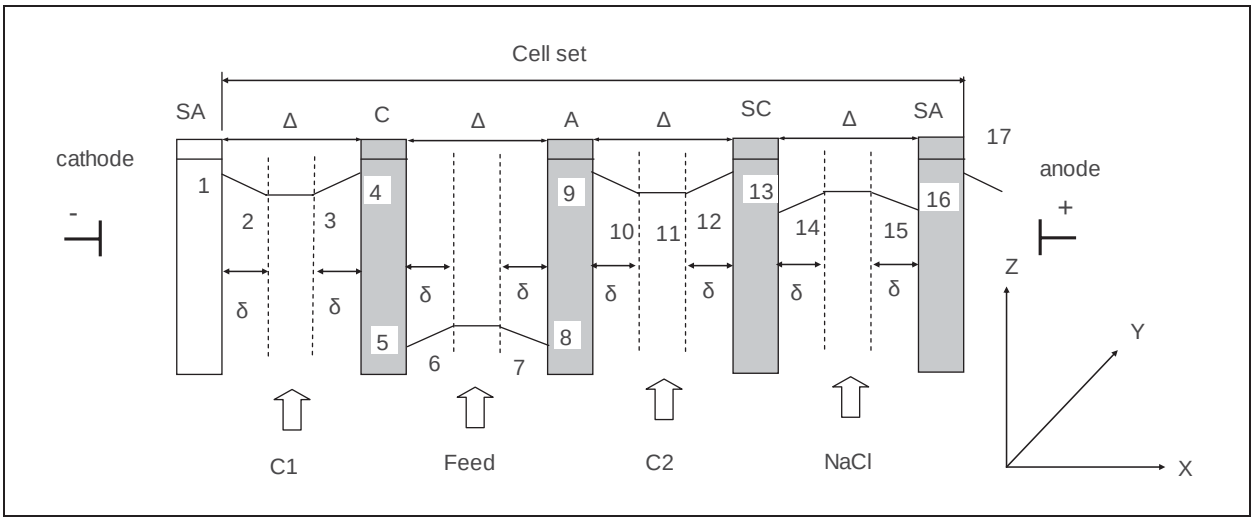

Figure B.2 Electrodialysis metathesis cell set illustrating the electrolyte concentration profile

$$\Delta U = \frac{\Re T}{F}\left[\ln\left(\frac{k_c}{k_d}\right) - \ln\left(\frac{k_d}{k_c}\right)\right] + \beta i\left[\frac{\Delta}{k_d} + \rho_{am} + \frac{\Delta}{k_c} + \rho_{cm}\right] \tag{B.2}$$

In an electrodialysis stack, not all of the electrical potential is utilized to transport ions. Several factors can contribute to incomplete current utilization including the following:

- Current can pass through the stack manifold.
- The membranes are not perfectly selective.
- There is water transfer across the membranes due to osmosis and electroosmosis.

A current efficiency factor, ζ, is applied to capture these inefficiencies.

$$\zeta = \frac{I_{theoretical}}{I_{actual}}$$

ELECTRODIALYSIS METATHESIS MODEL

The EDM cell set is illustrated schematically in Figure B.2. The cell set comprises from left to right: concentrate compartment 1, cation selective membrane C, diluate compartment, anion selective membrane A, concentrate compartment 2, monovalent cation selective membrane SC, NaCl compartment, and monovalent anion selective membrane SA. All flows are co-current in the Y direction, and the voltage applied to the electrodes causes an electrical potential gradient in X direction. The concentration profile is shown.

Voltage drops in the EDM cell set are analogous to the basic ED cell pair except the additional concentrate compartment, the NaCl compartment, and the two additional membranes must be accounted for. The equation for voltage drop across the EDM cell set is developed with assumptions used to develop the ED equation:

- The effects of concentration variations within each compartment are negligible.

- Cation and anion transport numbers in a solution are similar.
- Current is carried in membranes exclusively by counterions.

With the above assumptions, voltage drop due to diffusion potential in the EDM cell set is

$$\Delta U_{dp} = \frac{\Re T}{F}\left[-\int_{4}^{5} d(\ln \gamma C) + \int_{8}^{9} d(\ln \gamma C) - \int_{12}^{13} d(\ln \gamma C) + \int_{16}^{17} d(\ln \gamma C)\right]$$

$$\Delta U_{dp} = \frac{\Re T}{F}\left[-\ln\left(\frac{\gamma_d C_d}{\gamma_{c1} C_{c1}}\right) + \ln\left(\frac{\gamma_{c2} C_{c2}}{\gamma_d C_d}\right) - \ln\left(\frac{\gamma_{NaCl} C_{NaCl}}{\gamma_{c2} C_{c2}}\right) + \ln\left(\frac{\gamma_{c1} C_{c1}}{\gamma_{NaCl} C_{NaCl}}\right)\right]$$

If activity ratios are replaced with conductivity ratios,

$$\Delta U_{dp} = \frac{\Re T}{F}\left[-\ln\left(\frac{k_d}{k_{c1}}\right) + \ln\left(\frac{k_{c2}}{k_d}\right) - \ln\left(\frac{k_{NaCl}}{k_{c2}}\right) + \ln\left(\frac{k_{c1}}{k_{NaCl}}\right)\right]$$

With the assumption that concentration variations across each compartment are negligible and recognizing that $\Delta >> \delta$, the potential drop due to resistance in the EDM cell set is

$$\Delta U_{IR} = i\left[\frac{\Delta}{k_{c1}} + \rho^{cm} + \frac{\Delta}{k_d} + \rho^{am} + \frac{\Delta}{k_{c2}} + \rho^{scm} + \frac{\Delta}{k_{NaCl}} + \rho^{sam}\right]$$

Combining diffusion potential and resistance terms and applying the shadow effect factor, β,

$$\Delta U = \frac{\Re T}{F}\left[-\ln\left(\frac{k_d}{k_{c1}}\right) + \ln\left(\frac{k_{c2}}{k_d}\right) - \ln\left(\frac{k_{NaCl}}{k_{c2}}\right) + \ln\left(\frac{k_{c1}}{k_{NaCl}}\right)\right] + i\beta\left[\frac{\Delta}{k_{c1}} + \rho_{cm} + \frac{\Delta}{k_d} + \rho_{am} + \frac{\Delta}{k_{c2}} + \rho_{scm} + \frac{\Delta}{k_{NaCl}} + \rho_{sam}\right] \quad \text{(B.3)}$$

CALIBRATION OF THE EDM MODEL WITH PILOT DATA

Voltage Drop at the Electrodes

In addition to voltage drops across cell sets, there is also a voltage drop due to reactions at the electrodes. A typical full-scale EDM stack contains at least 100 cell sets between a pair of electrodes, and voltage drop at electrodes is negligible relative to voltage across all of the cell sets.

The EDM pilot stack, however, contained five cell sets between a pair of electrodes, and consequently voltage drop at the electrodes comprised a significant fraction of the stack voltage. In order to use pilot data to predict full-scale performance, voltage drop attributable to the pilot electrodes and electrode rinse solutions had to be quantified.

An experiment was conducted to determine voltage drop at the pilot stack electrodes. The pilot stack was disassembled and emptied of all membranes except a single cation exchange membrane. Four different strength Na_2SO_4 solutions were run through the stack while varying voltage and measuring current to evaluate electrode voltage drop as a function of solution conductivity.

The results of this experiment are shown in Figure B.3. A linear equation fit the data for each Na_2SO_4 solution with an intercept of 3 volts. Potential drop at electrodes is the sum of a fixed component due to resistance through stack materials and voltage drop due to solution and membrane resistances. Consequently, the intercept in Figure B.3 represents the fixed voltage drop at the electrodes (U_0), which includes the potential required for decomposition of water at each electrode

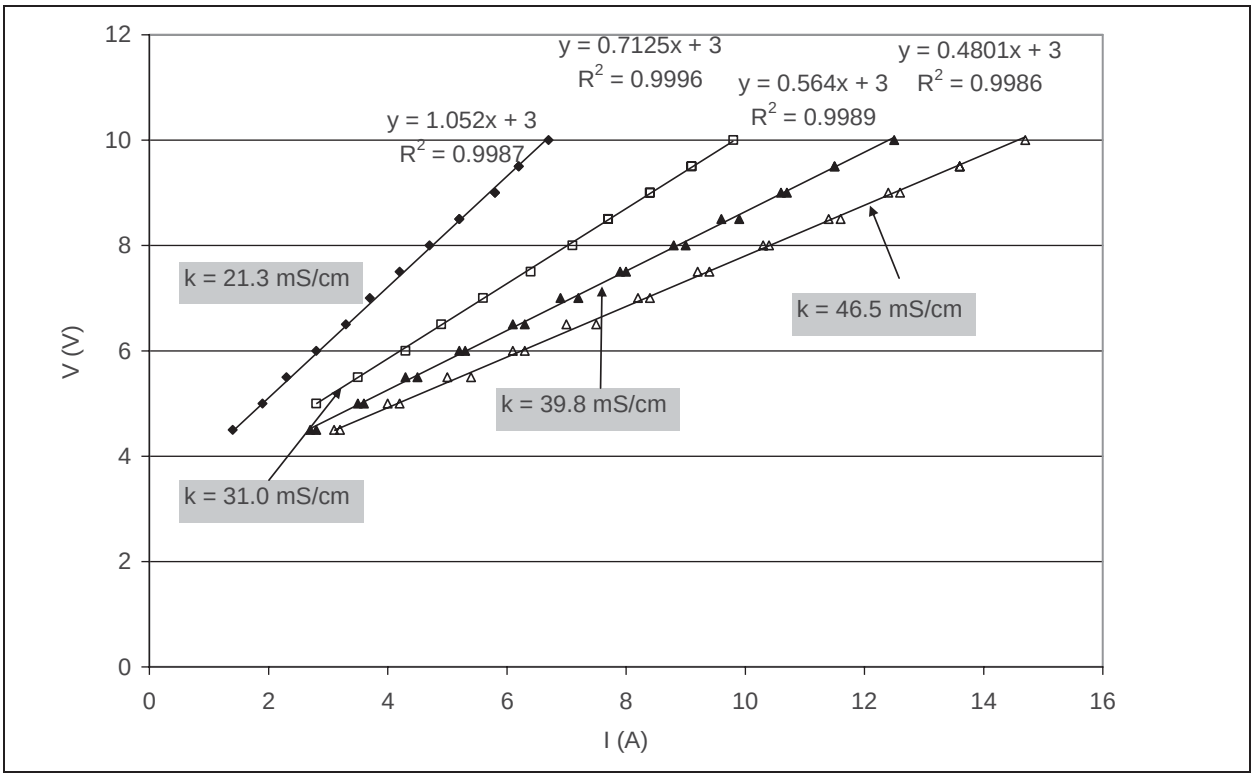

Figure B.3 Results of pilot experiment to isolate voltage drop at the electrodes

and the overvoltage required to generate gas bubbles of hydrogen at the cathode and oxygen at the anode, and the slope of each graph represents resistances across the membrane, R_m, and solution, R_{sol} at the solution conductivity tested. The resistance of the membrane is the area resistance, ρ (ohm·cm^2), divided by the membrane area A (cm^2). The voltage drop at the electrodes (U_e) is

$$U_e = U_0 + I(R_{sol} + R_m) = U_0 + I\left(R_{sol} + \frac{\rho}{A}\right)$$

The slope of the graph is $R_m + R_{sol}$. Therefore, R_{sol} can be calculated from the slope of the linear regression for each data set and the known area resistance of the membrane. The membrane used in the experiment had an area resistance of 3 ohm·cm^2 and a membrane area of 200 cm^2. Therefore, the membrane resistance was 0.015 ohm. Because solution resistance varies linearly with conductivity, the product of R_{sol} and k was a constant.

Calculated values of R_{sol} and $R_{sol} \times k$ are shown Table B.1. Solution resistance was the difference between the graph slope and the membrane resistance. The calculated values of $R_{sol} \times k$ were within 2 percent of one another, and the average value was 21.8 ohms mS cm^{-1}. Therefore, the relationship $R_{sol} = 21.8\ k^{-1}$ was used in the model to calculate solution resistance in the electrode compartments as a function of solution conductivity.

With all membranes replaced, the pilot stack contained two electrode membranes, a CMB membrane at the anode and an AHA membrane at the cathode. The area resistances were 4.5 Ω cm^2 for the CMB membrane and 4.1 Ω cm^2 for the AHA membrane. The total membrane resistance was 0.043 Ω. Therefore, the electrode voltage drop in the pilot unit at any conductivity k was calculated as

Table B.1
Calculated values of the product of solution resistance and conductivity ($R_{sol} \times k$)

k (mS cm^{-1})	21.3	31.0	39.8	48.7
Slope (Ω)	1.052	0.713	0.564	0.480
R_{cm} (Ω)	0.015	0.015	0.015	0.015
R_{sol} (Ω)	1.037	0.698	0.549	0.465
$R_{sol} \times k$ (Ω mS cm^{-1})	22.0	21.6	21.9	21.7

Table B.2
Area resistances of EDM pilot membranes

Membrane	Area resistance (Ω cm^2)
CMX	3.0
AMX	2.4
CMS	6.5
ACS	6.5

$$U_e = 3 + I\left(\frac{21.8}{k} + 0.043\right)$$

Area Resistance of Cell Membranes

The area resistances, ρ, of the four membranes in each cell set were as shown Table B.2.

Conductivity Temperature Correction Factor

The conductivity meter used to collect pilot data automatically corrected measured conductivity to a standard conductivity at 25 °C using a factor of 2 percent per degree Celsius. Actual conductivities, however, were needed for model calibration. Measured conductivities were converted to actual conductivities with a temperature correction factor, TCF, where T is the measured temperature (°C) and α = 0.02.

$$TCF = 1 + \alpha(T - 25)$$

Calculation of EDM Concentrations

Concentrations in the EDM concentrate cells must be known to calculate voltage requirements with Equation B.3. To use the model as a predictive tool in the absence of empirical data, these concentrations first must be calculated with equivalent balance equations.

Ion and water flux in an EDM cell set are represented in Figure B.4. Ions are transported from the diluate cell, D, to the two concentrate cells, C1 and C2, by the applied electrical potential gradient. Water is transported from the diluate cell to the two concentrate cells by osmosis and

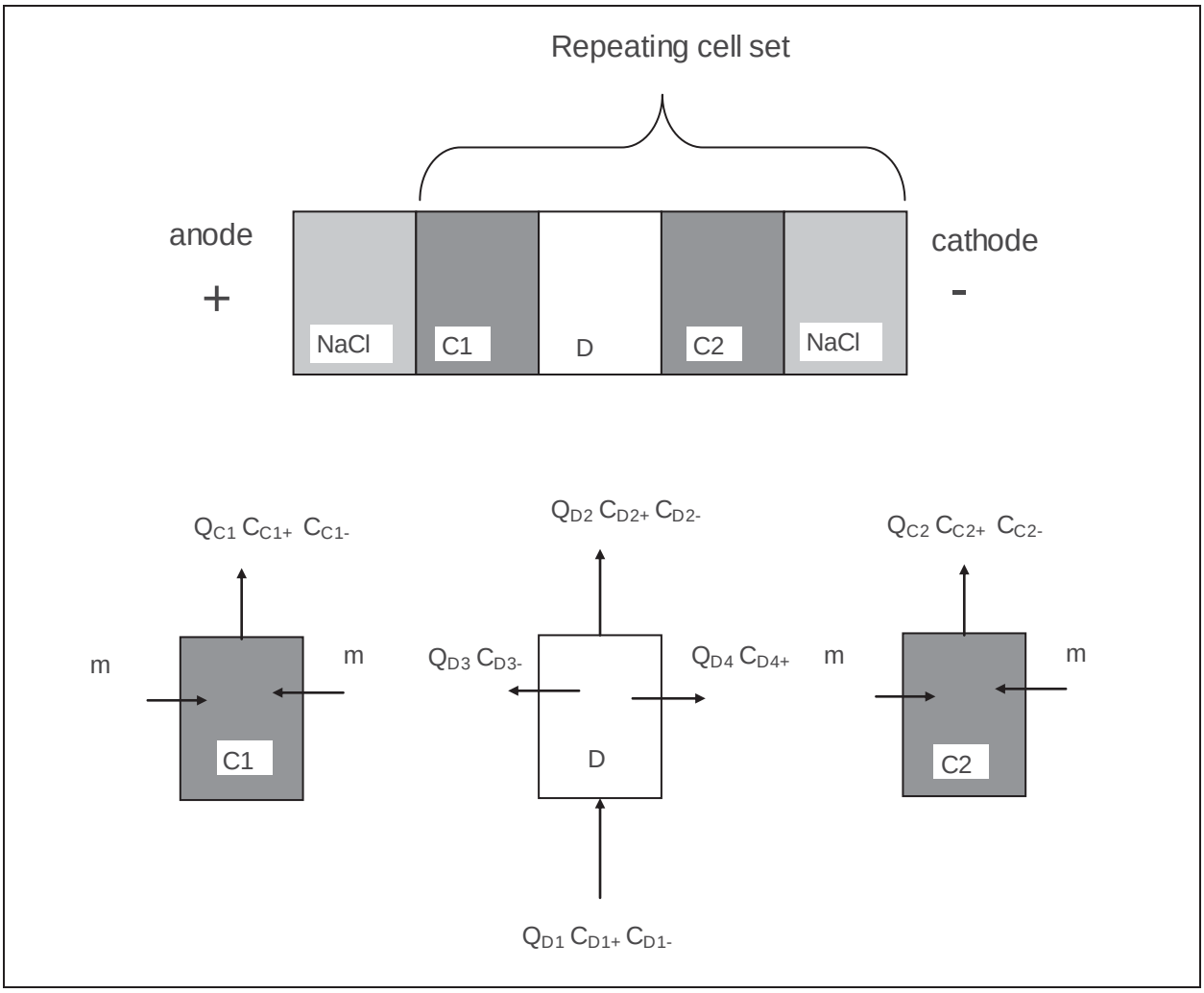

Figure B.4 Schematic of ion and water transport in an EDM cell set

electroosmosis. Likewise, ions and water are transported from the sodium chloride, NaCl, cells to the two concentrate cells.

Equivalent balance equations for the diluate cell are shown in Equations B.4 and B.5. Anions are transferred from the diluate cell to the cell C1, and cations are removed from the diluate cell to cell C2.

$$Q_{D1} C_{D1-} - Q_{D2} C_{D2-} = Q_{D3} C_{D3-} \quad \text{(B.4)}$$

$$Q_{D1} C_{D1+} - Q_{D2} C_{D2+} = Q_{D4} C_{D4+} \quad \text{(B.5)}$$

Flow of cations and anions can be described as a transfer rate of equivalents, m. The transfer rate of anion equivalents and cation equivalents from cell D and from the NaCl cells are equal to maintain electroneutrality.

$$Q_{D3} C_{D3-} = m$$

$$Q_{D4} C_{D4+} = m$$

Table B.3
Calculation of moles water transferred per meq from pilot data

Water source	I (A)	ζ	m (meq/h)	Q_{C1} (L/h)	λ (mole/eq)
LHGW	3.0	0.90	100.7	0.028	7.7
TGW	1.9	0.85	60.2	0.016	7.4
OBGW	1.6	0.80	47.8	0.013	7.6

Since concentrate flows are much smaller than the diluate flows, diluate influent and effluent flows are approximately equal, and ion transfer rates can be calculated as follows:

$$Q_{D1}(C_{D1-} - C_{D2-}) = Q_{D1}(C_{D1+} - C_{D2+}) = \frac{I\zeta}{F}$$

$$m = \frac{I\,\zeta}{F}$$

In electrodialysis, water transferred from the diluate to the concentrate cells is typically proportional to equivalents of ions transferred. A variable λ was defined as moles of water transferred per equivalent of ions transferred to each concentrate cell (λ can be viewed as the number of water molecules accompanying each ion that migrates through the membrane). Each mole of water comprises 0.018 L. Therefore, the volume of water transferred is 0.018 λ L per eq of ions transferred.

$$Q_{C1} = 0.018\lambda_1 2m$$

$$Q_{C2} = 0.018\lambda_2 2m$$

Concentrations (meq L^{-1}) in the C1 and C2 cells are

$$C_{C1+} = C_{C1-} = \frac{m}{Q_{C1}} = 27.8\lambda_1^{-1} \quad \text{(B.6)}$$

$$C_{C2+} = C_{C2-} = \frac{m}{Q_{C2}} = 27.8\lambda_2^{-1} \quad \text{(B.7)}$$

Pilot data were evaluated to determine λ values (Table B.3) using Equations B.6 and B.7. Based on pilot results, an λ value of 7.6 mol meq^{-1} was selected for model calculations.

Recovery, Y, of the EMD cell set is the ratio of diluate and feed flows.

$$Y = \frac{Q_{D2}}{Q_{D1}}$$

The net product water produced, Q_{D2}, is the feed flow less the two concentrate flows. This is not apparent in Figure B.4 because part of the concentrate flow comes from the NaCl cells. The NaCl solutions, however, are made up with product water, and the water transferred from the NaCl cells to the concentrate cells is a loss of product water that should be accounted for in the recovery calculation. Therefore,

Table B.4
Current utilization factors calculated from pilot data

Water source	ΔU model (V)	ΔU pilot (V)	ζ
LHGW	0.56	0.61	0.93
TGW	0.63	0.75	0.85
OBGW	0.66	0.80	0.82

$$Q_{D2} = Q_{D1} - Q_{C1} - Q_{C2} = Q_{D1} - 0.018 \times 2m(\lambda_1 + \lambda_2)$$

$$Y = \frac{Q_{D1} - 0.018 \times 2m(\lambda_1 + \lambda_2)}{Q_{D1}}$$

$$Y = 1 - \frac{0.036m(\lambda_1 + \lambda_2)}{Q_{D1}}$$

Current utilization factors (ζ) were calculated from ratios of theoretical voltage (model calculation) to voltage measured in the pilot (Table B.4).

$$\zeta = \frac{I_{theoretical}}{I_{actual}}$$

$$I = \frac{\Delta U}{R}$$

$$\zeta = \frac{\Delta U_{model}}{\Delta U_{pilot}}$$

APPENDIX C
COST CALCULATIONS

The methodology and factors used for the cost calculations are shown in this appendix. Capital costs were amortized over 20 years at an annual rate of return of 6 percent. The average cost of electricity was obtained from data provided by the U.S. Energy Information Administration using data through April 2010. Costs of chemicals were obtained directly from manufacturers, however it should be noted that the cost of chemicals vary with location and time. Process equipment capital cost estimates were provided from the equipment suppliers, and markups were applied to derive installed costs. Markups depended on the type of equipment and the capacity.

Unit costs used for each of the options evaluated are shown in Table C.1.

An example of the cost calculations is presented using Option 3A of TGW source to demonstrate the methodology. Table C.2 shows flow rates for the three process units for TGW Option 3A. Design parameters and unit costs used for the calculation of MIEX treatment costs are shown in Table C.3. Design parameters and costs for EDM in TGW Option 3A are shown in Table C.4. Costs used for the crystallizer in TGW Option 3A are shown in Table C.5. Total treatment costs used for TGW Option 3A are shown in Table C.6.

Table C.1
Unit costs used for treatment cost calculations

Parameter	Value
Cost recovery factor	0.0872
Electricity cost, $/kWh	0.12
Building cost, $/sf	200
NaCl cost, $/kg	0.11
NaOH cost, $/kg	0.66
CaO cost, $/kg	0.22
Na_2CO_3 cost, $/kg	0.44

Table C.2
Process stream flows for TGW Option 3A

Process	Total flow (m^3/d)	Recovery	Product water (m^3/d)
MIEX	10,000	99.7%	9,970
EDM	9,970	98.4%	9,810
Crystallizer	190	100.0%	190

Table C.3
MIEX costs for TGW Option 3A

Parameter	Value
Regeneration solution, g NaCl/L sol	100
Regeneration rate, g NaCl/L resin	360
TOC limit in regenerate Solution, g/L	10
SO_4 limit in regenerate Solution, g/L	30
Regeneration rate, BV	3.6
NaCl per regeneration, g	7,200
Initial TOC, mg/L	50
Treated water TOC, mg/L	20
NaCl exchange rate, g Cl per g TOC	1
NaCl consumed, g NaCl per m^3 treated	50
Regeneration waste, m^3 per m^3 water treated	0.003
MIEX attrition rate, L resin per m^3 water treated	0.002
MIEX resin unit cost, $ per L resin	14
MIEX resin replacement cost, $ per m^3 water treated	0.028
NaCl cost, $ per m^3 water treated	0.005
Total O&M cost, $/year	122,160
Capital cost, $	9,246,021
Amortized capital cost, $/year	806,110
Total annual cost, $/year	928,271
Unit capital cost, $/$m^3$	0.22
Unit O&M cost, $/$m^3$	0.03
Unit treatment cost, $/$m^3$	0.25

Table C.4
EDM costs for TGW Option 3A

Parameter	Value
NaCl transfer per cell	0.49 meq/s
NaCl consumption per cell, kg NaCl per day	2.5
Cell flow, m^3/d	1.452
NaCl consumption, kg/m^3	1.7
NaCl cost, $\$/m^3$	0.19
Membrane cost, $	53
Membranes per stack	400
Total number of stacks	70
Total number of membranes	28,000
Membrane replacement frequency, years	7
Annual membrane replacement cost, $/year	210,526
Annual membrane replacement cost, $\$/m^3$	0.06
Energy consumption, kWh/m^3	0.56
Energy cost, $\$/m^3$	0.07
Annual O&M cost, $/year	1,131,174
Capital cost, $	4,559,210
Amortized capital cost, $/year	397,493
Unit capital cost, $\$/m^3$	0.11
Unit O&M cost, $\$/m^3$	0.31
Unit treatment cost, $\$/m^3$	0.42

Table C.5
Crystallizer costs for TGW Option 3A

Parameter	Value
Capital cost, $	6,766,094
Amortized capital cost, $/year	589,899
Unit capital cost, $\$/m^3$	0.16
Energy consumption, kWh/m^3	88
Unit capital cost, $\$/m^3$	0.15
Unit O&M cost, $\$/m^3$	0.17
Unit treatment cost, $\$/m^3$	1.20

Table C.6
Total cost for Option 3A CCNF

Parameter	Value
Unit capital cost, $\$/m^3$	0.48
Unit O&M cost, $\$/m^3$	0.47
Unit treatment cost, $\$/m^3$	0.95

REFERENCES

Abdel-Wahab, A., and B. Batchelor. 2002. Chloride Removal From Recycled Cooling Water Using Ultra-High Lime With Aluminum Process. *Water Environment Research*, 74(3):256.

Aiken, G.R., and E. Cotsaris. 1995. Soil and Hydrology: Their Effect on NOM. *Journal AWWA*, 87(1):36.

Aiken, G.R., D.M. McKnight, R.L. Wershaw, and P. MacCarthy. 1985. *Humic Substances in Soil, Sediment, and Water*. New York: John Wiley and Sons.

Aldaco, R., A. Garea, and A. Irabien. 2006. Fluoride Recovery in a Fluidized Bed: Crystallization of Calcium Fluoride on Silica Sand. *Industrial and Engineering Chemistry Research*, 45:796–802.

Aldaco, R., A. Irabien, and P. Luis. 2005. Fluidized Bed Reactor for Fluoride Removal. *Chemical Engineering Journal*, 107:113.

Alheritiere, C., W.R. Ernst, and T.A. Davis. 1998. Metathesis of Sodium Salt Systems by Electrodialysis. *Desalination*, 115:189–198.

Allgeier, S.C., and R.S. Summers. 1995. Evaluating NF for DBP Control With the RBSMT. *Journal AWWA*, 87(3):87.

Amor, Z., S. Malki, M. Taky, B. Bariou, N. Mameri, and A. Elmidaoui. 1998. Optimization of Fluoride Removal From Brackish Water by Electrodialysis. *Desalination*, 120:263.

Astilleros, J.M., C.M. Pina, L. Fernandez-Diaz, and A. Putnis. 2002. Molecular-Scale Surface Process During the Growth of Calcite in the Presence of Manganese. *Geochimica et Cosmochimica Acta*, 66(18):3177.

Batchelor, B., and M. McDevitt. 1984. An Innovative Process for Treating Recycled Cooling Water. *Journal WPCF*, 56(10):1110.

Batchelor, B., M. McDevitt, and D. Chan. 1985. Removal of Sulfate From Recycled Cooling Water by the Ultra-High Lime Process. In *Proc. of the Water Reuse Symposium.* Denver, Colo.: AWWA.

Batchelor, B., M.B. Lasasla, M. McDevitt, and E. Peacock. 1991. Technical and Economic Feasibility of Ultra-High Lime Treatment of Recycled Cooling Water. *Research Journal WPCF*, 63(7):982.

Behrman, A.S., and H. Gustafson. 1940. Removal of Silica From Water. *Industrial and Engineering Chemistry*, (April):468–472.

Betz, L.D., C.A. Noll, and J.J. Maguire. 1940. Removal of Silica From Water by Cold Process. *Industrial and Engineering Chemistry*, (October):1320–1323.

Bishop, P., and G. Sansoucy. 1978. Fluoride Removal From Drinking Water by Fluidized Activated Alumina Adsorption. *Journal AWWA*, 70(10):554.

Bond, R.G., and S. Veerapaneni. 2007a. *Zero Liquid Discharge for Inland Desalination.* Denver, Colo.: AwwaRF and AWWA.

Bond, R.G., and S. Veerapaneni. 2007b. Reducing the Costs for Desalination With Zero Liquid Discharge. In *Proc. of the AWWA Annual Conference and Exposition.* Denver, Colo. AWWA.

Bouguerra, W., M. Ben Sik Ali, B. Hamrouni, and M. Dhahbi. 2007. Equilibrium and Kinetic Studies of Adsorption of Silica Onto Activated Alumina. *Desalination*, 206:141–146.

Braghetta, A., F.A. DiGiano, and W.P. Ball. 1998. NOM Accumulation at NF Membrane Surface: Impact of Chemistry and Shear. *Journal of Environmental Engineering*, November.

Chen, A.S.C., V.L. Snoeyink, and F. Fiessinger. 1987. Activated Alumina Adsorption of Dissolved Organic Compounds Before and After Ozonation. *Environmental Science and Technology*, 21:83–90.

Chen, J., and H. Yu. 2000. Lead Removal From Synthetic Wastewater by Crystallization in a Fluidized Bed Reactor. *Journal of Environmental Science and Health, Part A*, 35(6):817–835.

Chiang, P.-P., and M. Donohue. 1987. Crystallization From Ionic Solution. In *Fundamental Aspects of Crystallization and Precipitation Processes*. American Society of Chemical Engineers.

Choi, W., and K.Y. Chen. 1979. The Removal of Fluoride From Waters by Adsorption. *Journal AWWA*, 71:562.

Cicerone, D.S., A.E. Regazzoni, and M.A. Blesa. 1992. Electrokinetic Properties of the Calcite/Water Interface in the Presence of Magnesium and Organic Matter. *Journal of Colloid and Interface Science*. 134(2):423–433.

Cleary, J.G., and J. Grazdis. 1982. Treatment and Reuse of Gasifier Wastewater. In *Proc. of the Water Reuse Symposium.* Denver, Colo.: AWWA.

Clifford, D. 1999. Ion Exchange and Inorganic Adsorption. In *Water Quality and Treatment.* Edited by R.D. Letterman. McGraw Hill.

Clifford, D., J. Matson, and R. Kennedy. 1978. Activated Alumina: Rediscovered "Adsorbent" for Fluoride, Humics, and Silica.

Crozes, G., P. White, and M. Marshall. 1995. Enhanced Coagulation: Its Effect on NOM Removal and Chemical Costs. *Journal AWWA*, 87(1):78.

Davis, J.A., and R. Gloor. 1981. Adsorption of Dissolved Organics in Lake Water by Aluminum Oxide: Effect of Molecular Weight. *Environmental Science and Technology*, 15(10):1225.

Dempsey, B.A., R.M. Ganho, and C.R. O'Melia. 1984. The Coagulation of Humic Substances by Means of Aluminum Salts. *Journal AWWA*, 76(4):141.

Dennett, K.E., A. Amirtharajah, T.F. Morgan, and J.P. Gould. 1996. Coagulation: Its Effect on Organic Matter. *Journal AWWA*, 88(4):129.

Eberle, H., H. Stober, and D. Donnert. 1976. Study on the Adsorption Properties of Aluminum Oxide and Its Application for the Purification of Groundwater Containing Humic Substances. In *Translations of Reports on Special Problems of Water Technology.* Volume 9, Adsorption. EPA-600/9-76-030. Cincinnati, Ohio: U.S. Environmental Protection Agency. p. 380.

Egeberg, P.K., and J.J. Alberts. 2002. Determination of Hydrophobicity of NOM by RP-HPLC, and the Effect of pH and Ionic Strength. *Water Research*, 36:4997–5004.

Fonseca, A.C., R.S. Summers, A.R. Greenberg, and M.T. Hernandez. 2007. Extra-Cellular Polysaccharides, Soluble Microbial Products, and Natural Organic Matter Impact on Nanofiltration Membranes Flux Decline. *Environmental Science and Technology*, 41:2491–2497.

Ghosh, K., and M. Schnitzer. 1980. Macromolecular Structures of Humic Substances. *Soil Science*, 129:266–276.

Gratz, A.J., and P.E. Hillner. 1993. Poisoning of Calcite Growth Viewed in the Atomic Force Microscope. *Journal of Crystal Growth*, 129:789–793.

Graveland, J.C., P.J. de Moel, and J.H. Oomen. 1983. Developments in Water Softening by Means of Pellet Reactors. *Journal AWWA*, 75(12):619.

Greenberg, S.A., and T.N. Chang. 1965. Investigation of the Colloidal Hydrated Calcium Silicates. II. Solubility Relationships in the Calcium Oxide-Silica-Water System at 25°C. *Journal of Physical Chemistry*, 69:182.

Guillard, D., and A. Lewis. 2001. Nickel Carbonate Precipitation in a Fluidized Bed Reactor. *Industrial and Engineering Chemistry Research*, 40:5564–5569.

Hao, O.J., and C.P. Huang. 1986. Adsorption Characteristics of Fluoride Onto Hydrous Alumina. *Journal of Environmental Engineering*, 112(6):1055.

Harms, W.D., and R.B. Robinson, 1990. Characterization of Fluidized Bed Crystallizers Used for Softening in South Florida. *Environmental Engineering.*

Hoch, A.R., M.M. Reddy, and G.R. Aiken. 2000. Calcite Growth Inhibition by Humic Substances With Emphasis on Hydrophobic Acids From the Florida Everglades. *Geochimica et Cosmochimica*, 64(1):61.

Hong, S., and M. Elimelech. 1997. Chemical and Physical Aspects of Natural Organic Matter (NOM) Fouling of Nanofiltration Membranes. *Journal of Membrane Science,* 132:159–181.

Iler, R.K. 1979. *Chemistry of Silica*. New York: John Wiley and Sons.

Jucker, C., and M. Clark. 1994. Adsorption of Aquatic Humic Substances on Hydrophobic Ultrafiltration Membranes. *Journal of Membrane Science*, 97:37–52.

Kilduff, J.E., S. Mattaraj, and G. Belfort. 2004. Flux Decline During Nanofiltration of Naturally Occurring Organic Matter: Effects of Osmotic Pressure, Membrane Permeability, and Cake Formation. *Journal of Membrane Science*, 239:39–53.

Kim, W.-S., I. Hirasawa, and W.-S. Kim. 2004. Polymorphic Change of Calcium Carbonate During Reaction Crystallization in a Batch Reactor. *Industrial and Engineering Chemistry Research*, 43:2650–2657.

Lebron, I., and D.L. Suarez. 1998. Kinetics and Mechanisms of Precipitation of Calcite as Affected by PCO_2 and Organic Ligands at 25°C. *Geochimica et Cosmochimica Acta*, 62(3):405–416.

Leenheer, J.L., and E.W.D. Huffman Jr. 1976. Classification of Organic Solutes in Water Using Macroreticular Resins. *Journal of Research, U.S. Geological Survey*, 4:737–751.

Li, C., J. Jian, and J. Liao, 2004. Integrating Membrane Filtration and a Fluidized-Bed Pellet Reactor for Hardness Removal. *Journal AWWA*, 96(8):151.

Li, Q., and M. Elimelech. 2004. Organic Fouling and Chemical Cleaning of Nanofiltration Membranes Measurements and Mechanisms. *Environmental Science and Technology*, 38:4863–4693.

Liao, M.Y., and S.J. Randtke. 1985. Removing Fulvic Acid by Lime Softening. *Journal AWWA*, 77(8):78.

Lin, Y.P., P.C. Singer, and G.R. Aiken. 2005. Inhibition of Calcite Precipitation by Natural Organic Material: Kinetics, Mechanism, and Thermodynamics. *Environmental Science and Technology*, 39:6420–6428.

Lindsay, F.K., and J.W. Ryznar. 1939. Removal of Silica From Water by Sodium Aluminate. *Industrial and Engineering Chemistry*, 31(7):859.

Mazrou, S., H. Kerdjoudj, A.T. Cherif, A. Elmidaoui, and J. Molenat. 1998. Regeneration of Hydrochloric Acid and Sodium Hydroxide With Bipolar Membrane Electrodialysis From Pure Sodium Chloride. *New Journal of Chemistry*, 355–359.

Mortensen, E.R., T.Y. Cath, J.A. Brant, K.E. Dennett, and A.E. Childress. 2007. Evaluation of Membrane Processes for Reducing Total Dissolved Solids Discharged to the Truckee River. *Journal of Environmental Engineering*, (December):1136–1144.

Mouche, R., and J.V. Matson. 1980. Conservation of Cooling Water by Silica Removal With Activated Alumina. *National Science Foundation*, PFR 7919072.

Mujeriego, R. 1976. Silica Removal From Industrial Water. Ph.D. Dissertation, University of California, Berkeley.

Mullin, J.W. 1993. *Crystallization*. London: Butterworth-Heinemann, Linacre House, Jordan Hill, Oxford.

Nilson, J.A., and F.A. DiGiano. 1996. Influence of NOM Composition on Nanofiltration. *Journal AWWA*, 88(5):53.

Nilsson, O., and J. Sternbeck. 1999. A Mechanistic Model for Calcite Crystal Growth Using Surface Speciation. *Geochimica et Cosmochimica Acta*, 63(2):217–225.

Powell, S.T. 1954. *Water Conditioning for Industry*. New York: McGraw Hill Book Company.

Randtke, S.J. 1988. Organic Contaminant Removal by Coagulation and Related Process Combinations. *Journal AWWA*, 80(5):40.

Reardon, E., and Y. Wang. 2000. A Limestone Reactor for Fluoride Removal From Wastewaters. *Environmental Science and Technology*, 34:3247–3253.

Reddy, M.M., and K.K. Wang. 1980. Crystallization of Calcium Carbonate in the Presence of Metal Ions. *Journal of Crystal Growth*, 50:470–480.

Roller, P.S., and G. Ervin. 1940. The System Calcium Oxide-Silica-Water at 30°: The Association of Silicate Ion in Dilute Alkaline Solution. *Journal of the American Chemical Society*, 62:461.

Salt Industry Center of Japan. 2009 [Online]. Available: <http://www.shiojigyo.com/english/method/concentrate.html>.

Schaefer, A., A.G. Fane, and T.D. Waite. 1998. Nanofiltration of Natural Organic Matter: Removal, Fouling, and the Influence of Multivalent Ions. *Desalination*, 118:109–122.

Schoeman, J., and H. MacLeod. 1987. The Effect of Particle Size and Interfering Ions on Fluoride Removal by Activated Alumina. *Water SA*, 13(4).

Schwartz, M.C. 1938. *Journal AWWA*, 30:551.

Sehn, P. 2008. Fluoride Removal With Extra Low Energy Reverse Osmosis Membranes: Three Years of Large Scale Field Experience in Finland. *Desalination*, 223:73.

Semmens, M.J., and K. Ayers. 1985. Removal by Coagulation of Trace Organics From Mississippi River Water. *Journal AWWA*, 77(5):79.

Semmens, M.J., and A.B. Staples. 1986. The Nature of Organics Removed During Treatment of Mississippi River Water. *Journal AWWA*, 78(2):76.

Spiegler, K.S. 1958. Transport Process in Ionic Membranes. *Transactions of the Faraday Society*, 54:1408.

St. Johns River Water Management District. 2004. *Surface Water Treatability and Demineralization Study*. Special Publication SJ2004-SP20.

Strathmann, H. 2004. *Ion-Exchange Membrane Separation Processes*. Amsterdam: Elsevier.

Straub, F.G. 1936. Removal of Silica From Solution at Boiler Temperatures. *Industrial and Engineering Chemistry*, 28(1):36.

Stumm, W., and J.J. Morgan, 1996. *Aquatic Chemistry. Chemistry Equilibria and Rates in Natural Waters.* New York: John Wiley and Sons.

Tahaikt, M., R. Habbani, A. Haddou, I. Achary, Z. Amor, M. Taky, A. Alami, A. Boughriba, M. Hafsi, and A. Elmidaoui. 2007. Fluoride Removal From Groundwater by Nanofiltration. *Desalination*, 22:46.

Thompson, D.W., and P.G. Pownall. 1988. Surface Electrical Potential of Calcite. *Journal of Colloid and Interface Science*, 131(1):74–82.

Thurman, E.M. 1985. *Organic Geochemistry of Natural Waters*. Dordrecht, The Netherlands: Martinus Nijhoff/Dr. W. Junk Publishers.

Thurman, E.M., and R.L. Malcolm. 1981. Preparative Isolation of Aquatic Humic Substances From Different Lakes. *Environmental Sciences and Technology*, 15:463.

Tlili, M.M., B. Amor, C. Gabriella, S. Joiret, G. Maurin, and P. Rosseau. 2003. Study of Electrochemical Deposition of $CaCO_3$ by In Situ Raman Spectroscopy. *Journal of the Electrochemical Society*, 150(7):C485.

Turner, B.D., P. Binning, and S.L.S. Stipp. 2005. Fluoride Removal by Calcite: Evidence for Fluorite Precipitation and Surface Adsorption. *Environmental Science and Technology*, 39:9561.

U.S. Census Bureau. 2005. Table A1: Interim Projections of the Total Population for the United States: April 1, 2000, to July 1, 2030 (Online). Available: <http://www/census.gov/population/www/projections/projectionsagesex.html>. [cited October 16, 2008]

USEPA (U.S. Environmental Protection Agency). 1996. *ICR Manual for Bench- and Pilot-Scale Treatment Studies.* EPA 814-B-96-002. Cincinnati, Ohio: Office of Groundwater and Drinking Water.

USEPA (U.S. Environmental Protection Agency). 2003. Occurrence Summary and Use Support Document for the Six-Year Review of National Primary Drinking Water Regulations.

Van der Bruggen, B., L. Braeken, and C. Vandecasteele. 2002. Flux Decline in Nanofiltration Due to Adsorption of Organic Compounds. *Separation and Purification Technology*, 29:23–31.

Van der Veen, C., and A. Graveland. 1988. Central Softening by Crystallization in a Fluidized Bed Process. *Journal AWWA*, 80(6):51.

Van Dijk, J.C., and D.A. Wilms. 1991. Water Treatment Without Waste Material—Fundamentals and the State of the Art of Pellet Softening. *Journal Water SRT*, 40(5):263–280.

Weber, W.J., and A.M. Jodellah. 1985. Removing Humic Substances by Chemical Treatment and Adsorption. *Journal AWWA*, 77(4):132.

Wilhelm, F.G., I. Punt, N.F.A. van der Vegt, H. Strathmann, and M. Wessling. 2002. Asymmetric Bipolar Membranes in Acid-Base Electrodialysis. *Industrial and Engineering Chemistry Research*, 41:579–586.

Wu, Y.C., and A. Nitya. 1979. Water Defluoridation With Activated Alumina. *Environmental Engineering*, 105:357.

Yang, M., T. Hashimoto, N. Hoshi, and H. Myoga. 1999. Fluoride Removal in a Fixed Bed Packed With Granular Calcite. *Water Research*, 33(16):3395–3402.

Zhang, G., Y. Gao, Y. Zhang, and P. Gu. 2005. Removal of Fluoride From Drinking Water by a Membrane Coagulation Reactor (MCR). *Desalination*, 177:143.

Zhou, P., J. Huang, A. Li, and S. Wei. 1999. Heavy Metal Removal From Wastewater in a Fluidized Bed Reactor. *Water Research*, 33(8):1918–1924.

Zhou, P., S. Rowland, R.F.C. Mantoura, and J. Braven. 1994. The Formation of Humic Coatings on Mineral Particles Under Simulated Estuarine Conditions—A Mechanistic Study. *Water Research*, 28(3):571–579.

Zuddas, P., and A. Mucci. 1994. Kinetics of Calcite Precipitation From Seawater: I. A Classical Chemical Kinetics Description for Strong Electrolyte Solutions. *Geochimica et Cosmochimica Acta*, 58:4353–4362.

ABBREVIATIONS

a	activity
a_0	activity at equilibrium
AA	activated alumina
A_s	specific surface area
ASTM	American Society for Testing and Materials
AWWA	American Water Works Association
AwwaRF	Awwa Research Foundation
BV	bed volume
°C	degrees Celsius
°F	degrees fahrenheit
FBC	fluidized bed crystallizer
g	gram
hrs	hours
HRT	hydraulic residence time
IAP	ion activity product
IX	ion exchange
J	joule
K	degrees kelvin
kg	kilogram
Ksp	solubility product
L	liter
L/h	liters per hour
M	molar
m	meter
m^2	square meter
m^3	cubic meter
MF	microfiltration
mg	milligram
mg/L	milligrams per liter
mL	milliliter
ML	megaliter

N	normal (equivalents per liter)
nm	nanometer
NOM	natural organic matter
O&M	operation and maintenance
Q	flow rate
R	recovery
r	rejection
RO	reverse osmosis
S	supersaturation
SI	Système International (International System of Units)
T	temperature
t	time
TDS	total dissolved solids
TOC	total organic carbon
UF	ultrafiltration
USEPA	United States Environmental Protection Agency
UVA	ultraviolet absorption
ZLD	zero liquid discharge

The following organizations contributed financially to this Tailored Collaboration project:

- Orlando Utilities Commission
- Tampa Bay Water
- South Florida Water Management District
- Southwest Florida Water Management District
- Saint Johns River Water Management District

WATER RESEARCH FOUNDATION℠

6666 West Quincy Avenue, Denver, CO 80235-3098 USA

P 303.347.6100 • F 303.734.0196 • www.WaterResearchFoundation.org

ISBN 978-1-60573-143-8

4163

1P-2C-4163-06/11-FP